THE UNIVERSITY *of* EDINBURGH

Investigating cell cycle control mechanisms in CD8+ effector T cells

David Alexander Lewis

Degree of Doctor of Philosophy – The University of Edinburgh - 2023

Declaration

I, the undersigned, hereby declare that this thesis has been of my own composition, that all work presented within the thesis has been conducted by myself, that this work has not been submitted for any other degree of professional qualification, and that except where explicitly stated or acknowledged in the thesis or below, that all work was carried out by me.

Segments of Chapter 1 are expanded from material previously published as part of a review in Frontiers in Cellular Development Biology, which was co-authored with Tony Ly. The figures taken from that paper, as indicated in their respective figure legend, were produced by myself for the purpose of this review.

22/03/2023

Acknowledgements

This work would not have been possible without the support, guidance, and tutelage of my supervisors. Dr Tony Ly for his expertise in cell cycle biology and mass spectrometry, Professor Rose Zamoyska for her expertise in T cell activation and differentiation, and Professor Doreen Cantrell for her expertise in T cell proteomics for its input in the early design work conducted on this project.

I would like to thank Dr Van Kelly for lending his experience and time for Mass Spectrometry set up, and to Dr Christos Spanos for his instrumental role in enabling acquisition of MS samples utilising the Lumos, David Wright for his input in the design of the Cas9 CrispR procedures, Xiaoyen Zou for their assistance in basic lab procedures, and general advice with T cell tissue culture, Dr Martin Waterfall for his guidance and aid in utilising the flow cytometry facilities, and Dr Alan Score for his aid in processing the DIA datasets.

General aspects of T cell immunology, including lab procedures, discussion, and sharing of materials, protocols, and specimens, benefited greatly from the support and contributions of other members of Zamoyska lab, including Dr Patricia Castro Sanchez, Dr Sonja Haupt, Dr Thomas Tan, Dr Mate Ravasz, Dr Johanna Knipper, Nicola Logan, Peter Pukler, and Dr Alex Teagle.

Support for cell cycle and other aspects of molecular biology where made possible by members of Ly Lab, including fellow PhD students Aymen Al-Rawi, Rene, and Edward, as well as Dr Ananya Kar, all of whom provided discussion, ideas, and general aid at key points during the investigation.

Members of IIIR and the MSB groups in Edinburgh Universty as well as Alabert lab and Blow lab who are part of the Tri-lab meetings in Dundee. These groups provided alternative perspectives on the work I have done, and as such offered new insights. As the project is in part a molecular biology and an immunology project, having both these pools of expertise to draw from was essential to cover for any blindspots that only focusing on the one area may otherwise have lead to.

I'd like thank the BBSRC and the Eastbio programme for providing the funding for this work, as well as the framework for networking and allowed me to meet with a pool of diverse

project candidates from across the four universities involved, with special mention to Kiani, Holly, and Grace, with whom I was able to compare and contrast the various means of mental survival as we navigated the PhD programme.

The completion of this work is due in no small part to a support network of family and friends, especially my wife Xin, my parents, and brother Benjamin, who offered everything from light reprieve to much needed distraction. I also give thanks to Dr. Wu “Hazel“ Huang, who consistently hosted and invited me to a number of events and occasions in which to meet other PhD students in an entirely non-scientific setting. I owe a lot to GEAS and FAQ, the ttrpg society and board game society of Edinburgh respectively, for allowing me a means of escape and a network of non-scientific people to engage with, with special mention to Will, Jing Jing, Alex. I would also like to thank the WoD and CofD Discord communities, who provided me with a variety of different social groups while in the midst of intense isolation, from the pandemic or otherwise.

Abstract

CD8+ T cells have an important role in adaptive immunity. By possessing cytotoxic potential, CD8+ T cells are key effectors of the adaptive immune system, targeting diseased cells for destruction. CD8+ T cells are a key focus in the growing field of immuno-oncology because of their role in tumour cell killing. Naïve CD8+ T cells exist in a state of quiescence. Upon antigen recognition and co-stimulation, the CD8+ T cell escapes from this state of dormancy and towards a complex programme of cellular growth, cell cycle entry, and differentiation, leading to the production of short-lived effector T cells (SLECs), and memory progenitor cells (MPECs). The memory T cell pool which remains shares a lot of characteristics with the naïve cell including a capacity to remain dormant, engage in self-renewal, and maintain proliferative potential and multipotency upon restimulation, in a manner very similar to stem cells. Another characteristic shared with stem cells is a capacity for rapid proliferation.

Like stem cells, at the peak of expansion, CD8+ T cells are also predominantly found in S phase, however it is not currently known whether their cell cycle regulation is similar to stem cells. There is also a good body of evidence showing a correlation between the rate of proliferation and the route of differentiation in CD8+ T cells. Cells which rapidly re-enter S-phase post mitosis favour differentiation towards the SLEC phenotype, while cells which stall in G1 phase favour the MPEC phenotype. However, the exact nature of this correlation, and how such a switch in cell cycle regulation is governed during the expansion phase is not well understood. This is in part because CD8+ T cells are resistant to cell cycle inhibiting agents, making the synchronisation studies seen in classic cell cycle analysis experiments not possible to do with CD8+ T cells.

In order to investigate how the cell cycle is regulated in $CD8^+$ T cells, we used PRIMMUS (Proteomic analysis of Intracellular iMMUnolabelled cell Subsets), a method which utilises FACSorting to conduct proteomic analysis on sorted populations from asynchronous CD8+ T cells, thereby allowing a method to identify the cell cycle regulated proteins in CD8+ T cells without the need for synchronisation.

Our analysis identified 160 proteins which had a strong periodicity rating, indicating they were likely to be cell cycle regulated. The majority of these identities consisted of mitotic proteins

such as those involved in kinetochore assembly. In Embryonic Stem (ES) cells, rapid proliferation is facilitated by the inhibition of an E3 ubiquitin ligase known as the anaphase promoting complex cyclosome (APC/C) due to high expression of the pseudo-substrate Emi1. This prevents APC/C from binding with co-activator Cdh1, and thus preventing the degradation of many S phase promoting mechanisms, especially proteins which are involved with origin licensing such as Cyclins E and A, which stay constitutively active. This results in a shortened G1 and G2 phase, with the majority of stem cells found in S phase more than any other cell cycle phase. In CD8+ T cells we noticed that many targets of APC/C^{Cdh1}, including DNA replication enzymes and origin licensing components and regulators, showed either very low periodicity or very little fluctuation over the course of cell cycle, indicating a loss of cell cycle regulation. We also observed that Cyclin A was found to fluctuate far less in CD8+ T cells than has been observed in the somatic Nb4 cells, and that Emi1 had a very high level of periodicity. When comparing this dataset with other studies on asynchronous populations for ES and somatic cells, we found a greater overlap of processes shared between CD8+ T cells and ES cells than with somatic cells which suggested CD8+ T cells may share stem-like qualities in their cell cycle regulation. We therefore hypothesised that Emi1 has a role in defining cell cycle rate and by extension, the eventual differentiation fate.

To test this hypothesis, we conducted another proteomic analysis comparing IL-2 treated T effector cells to IL-15 treated memory T cells. Within these two phenotypes, we further divided them into G1 delayed and actively cycling cells. Absolute protein content was generally higher in effector cells. But when examining APC/C substrate abundance relative to total protein content, we found that G1 delayed memory T cells had a higher proportion of APC/C substrates compared with G1 delayed effector T cells. This was not the case with actively cycling cells, which showed similar proportions of APC/C substrates between effector and memory. This could imply that while memory T cells are encouraged to exit cell cycle, they retain much of the machinery to re-enter, maintaining a higher state of cell cycle "readiness" than arrested effector T cells possess. We also noted that Emi1 levels were consistent between memory and effector cells, with the true correlating factor of Emi1 expression being whether the cell was G1 delayed or actively cycling, with actively cycling cells expressing a high quantity of Emi1, while G1 delayed cells expressing very little.

To examine the role of Emi1 on CD8+ T cells more directly, we induced a knockout of Emi1 by Crispr. This knockout of Emi1 lead to T effector cells undergoing “re-replication”, in which the genome is duplicated a second time before the cells enter M phase. The cells that did not experience re-replication, experienced an apparent block to cell cycle re-entry. While re-replication was present in memory T cells, the effect on cell cycle re-entry did not appear. The re-replication is likely to have occurred as a consequence of insufficient APC/C^{Cdh1} inhibition. This results in the degradation of origin licensing regulating proteins like Cyclin A and geminin, resulting in inappropriate origin licensing, which is essential for commencement of DNA replication. However, if the cell becomes deficient in Emi1 before origin licensing occurs, it remains within G1 and becomes unable to progress, a phenomenon observed in Emi1 disruption within transformed cancer cells and stem cells. That we saw no increase in G1 phase in knockout memory T cells could imply that Emi1 was already significantly reduced in memory cells, rendering the knockouts impact on G1 phase bellow detection.

We therefore conclude that CD8+ T cells achieve a rapid proliferation phenotype via stem cell-like regulation of cell cycle, enabling steady re-entry into S-phase mediated by high levels of Emi1, and that IL-15 treated cells shift their cell cycle behaviour, reducing Emi1 and thus reducing their proliferative activity. Because we noticed in our dataset the fluctuation of deubiquitinase Usp1 mimics the pattern of Emi1 fluctuation, we hypothesise that SLEC associated transcription factor Id2 and MPEC associated transcription factor Id3, proteins which Usp1 preserves, may be the link between cell cycle speed and memory phenotype, as Id2 and Usp1 are both APC/C^{Cdh1} substrates, but Id3 is not. We suggest a model then in which Emi1 mediated APC/C^{Cdh1} inhibition promotes both rapid proliferation and survival of Id2, driving cells towards the effector cell fate. While in the absence of Emi1, cells remain in G1 where APC/C^{Cdh1} is active, degrades Id2, allowing Id3 to promote the memory cell fate.

Lay Abstract

CD8+ T cells have an important role in controlling the spread of infection and have a lot of potential as a novel tool for treating cancer. One of their key characteristics which allows them to carry out these roles is that they can divide very rapidly in response to infection. This results in a large pool of effector cells which are able to recognise and kill any infected cells, and memory cells which remain in the body after the infection has cleared and act as early responders upon repeat infection.

CD8+ T cells share a number of behaviors with stem cells in that they are both capable of self renewal, and as they divide both are capable of producing a variety of different types of cells. In addition, they share a rapid turnover of cell division.

Cell division is the final step in a wider process known as the cell cycle. The cycle consists of four phases, the first gap phase (G1 phase) in which the cells prepare to duplicate their genome (S phase), then a second gap phase (G2 phase) as the cells prepare to divide (M phase). Following M phase, cells return to G1 and remain within the cycle, or leave the cycle and stop dividing. To better understand how CD8+ T cells divide, we designed a method in which CD8+ T cells could be sorted based on which cell cycle phase they were in, collected, and processed for mass spectrometry, a technique which permits the identification of most proteins within cells. The protein content of each cell could then be quantified, allowing us to see which biological processes are active at each cell cycle phase.

CD8+ T cells were found to share a number of characteristics with stem cells, namely that a number of proteins which are typically degraded during G1 phase in other cell types did not fluctuate over the course of the cell cycle. A similar mechanism is seen within stem cells which enables them to maintain a rapid progression from M phase to S phase. The role of one of these proteins, called Emi1, was further characterised, with its expression seen as critical for successful cell division. Overall, these data indicates that CD8+ T cells share a number of mechanisms with stem cells which enable rapid cell division, with Emi1 being a key component that allows for rapid re-entry in to S phase.

Table of Contents

1 Introduction

Classical descriptions of the immune system separate it into two distinct arms, referred to as the innate and the acquired immune response. The innate arm consists predominately of myeloid lineage leukocytes including macrophages, neutrophils, dendritic cells (DCs), and NK cells, all of which have a role in the early response to infection, such as inflammation, the attraction of myeloid cells to the site of infection, phagocytosis, and other more generally applied means of controlling and containing pathogens. The acquired immune response instead is mediated predominately by lymphoid lineage leukocytes. Unlike the innate system which relies on generic danger signals, including pathogen associated molecular patterns (PAMPs), lymphocytes instead go through a process known as VDJ recombination upon their antigen recognising receptors, which enables a large repertoire of antigen specific recognition, and thus a more specified means of clearing infection.

These cells are primarily split into T lymphocytes and B lymphocytes. The former are responsible for targeted destruction of infectious agents and mediating the nature and strength of infection, while the latter is responsible for production of antibodies against the source of infection. The innate response is very rapid, immediately active shortly after the infectious agent appears. The acquired immune response however is slower typically only being apparent 5-7 days post infection. This is in part because lymphocytes require activation by certain cells of the innate immune response, known as antigen presenting cells (APCs), to phagocytose the infectious agent and present the peptide antigens to the lymphocytes within the lymph nodes. Following this antigen led activation, the lymphocytes proliferate and differentiate into a pool of effector cells which act to clear the infection, as well as a pool of long lived memory cells, providing long lasting immunity to repeat infections. These memory lymphocytes remain in circulation or in the tissue at the site of infection, ready to produce a targeted attack even without myeloid intervention (Dempsey, Vaidya, and Cheng 2003).

1.1 CD8 T cell immunology

$CD8^+$ T have a primary role in limiting viral infection and cancer progression through recognising key viral/tumour antigens on the infected cell surface and targeting them for destruction (Kim and Ahmed 2010). Once they are stimulated by pAPCs, they go through three stages of development known as the activation phase, the expansion phase, and the

contraction phase. The activation phase is characterised by major rewiring of their cellular proteomes and metabolism, including a shift in activity to cytokine production, most notably Interferon (IFN)-γ as well as a small amount of Interleukin (IL)-2. During the expansion phase, activated T cells rapidly proliferate, the doubling rate averages at 6-8 hours with some studies demonstrating a peak doubling time of 4.5 hours, or even as little as 2 hours (Kurts et al. 1997; Yoon, Kim, and Braciale 2010). During this phase, T cells will begin to differentiate towards one of two T effector (T_{eff}) phenotypes, the short lived effector cell phenotype (SLEC) which are have a high capacity for infection clearance die during the subsequent contraction phase, and the memory progenitor phenotype (MPEC) which remain (Mehlhop-Williams and Bevan 2014) Figure 1.

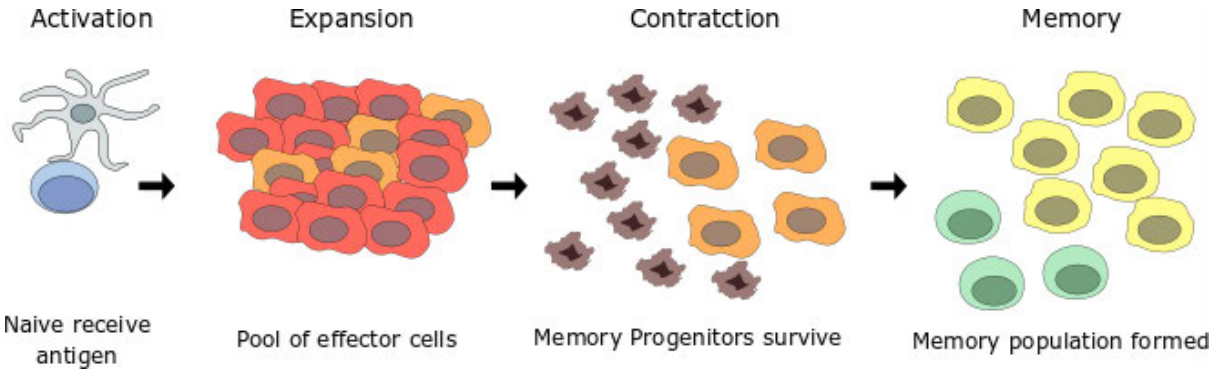

Figure 1 Naïve T cells are activated by APCs at Activation phase, this leads the T cells to enter the Expansion phase where the cells rapidly proliferate and differentiate to form a large pool of effector cells and a small pool of memory progenitor cells. During the Contraction phase, the effector cells die and leave behind the pool of memory progenitors which differentiate in to the stable pool of long lived memory cells, returning to a state of quiescence.

Because of their ability to target specific cells for destruction, there is a lot of interest in adapting these cells for use in cancer immunotherapy. One method is adoptive T cell transfer (ACT) in which tumour recognising $CD8^+$ T cells (commonly referred to as tumour infiltrating lymphocytes (TILs)) are extracted from the patient, grown *ex vivo* with IL-2, and then reintroduced to the patient. This method is however limited by the number of TILs which can be successfully extracted from the patient, and thus require additional time for expansion. This expansion period often require cytokine modulation or other forms of bioengineering materials such as biopolymer implants to both encourage growth of the pool for the length of time required, but must be done so in a manner which, also encourage a development of memory T cells for long lived tumour immunity (Morotti et al. 2021). Another method is chimeric antigen receptor (CAR) T cells, in which $CD8^+$ T cells from the patient are genetically modified to produce TCRs which are already specific for the tumour antigen of choice, getting

around the limited pool of tumour recognising cells in the patient, and the more recent generations of CAR T cells are engineered to produce more cytokine such as IL-2 following antigenic stimulation (Tomasik, Jasiński, and Basak 2022). However, a number of other problems face these therapies, a main one being the immunosuppressive microenvironment around the tumour which can prevent activation, proliferation, and effector function of re-introduced $CD8^+$ T cells (Martín-Otal et al. 2022; Sterner and Sterner 2021). A $CD8^+$ T cell's capability to expand is crucial for its function, with a weaker capability to proliferate resulting in reduced capability to control tumour growth following ACT (Chee et al. 2020).

1.1.1 Naïve T cells, Activation

A naïve $CD8^+$ T cell requires 3 stimulation signals to activate and initiate proliferation: antigenic stimulation via the TCR, co-stimulator signalling from pAPCs via molecules such as CD28, and cytokine stimulation primarily driven by IL-2. Stimulation of the TCR alone leads a cell to become anergic, meaning the cells do not express the IL-2 receptor CD25, fail to proliferate, and become unresponsive to further stimulation attempts. A dual signal of TCR and CD28 induces production of IL-2 and proliferation within the first 24 hours. IL-2 stimulation through the IL-2 receptor (IL-2R) enables rapid proliferation as the cells enter the expansion phase (Mondino et al. 2006).

TCR stimulation leads to phosphorylation of lymphocyte-specific protein tyrosine kinase (Lck), which in return phosphorylates the ζ chains of the TCR along the immunoreceptor tyrosine-based activation motifs (ITAMS). This enables recruitment of TCR-associated protein 70 (Zap70), which is subsequently phosphorylated by Lck. Zap70 then phosphorylates four key sites on the linker for activation of T cells (LAT) which allows for recruitment of proteins into the LAT signalosome. The downstream effect is activation of the Rat sarcoma (Ras)/ extracellular signal-related kinase (Erk)/Activator protein 1 (AP-1) pathway, Protein kinase C-θ (PKCθ)/ κB kinase (IKK)/ nuclear factor-κB (Nf-κB) pathway, and the calcium-dependent Calcineurin/nuclear factor of activated T cells (NFAT) pathway. (Brownlie and Zamoyska 2013; Hwang et al. 2020). The transcription factors downstream of these pathways, NFAT, Nf-κB, and AP-1 all contribute to the transcription of *IL2* and also contribute to the transcription of *IL2RA,* which encodes IL2RA/CD25, the alpha subunit of the IL-2 receptor (Liao, Lin, and Leonard 2013) **(**Figure 2**).**

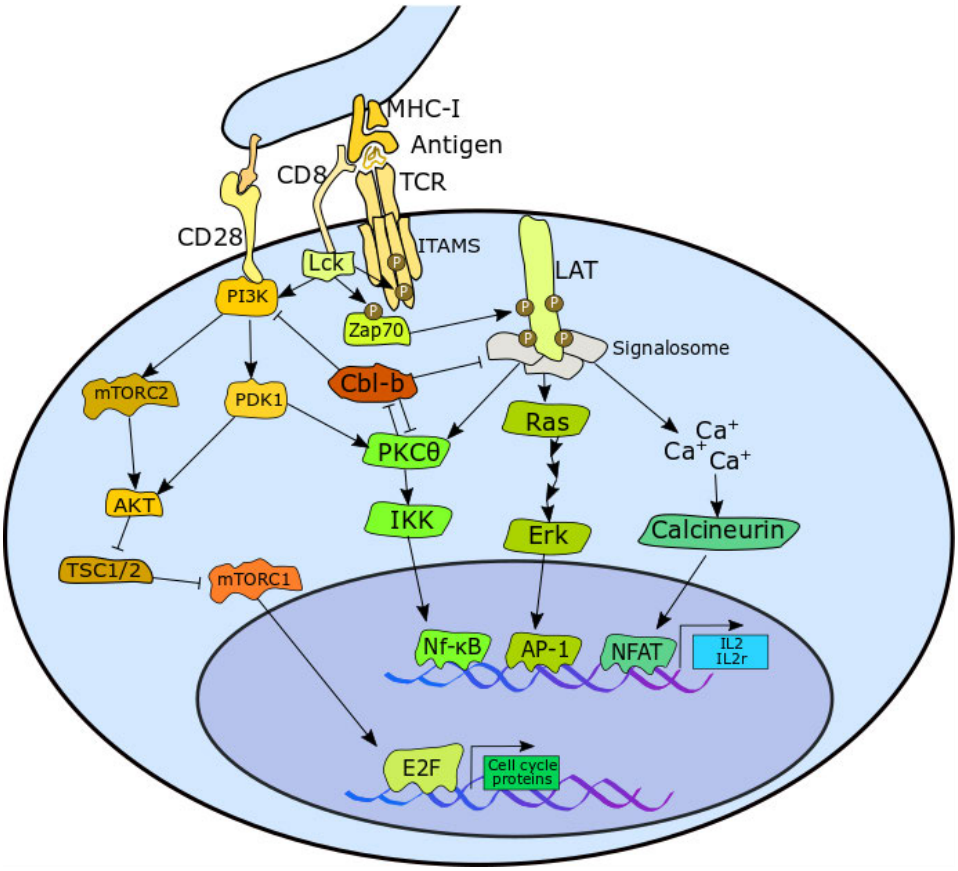

Figure 2 MHC-I presented peptide stimulated the TCR and CD8 leading to phosphorylation via Lck and autophosphorylation of kinases around the ITAMS, including phosphorylation of Zap70 which leads to phosphorylation events around LAT and recruitment of proteins around it forming the signalosome. This triggers three major pathways cascades, the PKCϑ/IKK/Nf-κB pathway, Map kinase pathway, and the Calcineurin pathway, leading to an upregulation of IL-2 and the IL-2 receptor. CD28 stimulation by the APC leads to activation of PI3K which enhances PKCϑ, deactivating Cbl-b which would otherwise inhibit the signalosome, promoting anergy. PI3K also leads to mTORC1 activation via AKT, resulting in activation of E2F and cell cycle initiation. Figure originally published in (Lewis and Ly 2021)

Lck positively regulates phosphoinositide-dependent kinase 1 (PDK1) activity, which stimulates two major pathways: PKCθ/IKK/Nf-κB pathway and the Ak strain transforming (AKT)/ mammalian target of rapamycin complex 1 (mTORC1) pathway. Lck mediates this via activation of phosphoinositide 3-Kinase (PI3K), which is enhanced by co-receptor CD28 stimulation. PI3K is also responsible for enabling the assembly of mTOR complex 2 (mTORC2), which activates AKT, enabling it to target its substrates, such as the mTORC1 inhibitor, TSC1/2, thereby upregulating mTORC1 activity. (Brownlie and Zamoyska 2013; Hwang et al. 2020; Jutz et al. 2016; Spolski, Li, and Leonard 2018).

With TCR stimulation alone, however, the components of the LAT signalosome, as well as PKCθ are targeted for degradation by the E3-Ubiquitin ligase Cbl-b. Cbl-b also has the effect of reducing PI3K activity by preventing formation of phosphatidylinositol-3-phosphate (PIP3).

The net effect of this is a sharp reduction in NFAT, NFκB, AP-1, and mTOR activity, resulting in the cell becoming anergic (Liu, Langdon, and Zhang 2014).

CD28 co-stimulation counteracts this effect by enhancing PKCθ activity, which promotes degradation of Cbl-b. Indeed, loss of PKCθ activity further decreases transcription factor activity downstream of LAT (Gruber et al. 2009), while knockout (KO) of CD28 reduces proliferation (Li et al. 2004). Conversely, either Cbl-b deletion, or a Cbl-b inactive mutant, enables T cell proliferation and production of IL-2 in the absence of CD28 signal. Loss of Cbl-b activity greatly enhances CD28-mediated proliferation and IL-2 production (Paolino et al. 2011). Consistent with a role in negatively regulating activation, Cbl-b also emerged as a top hit in a CRIPSR genetic screen for regulators of secondary activation in human $CD8^+$ T cells (Shifrut et al. 2018).

Interestingly, there is no requirement for Lck in the activation of memory T cells upon secondary infection by LCMV *in vivo*. The frequency of antigen-specific T cells after secondary challenge to antigen was unaffected in memory cells depleted of Lck compared to Lck-replete cells. Rechallenged Lck-depleted cells also produce comparable levels of interferon (IFN)-γ levels to Lck-replete cells (Tewari et al. 2006). This is in direct contrast to naïve cells depleted of Lck, which do not proliferate in response to antigen (Seddon et al. 2000). In addition, *ex vivo* memory T cells seem more reliant on cytokine signalling to induce proliferation, with antigen and CD28 stimulation alone proving insufficient to trigger proliferation in memory T cells (Cho et al. 1999).

1.1.2 Memory and Effector T cell Differentiation

During the expansion phase, $CD8^+$ T cells undergo a state of rapid proliferation, during which time the cells begin to differentiate towards two main phenotypes, SLECs and MPECS. SLECs are characterised by high expression of T-box transcription factor (T-bet) which upregulates receptor KLRG1 (Joshi et al. 2007)**.** SLECs have greater capacity for cytotoxicity via production of granzyme B and perforin, while MPECs have a greater capacity for survival via expression of the interleukin IL-7 α-chain receptor (CD127). T-bet is understood to contributes a great deal to the SLEC phenotype, and knockout studies has shown a severe decrease in SLEC development, with activation of T-$bet^{-/-}$ naïve T cells favouring MPEC fate (Fixemer et al. 2020). T-bet is shown to be essential for cytotoxicity (Sullivan et al. 2003) and has a role in downregulating CD127 expression (Knox et al. 2014; Yeo and Fearon 2011). Mechanistically,

loss of CD127 caused by high expression of T-bet reduces the cells access to survival signal IL-7, contributing to these cells being generally short lived (Kaech et al. 2003). However, T-bet KO studies have demonstrated no direct role in influencing cell cycle mechanisms (Sullivan et al. 2003).

MPECs are positive for another T-box transcription factor Eomesodermin (Eomes), along with reduced expression of T-bet (Joshi et al. 2007). While T-bet and Eomes both have the effect of downregulating CD127 expression in $CD8^+$ T cells, $Eomes^{hi}$ $T\text{-}bet^{lo}$ MPEC cells preserve far more CD127 expression than $T\text{-}bet^{hi}$ SLECs (Knox et al. 2014), Eomes also has a role in upregulating pro-survival protein Bcl-2 (Kavazović et al. 2020) enabling the MPECs to outlive the contraction phase, and differentiate towards one of the memory T cell phenotypes, including the central memory T cell (T_{cm}), and effector memory T cell (T_{em}).

T_{cm} cells revert to a more naïve-like phenotype, regaining expression of L-selectin (CD62L) and the chemokine receptor CCR7 characteristic of naïve T cells, both of which enable the T_{cm} to exit the periphery via the high endothelial venules (HEV) and localise within the secondary lymph nodes (Debes et al. 2005; Galkina et al. 2007).

T_{em} lack both CCR7 and CD62L, and as such localise predominately in peripheral blood and tissue. Just as T_{cm} are more naïve-like in response to re-stimulation, T_{em} more closely behave like T_{eff}, possessing greater cytotoxic capability than T_{cm}, but have much reduced proliferative capability (Cellerai et al. 2010). T_{cm} can differentiate into both T_{em} and T_{eff}, while T_{em} only differentiate towards the T_{eff} phenotype, indicating a hierarchy of memory phenotype through which T cells irreversibly progress upon re-stimulation, losing naïve-like qualities of longevity and proliferative potential as they become more cytotoxic (Gattinoni et al. 2011) (Figure 3). This hierarchy is encoded within the epigenome. Naïve cells possess a lot of closed chromatin states with very low levels of DNA methylation, hiding away key cell cycle genes. DNA Methylation is greatly enhanced within T_{eff} following activation, while methylation is much reduced in the memory pool following contraction. Within the memory pool, the closed chromatin suppresses the transcription of many cell cycle genes within T_{cm} in a manner resembling naïve cells, while T_{em} chromatin states resembles that of the more open T_{eff} phenotype (Barski et al. 2017; Youngblood et al. 2017).

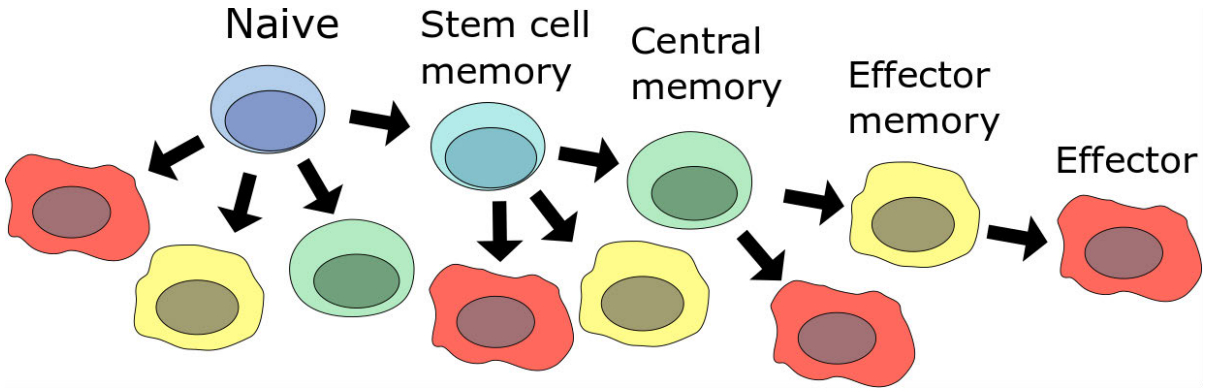

Figure 3 Hierarchy of differentiation from Naïve to Effector T cell. Each phenotype is capable of producing cells of its own phenotype or to the phenotype further down the hierarchy.

There seems to be a correlation with relative levels of T-bet vs Eomes within memory populations, with T_{cm} expressing less T-bet than T_{em}. While Eomes levels remain consistent between these populations, Eomes expression is generally lost in T_{eff} phenotype, where T-bet is predominantly expressed (Knox et al. 2014). It is interesting to note that levels of T-bet expression also seem to follow the above mentioned hierarchy, with only 20% of T_{cm} expressing low levels of T-bet compared to 50% of Tem cells, while high levels of T-bet are seen in 20% of Tem cells and 30% of fully differentiated T_{eff} (McLane et al. 2013).

One notable difference between naïve and memory T cells is the rate of proliferation they undergo for self-renewal. Studies analysing the amount of deuterium in glucose or the total amount of isotope labelled "heavy water" ($^2H_20$) over the course of a culture have determined that a mixed population of $CD8^+$ T memory cells have a resting dilution rate of between 0.007 – 0.015 d^{-1} (doubling time = 46 – 99 days)(Macallan, Busch, and Asquith 2019), far faster than that of naïve T cells at 0.00045 d^{-1} (doubling time = 1400 days)(del Amo et al. 2018). Proliferation time has not yet been determined for different memory T cell population. Such studies have been performed on $CD4^+$ T_{cm} and T_{em} which put their proliferation rate at as fast a 15 days and 48 days respectively (Macallan et al. 2004).

The events which determine whether cells differentiated in the expansion phase towards the short lived SLECs or the MPEC phenotype is still a topic of active debate, with many citing the role of antigen stimulation strength and type of cytokine stimulation as prevailing, though the exact mechanism of developing a diverse population of differentiated cells is still to be fully explored. Recent studies have demonstrated a link between rate of cell cycle progression and eventual fate of newly activated T cells. The Fluorescent Ubiquitination-based Cell Cycle

Indicator (Fucci) system offers us a means of directly tracking the cell cycle activity of cycling cells. This is done by using fluorescent markers tagged to two key cell cycle regulatory proteins, the licensing factor Cdt1 and its inhibitor Geminin, both of which will be described in greater detail further down. Cdt1 expresses predominately during early cell cycle, and can be an indicator of cells which stall in re-entry, while Geminin is expressed from mid cell cycle through to just before mitosis. (Zielke and Edgar 2015). Within Fucci mice (Kinjyo et al. 2015) it was observed that within the first 7 days post immunisations, proliferating T cells distinguish themselves into slow and fast proliferators, and that slow proliferating cells behaved as MPECs, and fast proliferating, as SLECs. Another study has demonstrated similar findings, where $CD62L^+$ MPEC cells transition through the cell cycle phases at a slower rate, demonstrating by a slower uptake of BrdU and EDU, than $CD62L^-$ SLEC at 3-6 days post immunisation irrespective of the strength of antigenic signal (Kretschmer et al. 2020).

1.1.3 Stemness and Exhaustion

The pool of memory T cells that remains following contraction phase return to a state of dormancy, similar to naïve cells. These cells share a lot of traits with stem cells in that within both naïve and memory populations is a capability to self-renew in the absence of antigenic stimulation, a good capacity for survival, and the potential to form a new pool of T_{cm}, T_{em}, and T_{eff} cells following (re-)stimulation with antigen. These characteristics are often referred to T cell "stemness" (Graef et al. 2014). Within the memory pool formed, T_{cm} would have more stemness than T_{em} being further up the differentiation hierarchy, while T_{eff} would have the least stemness. While naïve T cells arguably have the most stemness of all these phenotypes, there is a naïve-like phenotype of memory cell known as the T stem cell memory (T_{scm}) cell which has an enhanced capacity for self renewal and is capable of production of all other memory phenotypes (Gattinoni et al. 2011). T_{scm} express a similar array of markers as naïve T cells do ($CD62L^+$ $CD44^-$) but express elevated levels of CD95, and IL-2 receptor β-chain (CD122) (Gattinoni et al. 2009). They are produced directly from naïve cells, and rely on Wnt signalling mediated upregulation of the transcription factor Tcf1 in order for T_{scm} to maintain their stemness (Gattinoni et al. 2009; Kaech and Cui 2012).

When an activated T cell is exposed to a sustained consistent antigenic stimulation, as is often seen during chronic infection, it results in a dysfunctional cell state known as the exhausted T cell (T_{ex}). They are characterised by a range of exhaustion markers such as Pd-1, Tim-3, Lag-3,

and Tigit, all of which have an inhibitory role which leads to reduced cytokine production, proliferative capacity, and an impaired ability to clear infections, and therefore represent cells that have entirely lose their stemness (Wherry 2011). While typical T_{ex} are do not express Tcf1, there exists a subset of Tcf^{+} $Pd\text{-}1^{+}$ T cells, often referred to as precursor exhausted T cells (T_{pex}). These T_{pex} show many of the hallmarks of exhaustion, but still maintain a capacity for self-renewal and proliferative capacity in a manner similar to other memory phenotypes. When activated, they show themselves as capable of producing other T_{pex} and T_{ex}. Indeed, when a pool of exhausted cells are treated with PD-1 blockade, inducing proliferation, it is only the T_{pex} which proliferate as a result (Siddiqui et al. 2019).

A number of other proteins have been identified in maintaining stemness in T cells, this includes Bach2, Id3, and c-Myb, all of which have been shown to have a role in fostering production of Tcf1 and thus in preserving stemness across T cell phenotypes. Bach2 deficiency results in a reduction in T_{pex} within exhausted populations of T cells, while its overexpression promotes their production during chronic infection (Utzschneider et al. 2020; Yao et al. 2021). Id3 is understood to be essential for the formation of memory T cells (Ji et al. 2011), and is also observed to be highly expressed within T_{pex}, becoming lost along with Tcf1 as exhausted cells begin to express Tim3, terminally differentiating towards T_{ex} (Utzschneider et al. 2020). C-Myb is also a pivotal regulator of stemness in $CD8^{+}$ T cells by activating transcription of Tcf1, and is understood to promote T_{scm} and encourage T_{pex} cells, preserving stemness as cells move towards exhaustion (Z. Chen et al. 2019; Heuser and Gattinoni 2022)

These accounts provide more evidence towards the connection between proliferation and differentiation, as cells which proliferate more slowly are able to retain stemness. Taken together, it is thus quite likely that there is an intimate relationship between T cell fate post-immunisation and regulation of cell cycle progression.

1.2 Cell cycle

The cell cycle is divided into 4 phases (Figure 4), the first gap phase (G1) as the cell prepares for DNA replication (S) followed by a second gap phase (G2) when the cell prepares for mitosis (M). Quiescent, or G0 cells enter the cell cycle by first transiting through G1. During G1, cells pass through a commitment step called the restriction point (R). Before R, cells are susceptible to cell cycle arrest by mitogen starvation. However, beyond R, progression through the cell

cycle is mitogen-independent in human fibroblasts. The time cells spend in pre-R G1 is heterogeneous compared with the time spent in the remaining phases of the cell cycle (Zetterberg and Larsson 1985; Zetterberg, Larsson, and Wiman 1995). Additionally mitogen starved cells which exit to G0 and are reintroduced to mitogen have been observed to take up to an additional 8 hours to complete mitosis compared to cells cultured in mitogen-replete conditions (Zetterberg and Larsson 1991). Thus, G0, pre-R and post-R G1 are distinct phases that are distinguished in their mitogen responsiveness and in the length of time needed to progress to S-phase.

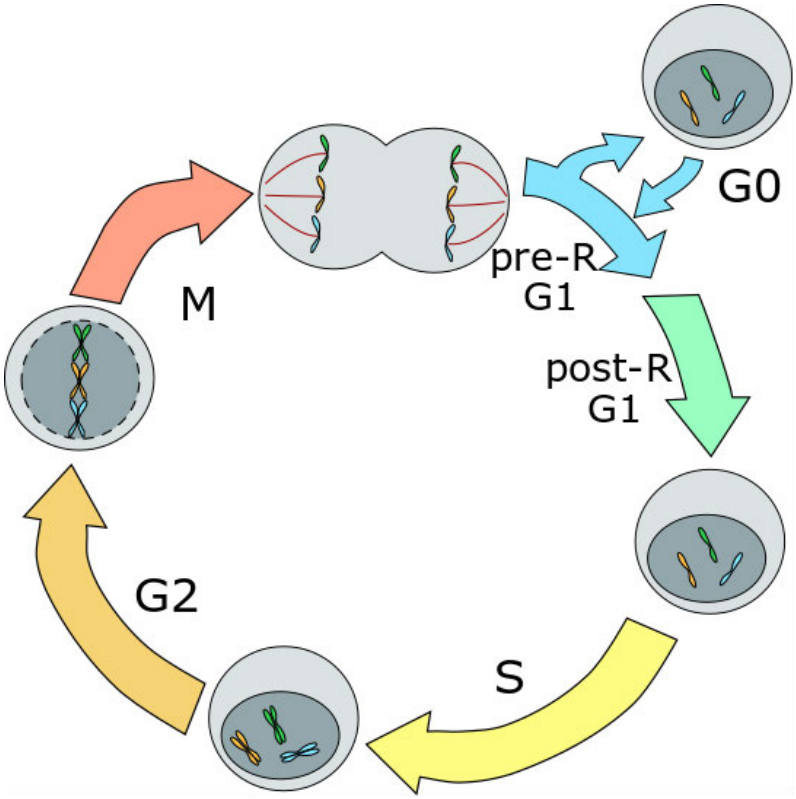

Figure 4 Cell cycle consists of two major events. DNA duplication which occurs in S phase, and cell division in M phase, with two gap phases before them known as G1 and G2 respectively. G1 can be further separated in to 2 phases as defined by the moment after which mitogen restriction does not prevent the cell from committing to cell cycle completion, referred to as the R point. Before the cells enter R point, they are able to exit the cell cycle entirely becoming quiescence/senescent, known as being in G0.

Key proteins that control cell cycle progression include 1) the cyclin proteins, which rise and fall in abundance at key stages of cell cycle, 2) the cyclin-dependent kinases (Cdks) which become active when bound to their cognate cyclins and 3) the Cdk inhibitor proteins (Cdki) which control cell cycle progression at key check points in response to mitogen starvation or cellular stress (e.g., DNA damage).

1.2.1 Cyclins and Cdks

Cyclins, Cdks and Cdkis have key roles in regulating the activity of E2F, a transcription factor that promotes the expression of cell cycle genes, including the cyclins and Cdks themselves. In G0 and pre-R G1, E2F mediated transcription is inhibited by pocket proteins Rb, p107, and p130, preventing the cell from progressing to S phase (Stengel et al. 2009). An active kinase complex is formed by interaction of cyclin D with either Cdk4 or Cdk6, and this kinase activity mediates hyperphosphorylation of Rb, causing Rb to decouple from E2F, and thereby enable E2F to promote upregulation of its targets. Such targets include a large number of S phase proteins, as well as cyclin E and cyclin A. Cyclin E will form a complex with Cdk2 which amongst other processes will contribute to Rb hyperphosphorylation, resulting in a positive feedback loop of E2F activation (Dyson 1998). Recent work suggests that Cdk4/6 regulates cellular processes other than those downstream of E2F (Figure 5).

Cyclin D3-Cdk6 phosphorylates key enzymes in the glycolysis pathway, diverting metabolites from glycolysis into the pentose phosphate pathway to promote redox balance (via production of NADPH) and cellular anabolism (e.g. by generating nucleotide precursors) production of nucleotide precursors to support DNA replication (Wang et al. 2017).

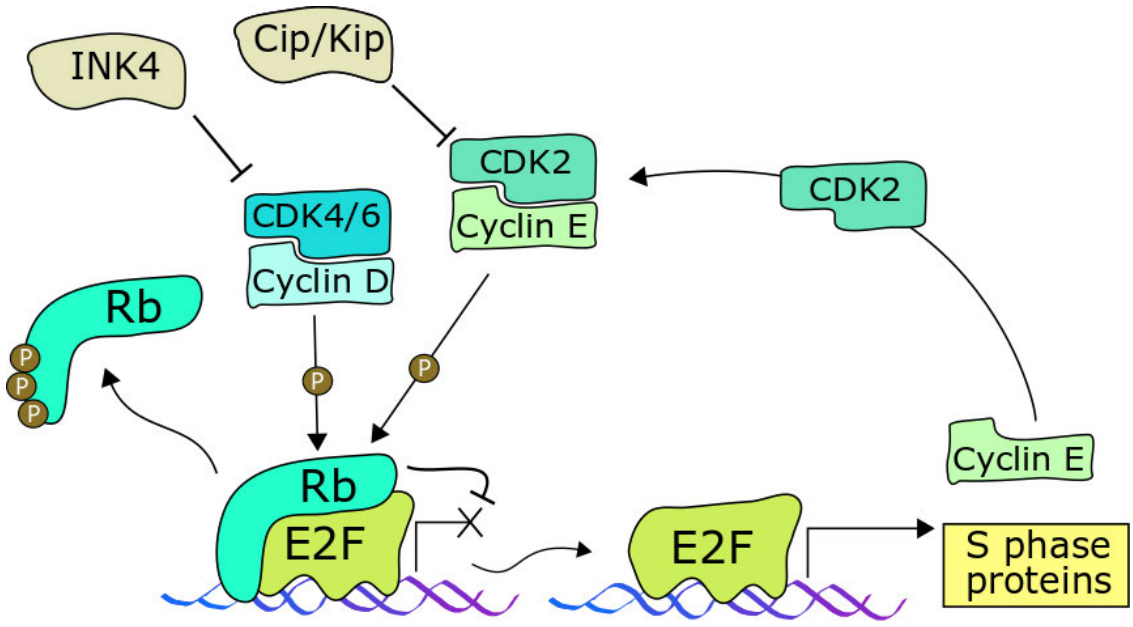

Figure 5 E2F upregulates S phase promoting proteins, but in early G1/G0 is inhibited by Rb. Activation of Cyclin D-Cdk4/6 leads to phosphorylation of Rb which decouples from E2F enabling transcription of its targets. One of its targets is Cyclin E, which when coupled with Cdk2 enables another means for Rb phosphorylation, resulting in a positive feedback loop. This can be slowed by the presence of Cdki of either the INK4 family or Cip/Kip family.

1.2.2 CdkIs

Cdk activities can be inhibited by stoichiometric binding to Cdkis, of which there are two main families: the INK4 family consisting of p16, p15, p18, and p19, which inhibit Cyclin D-Cdk4/6 complex; and the Cip/Kip family which consists of p27, p21, and p57, and are known to inhibit any cyclin-Cdk complexes within the cell cycle, and are able to induce cell cycle arrest at G1 phase (Sherr and Roberts 1999). The regulation of Cdk4/6 complexes by the Cip/Kip family members are more complex. Cip/Kip proteins can catalyse the formation of cyclin-Cdk complexes and in the absence of p21 or p27, cyclin D-Cdk complexes do not form (Cheng et al. 1999). Trimeric species containing p27 phosphorylated on tyrosine 74, cyclin D and Cdk4 retain kinase activity (Guiley et al. 2019). On the other hand, high levels of p21 inhibit Cdk4 (Labaer et al. 1997). Cip/Kip proteins are inactivated by post-translational modification and degradation. For example, tyrosine phosphorylation on p27 by mitogen-activated tyrosine kinases disrupts the inhibitory interaction of p27 with Cdk2 and promotes p27 degradation (Grimmler et al. 2007).

1.2.3 Cell Cycle Progression

There are a number of crucial checkpoints, some of which are specific to key phase transition points, such as G1/S and G2/M checkpoints, while others are not specific to any one phase. These checkpoints ensure cells do not continue along the cell cycle until properly fit to do so and in some cases will trigger the production of Cdkis, forcing the cell towards quiescence/senescence, or even apoptosis.

The phosphorylation of Rb as described above makes up the G1/S checkpoint, which ensures that the cell has sufficient quantity of activated Cdk2 to enable progress on to S phase. This starts with replication origin licensing in which the origin recognition complex (ORC) binds to the DNA. Cdc6 and Cdt1 are phosphorylated by both Cdk2/Cyclin E, Cdk2/Cyclin A, and Cdc7 (Ballabeni et al. 2009; Bermejo, Vilaboa, and Calés 2002), allowing them to be recruiting to the ORC. Cdt1 and Cdc7 recruitment then enables the formation of the minichromosome maintenance (Mcm) 2-7 to form a complex near the origin site, initiating replication (Evrin et al. 2009). Geminin inhibits origin licensing by binding to Cdt1, preventing it from being recruited to the ORC. Geminin expression increases in S phase and peaks a G2/M in order to prevent the possibility of premature origin-licensing which would then lead to re-replication (Bermejo et al. 2002; Klotz-Noack et al. 2012).

Another important checkpoint mechanisms is the DNA Damage Response which senses DNA damage, and induces cell cycle arrest to allow for DNA damage repair. These mechanisms can be divided into two broad pathways, the p53 pathway, and the Checkpoint Kinase (CHK)1 pathway. p53 in a transcription factor which responds to cellular distress. When not needed, p53 expression is kept low by degradation by the E3 ubiquitin ligase Mdm2. Mdm2 can be inhibited by sensor proteins which are activated in response to DNA damage such as ataxia telangiectasia mutated (ATM), which responds to double strand breaks in DNA, and ataxia telangiectasia and Rad3 related protein (ATR), which responds to replicative stress and are not cell cycle restricted, meaning these mechanisms operate at any time during the cell cycle when DNA damage is detected. ATM and ATR also phosphorylate p53, allowing it to form a tetramer and become activated as a transcription factor (Cheng et al. 2009; Davison et al. 1998).

This results in upregulation of a number of DNA repair mechanisms, as well as cell cycle arrest factors including p21, pausing cell cycle at any phase at which this may occur (Wade Harper et al. 1993). Chk1 is also activated by phosphorylation by activated ATR, and this enables Chk1 to phosphorylate Wee1 and Cdc25. Once phosphorylated, Wee1 becomes activated and phosphorylates Cdk1 in turn, inhibiting it and thereby inhibiting cell cycle at the G2/M border (Russell and Nurse 1987). Cdc25 is a phosphatase and is instead is inhibited by Chk1, rendering it unable to dephosphorylate either Cdk1 or Cdk2, ensuring these Cdks remain inactive (Dunphy and Kumagai 1991).

As the cells continue through M phase, they encounter the mitotic spindle checkpoint, which occurs between metaphase and anaphase and is predominately mediated by the E3 ubiquitin ligase Anaphase Promoting Complex Cyclosome (APC/C). During prometaphase, the kinetochore forms on the centromere and attaches to the microtubules protruding from the spindles as the cell enters metaphase. APC/C binds with its co-activator Cdc20 and polyubiquitinates both Cyclin B and Securin, tagging them for degradation (Thornton and Toczyski 2003). Securin is an inhibitor that binds to Separase. Once decoupled, Separase will cleave the cohesin complex which keep the chromatin together, allowing the sister chromatid to separate and the cell to enter anaphase (Sullivan, Lehane, and Uhlmann 2001; Uhlmann, Lottspelch, and Nasmyth 1999). To ensure this process does not occur too early, kinetochore complexes that remain unattached to chromatin can orchestrate the construction of the

mitotic checkpoint complex (MCC) consisting of BubR1, Bub3, Mad2, and Cdc20. This MCC will couple with a second subunit of Cdc20 already coupled with the APC/C, preventing APC/C^{Cdc20} from interacting with UbcH10, thought to be required for Ube2S mediated ubiquitin elongation. This 'closed' form of APC/C remains stable until APC/C^{Mcc} can initiate autoubiquitination of $Cdc20^{Mcc}$ upon complete chromatin attachment, and thereby triggering MCC disassembly and subsequent re-activation of APC/C^{Cdc20} (Alfieri et al. 2016; Sudakin, Chan, and Yen 2001; Uzunova et al. 2012). Thus, only when all kinetochores along the chromosome are properly attached and aligned can the chromatid pairs separate.

1.2.4 E3 Ubiquitin Ligases APC/C and SCF

In addition to mitotic spindle checkpoint, APC/C plays a role in aiding in controlling S-phase entry and mitotic exit. This is done with the aid of a different co-activator, Cdh1 (also known as Fzr1) (Figure 6). In Metaphase, Cdh1 is phosphorylated by Cdk1/Cyclin B, keeping it from forming a complex with APC/C. However, when APC/C^{Cdc20} reduces the abundance of Cyclin B, Cdk1/Cyclin B mediated phosphorylation is outcompeted by the Cdc14b phosphatase that removes the phosphate from Cdh1, enabling the formation of APC/C^{Cdh1}. One of the substrates of APC/C^{Cdh1} is Cdc20, so over the course of Anaphase, the APC/C^{Cdc20} becomes replaced by APC/C^{Cdh1} (Bassermann et al. 2008; Foe et al. 2011).

APC/C^{Cdh1} prevents origin licensing from taking place by targeting a number of E2F targets for degradation. This includes Cyclins E and A, ORC complex proteins, and inhibitors of Cdki such as Skp2, keeping cells from transitioning from G1 to S phase. Indeed, inactivation of the APC/C-Cdh1 has been shown to be a second crucial step after E2F activation in promoting the transition from G1 to S (Cappell et al. 2016). Thus, proteins required for G1/S are upregulated by increased synthesis via transcription by E2F and maintain an increased stability via APC/C inactivation. APC/C inactivation in G1 is mediated by multiple mechanisms, including phosphorylation of Cdh1 (Kramer et al. 2000) by Cdk2 (Lukas et al. 1999) and by the accumulation the pseudosubstrate inhibitor protein, Emi1 (also known as Fbxo5) (Cappell et al. 2018). Additionally, there are deubiquitinases (DUBs), including Usp37, which stabilise APC/C substrates by removing ubiquitin chains that would otherwise target these proteins for proteasomal destruction (Huang et al. 2011).

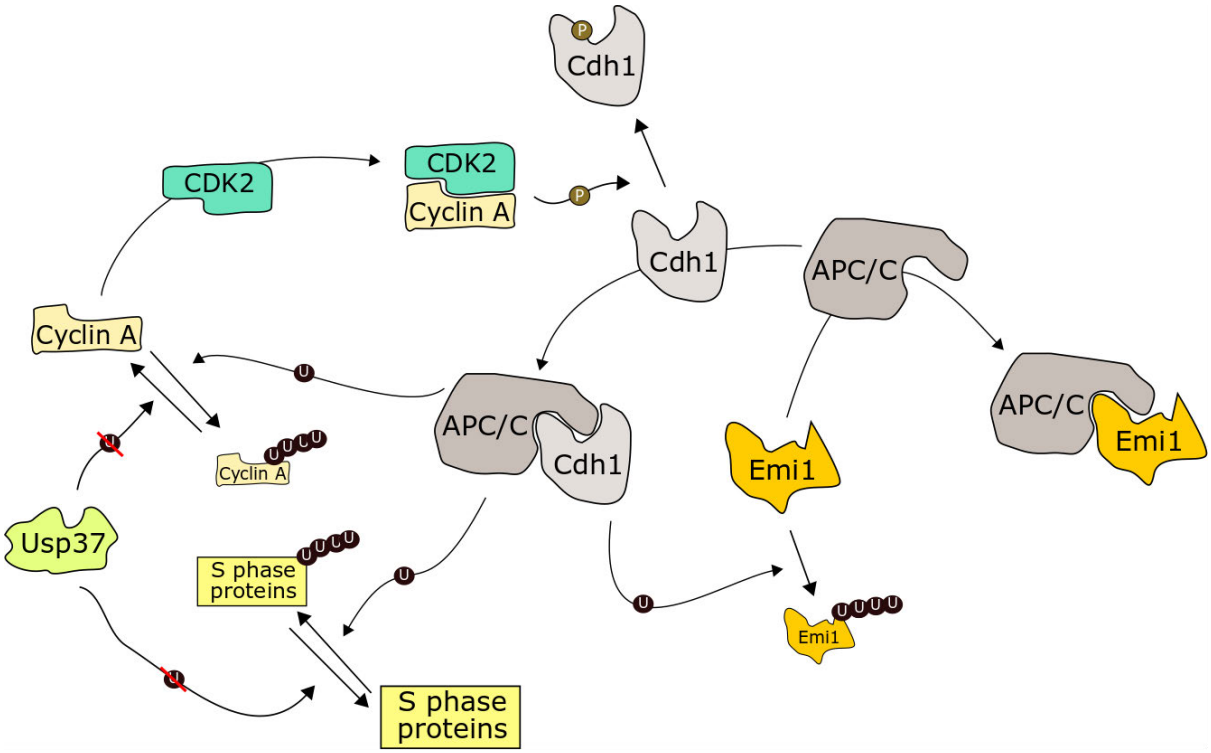

Figure 6 E3 ubiquitin ligase relies on co-activator Cdh1 in order to target its substrates. Once coupled, it is able to polyubiquitinate many proteins which promote S phase progression including Cyclin A, which tags them for proteolytic degradation. This can however be reverse by deubiquitinases such as Usp37. Once Cyclin A-Cdk2 is abundance enough to outpace APC/C^{Cdh1} activity, it can inhibit Cdh1 coupling with APC/C by phosphorylating it. Another mechanism is that of the pseudo-substrate Emi1 which binds to the co-activator pocket of APC/C, thereby preventing Cdh1 from forming a complex. and substrate of APC/C^{Cdh1}. Emi1 is also a substrate of APC/C^{Cdh1} and so will be degraded until the abundance of Emi1 can outpace APC/C^{Cdh1} activity.

Skp1-Cul1-F-box (SCF) complex is another E3 ubiquitin ligase which is important to mediating cell cycle control. Like APC/C, it has a number of co-activators which determine its targets, and while there are many such co-activators, there are four which are relevant to cell cycle regulation. S-Phase Kinase Associated Protein 2 (Skp2), β-Transducin repeats-containing protein (βTrCP), F-box and WD repeat domain containing 7 (Fbxw7), and Cyclin F. SCF^{Skp2} targets phosphorylated p27, which is phosphorylated by Cdk2/Cyclin E (Hao et al. 2005). This means once E2F activity will reach a threshold in which sufficient abundance of Cyclin E is produced to phosphorylate p27 which is then polyubiquitinated and subsequently degraded.

The resulting positive feedback loop allows high E2F activity to overcome p27 mediated inhibition. It has been observed that a similar mechanism occurs with p57 (Kamura et al. 2003) and p21 (Bornstein et al. 2003). SCF^{Skp2} also targets unbound Cyclin E (Nakayama et al. 2000), but because Skp2 is a substrate of APC/C^{Cdh1}, it is predominately active when APC/C^{Cdh1} is

already inhibited in late G1 through to S phase (Bashir et al. 2004). This means SCF^{Skp2} degrades Cyclin E while it is released from Cdk2 during S phase.

SCF binds to Cyclin F once it is phosphorylated by Akt (Choudhury et al. 2017), $SCF^{Cyclin\ F}$ forms as the cells approach G2 and targets activator E2Fs (E2F1, E2F2, E2F3a), preventing their activity post S phase (Dankert et al. 2016). In addition, $SCF^{Cyclin\ F}$ targets Cdh1, while APC/C^{Cdh1} targets Cyclin F (Choudhury et al. 2016), which may indicate that $SCF^{Cyclin\ F}$ has a role in aiding S phase progression, while APC/C^{Cdh1} enables a resurgence in activating E2Fs following M phase (Emanuele et al. 2020). Like Cyclin F, Fbxw7 requires phosphorylation by Akt to bind with SCF. Once formed, SCF^{Fbxw7} is known to predominately regulate the degradation of Cyclin E and Myc (Schülein, Eilers, and Popov 2011). Unlike Cyclin F, Fbxw7 is not a substrate of APC/C^{Cdh1} and as such can target Cyclin E for degradation during G1 phase, which has the consequence of promoting APC/C^{Cdh1} activity by preventing Cdh1 phosphorylation from Cdk2/Cyclin E (Lau et al. 2013).

$SCF^{\beta\text{-}TrCP}$ is not directly cell cycle regulated like Cyclin F, Cdh1, of Cdc20 is. Instead, regulation is governed by phosphorylation of its targets. Canonical degron motifs for $APC/C^{\beta\text{-}TrCP}$ must be phosphorylated (Paul et al. 2022), and as such its targets can be cell cycle regulated via phosphorylation by one or more kinases. For example, Wee1 is degraded following phosphorylation by Cdk1 and polo-like kinase (Plk1) (Watanabe et al. 2004); Cyclin F following phosphorylation by Casein Kinase 2 (Ck2) (Mavrommati et al. 2018); and Cdc25a phosphorylated by Chk1 and Chk2. This allows $SCF^{\beta\text{-}TrCP}$ to have a dual role in controlling APC/C^{Cdh1} activity by polyubiquitinating Cdh1 when it is phosphorylated by Plk1 and Cdk2 (Fukushima et al. 2013) , and Emi1 when it is phosphorylated by Cdk1 (Margottin-Goguet et al. 2003).

1.3 Cell Cycle Mechanisms in $CD8^+$ T cells

1.3.1 Naive

In many ways, T cells present a unique behavior in how cell cycle is regulated. Naïve $CD8^+$ T cells remain in a quiescent state, doubling at a time scale of months to years (Tough and Sprent 1994), requiring only minimal TCR stimulation from self-peptide expressed on MHC, as well as stimulation by IL-7 to maintain survival (Seddon and Zamoyska 2002). Though the exact mechanisms that suppress cell cycle entry in naïve cells are not clear, there are a

number of factors which are understood to contribute to this quiescence. mRNA expression of Klf4 correlates with that of p21, and knockout of Klf4 leads to an increase in proliferation upon activation (Yamada et al. 2009). Indeed, upon activation, it has been observed that the degradation of Klf4 is essential to enable cell cycle entry (Hao et al. 2017). Foxp1 is also understood to be an important mediator of quiescence in naïve T cells. Knockout experiments show that a loss of Foxp1 leads to enhanced expression of IL-7r, and allows for IL-7 mediated proliferation possibly by negatively regulating Mek and Erk signal (Feng et al. 2011), and a subsequent increase in activating E2F proteins (Wei et al. 2016). Stat1 is also observed to maintain quiescence via suppression of mTOR and cMyc pathways in response to type I interferons (Kye et al. 2021).

1.3.2 Activation induced proliferation

TCR/CD28 stimulation of naïve cells is sufficient to initiate proliferation. TCR/CD28 stimulation leads to phosphorylation of Rb, expression of cyclin E, cyclin A, and Cdk2, and the degradation of p27 (Appleman et al. 2000). Conversely, cells that become anergic from TCR stimulation alone have increased p27 (Boussiotis et al. 2000). Rapamycin, an inhibitor of mTOR, induces a severe delay in proliferation (D'Souza and Lefrançois 2003), resulting from decreased levels of cyclin D3 and cyclin E. And while cyclin D3 levels recover 3-5 days following rapamycin treatment, cyclin E remains low, suggesting a reliance on mTOR for antigen-induced E2F activation. Although the exact mechanism is unknown, expression of a rapamycin resistant mutant of $p70^{S6k}$ rescues E2F activity in rapamycin-treated cells; thereby demonstrating that mTOR activity promotes cell cycle progression by activating E2F through S6K (Brennan et al. 1999). In contrast to wild-type cells, proliferation of IL-$2^{-/-}$ cells is arrested completely by rapamycin. Together these results suggest that IL-2 signalling contributes to proliferation in an mTOR-independent manner. Interestingly, mTOR inhibition does not delay cells in the expansion phase (Colombetti et al. 2006).

mTOR also upregulates the c-Myc transcription factor, which has a crucial role in T cell metabolism (Vartanian et al. 2011; Waickman and Powell 2012; Wang et al. 2011) and expression of several cell cycle regulators, including p27, cyclins and Cdks (Dang et al. 2006). T cells lacking c-Myc have defects in glycolysis, glutaminolysis, cell growth and proliferation. Indeed, compared to wild type, c-Myc knockout cells show decreased levels of Cdk4, Cdk2 and CDC25A (Wang et al. 2011). Furthermore, in Raptor deficient cells that poses impaired

mTORC1 activity present attenuated transcription factors including Myc, but also Gabpa, YY1, and Srebf1, all of which are associated with mitochondrial function (Tan et al. 2017).

Cdki proteins interfere with the pathways downstream of TCR stimulation. p27 is a key negative regulator of IL-2 production in anergic $CD4^+$ T cells (Boussiotis et al. 2000). Ectopic expression of p27, but not p21, suppresses IL-2 production in control $CD4^+$ T cells. Depletion of p27 in stimulated Jurkat T cells enhances transcription of an IL-2 luciferase reporter construct and enhanced cellular AP-1 activity. The proposed mechanism is that p27 directly binds JAB1/COPS5, a subunit of the COP9 signalosome and a positive regulator of AP-1, inducing translocation from the nucleus to the cytoplasm (Tomoda, Kubota, and Kato 1999), thereby suppressing IL-2 transcription (Boussiotis et al. 2000). Whether this effect extends to $CD8^+$ T cells is yet to be determined.

There is significant interest in the roles of Cdk4/6 in immunomodulation, and how small molecule inhibitors of Cdk4/6 affect immune cell phenotypes. Recent data using Cdk4/6 inhibitors (Cdk4/6i) suggest a direct role in Cyclin-Cdks in controlling T cell differentiation. Three Cdk4/6i are FDA-approved for HR+ breast cancer: palbociclib (PD-0332991), abemaciclib (LY2835219) and ribociclib (LEE011). Numerous clinical trials are ongoing for the treatment of other solid tumours (Álvarez-Fernández and Malumbres 2020). Interestingly, recent evidence suggests these inhibitors function similarly to the INK4 family of proteins by binding to monomeric Cdk4/6 (Guiley et al. 2019). Proliferation of $CD4^+$ Treg cells is inhibited by Cdk4/6 inhibition whereas proliferation of $CD8^+$ cells is unaffected (Goel et al. 2017). Indeed, $CD8^+$ T cell function can be augmented by Cdk4/6 inhibition. Treatment of $CD8^+$ T cells with Cdk4/6 inhibitors enhances NFAT activity, increasing expression of the IL-2 receptor α (CD25) and production of IL-2 and granzyme B, indicating that Cdk6 may have a role in limiting T cell effector differentiation (Deng et al. 2018).

In summary, T cell activation produces a signalling cascade that triggers a change in gene expression that promotes cell growth, increased anabolic metabolism, and stimulation of nascent Cdk/E2F activities. The significant rewiring of the proteome and metabolism is important for supporting the next phase of $CD8^+$ T cell differentiation, in which activated cells rapidly proliferate to clonally expand antigen-specific CTLs.

1.3.3 IL-2 driven proliferation

A key regulator of $CD8^+$ T cell proliferation in the expansion phase is IL-2. IL-2 is a cytokine and potent T cell mitogen (Smith and Ruscetti 1981) that is produced primarily by activated $CD4^+$ and to a lesser extent $CD8^+$ T cells (Nelson 2004). The IL-2 receptor is composed of three chains. The IL-2Rα (CD25), IL-2Rβ (CD122), and the common γ-chain (CD132). CD25 itself has no intracellular interactions and instead provides greater affinity between IL-2 and the other two components of the IL-2 receptor. CD122 and CD132 form a dimer and recruit Jak1 and Jak3 respectively, but have low affinity for IL-2 (Kd ≈ 450nM). CD25 alone also has a low affinity with IL-2 (Kd ≈ 10 nM), but when in a tetramer with CD122 and CD132, the affinity for IL-2 increases almost 1000 fold (Kd ≈ 300 pM), enabling prolonged signal transduction through CD122 and CD132. Signal strength of IL-2 can therefore be regulated via regulation of CD25 expression (Stauber et al. 2006).

Upon activation, $CD8^+$ T cells secrete IL-2 and begin production and expression of CD25. While TCR stimulation alone has been shown to be sufficient to induce proliferation of $CD8^+$ T cells, the absence of IL-2 signal results in suboptimal expansion and slower cell cycle progression (D'Souza and Lefrançois 2003), and indeed, blockade of IL-2 leads to reduced proliferation (Mishima et al. 2017). In addition, the presence of IL-2 in culture reduces the minimum threshold of TCR signalling required to enter cell cycle (Au-Yeung et al. 2017).

Continuous exposure to IL-2 is essential for prolonged expansion. IL-2 starvation leads to reduced cell viability, loss of CD25 expression, and decreased cellular protein content, including many major cell cycle regulators: cyclin D2, cyclin D3, cyclin A, cyclin B1, cyclin B2, Cdk4, Cdk6, Cdk1, p15 and p21. Notably, p27 is one of the few proteins to increase as a result of IL-2 starvation (Rollings et al. 2018).

p27 is implicated in controlling cell cycle exit in the contraction phase. *In vivo* experiments utilising p27 KO $CD8^+$ T cells continued to expand up to day 11 post immunisation, while WT began contraction by day 8. The effect of p27 is more pronounced for MPECs than SLECs as MPEC cells maintained their higher populations as late as 30 days post immunisation, while SLEC p27 knockouts generally returned to similar cell numbers as WT cells by day 15. This difference in response is likely due to MPECS expressing higher pro-survival factors and having a greater capacity for IL-2 production than SLECs (Singh et al. 2010).

Whereas studies consistently show that $p27^{-/-}$ mice exhibit splenic and thymic hyperplasia (Fero et al. 1996; Kiyokawa et al. 1996; Nakayama et al. 1996), the data for $p21^{-/-}$ mice are conflicting (Balomenos et al. 2000). Activated $p21^{-/-}$, $p27^{-/-}$ double knockout (DKO) splenocytes are hyperproliferative *in vitro*. Freshly isolated splenocytes from $p21^{-/-}$ but not $p27^{-/-}$ mice, had a higher frequency of CD25 expressing naïve $CD4^+$ and $CD8^+$ T cells. The percentage of $CD25^+$ cells in activated DKO or $p27^{-/-}$ splenocyte cultures were elevated by ~10% relative to wild type, or to $p21^{-/-}$ (Wolfraim et al. 2004), which may enhance T cell sensitivity to IL-2, and therefore mitogen-induced proliferation.

Downstream of IL-2 receptor activation is the STAT5 pathway (Moriggl, Sexl, et al. 1999), which is known to positively regulate proliferation (Figure 7). STAT5 activation induces homeostatic proliferation in naïve $CD8^+$ T cells, even in the absence of cytokine stimulation (Burchill et al. 2003), and in activated T cells, STAT5 enhances E2F activity by activating $p70^{S6K}$ just as mTOR does following TCR stimulation. (Lockyer, Tran, and Nelson 2007). STAT5 KO T cells have reduced cell cycle regulators, including cyclin D2, cyclin D3, cyclin E, cyclin A, and Cdk6 (Moriggl, Topham, et al. 1999). All of these proteins play important roles in G1-S phase progression. STAT5 signalling upregulates levels of pro-survival proteins Bcl-2 and Bcl-X_L. Additionally, STAT5 upregulates c-Myc, further implicating it as an important mediator of $CD8^+$ T cell proliferation (Lord et al. 2000). Constitutively active STAT5 promotes homeostatic proliferation and survival of $CD8^+$ T cells. Interestingly, STAT5 also enhances presence of T memory cell phenotype, increasing the frequency of cells expressing CD127, CD122, CD62L and Bcl-2(Hand et al. 2010) .

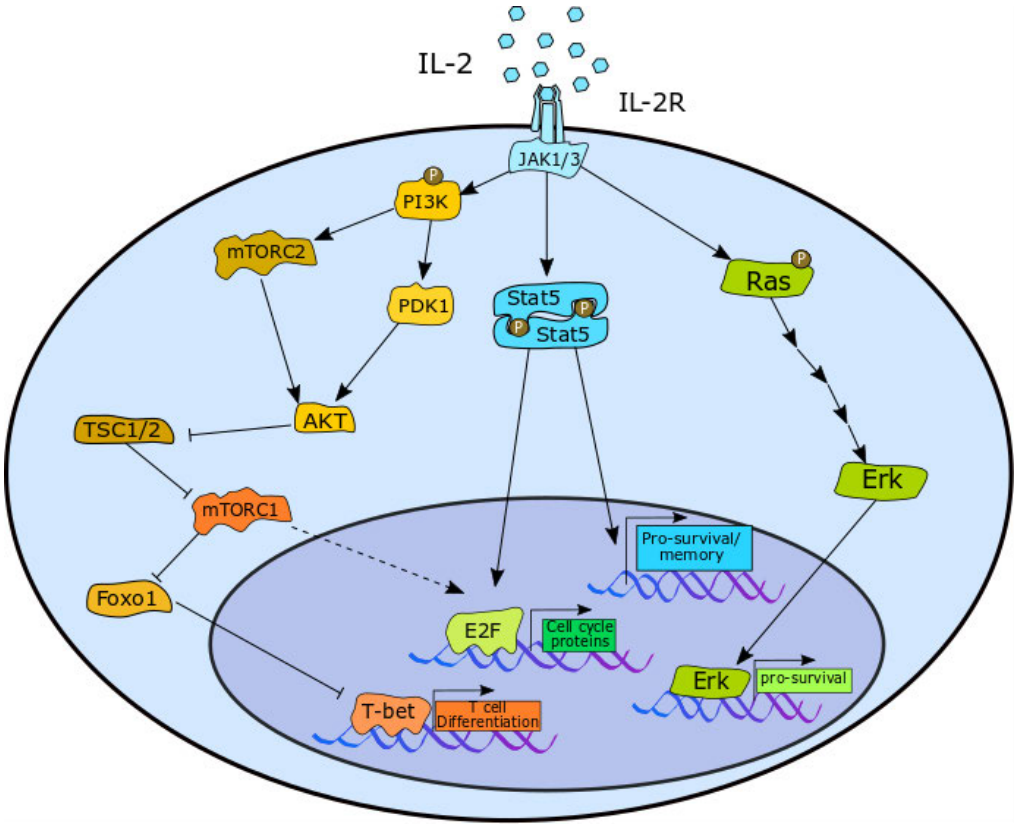

Figure 7 IL-2 stimulation of the complete IL-2 receptor triggers three major pathways. The PI3K pathways which mostly controls T-bet activity by inhibiting Foxo1 via mTORC1; the MapK pathways which allows Erk to mediate cell survival mechanisms; and Stat5 which activated E2F and enhances both survival and memory differentiation mechanisms, taking over from mTORC1 as the main promoter of cell cycle. Previously published in (Lewis and Ly 2021)

mTOR is also upregulated by IL-2 via the PI3K/AKT pathway. However, other pathways contribute more strongly to T cell proliferation in the expansion phase, as inhibiting mTOR in this phase does not arrest proliferation (Howden et al. 2019). Similarly, naïve $CD8^+$ treated with AKT inhibitors responded less to stimulation, with proliferation severely reduced by day 2 of the culture in a dose dependent manner (Cho et al. 2013). If treated three days post activation, however, AKT inhibition was shown to have little impact on proliferation (Macintyre et al. 2011).

Conversely, T cells expressing constitutively activated AKT were defective in memory T cell development in vivo. These cells have reduced CD127, CD122, CD62L and Bcl-2 (Hand et al. 2010). CD127 reduction is predominately controlled by PI3K/AKT activity in a STAT5 independent way, as STAT5 knockout cells had little impact on CD127 (Xue et al. 2002). Constitutively active AKT containing cells also showed poor STAT5 phosphorylation in response to any cytokine stimulation, and as a result had a defect in homeostatic proliferation.

Taken together, these data suggest that a principal role of the IL2R/PI3K/AKT/mTOR pathway is the differentiation of T cells towards the SLEC phenotype, which occurs in parallel to IL2R/STAT5. The latter is the dominant pathway that promotes upregulation of cell cycle regulatory proteins and therefore proliferation of $CD8^+$ T cells.

Cdk2/Cyclin E/A complexes phosphorylate numerous substrates, including targets outside of canonical cell cycle pathways that directly regulate DNA replication and mitosis. For example, cyclin E/A-Cdk2 phosphorylates and inhibits Foxo1 within a number of cancer cell lines (Huang et al. 2006). In T cells, mTOR drives differentiation towards SLEC phenotype by phosphorylation of Foxo1, an inhibitor of SLEC phenotype transcription factor T-bet. (Michelini et al. 2013; Pollizzi et al. 2015; Rao et al. 2010). Thus, Cdk2-mediated inhibition of Foxo1 raises the intriguing possibility that Cdk2 may also have a role in enhancing T-bet activity, and thus provide a mechanism by which high Cdk2 expression can enhance differentiation. However, this has yet to be demonstrated in T cells.

1.3.4 IL-15 stimulation

IL-15 is another cytokine which interacts with CD122 and CD132 with comparatively weak affinity (Kd = 25nM) (Meghnem et al. 2017), however the IL-15 specific subunit IL15Rα (CD215) has a very strong affinity to IL-15. Although IL-15 interacts with the same signal-transducing receptors that IL-2 does, and in one instance was shown to have a similar effect to IL-2 in lowering the antigen stimulation threshold required to induce proliferation (Au-Yeung et al. 2017), the effects of IL-15 are noted as being more active in promoting survival signal Bcl-2 than inducing proliferation, and as a result, in CD215 knockout mice, $CD8^+$ T cells produce less Bcl-2 and show increased sensitivity to death (Wu et al. 2002). IL-15 is often introduced to antigen experienced cells *ex vivo* in order to induce memory phenotype cells. The difference in outcome between IL-2 and IL-15 stimulation might be explained in the methods of delivery. While CD215 is expressed on $CD8^+$ T cells, it is reported that IL-15 signal is mostly delivered via trans signalling from antigen presenting cells which present CD215 and IL-15 together, letting them bind in the cytosol or binding externally and then being recycled to express at the immune synapse before presenting them as a presented ligand to interact with CD122/CD132 on the T cell as part of the immune synapse (Dubois et al. 2002; Nolz and Richer 2020). This proximity to antigen presenting cells may allow for a number of other

signalling events which could give way to some of the differences observed between IL-15 and IL-2 response.

Conversely, studies which artificially increased CD215 expression by transfection with IL-15RA mRNA have shown an increase of IL-15 induced signal transduction, resulting in enhanced proliferation and increased production of IFN-γ (Rowley et al. 2009). Another study compared WT $CD8^+$ T cells with $CD8^+$ T cells possessing mutant CD122 which had impaired association with STAT5. They observed that the impaired cells proliferated less than WT, retained CD62L and did not express KLRG1, in line with the T_{cm} phenotype, while T_{em} phenotype required a stronger CD122 signal, and in fact required IL-2 rather than IL-15 to be induced. These accounts therefore indicate weak CD122 signalling is enough to push for MPEC like behaviour, and furthermore that strength of CD122 signal determines whether the memory phenotype is closer to naïve or effector (Castro et al. 2011).

Another observation from this study was that both IL-15 and IL-2 signal resulted in similar expression of pSTAT5, but noted that IL-15 levels of pSTAT5 were more transient, decreasing over the course of an hour, while IL-2 mediated pSTAT5 expresion was more sustained, remaining relatively high even up to 3 hours(Castro et al. 2011). A similar observation of high pSTAT5 in response to IL-15 compared to IL-2 was made independently by another study(Grange et al. 2015) who then went on to examine $CD8^+$ T cells transduced to express active STAT5. They demonstrated that these cells had increased sensitivity to CD122 signalling, regardless of whether mitigated by IL-2 or IL-15, and that post immunisation, these cells demonstrated T_{em} like traits determined by KLRG1 expression and IFNγ production post re-stimulation (Grange et al. 2015). These observations when taken together suggest that intensity of IL-2R signal is the main driver of T cell differentiation. That high but transient STAT5 phosphorylation occur in response to weak CD122/CD132 signalling and favour memory phenotype with high survival and proliferative potential due to STAT5 mediated Bcl-2, Cyclin, and Cdk production, yet slow cell cycle progression, possibly due to a reduction of AKT mediated E2F activation.

As part of terminal differentiation to T_{eff}, $CD8^+$ T cells maintain high expression of T-bet, which results in downregulation of CD127, upregulation of CD122 and CD215. and a reduction in the expression of CD132 signal inhibit SOCS-1 (Yeo and Fearon 2011). This would have the effect of making the T_{eff} more reliant on CD122 mediated Bcl-2 upregulation for survival, while

upregulation of CD215 may enhance IL-15 mediated signal, and afford T_{eff} less reliance on the immune synapse to receive the signal.

Conversely, quiescent memory T cells pre-incubated with IL-15 have been shown to more rapidly proliferate following antigen re-stimulation than with antigen re-stimulation alone. This mechanism is mediated by both Stat5 and mTORC1 mediated $p70^{s6K}$ phosphorylation (Richer et al. 2015).

1.4 Proteomics

Due to the complexity of cell cycle regulation mechanisms, and the relatively unexplored territory that is cell cycle control in T cells, it would be beneficial to employ a method that provides an unbiased means of data acquisition. Bottom-up Proteomics is the method in which proteins are extracted from cells or tissue samples, broken down into peptides, and processed for acquisition via mass spectrometry. These peptides are then compared against a database of proteins in order to work out which proteins these peptides originally made up, with their numbers translating to a relative abundance of protein within the cell.

The standard protocol for acquisition can be typically broken down into six steps, following the culture of cells/tissue, as detailed below (Figure 8)

1. Extraction of proteins
2. Reduction and Alkylation
3. Digestion into peptides
4. Clean up
5. LC-MS/MS
6. Data Analysis

At the very beginning of the process, the samples are cultured, these could be from a variety of sources including, cell lines, tissues, *in vivo* and *ex vivo* experiments. Once a sufficient quantity of sample has been acquired, the proteins are extracted, typically by lysing the cell with the use of ionic detergents such as SDS.

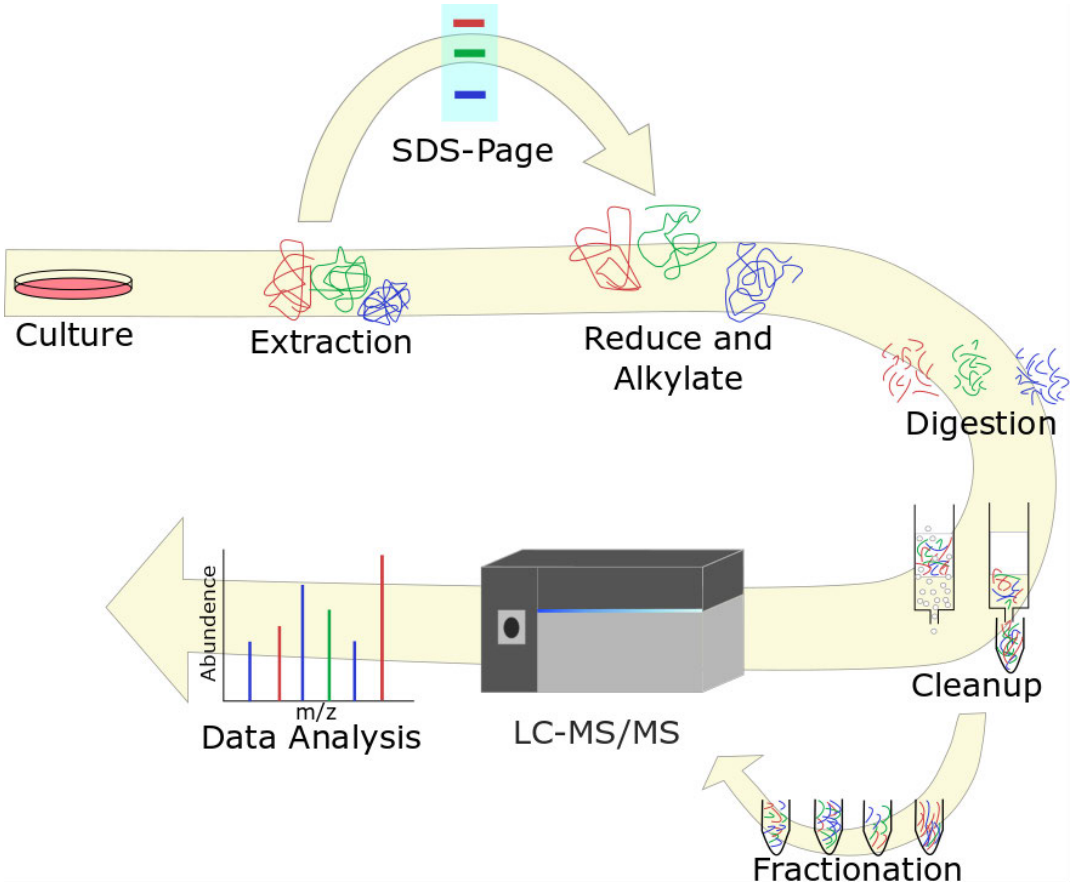

Figure 8 Cells or tissue are taken from culture and the proteins extracted by lysis. At this stage there is an option to run them through a gel in order to carry out size exclusion and remove impurities. Proteins are reduced to break up the disulphide bonds, and alkylated in order to prevent the re-formation of disulphide bonds on cysteine residues. Proteins are then digested into peptides with the preferred choice of enzyme. The peptides are then passed through c18 silica column to desalt the peptides. Peptides are then undergo liquid chromatography and are sprayed into a mass spectrometer for acquisition. For large samples, it may be desirable to fractionate the peptides by an additional step of liquid chromatography prior to running them through LC-MS. The peptide m/z readings are taken and can be used for data analysis.

Once extracted, there is the optional step run the samples through an acrylamide gel. The benefit of this step is to remove impurities which would otherwise obfuscate the MS reading, but can also be used for size-resolution, to remove proteins that are beyond a certain size range if they are not relevant to the analysis at hand. However, this step is not necessary if it is intended that entire proteome and if samples are kept free from most sources of contamination from the start. The proteins will then be reduced and alkylated. The reduction breaks the disulphide bonds, which will free up more cleavage sites for the enzymes during digestion, while Alkylation prevents the now free sulfhydryl groups on the Cysteine residues from reforming disulphide bonds. The proteins are then digested using proteolytic enzymes into peptides. The most common of these is Trypsin, which cleaves proteins at the C-terminal of Arginine and Lysine. However, other enzymes can be used, such as Lys-C, which cleaves only the C-terminal of Lysine.

In the case of fixed cells, it is possible to bypass the need of SDS and instead apply the digestion enzyme used for proteolysis directly to the cells. The enzymes will then simultaneously degrade the proteins into peptides and extract them from the cell into solution in a method which is referred to as the in-cell digest. The benefit of this system is that it reduces the chance for impurities to be introduced to the sample and enhances the amount of yield by cutting down on the steps required in sample processing (Kelly et al. 2022).

Following digestion, it is important to remove all impurities from the peptide sample, as any impurities will be detected by the mass spectrometer, and may mask the peptides themselves. This can be done via running the sample through an affinity column such as c18 silica, which binds to the peptides but not the salts, and then elutriate the peptide into a fresh tube. If the sample has not been separated prior to digestion, then it may be beneficial to separate the sample at this point using Liquid Chromatography in a step known as fractionation. This allows for more of the sample to be visualised by spreading it over multiple runs.

The sample, or fractions, will then be loaded into the mass spectrometer via high pH chromatography (known as LC-MS) where the sample/fractions is separated across a pH gradient and sprayed into the mass spectrometer for acquisition. Two scans will be performed by the Mass spectrometer, often referred as MS/MS, the first scan (MS1) will measure a chromatogram for every peptide, measuring the mass to charge ratio (m/z) against abundance of signal. Typically the top twenty most abundant peptides within a certain time frame are identified, and one at a time the machine will separate those peptides and perform the second scan (MS2) These approaches are known as Data Dependent Acquisition (DDA) in which the MS1 data informs the machine what to collect for MS2 acquisition (Karpievitch et al. 2010).

Data Independent Acquisition (DIA) instead focuses on peptides within a specific m/z window and carry out a MS2 scan on every peptide within this range. The scans are conducted in intervals of specific ranges, known as windows. For example, if set up to collect all peptides with a m/z between 500 and 900, the MS scans will be done in 20 windows of 20 m/z segments, starting with 500 – 520, and then 520 – 540, and so on until the entire range from 500 to 900 is covered. After this point the scan will cycle back to the first window, repeating the scan for the entire peptide spray. MS1 scans are conducted periodically in order to help

contextualise the data, but are not required to pull out peptides as they are in DDA (Krasny and Huang 2021).

While similar global analysis can be done much more easily via a transcriptomic approach, it has been well documented that transcriptomic and proteomic data do not correlate well. This is because, while transcriptomics can inform us which genes are being expressed, it cannot account for changes in translation or degradation rates (Ly et al. 2014). This is especially pertinent when examining cell cycle regulation as a large number of mechanisms are determined by different rates of degradation. It is therefore necessary to utilise proteomic data to get a more accurate impression of the fluctuations on protein content as cells progress through the cell cycle.

Another advantage of using proteomics, compared with more targeted techniques, is that it allows us to gain an unbiased view of cellular protein content, as well are providing information on global protein expression within the cell. This in turn will enable us to obtain a comprehensive look at how all mechanisms within T cells change over the course of the cell cycle, providing new insight into the factors which mediate cell cycle control of $CD8^+$ T cells post activation.

Utilising the PRIMMUS (Proteomic analysis of Intracellular iMMUnolabelled cell Subsets) technique, it is possible to carry out proteomic comparisons of different cell populations sorted by FACS. Chromatin staining will separate between G1, S and G2/M phase, as DNA content is expected to double between G2 and G1. While phosphorylated histone 3 can be used to separate M phase from the G2 population, as such a phenotype is only seen in mitotic cells (Ly et al. 2017)

1.5 Aims and objectives

The aims for this project are:

- Examine the proteome of $CD8^+$ T cells at key cell cycle stages and identify any novel cell cycle regulated mechanisms
- Analyse the proteomes of cycling $CD8^+$ T cells following stimulation with IL-2 or IL-15 and observe how cell cycle is differentially regulated between them.

- Identify the mechanisms of cell cycle which are prominent within $CD8^+$ T cells which differ when compared to somatic cell cycle processes; create and test hypothesis based on these findings.
- Determine a molecular mechanism which explains the relationship between proliferation and differentiation.

2 Methods

2.1 OT-1 Mouse

C57BL/6J *RAG1*-/- OT-1 mice were selected as our model organism due to the ease at which OT-1 T cell proliferation can be triggered *ex vivo*. Homozygous RAG1 knock out ensures that the mouse is unable to produce its own supply of mature T cell due to an inability to perform V(D)J recombination, required for TCR development (Mombaerts et al. 1992). These mice express a transgenic TCR specific for the ovalbumin peptide OVA257-264 (SIINFEKL), also known as N4 peptide. This ensures these mice only be able to produce $CD8^+$ T cells which are activated by the SIINFEKL antigen, which is not naturally expressed within the mouse (Kelly et al. 1993).

2.2 T cell culture

Inguinal, Brachial, Axillary, and Mesenteric lymph nodes were dissected from the mice and disrupted via passage through a 70 µm NylonG cell strainer (352350; Falcon). Naïve cells harvested from the lymph nodes were placed into culture in complete media consisting of Iscove's Modified Dulbecco's Medium (IMDM)(I3390-1L; Merck) supplemented with 10% heat inactivated Fetal Bovine Serum (FBS)(f9665; Sigma-Aldrich), 1% Penicillin/Streptomycin (P4333-100ML; Sigma-Aldrich), 1% L-glutamine (11500626; Fisher Scientific), and 50 µM β-Mercaptoethanol (M6250; Sigma-Aldrich).

Activation was induced by incubation with 6 nM N4 antigen peptide SIINFEKL (HY-P1771A-5mg; Cambridge bioscience) for up to 48 hours. To produce memory T cells along with effector T cells, naïve cells were incubated with N4 and 1:500 αCD28 (Cat:553294 Clone:37.51 ; BD Pharmigen) for 48 hours. Activated T cells were then washed in media and returned to culture with 20 ng/ml human IL-2 (200-02; Peprotech), or 10 ng/ml IL-15 (200-15; Peprotech) with daily supplements of equivalent volume cytokine added in 24 hour intervals for the duration of the culture. Confirmation of activation was made with a combination panel of CD25, CD68, and CD44 (see Appendix, figure 1). Confirmation of T cell phenotype was made with a panel of CD25, CD62L and CD44 (see Appendix, figure 2). Application of daily supplementation of IL-2 vs supplementation only at days 2 and 4 over the course of the culture were stained with pRb and pH3 S10 to determine the impact such regimes had on cell cycle distribution (see Appendix, figure 3)

2.3 Flow Cytometry

Cells were removed from culture and stained with Live/Dead fixable near-IR Dead cells stain kit (L34975;Thermofisher) as per manufacturer's instructions.

Surface staining was done in FACS buffer (0.1% BSA (Fisher bioreagents; BP9702-100), 0.01% Sodium Azide (S8032; Sigma-Aldrich), PBS (D1408-500ml; Sigma-Aldrich) with antibodies at the appropriate concentration for 20 minutes at 4^{o}c.

Cells were centrifuged at 400g for 2 minutes, washed in PBS and resuspended and fixed in 2% Formaldehyde (28908; Thermofisher) for 30 minutes at room temperature in constant rotation.

Cells requiring intracellular staining were centrifuged, supernatants removed, and pellets were resuspended by vortexing and permeablised by addition of 500µl ice cold 90% MeOH (M/4000/PC17; Fisher bioreagents) dropwise with gentle vortexing to the cells, and stored at -20^{o}C.

Prior to the intracellular stain, the cells were washed twice with FACS buffer and then incubated with antibodies at the appropriate concentration for 1 hour at 4^{o}C. The cells were then washed and acquired in FACS buffer or FACS buffer with 1 µg/ml Hoechst 33342

Data were acquired using either a MACSQuant Analyzer (Miltenyi), or a Fortessa (BD Biosciences). FACS sorting was performed using a FACSAria IIu (BD Biosciences).

2.4 EdU Click reaction

Cells were stained for EdU with use of the Click-IT EdU imaging kit (C10337;Invitrogen) as per manufacturer's instructions with some modifications. Cells in cultured were pulsed with 1 µM EdU for 30 minutes prior to removal from culture and processed for Flow Cytometry as above. Prior to intracellular staining, the cells were incubated with the click reaction mix, swapping out the azide-488 that came with the kit for azide-AF594 (CLK-1295-1; Jena Bioscience).

2.5 Proliferation assay

Naïve cells were washed with PBS and incubated at 37^{o}C for 20 minutes with 5 µM Cell Trace Violet (C34571A; Invitrogen) at a volume of 1ml per 1e7 cells. Following incubation, the cells were quenched with 2x volume of media and incubated at 37^{o}C for 5 minutes.

2.6 Western Blot

Cell pellets were lysed using 2% SDS + protease inhibitor cocktail (P8340ML; Sigma-Aldrich) and incubating at 65°C for 5 minutes, then 1 µl Benzonase (70664-3; Sigma-Aldrich) was added and incubated for a further 15 minutes. The lysates were then sonicated with a Ultrasonic Processor (UP200ST;Hielscher) at full power for two cycles of 20s on 30s off. Protein content for lysates were then assessed using Micro BCA Protein Assay Kit (23235; Thermofisher) as per manufacturer's instruction.

Lysates were incubated with NuPage LDS Sample Buffer (NP0007; Invitrogen) and incubated at 95°C for 5 minutes and loaded into NuPage 4%-12% Bis-Tris gradient MOPS gel (NP0323BOX; Invitrogen) in MOPS SDS Running Buffer (NP0001; Invitrogen) and run at 70 volts for 15 minutes and then 140 volts for 75 minutes. The gel was blotted on to an Immobilon-FL PVDF membrane (IPFL00010; Millipore Sigma) submerged in transfer buffer (24mM Tris Base (BP152-1; Fisher Bioreagents), 192mM Glycine (G8898-1KG; Sigma-Aldrich), 20% Ethanol (20821.330; VWR)) at 120 volts for 105 minutes, and then left to block in Intercept Blocking buffer (927-70001; Li-cor) for 1 hour or overnight.

The membrane was stained in primary antibody diluted in blocking buffer + 0.1% tween 20 (H5151; Promega) for 4 hours or overnight, and the secondary antibody diluted in blocking buffer 0.1% tween 20 and 0.01% SDS. The membrane was washed following both stains in PBS + 0.1% tween.

The membrane was imaged using a Li-Cor Odyssey CLx (Li-Cor) and analysed using ImageJ.

2.7 Antibodies

Specificity	Conjugate	Clone	Company	Cat. number	Dilution
m CD8a	PerCP	53-6.7	BioLegend	100732	1:100
m CD8a	AF647	53-6.7	Biolegend	100724	1:400
m CD8b	PE-Cy7	H35-17.2	Invitrogen	25-0083-82	1:400
m CD25	PE	PC61	BioLegend	102008	1:400
m CD25	PE-Cy7	PC61	BioLegend	102016	1:100
m CD25	APC	PC61	BioLegend	102012	1:400
m CD44	ef450	IM7	eBiosciences	48-0441-82	1:200
m CD44	APC-eF780	IM7	Invitrogen	47-0441-82	1:200
m CD69	AF488	H1.2F3	BioLegend	104516	1:300
m CD69	APC	H1.2F3	BioLegend	104514	1:200
m CD62L	APC	MEL-14	BioLegend	104412	1:100
p-H3(Ser10)	PE	D7N8E	Cell Signaling	29237S	1:350
p-Rb(Ser807/811)	AF488	D20B12	Cell Signalling	4277S	1:300
Emi1	AF546	B-3	Santa Cruz	Sc365212 AF546	1:400
Eg5	AF647	EPR23276-52	Abcam	ab283273	1:1,600
γH2AX	PE	20E3	Cell Signalling	5763S	1:50
Emi1	(Rabbit Ab)	EPR15320	Abcam	AB184950	1:5,000
Zap70	(Mouse Ab)	29/Zap70 Kinase	BD Biosciences	610239	1:5,000
Mouse IgG	IRDye 800CW	Polyclonal Goat	Li-Cor	926-32210	1:10,000
Rabbit IgG	AF680	Polyclonal Donkey	Life Technologies	A10043	1:10,000

2.8 Sample preparation for MS

Sorted cells for mass spec analysis were washed and resuspended in triethylammonium bicarbonate (TEAB) digestion buffer (100 nM TEAB, 50 µM $CaCL_2$, 50 µM $MgCL_2$), incubated

with 1 µl Benzonase at 37°C for 15-30 minutes, and then digested using the in-cell digestion protocol (Kelly et al. 2022) in Pierce Trypsin Protease (90057; Thermo Fisher) overnight at a ratio of 1 µg trypsin per 20 µg of protein. The lysates are then reduced with either 20 mM dithiothreitol (DTT) or 5 mM Bond-Breaker TCEP solution (77720; Thermo Fisher).

TMT tagging was done using TMT10plex™ Isobaric Label Reagent Set (90110;Thermo Fisher) as per manufacturer's instructions

Peptides were acidified in either 1% trifluoroacetic acid (TFA), or if destined for fractionation later, 1% formic acid. Fragments of C18 silica membrane were placed in 200 µl tips, wetted with 100% acetonitrile (MeCN) (A955-1; Fisher Chemicals) and primed with 1% TFA/formic acid (10596814; Thermo Fisher). For samples in excess of 100 µg, higher capacity Sep-Pak Vac tC18 cartridges (WAT036790; Waters) were used instead.

The sample was loaded onto pre-conditioned columns, washed with 0.1% TFA/formic acid, and then eluted into fresh tubes with 70% MeCN diluted in either 0.1% TFA, or 0.1% formic acid. Samples with TMT labels were additionally washed with 0.5% acetic acid and were eluted with 70% MeCN in 0.5% Acetic acid before being dried.

2.9 Mass Spectrometry

2.9.1 Data Dependent Analysis

LC-MS analyses were performed on an Orbitrap Fusion™ Lumos™ Tribrid™ Mass Spectrometer (Thermo Fisher Scientific, UK) coupled on-line, to an Ultimate 3000 HPLC (Dionex, Thermo Fisher Scientific, UK). Peptides were separated on a 75x50 cm (2 µm particle size) EASY-Spray column (Thermo Scientific, UK), which was assembled on an EASY-Spray source (Thermo Scientific, UK) and operated constantly at 50°C. Mobile phase A consisted of 0.1% formic acid in LC-MS grade water and mobile phase B consisted of 80% acetonitrile and 0.1% formic acid. Peptides were loaded onto the column at a flow rate of 0.3 µL min-1 and eluted at a flow rate of 0.25 µL min-1 according to the following gradient: 2 to 40% mobile phase B in 120 min and then to 95% in 11 min. Mobile phase B was retained at 95% for 5 min and returned back to 2% a minute after until the end of the run (160 min in total for each fraction).

The spray voltage was set at 2.2kV and the ion capillary temperature at 280°C. Survey scans were recorded at 120,000 resolution (scan range 380-1500 m/z) with an ion target of 4.0E5,

and injection time of 50ms. MS2 was performed in the Ion Trap (at a rapid mode), with ion target of 2.0E4 and HCD fragmentation (Olsen et al, 2007) with normalized collision energy of 28. The isolation window in the quadrupole was 0.7 Thomson. Only ions with charge between 2 and 6 were selected for MS2. Dynamic exclusion was set at 60 s and the injection time at 50ms. MS3 performed in the orbitrap at 50,000 resolution with isolation window of 0.7 Thomson. Ions were further fragmented by HCD with normalised collision energy of 55. The scan range was set between 100 and 500 m/z the AGC target at 5.0e4. The maximum injection time was set to 90ms and 5 precursor ions were chosen to perform SPS on. Data Dependent Acquisition was carried out on TMT labeled peptides. The peptides were analyzed using an Ultimate 3000 RSLCnano HPLC (ULTIM3000RSLCNANO;Dionex, ThermoFisher) coupled via electrospray ionisation to an Orbitrap Fusion Lumos Tribrid Mass Spectrometer (ThermoFisher) .

2.9.2 Data Independent Analysis

Peptides (equivalent of 1 µg) were injected onto a C18 reverse-phase chromatography system (UltiMate 3000 RSLC nano, Thermo Scientific) and electrosprayed into an Orbitrap Exploris 480 Mass Spectrometer (Thermo Fisher). For liquid chromatography the following buffers were used: buffer A (0.1% formic acid in Milli-Q water (v/v)) and buffer B (80% acetonitrile and 0.1% formic acid in Milli-Q water (v/v). Samples were loaded at 10 µL/min onto a trap column (100 µm × 2 cm, PepMap nanoViper C18 column, 5 µm, 100 Å, Thermo Scientific) equilibrated in 0.1% trifluoroacetic acid (TFA). The trap column was washed for 3 min at the same flow rate with 0.1% TFA then switched in-line with a Thermo Scientific, resolving C18 column (75 µm × 50 cm, PepMap RSLC C18 column, 2 µm, 100 Å). Peptides were eluted from the column at a constant flow rate of 300 nl/min with a linear gradient from 3% buffer B to 6% buffer B in 5 min, then from 6% buffer B to 35% buffer B in 115 min, and finally from 35% buffer B to 80% buffer B within 7 min. The column was then washed with 80% buffer B for 4 min. Two blanks were run between each sample to reduce carry-over. The column was kept at a constant temperature of 50^{o}C.

The data was acquired using an easy spray source operated in positive mode with spray voltage at 2.40 kV, and the ion transfer tube temperature at 250^{o}C. The MS was operated in DIA mode. A scan cycle comprised a full MS scan (m/z range from 350-1650), with RF lens at 40%, AGC target set to custom, normalised AGC target at 300%, maximum injection time

mode set to custom, maximum injection time at 20 ms, microscan set to 1 and source fragmentation disabled. MS survey scan was followed by MS/MS DIA scan events using the following parameters: multiplex ions set to false, collision energy mode set to stepped, collision energy type set to normalized, HCD collision energies set to 25.5, 27 and 30%, orbitrap resolution 30000, first mass 200, RF lens 40%, AGC target set to custom, normalized AGC target 3000%, microscan set to 1 and maximum injection time 55 ms. Data for both MS scan and MS/MS DIA scan events were acquired in profile mode.

2.10 Proteomic analysis

RAW data files from DDA experiments were processed using MaxQuant software (Ver 1.6.2.6) (Tyanova, Temu, and Cox 2016). The raw files were submitted along with a M.musculus FASTA file obtained from Uniprot.org on 2019-09-10 (55,197 entries). Group specific parameters were set to Reporter ion MS3, selecting that 10plex preset. Variable modifications included Oxidation (M) and Acetyl (Protein N-tem), and fixed modifications were set to include Carbamidomethyl (C). The Digestion model was set as Trypsin/P. Within the global parameters, for Protein Quantification, a minimum ratio count of 2 was selected, utilizing Unique and razor for quantification of peptides. Both unmodified peptides and peptides with Oxidation (M) and actetyl (Protein N-term) modifications were selected for quantification, with unmodified counterpart peptides discarded.

RAW data files from DIA experiments were processed using Spectronaut (version 16.2.220903.53000, Biognosys, AG). The directDIA workflow, using the default settings (BGS Factory Settings) with the following modifications was used: decoy generation set to mutated; Protein LFQ Method was set to QUANT 2.0 (SN Standard) and Precursor Filtering set to Identified (Qvalue); Precursor Qvalue Cutoff and Protein Qvalue Cutoff (Experimental) set to 0.01; Precursor PEP Cutoff set to 0.1 and Protein Qvalue Cutoff (Run) set to 0.05. For the Pulsar search the settings were: maximum of 2 missed trypsin cleavages; PSM, Protein and Peptide FDR levels set to 0.01; scanning range set to 300-1800 m/z and Relative Intensity (Minimum) set to 5%; cysteine carbamidomethylation set as fixed modification and acetyl (N-term), deamidation (asparagine, glutamine), dioxidation (methionine, tryptophan), glutamine to pyro-Glu and oxidation of methionine set as variable modifications. The database used was M.musculus downloaded from uniprot.org on 2022-10-25 (55,311 entries).

The output from MaxQuant or Spectronaut was then processed in R (4.0.3). TMT data sets were filtered to contain only samples with tmt values which appeared in the S phase samples shared between both runs. All values were normalised to a proportion of S phase proteins in order to combine the two datasets. These datasets were further normalised to ratios of the G0 data. T-sne was used to verify the impact of grouping on these measures. Both TMT and DIA datasets where otherwise normalised by calculating parts per million (PPM) by dividing the value by the sum of the total and multiplying the result by 1e6. Approximate protein copy number was determined by making use of the proteomic ruler. This was done by determined that the mass of DNA within mouse CD8 T cells was estimated to be 3.006e-12 for cells within 2n such as the pRb- cohort and 4.008e6-12 for the pRb+ cohort based on taking a weighted average on how many cells were likely to be 2n vs 4n within the cohort. Copy number for each protein identified in the DIA was then calculated as the product of DNA mass divided by the total histone intensity recorded, Avogadro's number divided by the Molar mass of the protein, and the protein's intensity. GO term analysis was done by exporting a list of proteins from the dataset and retrieving the Gene Ontology (GO) terms from Uniprot.org

The list of GO terms used to identify proteins with cell cycle terms is as follows: "cell cycle|cell division|cytokinesis|kinetochore|mitotic|chromosome segregation|replication"

Further analysis of GO terms was done utilizing the DAVID Bioinformatics resources https://david.ncifcrf.gov/

2.11 Crispr

Target sights for Crispr were identified by use of the online tool ChopChop (https://chopchop.cbu.uib.no/) under the default settings. Candidates were selected for their high GC content, low number of mis-match pairs, and high efficiency. These candidate target sequences were then mapped to the gene using SnapGene. Candidates which targeted exons 2-4 of the guide RNA sequences were selected and obtained from Integrated DNA Technologies

Emi1 Oligos	Sequence
G44	ACAGGTGCACGAATCCCCTG
G12	CCGGCACAATGAGTTCGTGG
Thy1 Oligo	ACAGACAAGCTGGTCAAGTG

Transfection of the guides was done with use of the Neon Tranfection 100 µl kit (MPK10096; Invitrogen). Guide RNA was incubated with TracrRNA (B00817; IDT) in Nuclease free duplex buffer (1072570; IDT) for 5 minutes at 98°C. Samples were then allowed to cool down before incubating with the TrueCast Cas9 protein V2 (A36499; Thermo Fiasher) and Resuspension Buffer T from the kit 20 minutes at 37°C. T cells were prepared for transfection by centrifugation at 300g for 5 minutes and resuspended in Resuspension Buffer T at a concentration of roughly 1.2e6 cells/100ul. 1.2e6 cells were mixed with the assembled Cas9 complex and transfection was carried out utilizing the Neon 100µl Tips within a solution of Electrolytic Buffer E2 provided by the kit. Electroporation was induced using the Neon Transfection System (Invitrogen) with a programme of 3 pulses of 10ms 1600V for Activated T cells and 4 pulses of 5ms 2500V for naive T cells.

2.12 PCR

Guides were designed to assess CrispR KO efficiency via TIDE Analysis. The criteria for their design were 1) the guide needed to be at least 250bp away from the cut site but no more than 450bp away, and 2) the product size would need to be at least 500bp long. These criteria were placed into a Primer-BLAST webtool (https://www.ncbi.nlm.nih.gov/tools/primer-blast/) with primers identified prioritised by having the fewest number of off-target areas.

PCR mixes were created using the Phusion High-Fidelity DNA Polymerase Reagents (M0530L; New England Biolabs) as per manufacturer's instructions. Samples were spun down and removed of liquid before being lysed with PCR Lysis buffer (0.1% SDS, 0.05% Tween, 400ug/ml Proteinase K (25530-015; Life Technologies). PCR was then conducted with the following settings on a T100 Thermo Cycler (Biorad). 98°C for 1 minutes, 98°C for 15 seconds, optimal temperature (between 62°C and 72°C) for 15 seconds, 72°C for 45 seconds, then repeat from step 2 34 times, then 72°C from 10 minutes, and finally hold at 12°C. A fraction of the PCR product was run through a 1.5% Agarose gel constituted from UltraPure Agarose (16500-500; Invitrogen) in TAE buffer (;Fisher Bioreagents) run at 120V for 20 minutes and imaged on a Li-cor D-Digit (Li-Cor). The remaining product was then purified using the Monarch PCR & DNA Cleanup Kit (T1030L;New England Biolabs) as per manufacturer's instructions. The purified product was then quantified with a Qubit 3.0 (Invitrogen) and sent to the MRC Protein

Phosphorylation and Ubiquitylation Unit in Dundee (https://dnaseq.co.uk/) for sequencing. The returned sequences were then analysed using the TIDE analysis webtool (https://tide.nki.nl/).

3 Proteomics on CD8 T cells reveal stem and somatic cell cycle regulatory characteristics

3.1 Introduction

A key regulatory mechanism of mitotic cell cycle progression in somatic cells (Figure 9 top) is the periodic expression of cyclin proteins. For example, Cyclin E peaks as cells approach the G1/S checkpoint, Cyclin A upon reaching G2, and Cyclin B at the G2/M checkpoint (Dyson 1998; Gookin et al. 2017). In contrast to somatic cells, mouse Embryonic Stem Cells (mESCs) have a much more rapid proliferative phenotype (Li and Kirschner 2014), and their cycle differs from that observed within somatic cells in a number of key ways to facilitate this phenotype (Figure 9 bottom). First it is understood that mESCs have a much shorter G1 phase, with mESCs more rapidly entering S phase (Coronado et al. 2013). Second, the periodic nature of the cyclins are altered, with Cyclin's A and E reported as constitutively active along with a number of other E2F targets, while Cyclin B retains periodic fluctuating behavior between the two models (Stead et al. 2002; White et al. 2005).

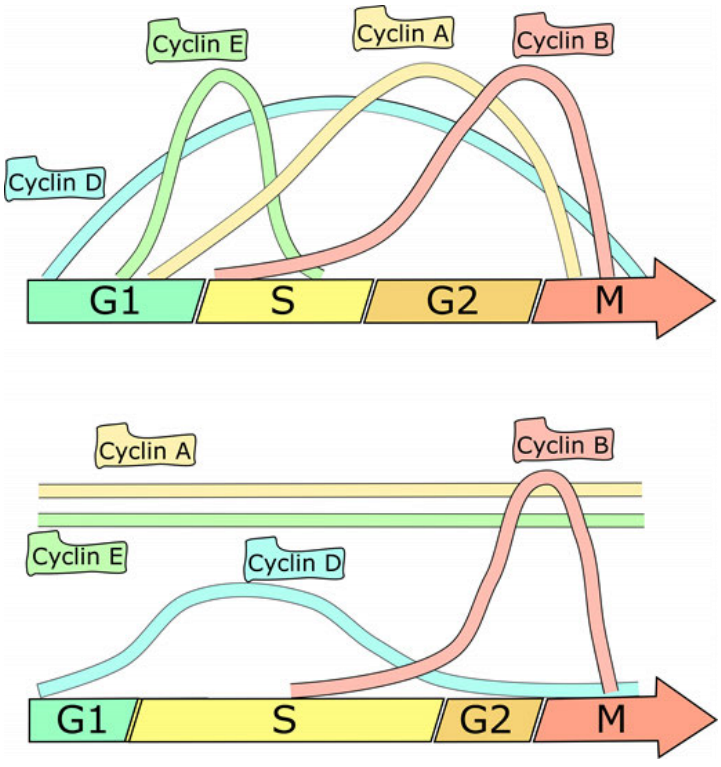

Figure 9 Models of cyclin activity over the course of the cell cycle in both somatic (top) and stem cell (bottom) models.

Sustained levels of Cyclins E and A are understood to result from decreased APC/C activity in mESCs as a result of high levels of the inhibitor Emi1 (Bar-On, anit Shapira, et al. 2010).

Naïve and memory $CD8^+$ T cells share many features with stem cells, such as self-renewal when unstimulated, and a level of multipotency in the differentiation towards the various memory and effector phenotypes (Gonzalez et al. 2021; Graef et al. 2014). Once stimulated with IL-2, $CD8^+$ T cells exhibit a very rapidly proliferative phenotype (Mondino et al. 2006) as is typically observed in cycling mESCs. It is therefore the aim of this study to identify the cell cycle regulated protein network in $CD8^+$ T cells in order to assess how closely their cell cycle regulated proteome follows either the stem cell model or the somatic model of cell cycle regulation.

To produce a population of CTL differentiated cyling CD8 T cells, OT-1 T cells were placed in to culture with N4 antigen for 48 hours, and then removed from antigen and placed in IL-2 for a further 72 hours, harvested at the 120 hour time point. IL-2 was provided at the 96 hour time point in order to maintain cell cycle re-entry over the course of the culture.

3.1.1 PRIMMUS

Traditionally, cell cycle analysis has been reliant on the use of synchronisation, where cells are exposed to a cell cycle inhibitory agent. Frequently used inhibitors include the Cdk4/6 inhibitor Palbociclib and the microtubule polymerization inhibitor Nocodazole. Arrested cells are then released and harvested at different times following inhibitor removal to obtain synchronous cell populations for downstream experimentation, including biochemistry. Such approaches come with the inherent drawback of directly interfering with physiological cell cycle mechanisms, introducing an inherent bias into the regulatory networks (Ly, Endo, and Lamond 2015). In addition to this, it has been observed that T cells in particular are resistant to arrest by such agents, which slow down their proliferation but do not stop it entirely (Heckler et al. 2021).

This makes attempts to synchronise them very challenging, and as of yet there is no published viable protocol to synchronise $CD8^+$ T cells. For these reasons, we decided to make use of the PRIMMUS technique, as defined by (Ly et al. 2017). This process involves a mixture of DNA and antibody based staining of key cell cycle markers so that the cell cycle phases can be separated by cell sorting from an asynchronous population. As illustrated in Figure 10, we

used p-Rb staining as a means to separate early and late G1 within the 2n peak of the DNA stain. The p-Rb negative group provides an indicator of E2F activity, with a high level of p-Rb indicating cell cycle entry (Weinberg 1995), while low levels of p-Rb are likely to indicate earlier G1 phase, and would also include cells which are in G0 (Figure 10). The 4n peak can be separated into G2 and M by the inclusion of the p-Histone 3 antibody, which has been used in PRIMMUS before to separate cells undergoing mitosis from cells in G2 previously. S phase is then crudely defined as any events that fall between these two gates.

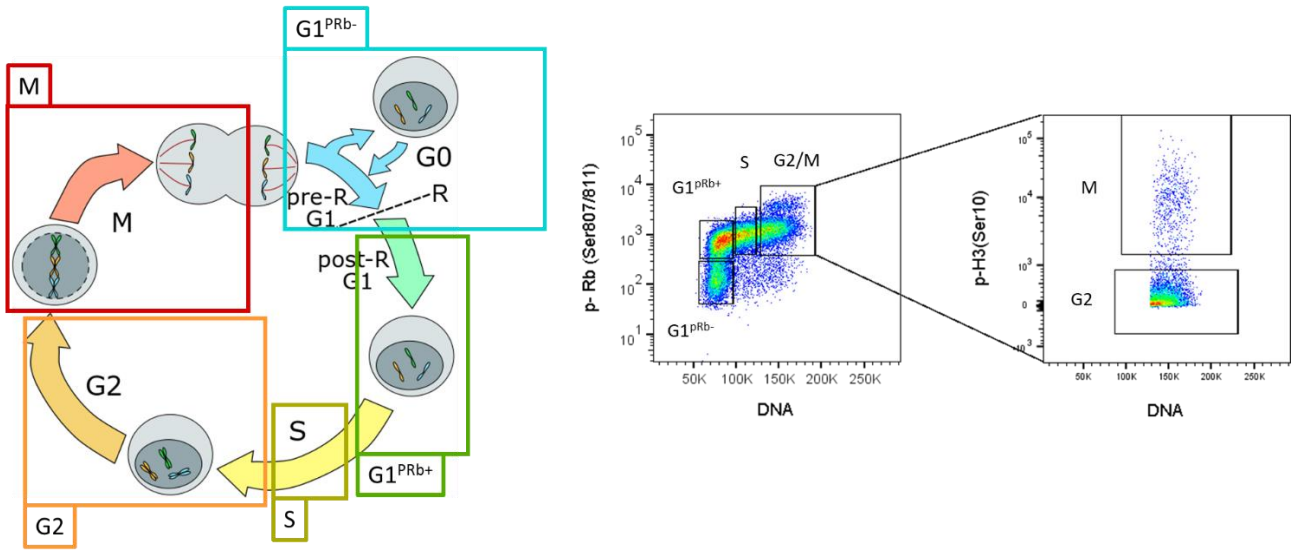

Figure 10 Schematic of how the cell cycle phases were separated via FACS. The DNA vs p-Rb separated early G1 from late G1 within what would be the 2n peak. The 4n peak designated as G2/M was further divided by p-H3 at Serine 10 into G2 and M phase populations. Events between the 2n and 4n peak were designated as S phase cells.

3.1.2 Tandem Mass Tagging (TMT) dyes

TMT dyes are isobaric labels which are made up of three components. A peptide reactive group which binds to free amines; a reporter group which will contain a different combination of ^{13}C and ^{15}N isotopes, and a spacer which ensures all TMTs have the same mass while they are intact. Peptides from each sample were incubated with each unique TMT and then pooled together prior to the desalting step. During acquisition, after undergoing the MS2 scan, the machine can break down the TMT tags on the peptide in the quantification scan (MS3 scan), causing cleavage of the TMT at the balance group, releasing the reporter group which is then measured by the mass spectrometer.

The unique combination of isotopes allows each tag to appear as a distinct peak making it possible to trace back how much each sample contributed to the total protein content detected in the pool. This allows for a quantifiable comparison of protein content across all

samples from a single MS run while having the added benefit of enhancing the signal of otherwise low abundance proteins.

The sorted cells from three separate specimens were treated for mass spectrometry and labeled with TMT dyes and pooled. At the time the highest multiplex available was the 10-plex kit, which meant in order to fit all 5 cell cycle phases in triplicate, it was necessary to use 2 separate runs with a common set of samples between the pools (Figure 11).

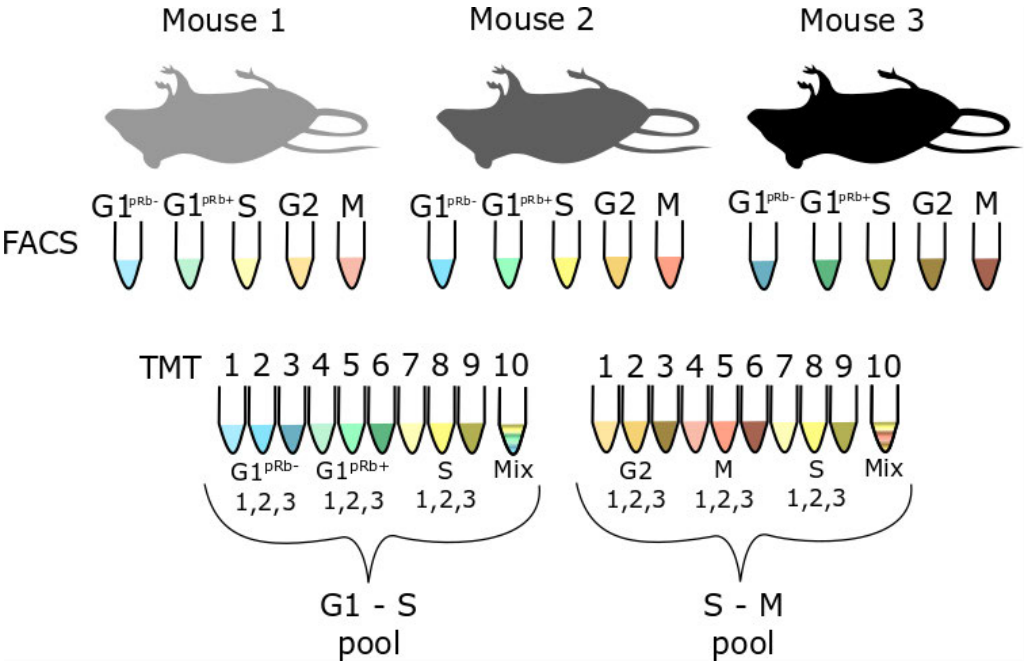

Figure 11 T cells cultures from three separate mice were separated by FACS and organised into two groups of TMT mixtures, with the S phase samples of each mouse shared between both pools so they may be normalised.

3.2 Processing of Proteomic Data

3.2.1 Normalisation of TMT pools

The readout was first mapped against the same fasta file used to generate the list with Maxquant, which initially contained 6267 unique protein identities. Removing any proteins that had zero intensities in all conditions left 6243 identities. The list was then filtered to only include proteins that appeared in the S phase samples of both the G1-S pool and the S-M pool, with proteins that only appeared in one but not the other excluded, leaving 5612 identities. The reporter intensity values within the filtered list was then normalised by dividing each protein by the average of the S phase values contributed from each of the three specimens, combining the two pools into one complete dataset. A t-SNE was conducted on the samples before and after normalisation. While the non-normalised

samples showed greater clustering by TMT pool than by cell cycle phase as seen with the S phase samples (Figure 12). As a consequence of S phase normalisation, the fluctuation patterns of all proteins were distorted, causing even expected periodic proteins like Cyclin B1 to have similar patterns of expression as non-periodic proteins like GAPDH around S phase (Figure 13 left). To restore their fluctuation patterns, we normalised each data point against its respective $G1^{pRb-}$ value (Figure 13 right). A t-SNE (Figure 12 bottom) showed that as a result, the grouping of the datasets was now much stronger by specimen of origin rather than cell cycle phase, however, there was still a general trend of each phase grouping together, with $G1^{pRb+}$ on the top left of each cluster, and G2 at the bottom right of each cluster. In addition, there was no longer any noticeable grouping based on run, indicating that any large biases that may have been present because the samples were carried out on two different runs were no longer predominate factors.

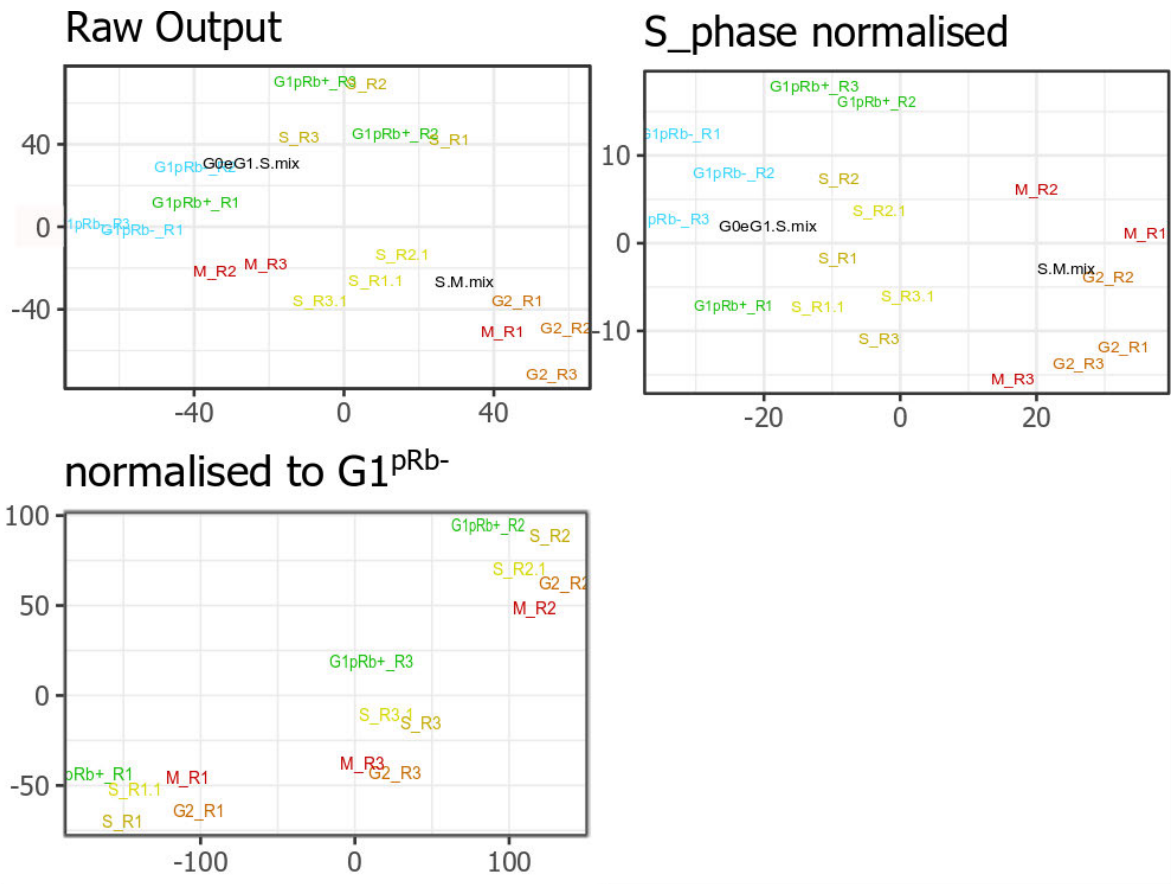

Figure 12 The datasets separated by each TMT signal were grouped using s t-SNE showing output of raw intensities (top-left) S-phase normalised intensities (top-right) (perplexity = 6), and normalised to $G1^{pRb-}$ (bottom-left) (perplexity = 4). R1 = Mouse 1, R2 = Mouse 2, R3 = Mouse 3, S_Rx = S phase from G1-S pool, S_Rx.1 = S phase from S-M TMT pool, G0eG1.S.mix = a mixed sampling of all samples from G1-S pool. S.M.mix = a mixed sampling of all samples from S-M pool, n=3.

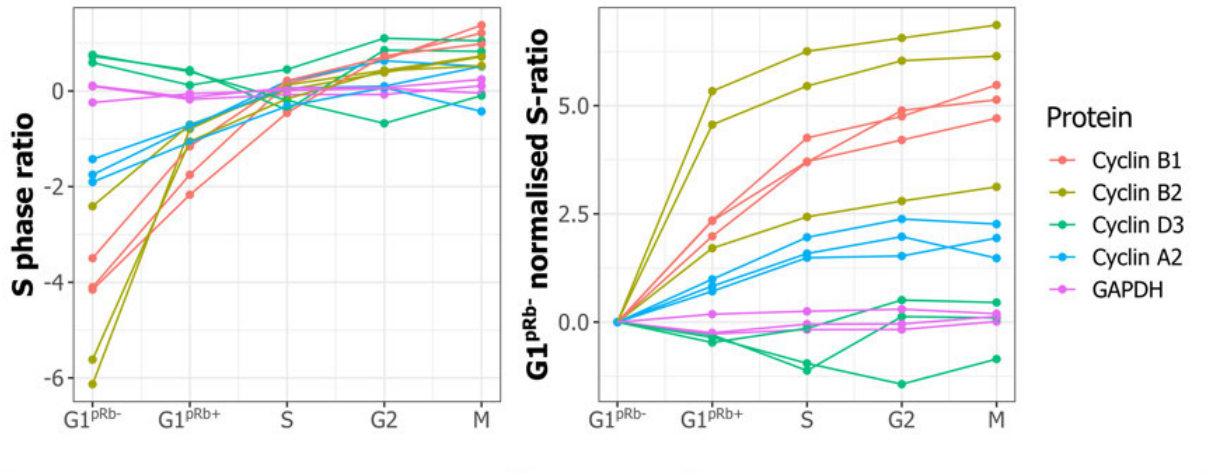

Figure 13 The general pattern of fluctuation across the phases of the cell cycle for a number of identified cyclins and GAPDH as a non-fluctuating protein to compare. Raw intensities from the two TMT groups were normalised on S-phase (left) where they share sample, each sample was then normalised against their respective $G1^{pRb-}$ value (right) to recover the fluctuation pattern.

3.2.2 Periodicity

A hallmark of cell cycle regulated proteins is that they show regular fluctuations of increase and decrease over the course of a cell cycle. This can be statistically determined by use of the Fisher's test for periodicity which evaluates the pattern of protein abundance over a time course extending to several cycles (Wichert, Fonkianos, and Strimmer 2004). Due to the difficulties of synchronising T cells mentioned above, it is not possible to have all T cells at the same phase of cycle at a given time point. However, by taking FACSorting T cells based on cell cycle phase, and putting the resulting intensities from each specimen together, it is possible to forge a pseudo-time course, with each mouse in place of a new cycle (Figure 14). The test looks for the general pattern between the set of triplicate in order to determine periodicity, with a non-periodic protein showing an inconsistent pattern of fluctuation and thus generating a high p value, and a periodic protein showing very consistent patterns and thus a lower p value.

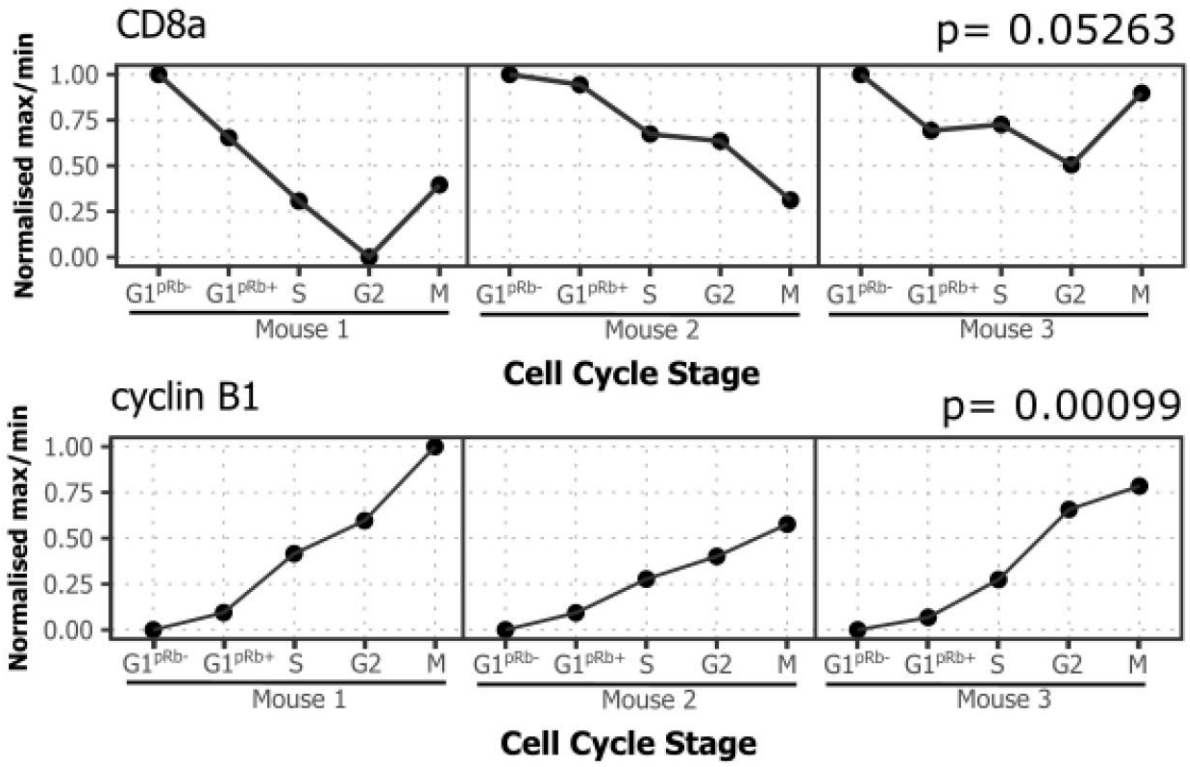

Figure 14 Periodicity is determined by putting the intensity of a protein at each phase in cell cycle order, and then arranging the intensity change in each mouse together, creating a pseudo-timecourse. CD8a (above) shows an example of a non-periodic protein, Cyclin B1 (below) shows an example of a periodic protein.

3.3 Analysis of Periodic Proteins

Our criteria for identified proteins within our data set that were likely to be cell cycle regulated were that they needed a consistent pattern of fluctuation across all three samples, and that the fluctuation needed to be substantial. The first of these criteria was determined by the protein demonstrating a p-value of less than 0.05 on the Fisher's test for periodicity. The second by setting a threshold of change between the highest and lowest of the normalised intensities to be at least of 2-fold change. Application of these criteria resulted in a set of 160 proteins which were deemed to be likely cell cycle regulated (Figure 15). In order to ascertain how many CTL unique cell cycle proteins were within contained within this dataset, the data was filtered to focus on proteins that did not have cell cycle associated GO terms. Within our list, we identified 88 proteins with cell cycle GO annotations leaving the remaining 72 proteins lacking cell cycle annotations. However, further analysis of GO terms was unable to determine any specific pathways or mechanisms from these novel cell cycle regulated proteins.

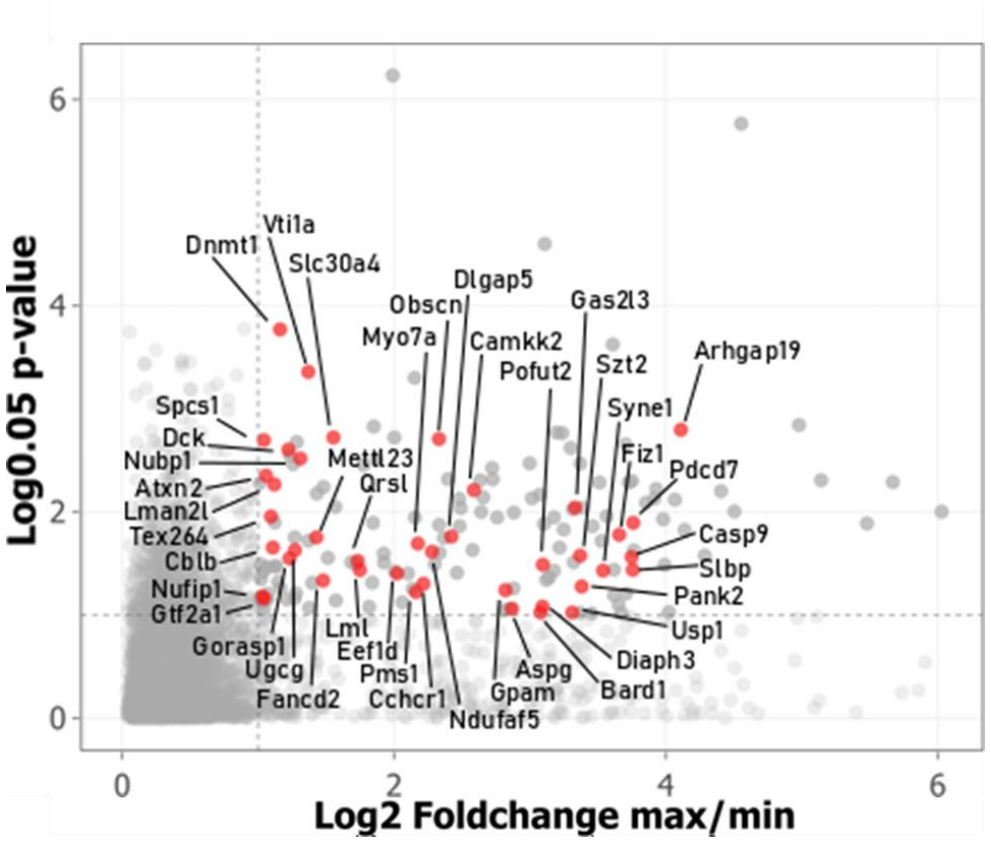

Figure 15 Proteomics identified 160 proteins as cell cycle regulated. These proteins met the criteria of being less than 0.05 on the Fisher's Periodicity Test and for the range of the normalised intensity fluctuation to be greater than a 2 fold different. red = proteins identified as being without cell cycle specific GO term, each one is labelled by name. n=3.

3.3.1 Meta-analysis with other periodic datasets

To better assess how well CD8⁺ T cells compare with other established cell cycle models, a meta analysis was conducted in which datasets that had identified cell cycle regulated genes were compared against the 160 genes identified in CD8 T cells as periodic. We included the proteomic dataset on NB4 cells, due to the similar utilisation of PRIMMUS for cell cycle phase comparison (Ly et al. 2014), to represent a more somatic model of cell cycle. Due to a paucity of similar proteomic studies, we broadened our search to include transcriptomic datasets, allowing the inclusion of a study which followed a similar model of FACSorting cells for RNA-seq carried out on haematopoetic stem cells (HSC) (Kowalczyk et al. 2015). This would serve as a more stem-like cell cycle model. These datasets of cell cycle regulated genes were then compared together with our own list obtained from CD8⁺ T cells (Figure 16). We observed 43 genes which were in both CD8 T cells and the HSC dataset, 39 genes which were common to all three cell types, and only 4 which were specifically common to

both $CD8^+$ T and NB4 cells. To better assess the contents of these gene sets, Functional Annotation Clustering was conducted. In all of these gene sets, the more highly enriched GO term was Cell Cycle and we extracted each gene which appeared with this term (Table 1). Many genes in the Common gene set, which are the set of genes identified as periodic in all three datasets, included genes which are active in the G2/M border, such as kinetochore components *Cenpe*, *Aurkb*, *Bub1*, *Bub1b*, and *Plk1*, as well as spindle formation including *Kif11*, *Kif23*, *Aruka*, *Nusap1* and *Tpx2* as well as genes which encoded a number of APC/C associated proteins including *Cdc20*, *Claspin*, and *Plk1*. It was also noted that two different APC/C associating E2 ubiquitin ligases Ube2c and Ube2s were considered periodic in CD8 T cells, one with HSC and the other with NB4 respectively. Two observations of interest were that Cyclin A2 was common between $CD8^+$ T cells and NB4 cells, while Emi1 appeared as common between CD8 cells and HSC, indicating that Cyclin A2 still fluctuates as seen in somatic cells, yet they still have a reliance of Emi1 for cell cycle control as observed in more stem-like models.

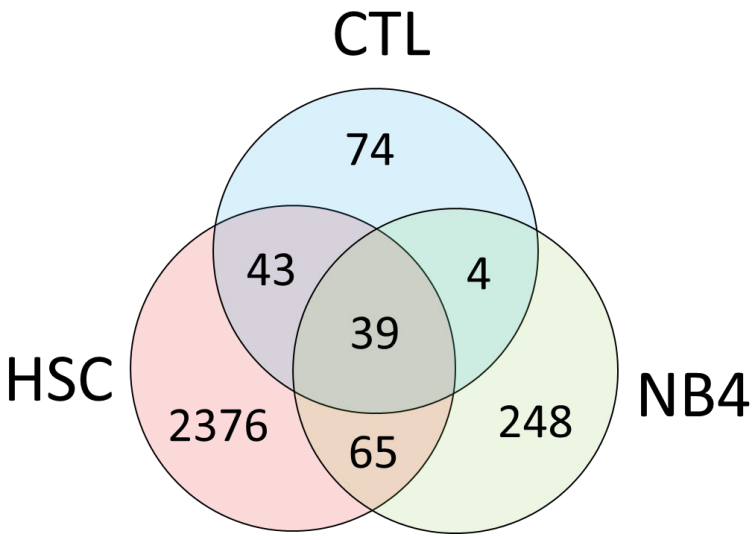

Figure 16 intersection of periodic gene expression which were identified in any of the four datasets. HSC = Haematopoetic stem cells, transcriptomic, 2523 genes, CTL = CD8 T cells, proteomic, 160 genes, NB4 = NB4 leukaemia cells, 356 genes, proteomic.

Periodic Genes identified in CD8⁺ T cells			
CTL only	CTL+HSC	CTL+NB4	Common
Ccdc117	Birc5	Ccna2	Anln
Cchcr1	Cdca2	Kif18b	Aurka
Cdkn2b	Ckap5	Kifc1	Aurkb
Cep131	Emi1	Ube2s	Bub1
Cep170b	Fam111a		Bub1b
Cep85	Fancd2		Ccnb1
Diaph3	Kif20b		Ccnb2
Espl1	Kif2c		Cdc20
Gbp9	Kif4		Cdca3
Haspin	Melk		Cdca5
Itpr2	Mis18a		Cdca8
Kif14	Mis18bp1		Cenpe
Knl1	Ndc80		Ckap2
Knstrn	Nuf2		Clspn
Med9	Psrc1		Dlgap5
Myo7a	Ska3		Ect2
Obscn	Spag5		Esco2
Pdcd7	Spc24		Hjurp
Ppp1r12c	Ttk		Incenp
Sgo1	Ube2c		Kif11
Ska1			Kif23
Spdl1			Nusap1
Tada3			Plk1
Tex264			Prc1
Wee1			Racgap1
			Tacc3
			Tpx2

Table 1 Genes which were highlighted as periodic within each overlapping category were submitted to GO term analysis via DAVID. Lists of genes within the Cell Cycle enrichment cluster of each group were then gathered together. CTL only were genes identified as periodic only within our CD8⁺ T cell dataset, CTL+HSC were genes that were periodic in both the CD8⁺ T data set and HSC dataset, CTL+NB4 were genes periodic in both the CD8⁺ T cell and NB4 dataset, and Common were genes identified as periodic in all three datasets.

3.3.2 Fluctuations of Cyclins and Cdk inhibitors in T cells

We then examined how known cell cycle regulated proteins, cyclins and Cdk inhibitors, behaved within the T cells. We observed Cyclins B1, B2, and A2 to be cell cycle regulated, while Cyclin D3 was deemed to not be cell cycle regulated, and other cyclins were not detected (Figure 17). INK family inhibitors P15, p16, p19 were also detected within our dataset, but only p15 was above threshold for periodicity. It was noted that the fold-change of both Cyclin B proteins, which showed a 32-fold change for Cyclin B1 and a 64-fold change for cyclin B2, was substantial over the course of the cell cycle. By comparison, Cyclin A2

changed by considerably less (4-fold). When examining the fluctuation of intensity over the course of the cell cycle (Figure 18 top), we observed that Cyclin A2 and Cyclin B1 behaved as expected, namely, Cyclin A2 peaking as it approached the G2M border and Cyclin B1 peaking in M phase. But the extent of this change was far shallower in Cyclin A2. Comparing this with a similar proteomic dataset on NB4 cells, separated via elutriation (Ly et al. 2014), we observed that the increase in Cyclin A2 and B1 were much more comparable to each other in NB4 cells (Figure 18 bottom). In addition to this, we observed that levels of Orc1, which decreased upon G1 phase exit in NB4 cells showed no such fluctuation in CD8 T cells, remaining constitutively expressed. This loss of periodic behavior, along with the diminished fold-change in Cyclin A2 abundance over the course of a cell cycle is reminiscent of the stem cell model of cell cycle control rather than that seen in somatic cells.

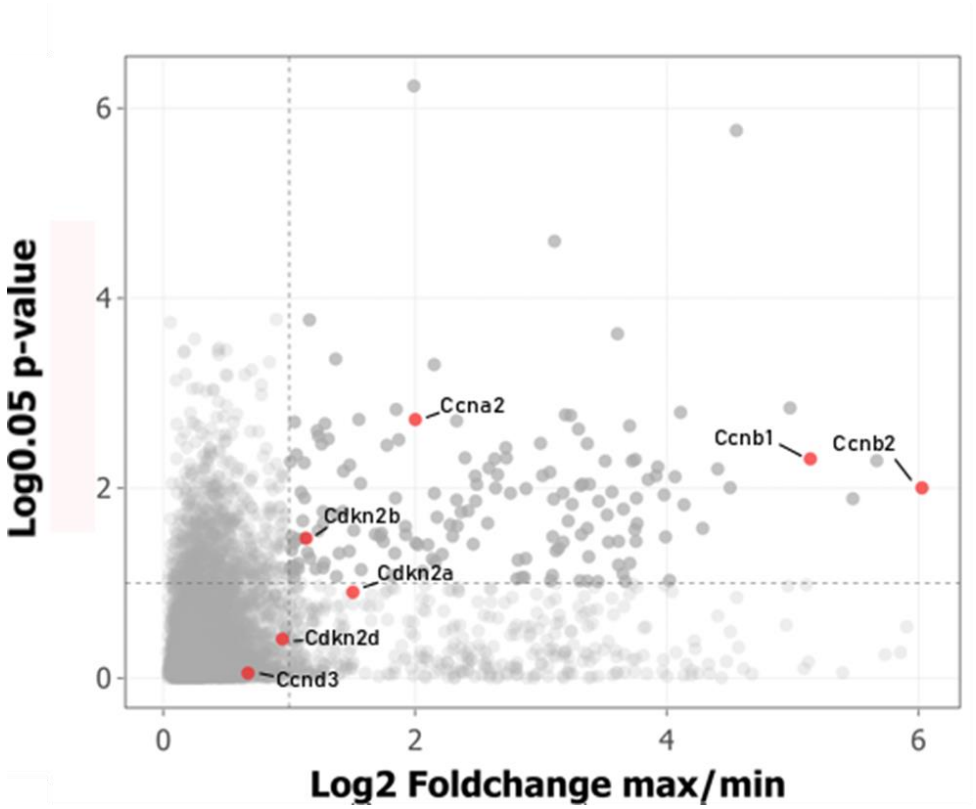

Figure 17 proteomics identified 7 proteins of the common Cyclins and Cdk inhibitors (red) labelled here by name. Dotted lines mark the boundary for proteins which were less than 0.05 on the Fisher's Periodicity Test and that the range of the normalised intensity fluctuation to be greater than a 2 fold different. n=3.

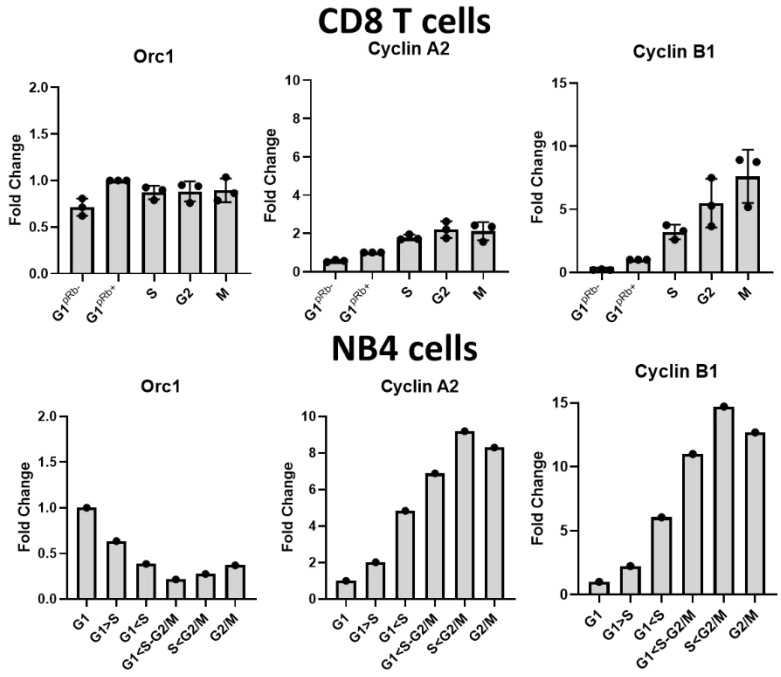

Figure 18 Fold change of Orc 1 (left), Cyclins A (middle) and B (right) over the course of cell cycle between collected data from CD8⁺ T cells (top) and published dataset of NB4 cells (bottom). In both instances fold change shows change in intensity from the earliest phase separated. Both datasets were produced via PRIMMUS. n=3.

3.3.3 Cell Cycle regulated status of APC/C substrates in T cells

Because Cyclin A degradation is mediated by APC/C, and because APC/C inhibition is a known regulatory feature of stem cell cycle progression, we next checked the periodicity of 145 known APC/C target proteins within the dataset. Of this list, 97 of them were present in the dataset, of which 35 were identified as cell cycle regulated (Figure 19). It was noted that Emi1 was most significantly periodic protein of the APC/C substrates while one of the proteins which was not considered periodic was Geminin, which is responsible for inhibition of origin re-licensing (Li and Blow 2005). This finding echoes what has been observed in ES cells, in which Geminin degradation is reduced via inhibition of APC/C, enabling for high levels of Cdt1 which are instead regulated by Cdk2 activity (Ballabeni et al. 2011).

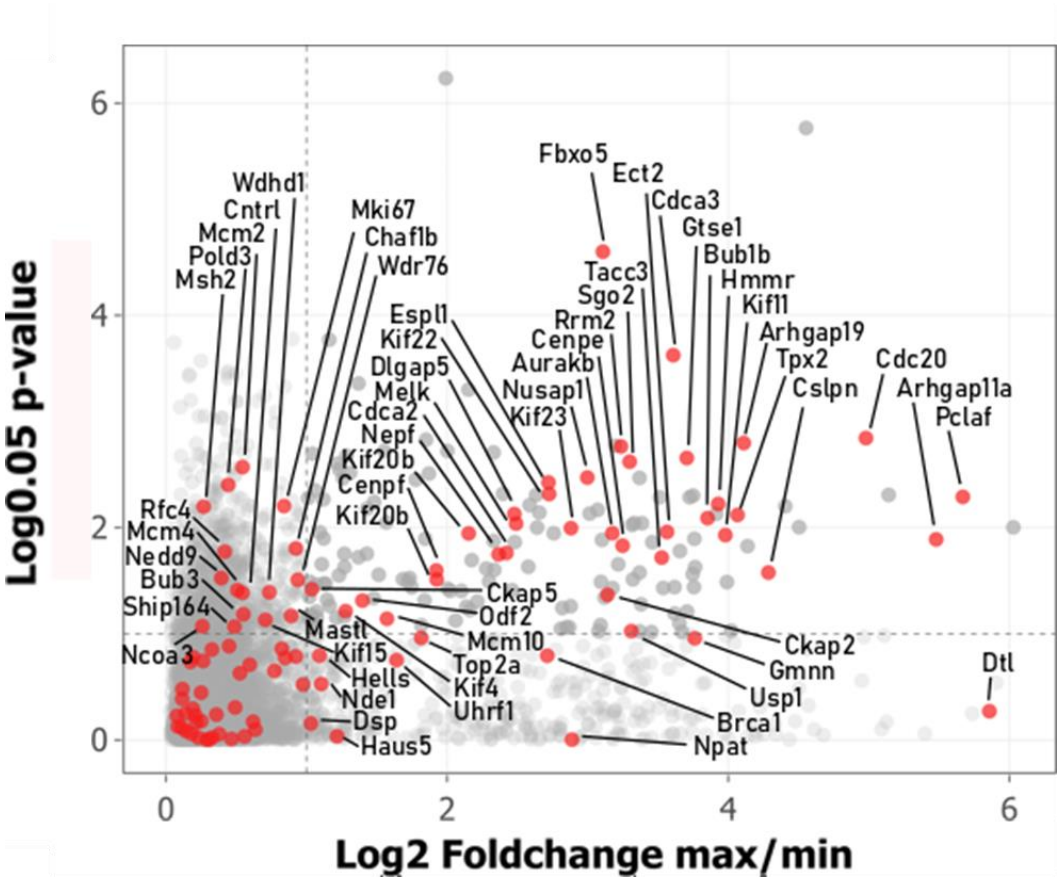

Figure 19 Proteomics identified a large number of APC/C substrates (red) within the dataset. Dotted lines mark the boundary for proteins which were less than 0.05 on the Fisher's Periodicity Test and that the range of the normalised intensity fluctuation to be greater than a 2 fold different. Each protein which met either of these criteria is here labelled by name. n=3.

In order to better assess the significance of which APC/C substrates were cell cycle regulated within T cells, two lists of proteins were constructed based on whether or not these substrates met or did not meet our threshold for being cell cycle regulated and on these we conducted Functional Annotation Clustering of GO terms on DAVID. Of the cell cycle regulated APC/C substrates group (Figure 20 right), the most strongly enriched GO term was Cell cycle, but the more mechanistic GO terms which enriched included Microtubules, Kinesin motor, Mitotic spindle midzone, and Kinetochore, all of which are mechanisms based around Mitosis. Non-cell cycle regulated APC/C substrates (left) were most enriched with DNA replication and DNA Damage/repair, but also included DNA origin binding, and duplex unwinding. All processes which are associated with S-phase progression.

Closer examination showed the genes that made up the DNA Replication term included Origin licensing components Mcm2, Mcm4, and Cdc45; Replication enzymes Top1 and Pold3;

scaffold proteins Rfc4; Histone chaperone Nasp; and E3 ubiquitin ligases Rbbp6, which is associated with Mcm10 (Miotto et al. 2014), and Dtl, which regulates Cdt1 (Sansam et al. 2006). While the cell cycle regulated gene set also showed enrichment in DNA damage/repair, it was notably a much weaker enrichment than within the non-cell cycle regulated gene set. Together, this indicates that the APC/C substrates which are cell-cycle regulated in T cells are strongly associated with the M phase side of cell cycle processes, while those which are not cell cycle regulated are associated with S phase entry side. This may indicate that $CD8^+$ T cells have a similar strategy of cell cycle progression as seen in stem cells, in which S phase promoting proteins evade degradation as a result of inhibition of APC/C, thereby enabling rapid re-entry into S phase.

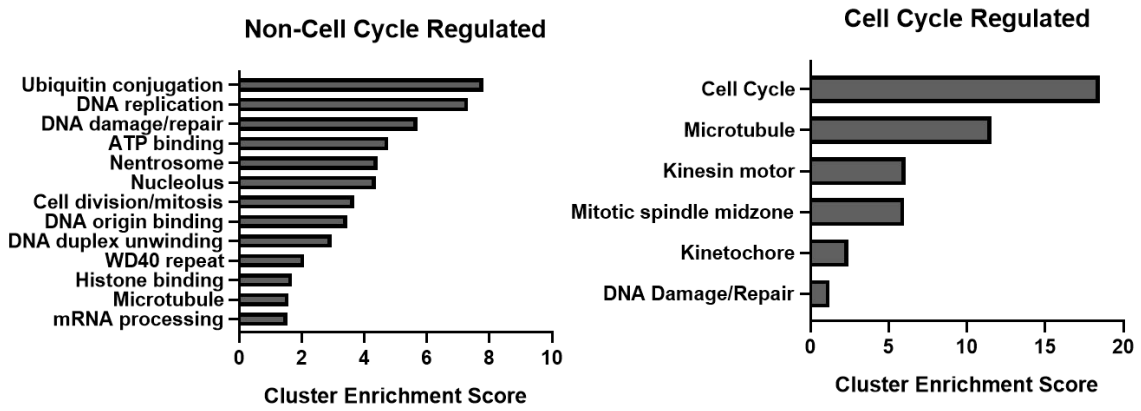

Figure 20 DAVID GO terms and enrichment scores generated from proteins selected from APC/C substrates, 62 of which were non-periodic (left) (p>0.05 fisher's periodicity or fold-change <2), and 35 were periodic substrates (right) (p<0.05 fisher's periodicity and fold-change>2). Top 15 most enriched clusters selected (Cell Cycle Regulated selection only returned 6 clusters). Enrichment score denotes importance of the group term to the list by ranking biological significance of gene groups based on all p-value EASE scores of all enriched terms.

3.4 Discussion

This study identified 160 cell cycle regulated proteins within IL-2-mediated proliferating $CD8^+$ T cells. Broadly speaking, the meta-analysis showed a much larger number of cell cycle regulated proteins in common between HSC and $CD8^+$ T cells than seen in common between CD8 and NB4 cells. On the surface this could indicate that T cells regulate proliferation in manner similar to that seen in HSC rather than that observed in somatic cells. However, it is difficult to draw such conclusion from this comparison due to the inherent differences between proteomic and transcriptomic datasets. This is because while transcriptomic data can provide a lot of information on which genes are currently being expressed, other factors

including the rate of translation, and rates of degradation, have a big impact in the behavior of the proteome that cannot be accounted for by RNA alone. We were able to detect Cyclins D3, A2, B1, and B2, however no isoforms of Cyclin E were detected, though this is likely due to the relatively low abundance of the E cyclins within T cells, as was the case in other T cell proteomic datasets (Rollings et al. 2018). We were also unable to detect all but one of the Cip/Kip family of Cdk inhibitors within our dataset. The exception to this is p21 which was only detected in one of the two runs, and so was excluded from analysis. It has been observed that Cip/Kip proteins are typically absent within mESCs (Fujii-Yamamoto et al. 2005). If Cip/Kip abundance falls below detection within $CD8^+$ T cells, this too may further indicate a more stem cell like proliferative environment.

As has been mentioned previously, APC/C plays an important role in mediating cell cycle regulation at two key time points across the cell cycle (Figure 21). The first is in mitosis, where the APC/C forms a complex with Cdc20, allowing it to polyubiquitinate targeted proteins, promoting the cells traversal through stages of mitosis. APC/C^{Cdc20} mediates the degradation of both Cyclin A and Nek2a once the centrosome has been constructed, enabling transition into metaphase (Hames et al. 2001). APC/C^{Cdc20} also mediates degradation of Securin, releasing active seperase, which will then cleave the cohesin rings, initiating sister chromatid separation. This enables entry into anaphase (Uhlmann et al. 1999). APC/C^{Cdc20} also mediates transition through anaphase by initiating spindle disassembly and spindle-pole separation though degradation of Kinesins such as Kip1, Cin8, and Kinesin related protein Xkid, as well as spindle related proteins Ase1 (Castro et al. 2005).

The second time point is the approach to mitotic exit and up until entry into S phase, in which APC/C forms a complex with Cdh1. APC/C^{Cdh1} and APC/C^{Cdc20} share many targets which aid in mitotic exit. This includes Cyclin B (Clute and Pines 1999), key kinetochore components such as Aurora kinase B, Cenp family proteins, and Sgo2, as well as geminin, an inhibitor of origin licensing post mitosis. All these proteins typically increase in abundance as the cells approach M phase (Alfieri, Zhang, and Barford 2017; Honda et al. 2000; McGarry and Kirschner 1998). APC/C^{Cdh1} also targets Cdc20 for degradation, reducing the population of APC/C^{Cdc20} complexes, leading to the transition seen in late stage mitosis where APC/C^{Cdh1} becomes the dominant APC/C complex (Foe et al. 2011).

APC/C^{Cdh1} remains within the daughter cells and predominately targets for degradation promotors of S-phase progression, such as origin licensing proteins including Cdc6, Cdki inhibitor Skp2, and Cyclin E, ensuring that the cell remains within pre-R G1 or exits from cell cycle entirely. APC/C^{Cdh1} also targets factors which inhibit origin licensing, such as Geminin which prevents MCM2-7 formation around chromatin, and Cyclin A which can inhibit origin licensing proteins such as Cdc6 and Cdt1. In so doing, the potential for origin licensing remains high yet unable to begin until APC/C^{Cdh1} is sufficiently inhibited (Mailand and Diffley 2005; Sivaprasad, Machida, and Dutta 2007).

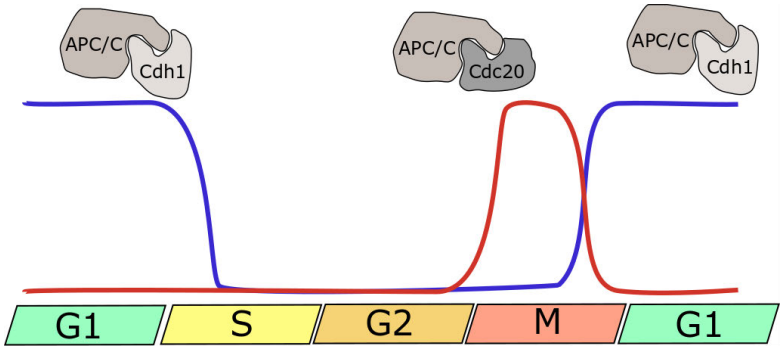

Figure 21 APC/C binds with one of two co-activators Cdh1 or Cdc20, which allow the E3 Ubiquitinase to locate its targets. Abundance of the APC/C^{Cdh1} complex rises as the cells exit M phase and decreases as they approache the beginning of S phase. APC/C^{Cdc20} abundance rises as the cells enter in to M phase and decreases as the cells are about to exit mitosis.

The APC/C has a dynamic relationship with the cyclins, which can act as substrate, activator, and suppressor of the complex depending on the context. Cdk1/Cyclin B and Cdk1/Cyclin A mediated phosphorylation both enables coupling of Cdc20 to APC/C and inhibits coupling of Cdh1 as the cells approach G2. As the cells being M phase entry, APC/C^{Cdc20} targets Cyclin B for degradation, reducing Cdk1 activity and thus enhancing instances of APC/C^{Cdh1}, which in turns leads to degradation of Cyclin A and Cyclin B seen around mitotic exit (Fujimitsu, Grimaldi, and Yamano 2016; Greil, Engelhardt, and Wäsch 2022; Parry and O'Farrell 2001; Reber, Lehner, and Jacobs 2006). Phosphorylation of Cdh1 also occurs during G1 phase of cell cycle, mediated by Cdk2/Cyclin E and A. Once E2F regulated transcription is uninhibited by Rb, levels of Cyclin E and A can surpass the proteolytic capacity of the APC/C^{Cdh1}. This leads to an increased phosphorylation of Cdh1 and thus a reduction of APC/C^{Cdh1}, from late G1 through to G2 (Reber et al. 2006; Zielke et al. 2008).

Emi1 inhibits APC/C activity by competing with Cdh1 for the coactivator binding pocket, thereby permanently preventing Emi1 from forming a complex with its coactivator. Emi1 is both a substrate and an inhibitor of APC/C^{Cdh1} in a phenomenon known as a bistable switch. While APC/C^{Cdh1} is dominant, Emi1 remains low until sufficient levels of E2F activity allows for both the Cdk2/Cyclin E to impair APC/C^{Cdh1} and Emi1 mRNA levels to increase, enhancing translation of Emi1 until the abundance of Emi1 reaches a critical point that it overwhelms APC/C^{Cdh1} ability to degrade it (Cappell et al. 2018). This is because Emi1 has a relatively weak D-box domain, the degron target of APC/C^{Cdh1} and the C-terminal sequences of Emi1 are understood to be able to block Ube2S mediated ubiquitin elongation. These factors together act in concert to reduce the efficacy of APC/C^{Cdh1}, resulting in a reduction in degradation for its other substrates (Frye et al. 2013).

Within the classic cell cycle model (Figure 22 top) generally thought to apply to most somatic cells, inhibition of APC/C^{Cdh1} is predominately mediated by phosphorylation. Cdh1 phosphorylation by either Plk1 or Cdk2/Cyclin E/A allows another E3 ubiquitin ligase $SCF^{\beta\text{-}TrCP}$ to polyubiquiniate it and thereby trigger its degradation (Fukushima et al. 2013). Within stem cells however, it is reported that APC/C^{Cdh1} substrates such as Cyclins A and E, remain constitutively expressed, their periodic fluctuations much shallower than that seen in somatic cells. This is due to a greatly increased abundance of Emi1 preventing formation of APC/C^{Cdh1} complexes (Figure 22 bottom). To avoid issues with origin licensing that APC/C^{Cdh1} would otherwise protect against, stem cells also have increased abundance of Cdc6 and Cdt1, allowing for safe rapid re-entry into S phase. This also results in a much shorter G1 phase (Ballabeni et al. 2011).

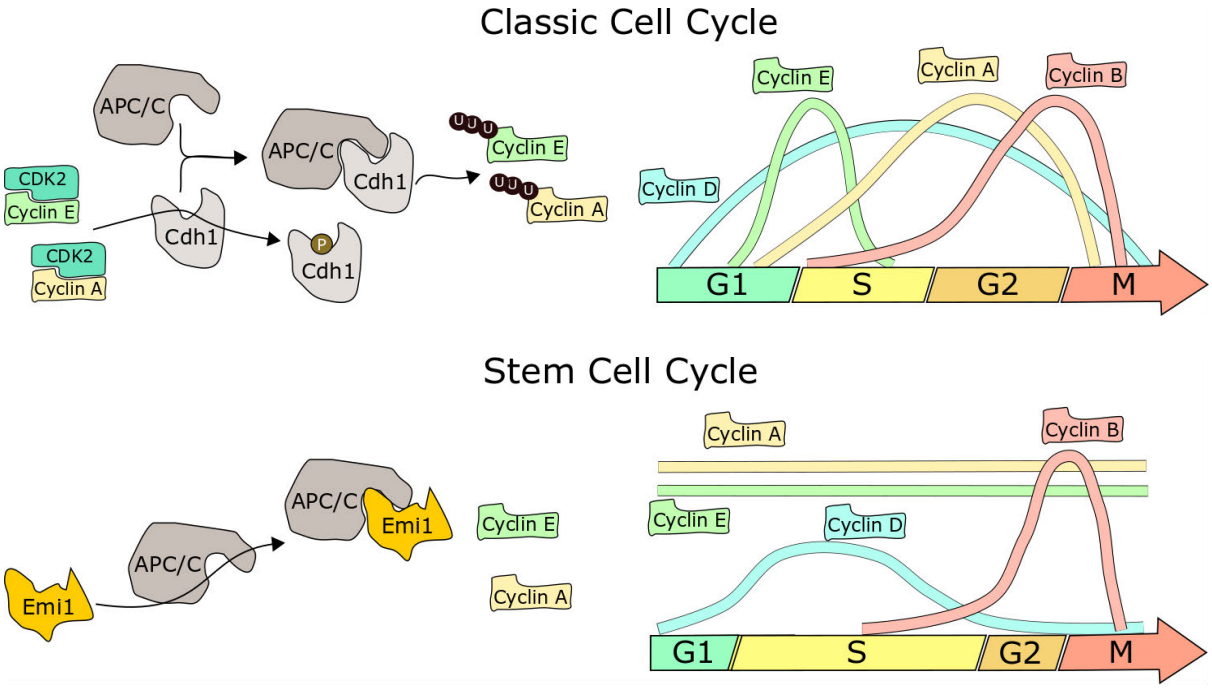

Figure 22 Classical cell cycle models state that APC/C contributes to the cyclic nature of Cyclins E and A by tagging them for degradation as the cells enter G1 phase. Once Cdk2-Cyclin E/A concentrations reach a critical point, however, they can disable APC/C^{Cdh1} by phosphorylation of Cdh1, preventing it from coupling with the APC/C. Within Stem cells however, APC/C is permanently inhibited by Emi1, preventing APC/C from accessing Cdh1, and as a result Cyclins E and A remain constitutively expressing throughout the cell cycle.

It is interesting that Cyclin A2 was identified as cell cycle regulated as, in the absence of Cyclin E, this is one of the key differences cited between the models of stem cell and somatic cell cycle regulation (Dyson 1998; Gookin et al. 2017; Li and Kirschner 2014). Especially as Cyclin A2 was identified as cell cycle regulated within NB4 cells but not within HSC. Yet we also demonstrated that, in comparison to NB4 cells, Cyclin A2 fluctuated to lesser degree possibly indicating that its overall abundance is not being depleted as dramatically as within NB4. Such a reduction in fluctuation may be indicative of a reduction in degredation, such as might be seen with an inhibited APC/C activity as predicted by the Stem cell model.

Of the APC/C substrates detected within CD8$^+$ T cells, those which were cell cycle regulated were strongly M phase associated, while those which were not cell cycle regulated were S phase associated, possibly indicating targeted inhibition of APC/C^{Cdh1} which is predominately active from mitotic exit to the entry into S phase, and is known to target S phase progression proteins such as A and E cyclins, and Cdc6 for degradation (Araki et al. 2003). Complementing this was the observation that Ube2c, an E2 ubiquitin ligase required for the activation of APC/C^{Cdh1} (Brown et al. 2016) was common between HSC and CD8$^+$ T cells further demonstrating how aligned CD8$^+$ T cells are with the APC/C^{Cdh1} reliant model of stem cell

control. Conversely, $CD8^+$ T cells also shared cell cycle regulated Ube2s with NB4 cells. While Ube2s is also associated with APC/C^{Cdh1} and is essential for the elongation of the polyubiquitin chain (Brown et al. 2016), it is also an essential component of the M phase oriented APC/C^{Cdc20} complex, forming a stable association with Cdc20 (Craney et al. 2016).

It is difficult to say definitively with this dataset what the implications are for T cells to have both Ube2s and Ube2c present as cell cycle regulated, though it does demonstrate an aspect of somatic cell cycle control seen in $CD8^+$ T cells.

APC/C^{Cdh1} moderation plays an important role in the cell cycle of mESC, and what this analysis indicates is it is likely the case with $CD8^+$ T cells as well. However, it is clear that while $CD8^+$ T cells share a lot of properties with Stem cell model, it is not an exact match. It is therefore likely that $CD8^+$ T cells share aspects of cell cycle regulation between the two models.

4 APC/C activity identified as important factor in T cell proliferation

4.1 Introduction

4.1.1 T cell fate and S-phase entry

Following antigenic stimulation, $CD8^+$ T cells begin to differentiate towards the SLEC phenotype, which rapidly proliferate into T_{eff} cells, or the MPEC phenotype which produce the pool of T_{cm} and T_{em} cells. It is not yet certain when lineage commitment is established, and exactly what triggers it, but there is a good body of evidence which correlates division speed with T cell fate. One study observed that MPECs fated to become T_{cm} had markedly less uptake of BrdU than T_{em} progenitors or SLECs, indicating SLECS were more likely to enter into S phase. This behavior was independent of signaling strength, either from antigenic stimulation or cytokine stimulation, with the effect of IL-2 stimulation enhancing EdU uptake only impacting non-T_{cm} progenitors (Kretschmer et al. 2020).

Another study looking at the Fucci/OT-1 mouse observed that $CD8^+$ T cells which mostly expressed Cdt1 and thus were predominately in G1/G0 had greater expression of memory markers such as CD62L and IL-7R, known markers of memory phenotype. Furthermore, by isolating single cells on the basis of the number of times they had divided using CTV to label the generations they confirmed greater expression of Cdt1 correlated with slower division time, and microarray analysis of these slower dividing cells confirmed a more memory like profile. Likewise, the faster proliferating cells presented a more effector like profile (Kinjyo et al. 2015). Another study noted that after incubating $CD8^+$ T cells in the Cdk4/6 inhibitor Palbociclib and reducing their rate of division, the proportion of T_{cm} produced were much higher. The production of T_{cm} increased in a dose dependent manner with palbociclib, with T_{cm} going from roughly 10% of the population to close to 50% at the strongest concentration of the inhibitor. This effect was seen both immediately after and 24 hours post activation (Heckler et al. 2021).

Having established in Chapter 3 that IL-2 stimulated cycling $CD8^+$ T cells share characteristics of ES cell cycle, we compared the uptake of EdU within the 2n peak of IL-2 treated activated $CD8^+$ T cells to Retinal Pigment Epithelial-1 (RPE-1) cells as a model of somatic cells which are in exponential growth (Figure 23). We found that $CD8^+$ T cells had a substantially higher

concentration of EdU^{+} cells within the 2n peak, indicating that a greater proportion of cells were entering S-phase.

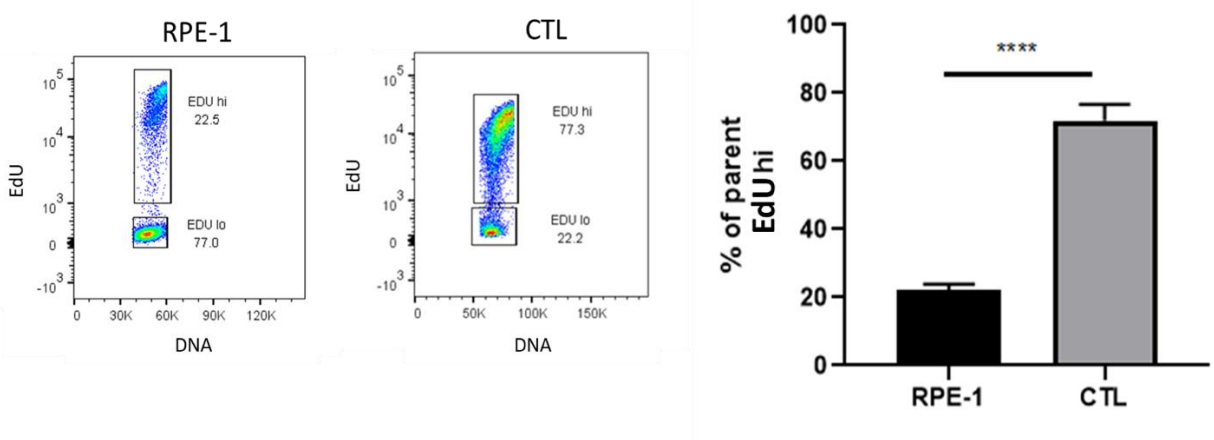

*Figure 23 Distribution of EdU of the population within the 2n DNA peak of RPE-1 cells mid cycle (left) and CD8^{+} T cells (CTL) (middle) activated for 48 hours and incubated in IL-2 for 72 hours. Quantification of EdU (right) with Student's T-Test conducted, **** = p<0.0001, n=3 from one experiment.*

To investigate the relationship between T cell fate and cell cycle, we examined the cell cycle phase distribution of TCR activated T cells treated either with IL-2 or IL-15, which promote effector or memory fate, respectively. To do this, we set up a culture of CD8^{+} T cells and following 48 hours of antigenic stimulation, incubated them with IL-2 or IL-15 for a further 48 hours, collecting the cells at 24 hour intervals. Cell cycle phases were separated by DNA, denoting the 2n peak for G1, the 4n peak for G2/M and the area between these peaks as S-phase. G1 and G2 were further subdivided based on staining of p-Rb and uptake of EdU after a 30 minutes pulse. Cells within the 4n peak that showed high intensity p-Rb staining were identified as being mitotic (Figure 24) (Jacobberger et al. 2008).

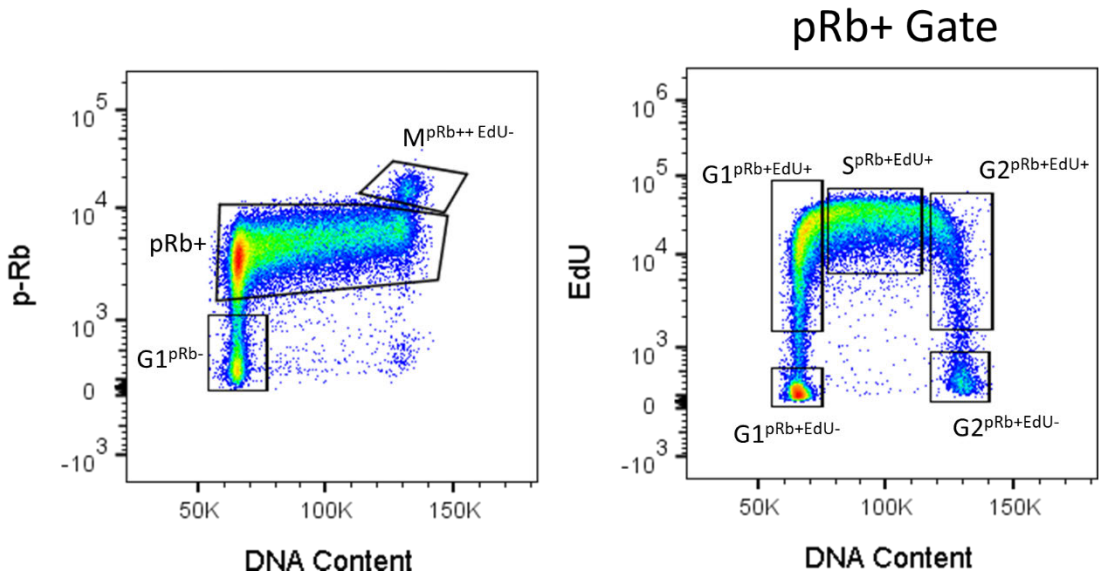

Figure 24 Gating strategy for the quantification of cell cycle distribution of IL-2 and IL-15 treated cells. Events which were in either $G1^{pRb-}$ and $M^{pRb++EdU-}$ were selected by p-Rb vs DNA content (left) as well as a general pRb+ group. This group is then further dissected (right) by EdU staining.

We observed that after 48 hours of antigenic stimulation (Figure 25), the majority of the $CD8^+$ T cells were found to be EdU positive (69%). This level of EdU uptake was maintained at the 72 hour point (24 hours post cytokine treatment) regardless of cytokine treatment, instead there was a shift in the proportion of G1 cells. IL-15 treated cells had a larger proportion (23.0%) of G1 cells without EdU compared with IL-2 treated (14.9%) or even to the 48 hour time point prior to cytokine stimulation (10.7%). By the 96 hour point (48 hours post cytokine treatment), the phenotype of the cells in the two cytokines was completely different. IL-2 treated cells had more EdU negative G1 cells (36.5%) indicating a moderate slowing down of cell cycle progression, while IL-15 treated were predominately EdU negative (88.5%), indicating a shift towards cell cycle arrest.

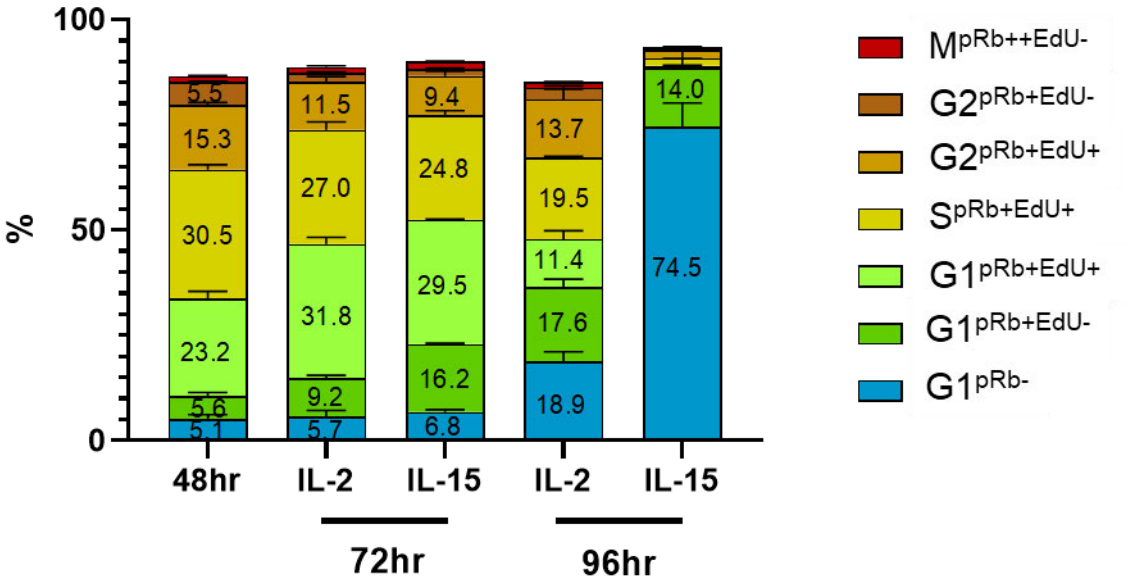

Figure 25 Cell cycle distribution of CD8⁺ T cells stimulated with antigen for 48 hours, and then either IL-2 or IL-15 for a further 48 hours, G1 is defined as events within the 2n gate, S as events between the 2n and 4n gate. G2 as events within the 4n gate and M as events within the 4n gate and with exceptionally high p-Rb staining. n=3

4.1.2 Proposed model for cell cycle control

Because the cell cycle of CD8⁺ T cells shares a number of features observed in the regulation of cell cycle in stem cells, it is possible that the mechanisms used to allow stem cells faster entry in to S-phase are present within CD8⁺ T cells. The main driving mechanism being a greater abundance of Emi1 at early cell cycle, allowing for constitutively active APC/C substrates between mitotic exit and S phase re-entry. To investigate this, we looked into a published proteomic dataset comparing the estimated copy number across a variety of CD8⁺ T cell subtypes, including IL-2 treated and IL-15 treated (Brenes et al. 2022 pre-print).

This dataset (Figure 26) showed that naïve cells do not express Emi1 or Cdh1 above detectable limits, but after 24 hours of TCR stimulation, Emi1 copy numbers increased to just over 8600 copies. This abundance increases 2-fold following treatment with IL-2, but decreased 4-fold in IL-15. Cdh1 by comparison changes very little, not above detectable limits in TCR stimulated CD8⁺ T cells, rising to just under 1000 copies in IL-2 treated and just about 3500 copies in IL-15 treated cells. When we consider that Emi1 inhibits APC/C^{Cdh1} by obstructing the binding pocket of APC/C^{Cdh1} and thereby reducing the amount of active APC/C^{Cdh1} available, the relative abundance of these proteins could be an indicator of the state of APC/C^{Cdh1} activity

within these phenotypes, with a high Emi1 to Cdh1 ratio indicating suppressed APC/C^{Cdh1} activity as seen in the IL-2 treated cells.

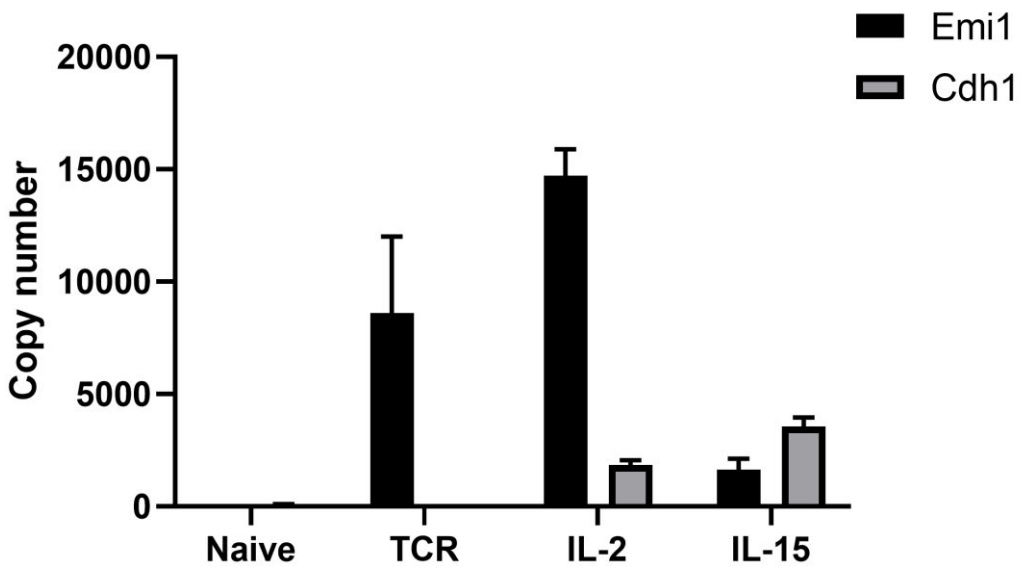

Figure 26 Emi1 and Cdh1 levels in p14 T cells from naïve, stimulated with antigen for 24hrs, stimulated and then treated with IL-2, or with IL-15. Copy number from DIA dataset calculated using the Histone Ruler. Data was taken from Immpres.co.uk on 16/11/2022

Together these data suggest that within cycling CD8$^+$ T cells, there are distinct mechanisms of cell cycle control (Figure 27). A slow, more somatic like model in which cells are kept in an extended G1 by APC/C^{Cdh1} as is seen in a classical somatic cell cycle model, and a fast more stem cell-like model whereby a high abundance of Emi1 enables for faster re-entry into S phase similar to that observed in stem cells. Exposure to different cytokine stimulation may be an important factor in how CD8$^+$ T cells become programmed towards either model. In order to address this hypothesis, we have analysed both the original TMT dataset and a newly obtained proteomic dataset comparing the differences between T cells during cycle in response to IL-15 and IL-2. What follows is an exploratory approach to the proteomic data collected with the intention to get a broad overview on the nature of cell cycle progression in either phenotype. A more direct look at the effect of Emi1 on cell cycle progression will be described in chapter 5.

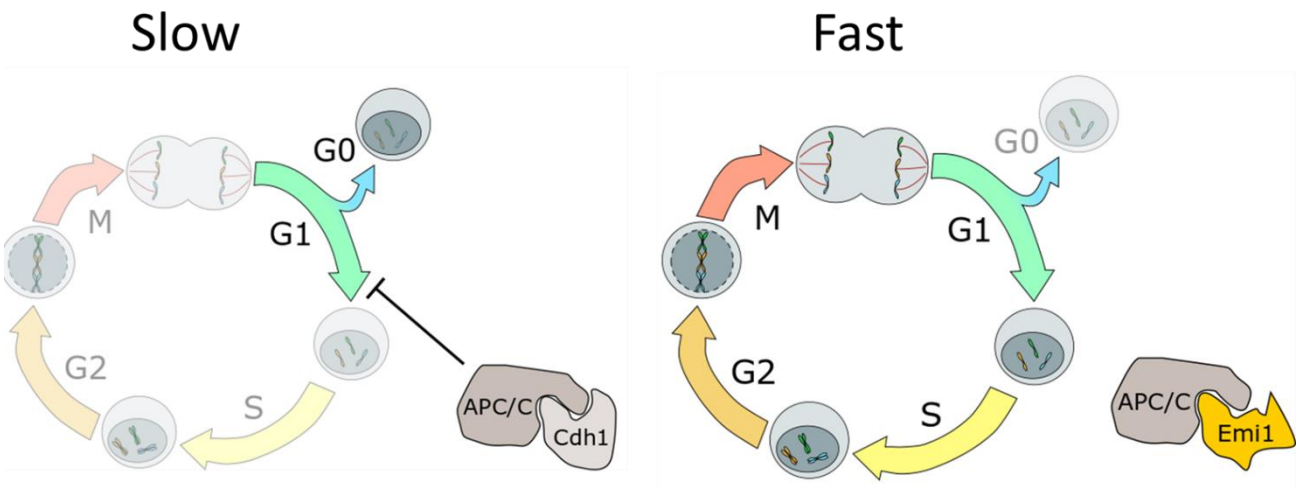

Figure 27 Proposed model for control of cell cycle behaviour between slow and fast cycling T cells is predominately mediated by Emi1. Slow proliferating cells have a lower Emi1 to Cdh1 ratio, allowing APC/C^{Cdh1} to form and target S-phase promoting proteins for degradation, keeping the cell in G1 phase for a prolonged period of time. Fast proliferating cells instead have a high Emi1 to Cdh1 ratio, successfully reducing the amount of active APC/C^{Cdh1}. This results in a shortened G1 phase and therefore a faster rate of proliferation.

4.2 Breakdown of DDA dataset

4.2.1 Kmeans clustering of fluctuation patterns

Having identified 160 proteins in CD8$^+$ T cells that were cell cycle regulated, we decided to further analyse the fluctuation patterns of these proteins. To do this we applied K-means clustering to these cell cycle regulated proteins within the TMT dataset. Using an elbow plot to examine the optimal number of clusters within the dataset (Figure 28), it was shown that 3 clusters represented over 75% of the variance, with 4 clusters pushing this to just over 80%. Any higher value for K only increased the representation by small increments and in some cases returned a cluster of 1 protein. We decided to accept the 4 cluster Kmeans as this was the point just before the improvement plateaued.

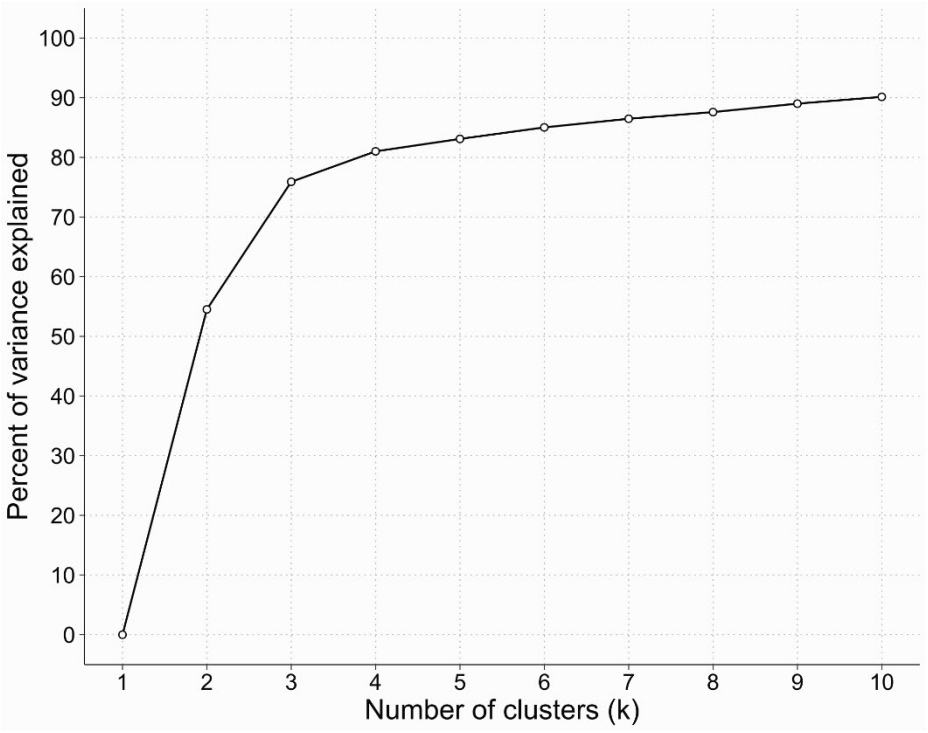

Figure 28 Analysis of the variance provided by separating the TMT data into different numbers of clusters via Kmeans clustering.

Four distinct clusters of fluctuation patterns emerged (Figure 29). The largest cluster consisting of 88 identities followed a pattern of gradually increasing in abundance from the start of the cell cycle through to the end, peaking at M phase (M peaking). The other clusters were of a more similar size, containing 21-28 identities each. What was shared between these three clusters was the difference in abundance between pRb+ and pRb- populations of G1. This included a cluster of proteins that had an abundance peaking at the earliest point of cell cycle, possible prior to restriction point, but decreased as the cells transitioned towards entered S phase ($G1^{pRb-}$ peaking). The other two clusters of proteins were defined by having a fairly low abundance prior to restriction point, but were generally high in all other phases of cell cycle, one of which show very high abundance specifically within the late G1/early S phase population ($G1^{pRb+}$ peaking), while the other showed no specific pattern of differentiation beyond being low pre-restriction point ($G1^{pRb-}$ low).

In order to assess these clusters for novel mechanisms, we took the protein list of each cluster and filtered them to exclude any GO terms which were associated with processes of cell cycle (Table 2). This revealed that while the M peaking cluster was the largest of the four, it only contained a small fraction of proteins which were not already associated with

cell cycle terms, and were therefore considered cell cycle regulated proteins specific to $CD8^+$ T cells.

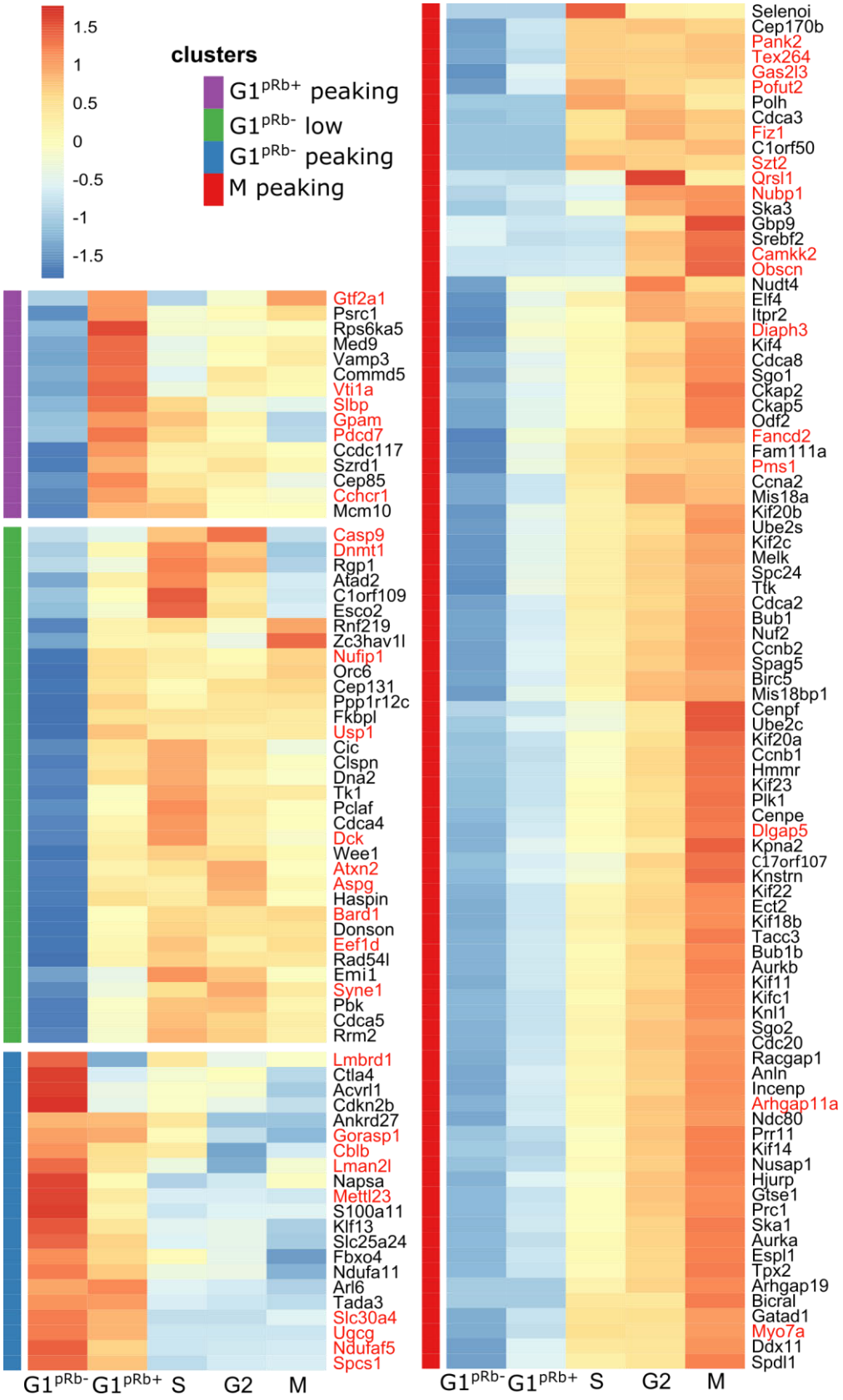

Figure 29 TMT dataset was submitted for Kmeans clustering on the basis of their fluctuation patterns over the course of a cell cycle utilising Ward's minimum variance method for clustering, with dissimilarities squared prior to clustering. Genes which did not have cell cycle related GO terms highlighted in red, K= 4, n=3

Identifying Novel Cell Cycle Proteins		
Cluster	Total	Lacking Cell Cycle GO terms
G1pRb+ peaking	23	14
G1pRb- low	21	19
G1pRb- peaking	28	15
M peaking	88	24

Table 2 The TMT dataset was clustered via Kmeans clustering and filtered for any Gene Ontology terms which were associated with aspects of cell cycle. The total column includes the number of proteins identified in each cluster.

4.2.2 Defining proteins that fluctuate greatly between pRb+ and pRb- G1

Because three out of four clusters were defined by a change in abundance between pRb+ and pRb- G1, and with it the majority of identified novel proteins, we looked at the differences in abundance between these two populations within the TMT dataset. Because the $G1^{pRb+}$ and $G1^{pRb-}$ specimens were a part of the same multiplex experiment, there was no need to normalise them against the S-phase. Instead, the raw intensities were calculated as parts per million (ppm) by dividing the intensity by the sum of all intensities detected within the specimen, and multiplying the result by 1e6.

Generally, there was a greater abundance of proteins within $G1^{pRb+}$ populations, which had 96 proteins significantly higher compare to only 6 found higher in $G1^{pRb-}$ (Figure 30). However, of these 96, only 6 of them where of our previously identified list of novel cell cycle regulated proteins, and within the proteins higher in $G1^{pRb-}$ only 2 were novel. A detailed analysis of each of these proteins can be found in the discussion section of this chapter.

We then examined the change in abundance of APC/C targets between $G1^{pRb+}$ and $G1^{pRb-}$ (as highlighted in Figure 31). We noted that a number of Kinetochore components were raised in the $G1^{pRb+}$ subset including Cenpe, Aurkb, Bub1, Bub1b, and Clspn as well as other M phase associated proteins like Kif11 which makes up part of the kinesin motor, Geminin which inhibits Cdt1, Tpx2 which stimulates microtubule assembly, and Tacc3 which contributes to spindle formation.

There were example of APC/C targets raised in $G1^{pRb+}$ which were not typically associated with M phase, such as Mcm10 which enables chromosome replication in S phase by allowing activation of the MCM complex (Quan et al. 2015), HMMR which lies downstream of Mek/Erk

signalling and is understood to aid proliferation in a number of cancer models more globally (Jiang et al. 2022), and Uhrf1 which works with Dnmt1 to maintain DNA methylation during DNA replication in S phase (Zhang et al. 2011). But looking at the general clustering enrichment of GO terms for the p-Rb+ group of APC/C substrates (Figure 32), terms associated with M phase processes such as Kinetochore, Mitotic spindle, and Kinesin motor are dominant, echoing much of what was observed in the broader cell cycle regulated analysis (Figure 20).

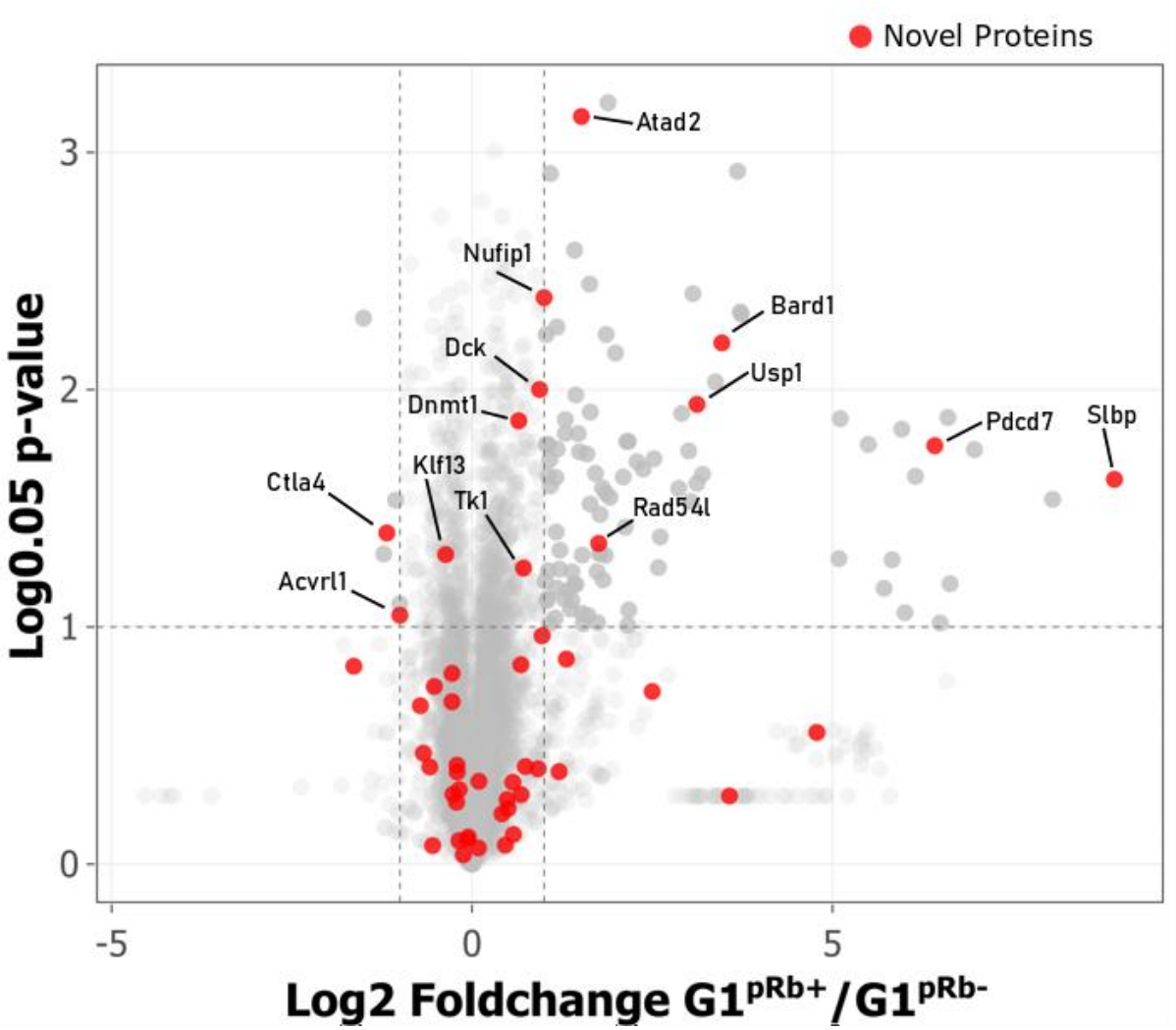

Figure 30 Distribution of proteins between p-Rb positive and p-Rb negative populations within the 2n gate. Fold change calculates from ppm normalisation of intensities from $G1^{pRb-}$-S phase dataset. Highlighted red are proteins identified as novel cell cycle regulated proteins by not having cell cycle associated GO terms. Significance was determined by Student's t-test.

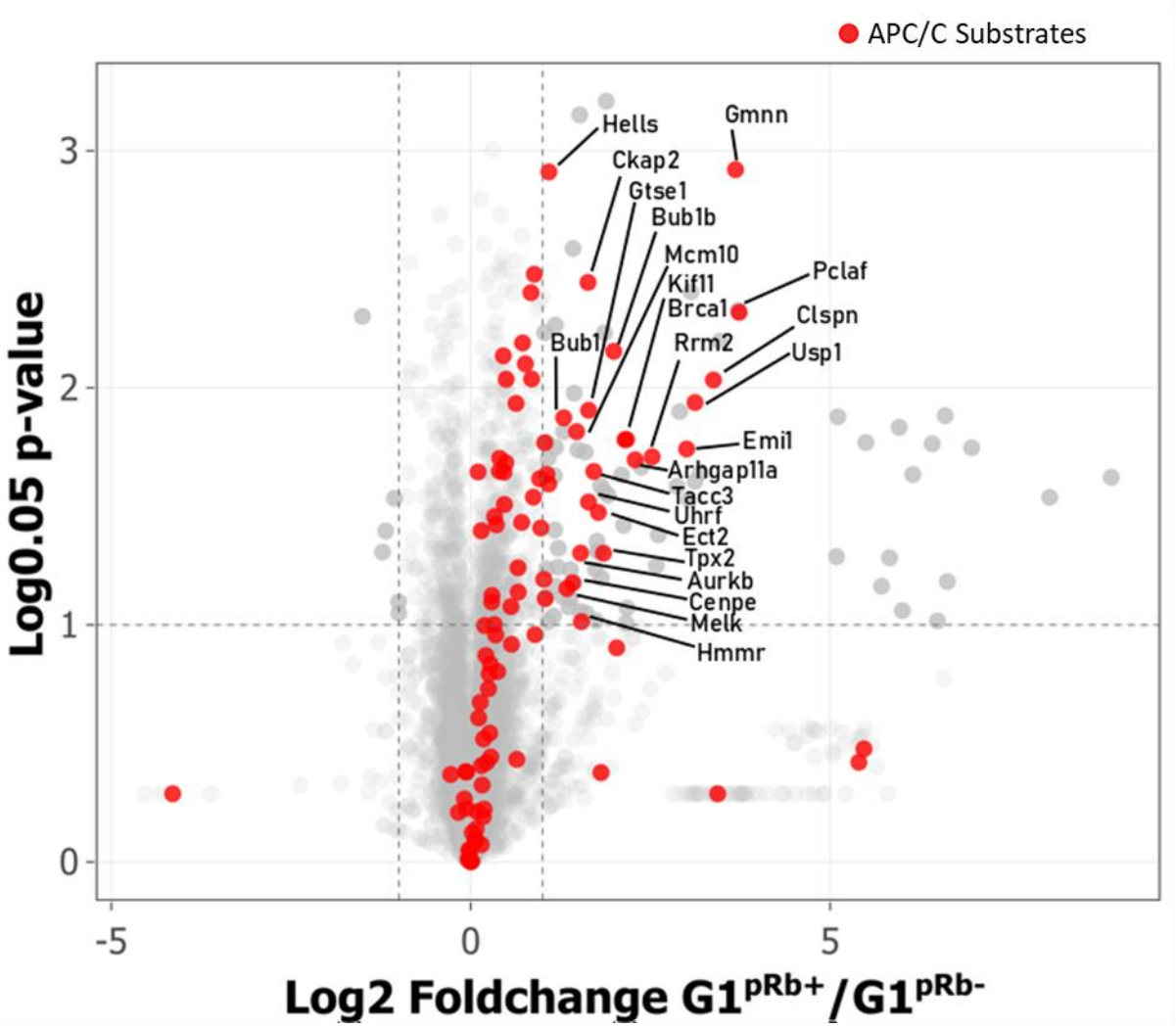

Figure 31 Distribution of proteins between p-Rb positive and p-Rb negative populations within the 2n gate. Fold change calculates from ppm normalisation of intensities from G1^{pRb-}-S phase dataset. Highlighted red are proteins identified as APC/C targets. Significance was determined by Student's t-test.

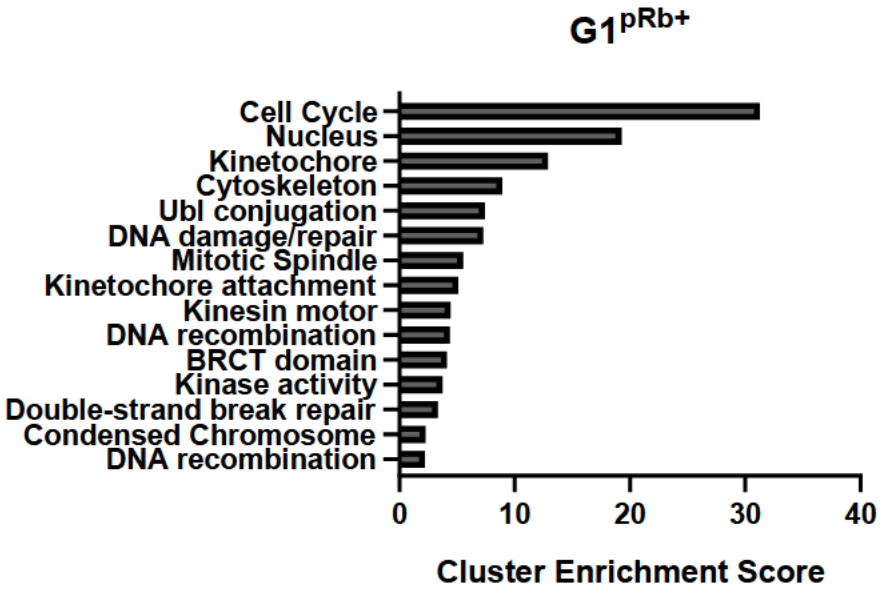

Figure 32 DAVID GO terms and enrichment scores generated from proteins selected from 96 APC/C proteins that were at least 2-fold increase in $G1^{pRb+}$ compared to $G1^{pRb-}$. First 15 most enriched selected. Enrichment score denotes importance of the group term to the list by ranking biological significance of gene groups based on all p-value EASE scores of all enriched terms.

4.3 DIA dataset of IL-2 and IL-15 cells

In order to assess our model for fast and slow proliferating cells, we activated OT-1 T cells and then incubated with either IL-2 to produce T_{eff} as examined thus far, or IL-15 to produce a pool of memory-like phenotype cells (T_{mem}). OT-1 cells were incubated for 48 hours in N4 and anti-CD28 antibody. They were then placed with either IL-2 or IL-15 which was replenished daily for three further days to ensure consistent exposure to cytokine, with the cells taken at the 120 hour time point (Figure 33) when we estimated there should still be a cycling population. The cells were then sorted into two populations of pRb+ and pRb-. This was done because there are relatively few T_{mem} which are pRb+ and thus further subdividing this scarce group by DNA content would have reduced the protein yield below that required for MS analysis.

The Proteomic ruler offers a method of post-hoc normalisation which provides an estimation on total copy number within the population (Wiśniewski et al. 2014). While it is possible to utilise the proteomic ruler on TMT normalized samples, it has been shown that the application of the proteomic ruler on TMT labeled samples does not improve the dataset compared to one obtained via a label free approach (Brenes et al. 2019). Therefore, to reduce loss from sample processing, we opted for a label free DIA approach instead of a TMT based method of quantification.

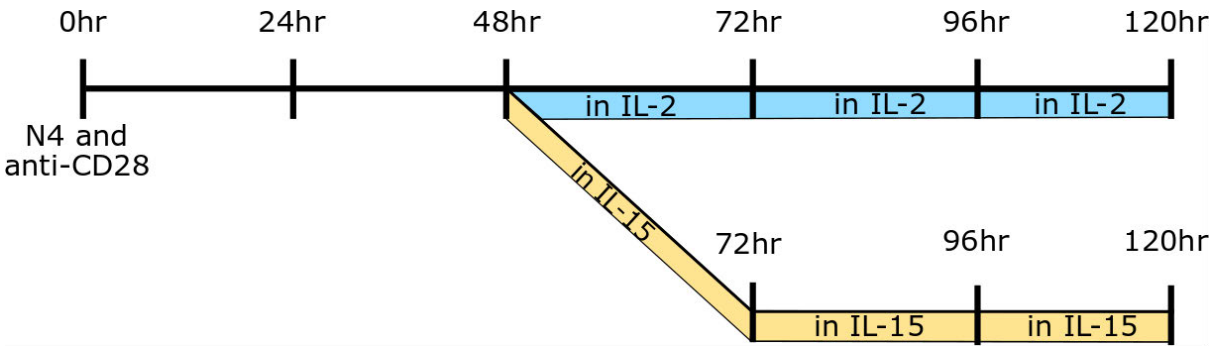

Figure 33 OT-1 T cells were activated with N4 and anti-CD28 and incubated for 48 hours. The cells were then divided, with half given IL-2 and the other half given IL-15 daily for a further 72 hours.

Our DIA analysis returned 6901 proteins to which we applied the Proteomic ruler technique, using a list of mouse histone uniprot ids to identify the histones within the dataset.

4.3.1 Mechanisms of APC/C control

We first examined the distribution of known T cell markers between IL-2 and IL-15 treated cells in order to confirm the effector status of the samples (Figure 34). In both the pRb+ and pRb- populations known T_{mem} marker CD62L was raised in the IL-15 treated, and T_{eff} markers CD25 and Granzyme B were raised in IL-2 treated samples. IL-7 receptor was elevated in T_{mem} in the pRb- population, but was lost in the pRb+ group. This is in fitting with observations that $CD8^+$ T cells expression of IL-7 receptor is higher in the memory phenotype, and that the expression of IL-7 receptor is inversely correlated with proliferation (Koenen et al. 2013). While T-bet levels were similar in both T_{mem} and T_{eff}, it is difficult to judge what this implies. Phenotype of MPEC vs SLEC relies on the relative levels of both T-bet and Eomes, and in our dataset Eomes was not detected (Li et al. 2013). In contrast to what had been recorded previously (Immpress.co.uk accessed 2023), Emi1 showed no difference between IL-2 and IL-15 treated $CD8^+$ T cells.

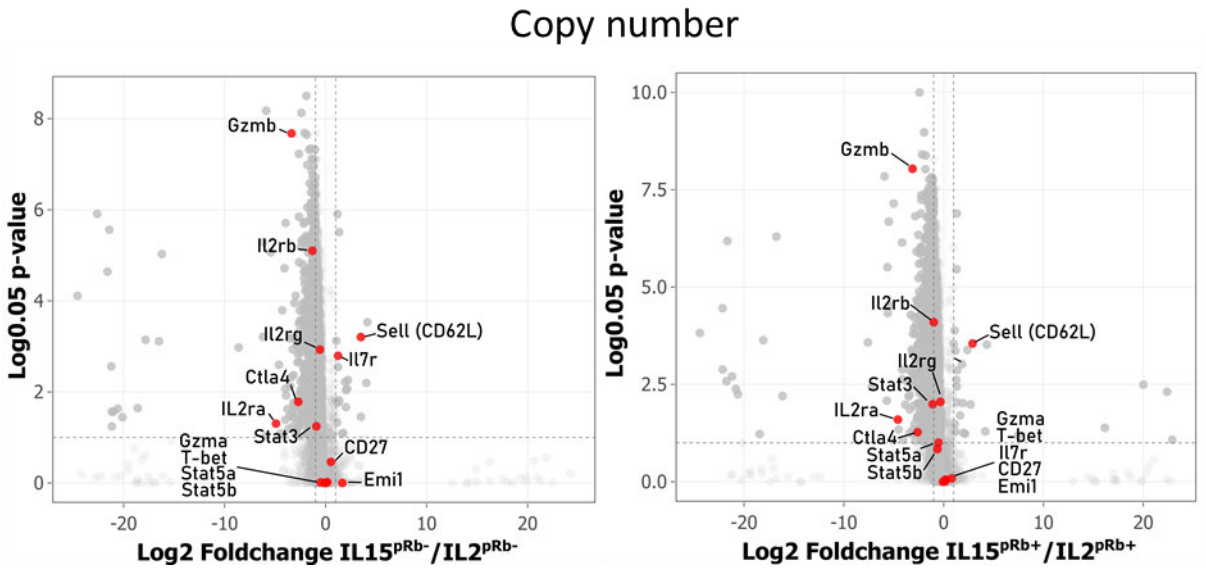

Figure 34 Proteomic analysis comparing IL-15 and IL-2 copy number in the p-Rb⁻ gate (left) and the p-Rb⁺ gate (right). Proteins in red represent selected markers of T cell phenotype. Significance was calculated using ANOVA followed by Tukey's test. n=3

To examine in more detail the state of APC/C^{Cdh1} activity between T_{eff} and T_{mem}, we extracted the copy number of key proteins in APC/C^{Cdh1} regulation. Copy number of Emi1 revealed that when accounting for Rb phosphorylation, Emi1 expression between T_{eff} and T_{mem} is identical (Figure 35). When looking at both E2 ubiquitin ligases required for APC/C^{Cdh1} functionality, they appear significantly higher in T_{eff}, but not by much, and indeed when comparing the fold increase from pRb- to pRb+ of either protein, neither T_{eff} nor T_{mem} show any difference in their expression of Ube2c or Ube2s (Figure 36).

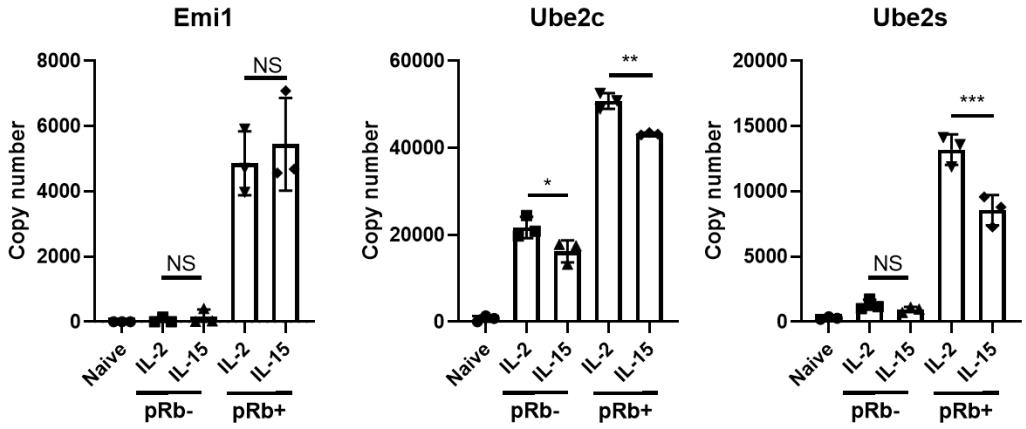

*Figure 35 Copy number of Emi1(left), Ube2c(middle), and Ube2s(both) from DIA dataset. Copy number was calculated using the Histone Ruler. Significance was determined by ANOVA, ***p<0.001, **p<0.01, *p<0.05, NS= Not Significant, n=3*

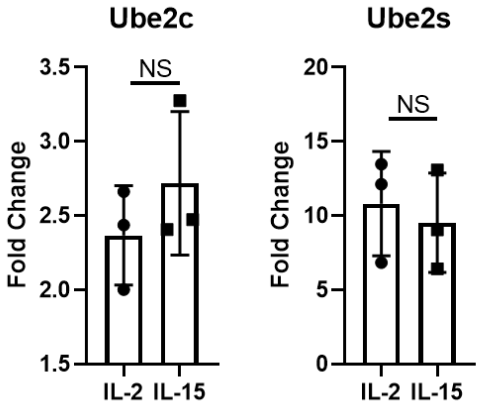

Figure 36 Fold change of copy number for Ube2c (left) and Ube2s (right) between pRb+ and pRb- populations of cells. Copy number was calculated using the Histone Ruler applied to DIA acquired intensities. Significance was determined by Student's T test NS= Not Significant. n=3

T_{mem} cells seems to have significantly more Plk1 copies that T_{eff}, which could indicate a greater extent of Cdh1 phosphorylation (Figure 37), but the increase was fairly marginal and so unlikely to be a major factor in APC/C activity. The only component of SCF $^{\beta\text{-TrCP}}$ complex itself which was increased in T_{eff} was the scaffold component Cul1, other components such as the E2 ubiquitin ligase binding Rbx1 and the substrate targeting Fbxw11 (Wu et al. 2003) showed no difference between either phenotype. Comparing fold change from pRb- to pRb+ of these proteins did not reveal any difference in behaviour between how these proteins behaved in either T_{eff} or T_{mem}, making it very unlikely that this pathway has been altered as a result of cytokine treatment.

Looking at proteins involved in mediating origin licensing, T_{eff} had increased copies of Cdt1, Cdc6 and Geminin, though notably Cyclin A2 levels were identical (Figure 38), possibly indicating a greater readiness for S-phase re-entry. Comparing fold change of pRb- to pRb+, the only significant difference was seen in Geminin levels, which increased in T_{mem} by 2.6 fold compared to the 2-fold change in T_{eff}.

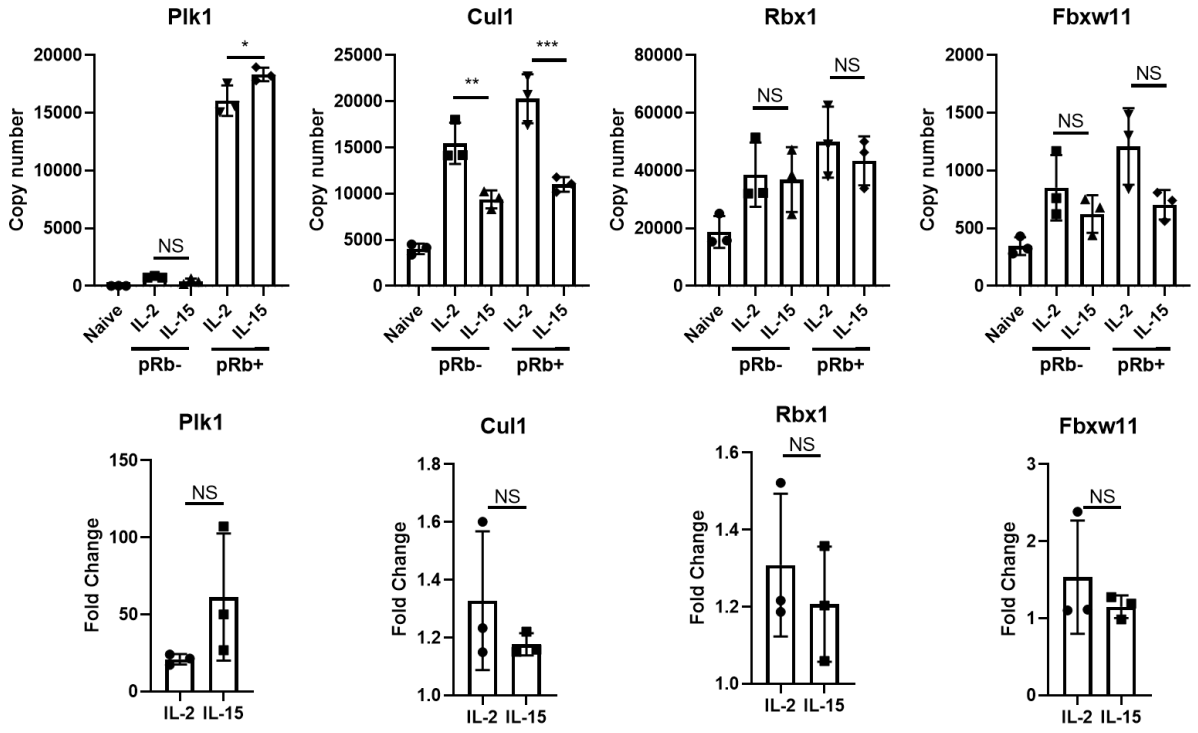

*Figure 37 Copy number (top) and fold-change from pRb+ to pRb- (bottom) of components of the SCF $^{\beta\text{-}TrCP}$ pathway for degrading Cdh1. Copy number was calculated using the Histone Ruler. Significance was determined by ANOVA (top) or by student's T test (bottom) ***p<0.001, **p<0.01, *p<0.05, NS= Not Significant, n=3*

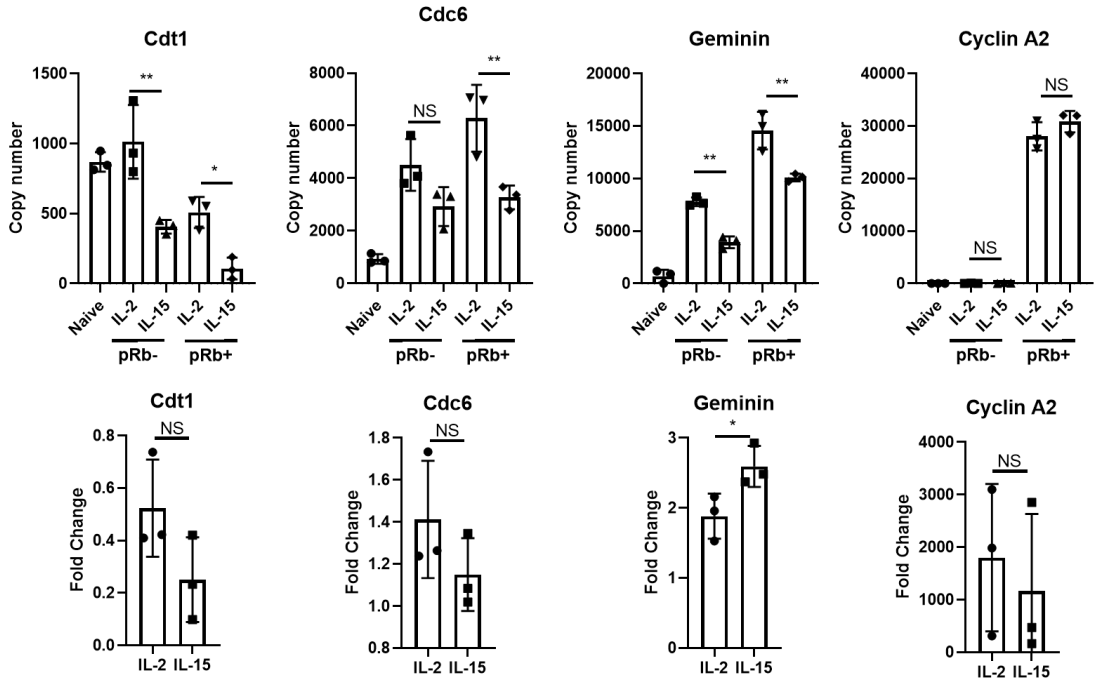

*Figure 38 Copy number (top) and fold-change from pRb+ to pRb- (bottom) of proteins important with mediating origin licensing. Copy number was calculated using the Histone Ruler. Significance was determined by ANOVA (top) or by student's T test (bottom) **p<0.01, *p<0.05, NS= Not Significant, n=3*

4.3.2 Global differences between T_{eff} and T_{mem}

As a general trend, T_{eff} had a greater number of copies of APC/C targets and indeed more widely on proteins across the board than T_{mem}, a disparity which is seen in both the pRb+ and pRb- populations. A similar pattern is observed between pRb+ and pRb- when focusing on only one of the two T cell phenotypes, where pRb+ T cells tend to have a richer number of copies (Figure 39). It is likely that this disparity is a result of the difference in cell size and density that each of these phenotypes have. Upon activation a naïve T cell blasts, growing in size as it gets ready to proliferate, but it has been observed that memory T cells revert back to a more naïve-like state, decreasing in both size and density (Allam et al. 2009).

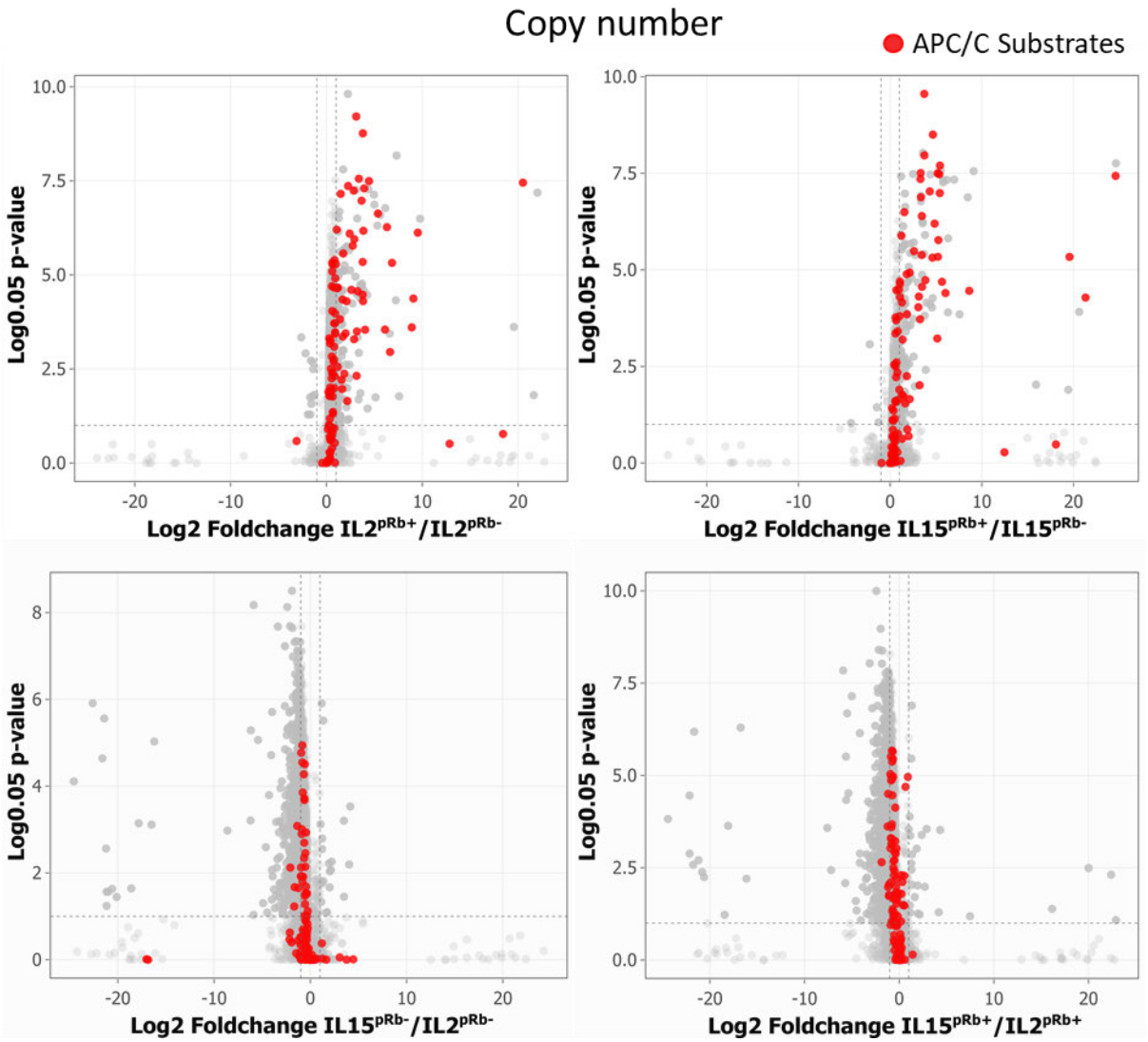

Figure 39 Volcano plots showing the comparison of the copy number between pRb+ pRb- groups in IL-2 (top left) and IL-15 (top right) treated T cells, and between IL-15 and IL-2 treated cells both within the p-Rb negative (bottom left) and the p-Rb positive (bottom right) populations. Red highlights proteins identified as APC/C substrates.. Significance was calculated using ANOVA followed by Tukey's test. n=3

To compensate for this, we examined the proteomes of T_{eff} and T_{mem} using ppm calculations (Figure 40), which shows that protein content ias more evenly distributed between IL-15 and IL-2 treated samples, yet the increase in protein content seen between pRb- and pRb+ was still apparent even in the analysis of ppm. What ppm revealed is that most APC/C substrates were significantly higher in abundance within the T_{mem} population for all pRb+ cells. Very few of these substrates reach a 2-fold increase from T_{eff} and thus are below the threshold of what could be considered a substantial shift in abundance. However, the general trend of distribution in samples between pRb- and pRb+ show APC/C substrate expression is skewed in favour of T_{mem} within pRb+ T cells (Figure 41), indicating that cycling T_{mem} may have a greater capacity for proliferation than cyclin T_{eff}.

A closer examination of the GO terms enriched in the pRb- populations (Figure 42) revealed a good enrichment score for terms associated with both cell cycle, protein manufacture, and cholesterol metabolism within T_{eff}, while T_{mem} showed a generally very low enrichment score, with terms mostly pertaining to a few domains.

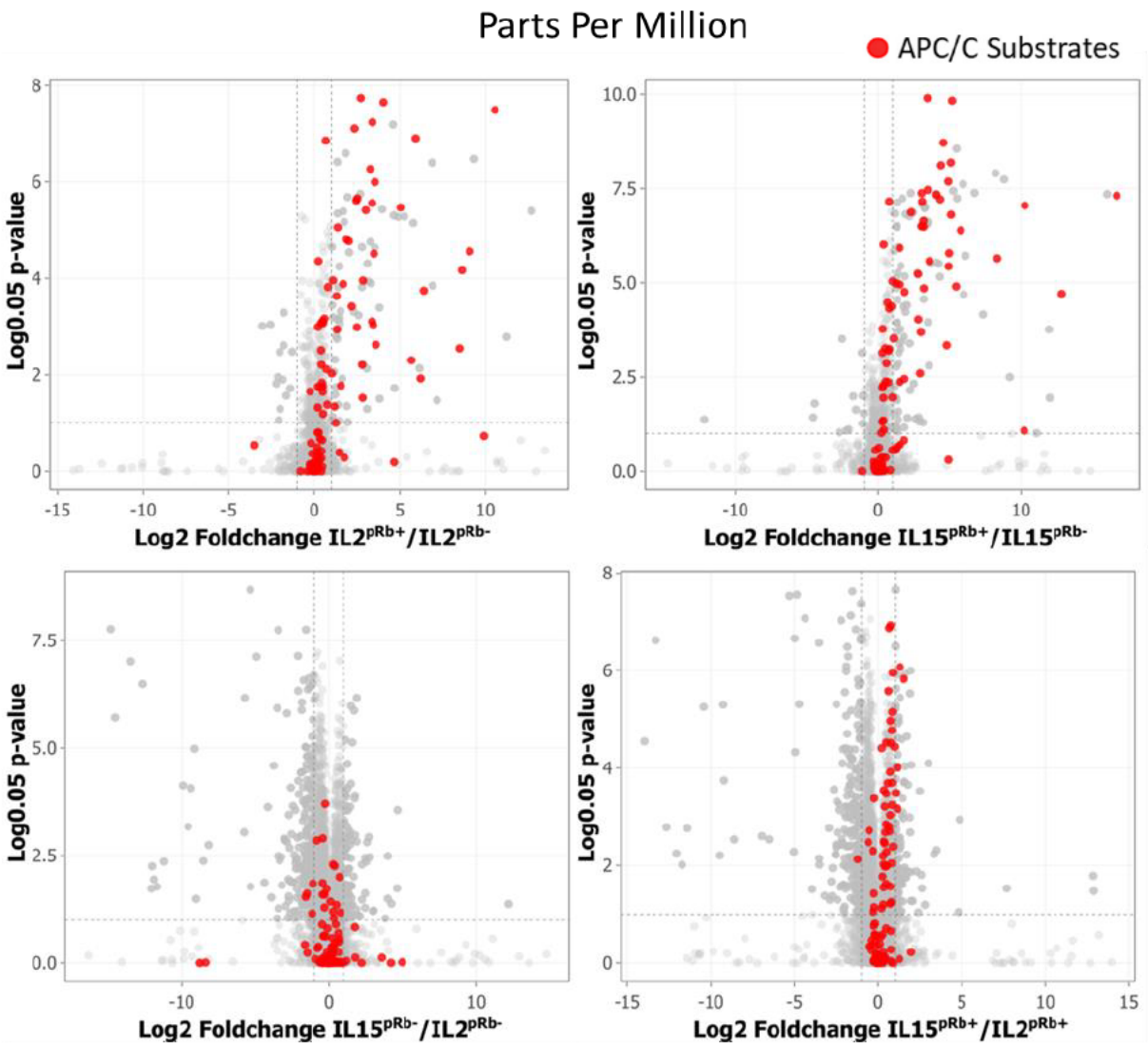

Figure 40 Volcano plots showing the comparison of ppm for each protein within the proteome between p-Rb positive and p-Rb negative groups in IL-2 (top left) and IL-15 (top right) treated T cells, and between IL-15 and IL-2 treated cells both within the p-Rb negative (bottom left) and the p-Rb positive (bottom right) populations. Red highlights proteins identified as APC/C substrates.. Significance was calculated using ANOVA followed by Tukey's test. n=3

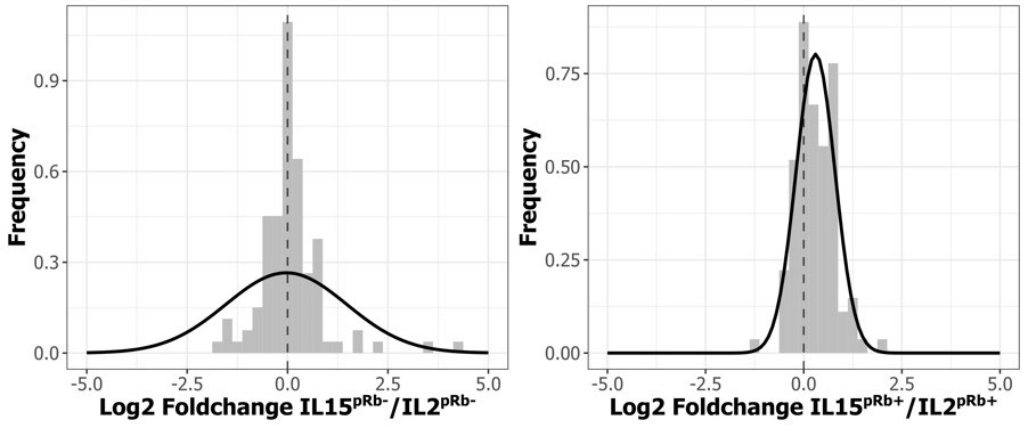

Figure 41 Histograms showing range of fold change of the parts per million calculation for APC/C substrates acquired from DIA proteomic dataset. Fold change of IL-15 against IL-2 for population of p-Rb- (left) and p-Rb+ (right). Dotted line shows the central bar where a fold change of 0 is recorded for these proteins. Curve shows the distribution. If the apex of the curve's peak is on the dotted line, the data is normally distributed.

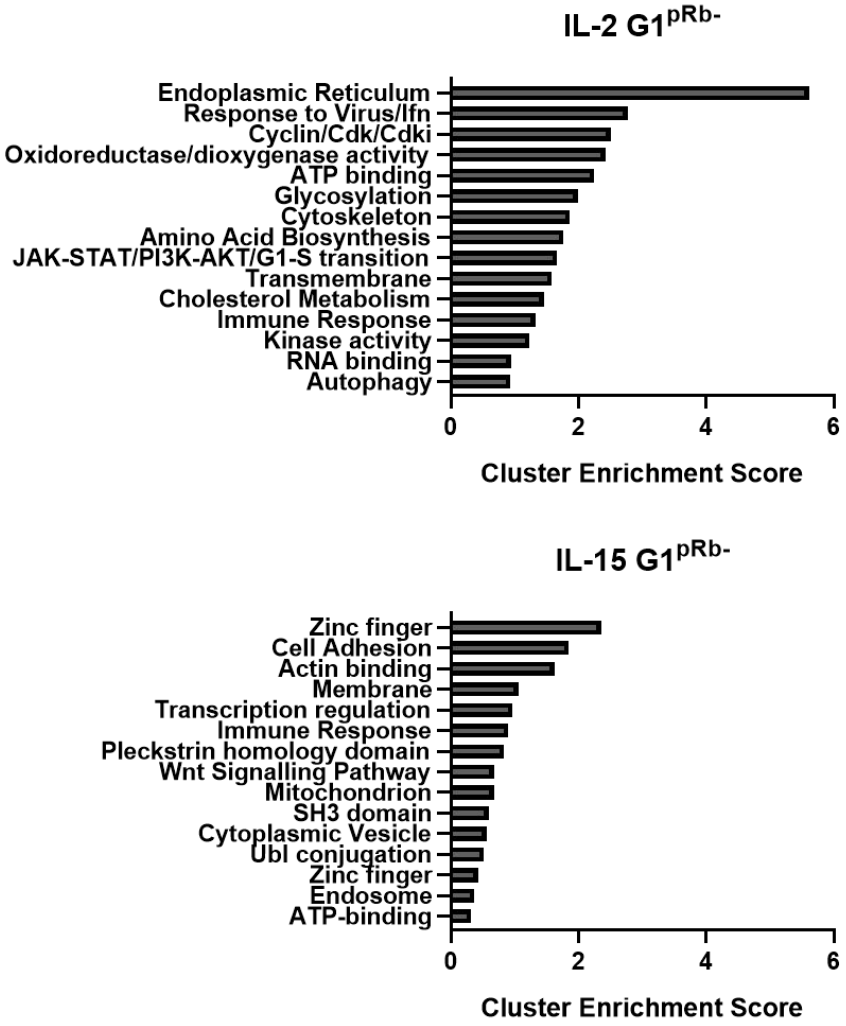

Figure 42 DAVID GO terms and enrichment scores generated from proteins which were significantly different between, and at least 2-fold greater in parts per million between IL-2 (top) and IL-15 (bottom) treated samples which were p-Rb+. 223 proteins were included for IL-2 dataset and 103 proteins from the IL-15 dataset. First 15 most enriched selected. Enrichment score denotes importance of the group term to the list by ranking biological significance of gene groups based on all p-value EASE scores of all enriched terms.

4.3.3 pRb- populations and Naïve T cells

Having examined the proteome of both cycling pRb+ $CD8^+$ T cells and the potentially more dormant pRb- $CD8^+$ T cells, we considered it necessary to establish how different the pRb- group was from the far more quiescent naïve phenotype. Even when using the more proportional measure of ppm to calculate fold change between naïve and pRb- T_{eff} (Figure 43), compared with naïve $CD8^+$ T cells there is a skew of distribution with 1395 proteins identified as significantly greater than 2-fold increased in IL-2 treated cells versus 498 proteins in naïve cells. The same can be seen between naïve and $T_{mem,}$ with 873 proteins higher in IL-15 treated versus 329 proteins higher in naïve, all of which supporting naïve T cells having a generally lower protein content.

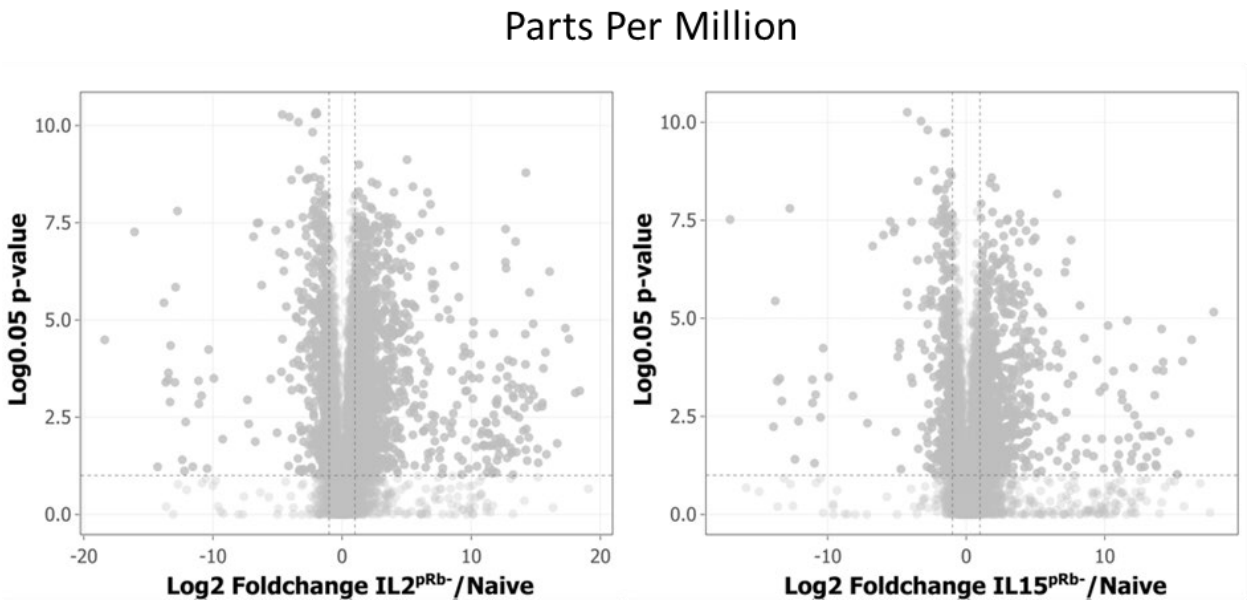

Figure 43 Volcano plots showing the comparison of ppm for each protein within the proteome between naïve T cells, and the pRb- population of either IL-2 (left) or IL-15 (right) treated cells. Significance was calculated using ANOVA followed by Tukey's test. n=3

Between pRb- T_{eff} and Naïve T cells, the naïve cells are enriched with proteins associated with metabolism with terms such as Mitochondrion, Lipid metabolism, and Respiratory chain appearing with good enrichment scores (Figure 44).

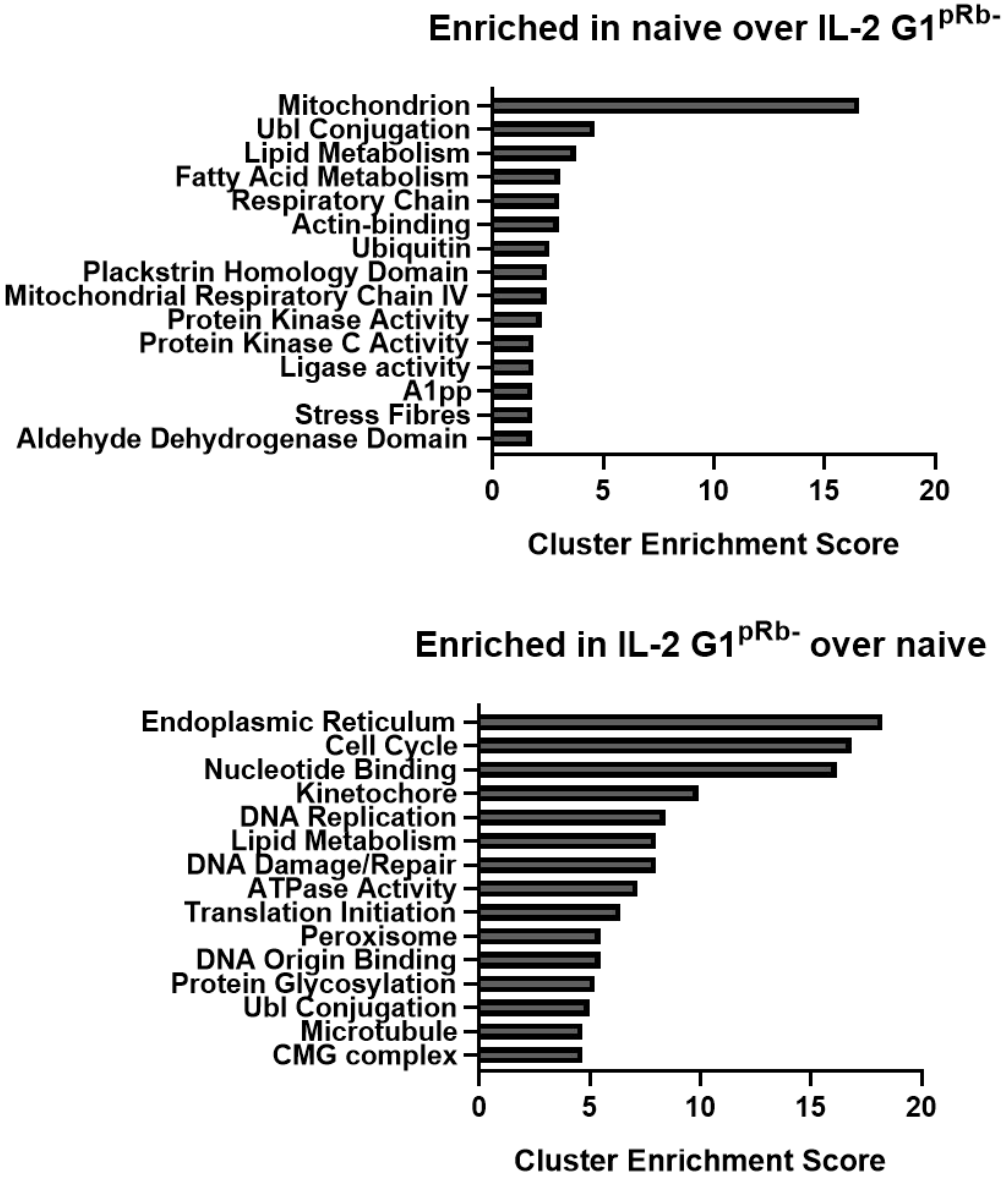

Figure 44 DAVID GO terms and enrichment scores generated from proteins which were significantly different between, and at least 2-fold greater in parts per million between naïve T cells (top) and pRb- IL-2 treated T cells (bottom). 498 proteins were included for IL-2 dataset and 1395 proteins from the IL-15 dataset. First 15 most enriched selected. Enrichment score denotes importance of the group term to the list by ranking biological significance of gene groups based on all p-value EASE scores of all enriched terms.

While T_{eff} instead show a high enrichment of protein manufacture processes including terms like Endoplasmic Reticulum, Glycosylation, and Translation initiation, as well as general cell cycle terms, all of which indicate that the Teff cells in $G1^{pRb-}$ are still very much a part of the cell cycle when compared with the more G0 naïve T cells. A similar pattern of enrichment distribution can also be seen between naïve and T_{mem} (Figure 45) demonstrating that neither pRb- T_{eff} nor T_{mem} closely resemble the naïve quiescent state.

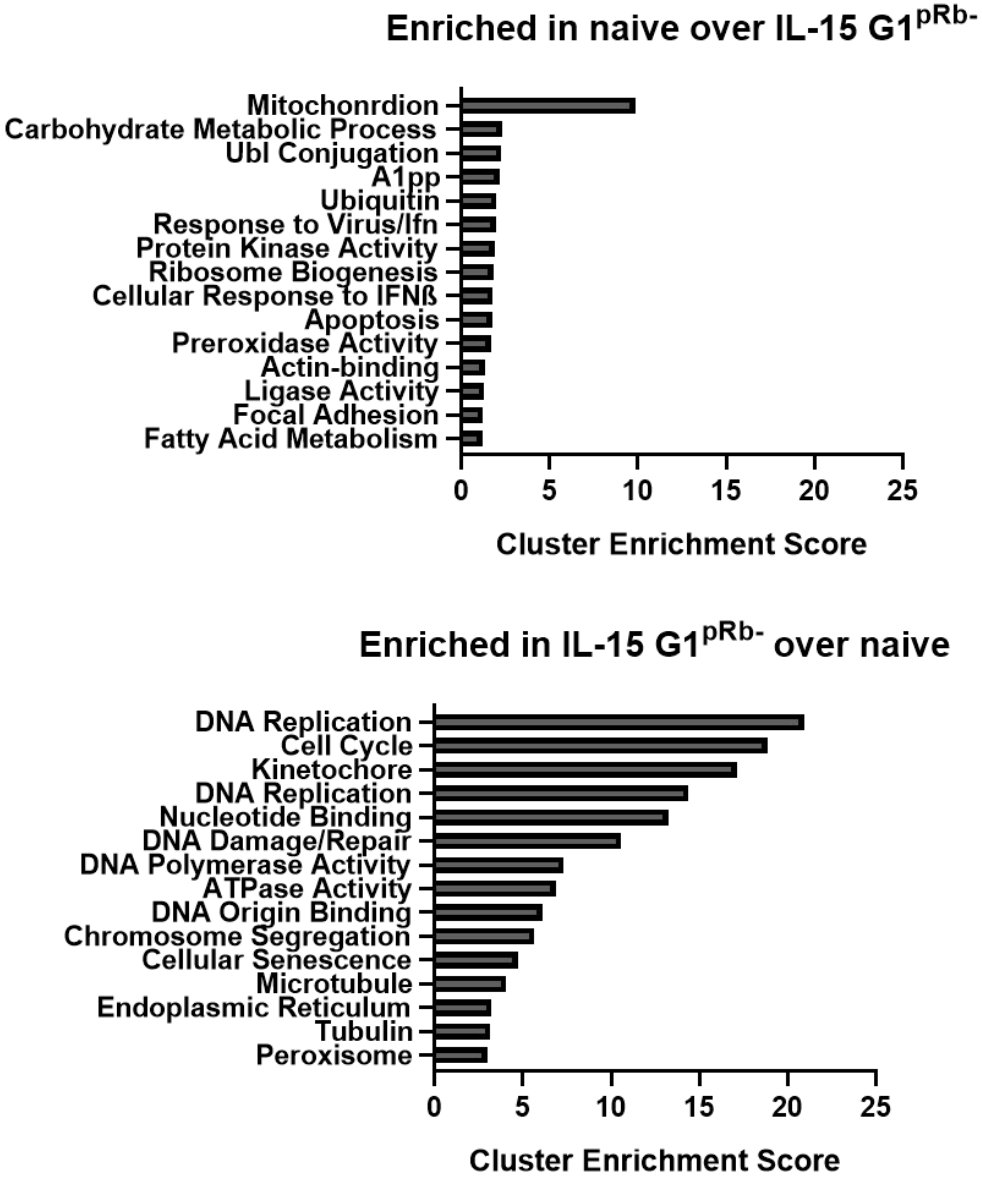

Figure 45 DAVID GO terms and enrichment scores generated from proteins which were significantly different between, and at least 2-fold greater in parts per million between naïve T cells (top) and pRb- IL-15 treated T cells (bottom). 329 proteins were included for IL-2 dataset and 873 proteins from the IL-15 dataset. First 15 most enriched selected. Enrichment score denotes importance of the group term to the list by ranking biological significance of gene groups based on all p-value EASE scores of all enriched terms.

4.3.4 pRb+ populations of T_{eff} and T_{mem}

Proteins which were high in the pRb+ groups would indicate proteins which are upregulated in both T_{eff} and T_{mem} which were already committed to cell cycle completion. Looking at the enrichments of GO terms within the pRb+ of T_{eff} and T_{mem} (Figure 46) we found that T_{eff} had a higher enrichments in proteins associated with metabolic processes such as Amino Acid Biosynthesis, Glycolysis, and Oxidoreductase activity. In addition there was a higher enrichments in terms linked with vesicle transport, and vesicles such as Lysosome, Endosome

and Autophagy, possibly pointing to an increase in protein trafficking and degradation. Conversely, T_{mem} which instead showed more typical enrichments to cell cycle processes such as of DNA damage repair and the general Cell cycle GO terms, in and amongst the protein domain terms.

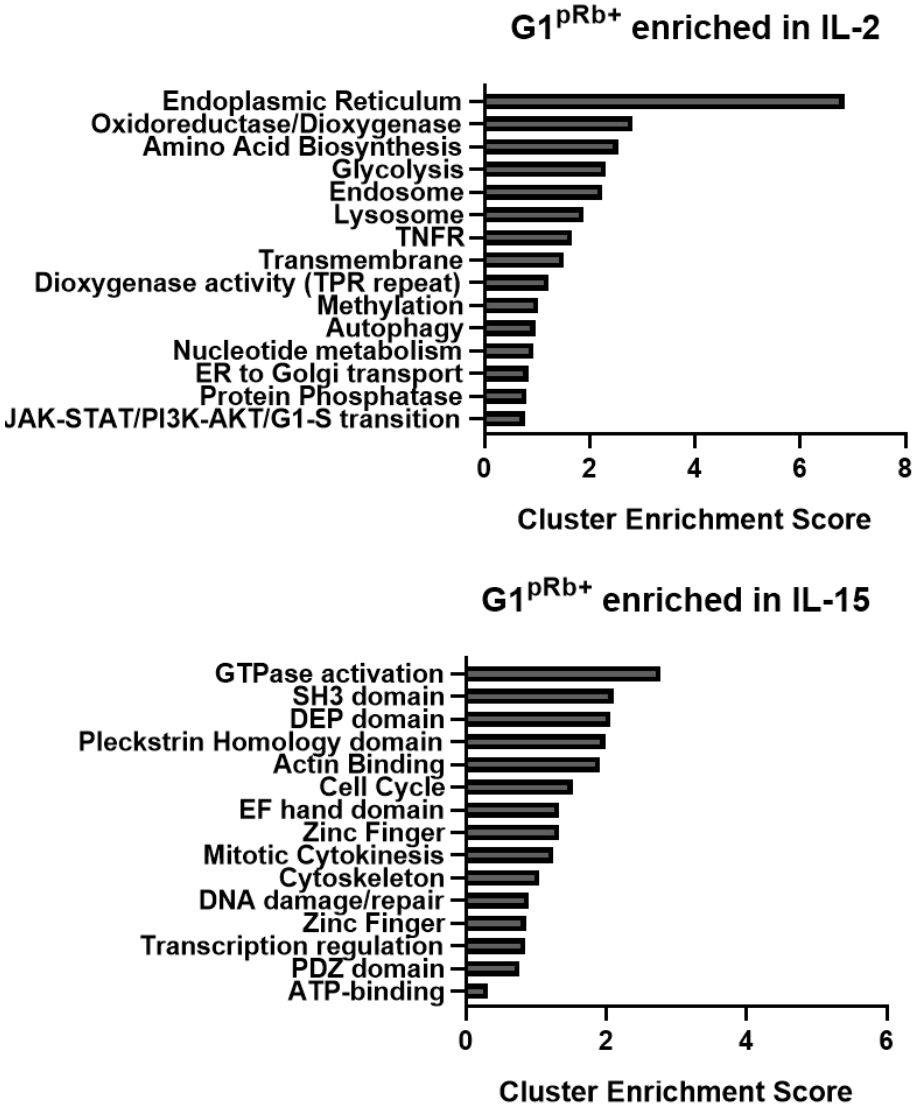

Figure 46 DAVID GO terms and enrichment scores generated from proteins which were significantly different between, and at least 2-fold greater in parts per million between pRb+ populations of IL-2 (top) and IL-15 (bottom) treated T cells (right). 219 proteins were included for IL-2 dataset and 112 proteins from the IL-15 dataset. First 15 most enriched selected. Enrichment score denotes importance of the group term to the list by ranking biological significance of gene groups based on all p-value EASE scores of all enriched terms.

To compare which cell cycle proteins featured more prominently in these two cycling groups, the cell cycle GO cluster of the IL-15 treated and the G1-S transition GO cluster of IL-2 treated groups were examined to see which genes were included (Table 3).Within the T_{eff} we find both Cyclin D3 and Cdk6, but also two Cdk inhibitors, p21 and p15, while the T_{mem} has mostly M

phase associated proteins, including the APC/C^{Cdc20} components, Cdc20 and Ube2s. This could indicate a difference in emphasise over aspects of cell cycle control, with T_{eff} more focused on controlling S-phase re-entry, and T_{mem} on Mitotic exit.

IL2pRb+ JAK-STAT/PI3K-AKT/ G1-S transition	IL-15pRb+ Cell Cycle
Cdkn1a	Esco2
Cdk6	Cep131
Ccnd3	Rabgap1
Cdkn2b	Racgap1
Bcl2	Ube2s
Eif4ebp1	Nusap1
IL2ra	Cdc20
Pim2	Cenpx
Cinp	Pimreg
Nek6	
Il12rb1	
Kif7	
Rasgrp1	
Junb	
Pik3ap1	
Pck2	
Sqstm1	
Nedd4	
Abcc1	

Table 3 List of gene names that made up the JAK-Stat/PI3K-AKT/G1-s transition cluster in IL-2^{pRb+} (left) and the cell cycle cluster of the IL-15^{pRb+} (right) groups as clustered by DAVID.

To better assess how the transition from pRb- to pRb+ differed between T_{eff} and T_{mem}, we selected proteins that were significantly greater in copy number by more than 2-fold in pRb+ compared with pRb- in both the IL-2 treated and IL-15 treated samples and conducted an enrichment analysis of the GO terms on the protein list that came up for both these selections. We found that the types of GO terms which were enriched in either T_{eff} and T_{mem} were fairly similar to one another (Figure 47), with both featuring typical cell cycle terms including Microtubule, Kinetochore, Kinesin, DNA Damage/Repair, etc.

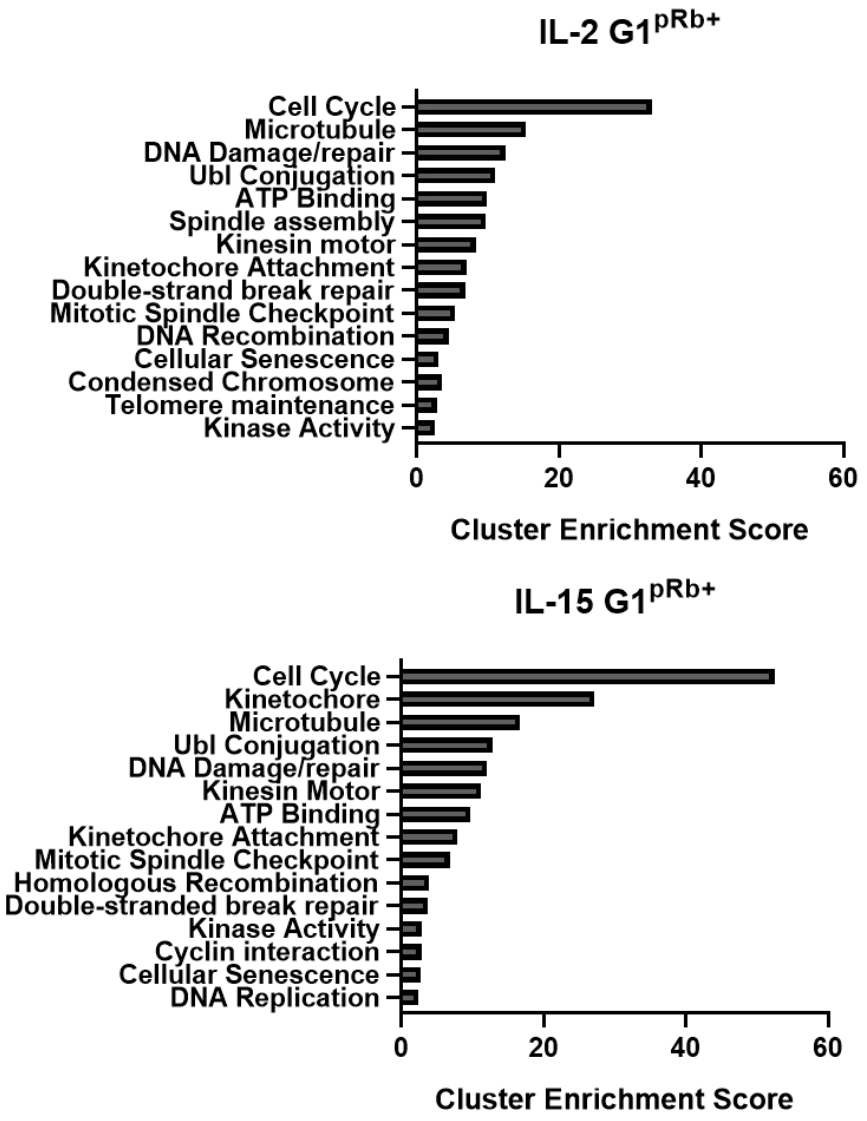

Figure 47 DAVID GO terms and enrichment scores generated from proteins which were significantly different between and at least 2-fold greater in copy number between $G1^{pRb+}$ and $G1^{pRb-}$ in IL-2 treated cells (top) and IL-15 treated cells (bottom). 179 proteins were included for IL-2 dataset and 159 proteins from the IL-15 dataset. First 15 most enriched selected. Enrichment score denotes importance of the group term to the list by ranking biological significance of gene groups based on all p-value EASE scores of all enriched terms.

To better identify the differences between these two cycling phenotypes, we assessed that 177 proteins appeared in both groups, 42 proteins were unique to T_{eff}, and 62 unique to T_{mem} (Figure 48). Another GO term enrichment analysis was conducted on the list of proteins unique to T_{eff} and to T_{mem} (Figure 49), the results of which yielded fairly low number of GO terms, though this is likely due to the relatively short gene list provided for the analysis. The terms that did come up however where still fairly similar between both T_{eff} and T_{mem}.

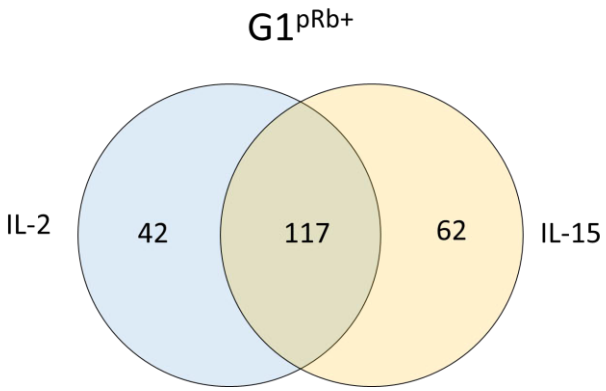

Figure 48 Venn diagram of genes which were significantly different between, and at least 2-fold greater in copy number between G1^{pRb+} and G1^{pRb-} Total list was made from list of statistically significant increase of ≥2-fold change within IL-2 stimulated cells (179 genes) and IL-15 stimulated cells (159 genes)

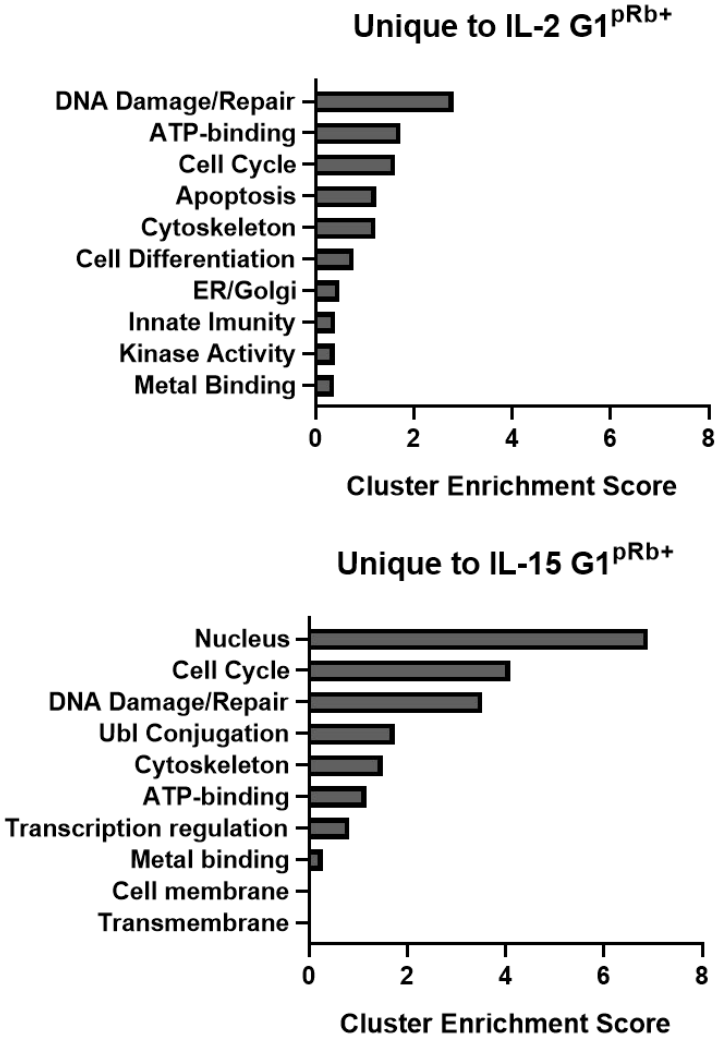

Figure 49 DAVID GO terms and enrichment scores generated from proteins which were identified as unique to G1^{pRb+}T cells from both IL-2 treated (top) and IL-15 treated cells (bottom). Unique proteins are proteins which appeared as significantly above 2-fold change higher in pRb+ against pRb- populations which only appeared in one dataset. 42 proteins were included for IL-2 dataset and 62 proteins from the IL-15 dataset. First 10 most enriched selected. Enrichment score denotes importance of the group term to the list by ranking biological significance of gene groups based on all p-value EASE scores of all enriched terms.

To discern whether there were any differences between proteins that were upregulated for cycling T_{eff} and T_{mem}, a list of genes from the Cell Cycle GO term cluster from both lists was compiled to compare which proteins were unique to either group and which were common to both (Table 4).

IL-2 unique Cell Cycle	IL-15 unique Cell Cycle	Common Cell Cycle			
Anapc16	Cdc45	Anln	Chek1	Incenp	Prr11
Cdca5	Cdk4	Arhgap19	Cit	Kif11	Pttg1
Cenps	Cenpj	Asf1b	Ckap2l	Kif18a	Racgap1
Cks1b	Chaf1b	Aspm	Ckap2l	Kif18b	Rbl1
Helq	Gmnn	Aurka	Ckap5	Kif20a	Rrm2
Melk	Kif14	Aurkb	Cuedc2	Kif20b	Sgo1
Rad51	Kif2c	Birc5	Dck	Kif22	Ska1
Rad51d	Mis18a	Blm	Diaph3	Kif23	Ska3
Sass6	Ppm1d	Brca1	Dlgap5	Kifc1	Slbp
Zwilch	Tipin	Brip1	E2f2	Knl1	Slfn9
	Triobp	Bub1	E2f7	Knstrn	Spag5
	Ube2c	Bub1b	E2f8	Kpna2	Spc24
	Zwint	Ccna2	Ect2	Mastl	Spc25
		Ccnb1	Emi1	Ndc80	Spdl1
		Ccnb2	Esco2	Nde1	Tacc3
		Ccp110	Espl1	Nuf2	Tk1
		Cdc20	Fam111a	Nusap1	Top2a
		Cdca2	Fancd2	Pclaf	Tpx2
		Cdca3	Fignl1	Pimreg	Ttk
		Cdca7	Foxm1	Pkmyt1	Ube2s
		Cdca8	Gtse1	Plk1	Uhrf1
		Cenpe	Hjurp	Polr3g	
		Cenpf	Hmmr	Prc1	

Table 4 List of gene names that made up the Cell Cycle cluster in IL-2^{pRb+} (left) the IL-15^{pRb+} (middle), and where common between both groups (right). Clustered were provided by DAVID GO Enrichment Analysis.

90 Cell Cycle associated genes were found to be common between both cycling T_{eff} and T_{mem}, 10 were found to be unique to cycling T_{eff} and 13 unique to cycling T_{mem}.

It is possible that some proteins which have been identified as unique to either cycling T_{eff} or T_{mem} may have been on the cusp of being at 2-fold change and were in fact just over the cut-off for one set and just below for the other. To better scrutinise how unique these proteins were to their respective phenotype, we checked the fold change originally calculated and plotted it back on the original volcano plot.

Most proteins identified as unique to cycling T_{mem} were actually very similar in how they behaved between pRb- and pRb+ T_{eff}, with only a small shift in fold change (Figure 50).

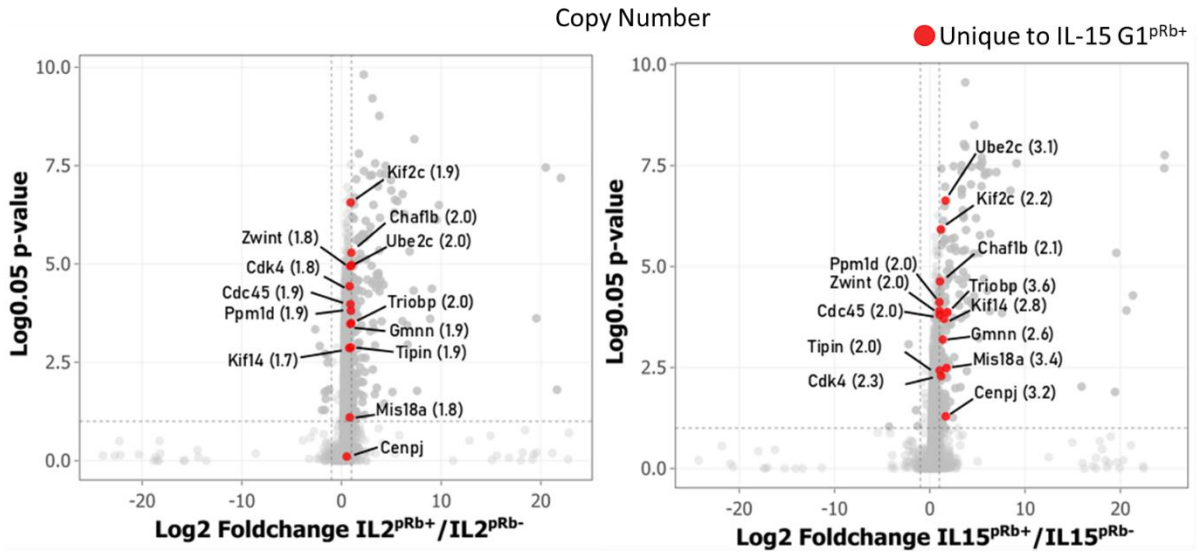

Figure 50 Volcano plots showing the comparison of the copy number between p-Rb positive and p-Rb negative groups in IL-2 (left) and IL-15 (right) treated T cells, Red highlights proteins identified as unique to cycling IL-15 treated cells. Numbers in brackets depict fold change difference for all proteins that are p<0.05. Significance was calculated using ANOVA followed by Tukoys test. n=3

The only exception to this was Cenpj which was not significantly different between pRb+ and pRb- IL-2 treated cells. The proteins unique to T_{eff} on the other hand did not show such similarity, with many of them not significantly different between pRb+ and pRb- subpopulations of T_{mem} cells. The most notable of which were Melk, Sass6 and Cdca5, which showed a significant increase of greater than 30-fold change only within T_{eff} (Figure 51).

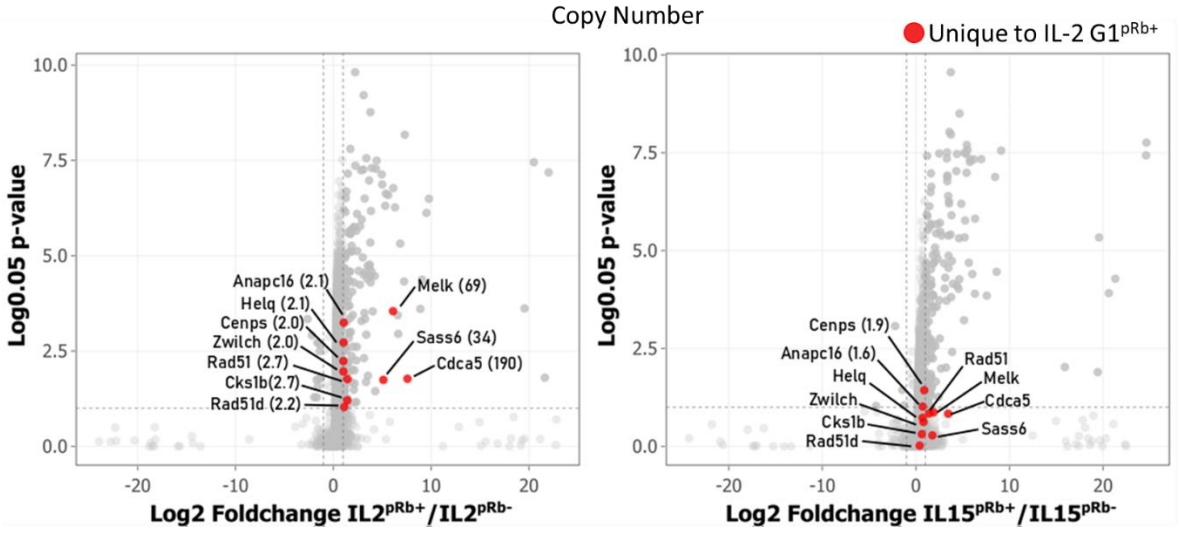

Figure 51 Volcano plots showing the comparison of the copy number between p-Rb positive and p-Rb negative groups in IL-2 (left) and IL-15 (right) treated T cells, Red highlights proteins identified as unique to cycling IL-2 treated cells. Numbers in

brackets depict fold change difference for all proteins that are p<0.05. Significance was calculated using ANOVA followed by Tukey's test. n=3

4.4 Discussion

In this chapter we examined the proteome of cycling $CD8^+$ T cells, and identified a number of mechanisms which help define the regulatory network of cell cycle, and how it differs following differentiation between memory and effector phenotypes, both in relation to APC/C control and more globally.

Of the proteins identified as novel cell cycle regulators that were significantly different between $G1^{pRb+}$ to $G1^{pRb-}$, most were already known to be cell cycle regulated, despite lacking the GO terms. Slbp is understood to bind to histone mRNA, and is required for histone pre-mRNA processing in late S phase (Zheng et al. 2003). Slbp is known to be cell cycle regulated, degraded by $SCF^{Cyclin\ F}$ as the cells exit S phase (Dankert et al. 2016). Bard1 forms a complex with Brca1, becoming a ubiquitin ligase which is influences DNA repair, centrosome regulation, and transcription (Parvin 2009) and is a known target of APC/C^{Cdh1} (Song and Rape 2010). Atad2 is expressed predominately in S phase, and is shown to promote proliferation in a number of different cancer models (Dutta et al. 2022; Koo et al. 2016; Zhou et al. 2020), while Rad54l is involved with DNA damage repair and is seen to enhance S phase entry in bladder cancer by inhibiting p53 and p21 activity while promoting Rb phosphorylation (Wang et al. 2022).

Pdcd7 has yet to be identified as cell cycle regulated, but is known to trigger apoptotic pathways within T cells (Jung Park et al. 1999), and is upregulated in anergic $CD8^+$ T cells (Baas et al. 2016). It is part of the $G1^{pRb+}$ peaking group, and thus only especially high as the $CD8^+$ T cell first approaches S phase but lowers once DNA replication begins. It may be that this rise is a kind of protection measure, ensuring that the cell is prepped to die at the first sign of genomic instability.

Within the $G1^{pRb-}$ group, Ctla4 and Acvrl1 were identified as raised, both of which are surface markers which are associated with decreased TCR mediated activation, Ctla4 by decreasing CD28 co-stimulation and thus increasing the likelihood of anergy and Acvrl1 by making up part of the TGFβ receptor (Oh et al. 2000; Rowshanravan, Halliday, and Sansom 2018; Tinoco et al. 2009).

Most intriguing was the finding of Usp1, a deubiqutinase which has been reported to target APC/C^{Cdh1} substrates to prevent their degradation which we identified as having a periodic pattern which clustered in the $G1^{pRb-}$ group. Particularly notable substrates include Id proteins (Williams et al. 2011). Id proteins have a role in directing T cell differentiation, with Id2 inhibiting factors which otherwise promote the MPEC phenotype, and Id3 instead promoting them, though the exact mechanism is yet to be (Hwang, Im, and Rudra 2022).

Interestingly, while Id2 is a known target of APC/C^{Cdh1}, and has been shown to increase in abundance with expression of Emi1, Id3 lacks the targeted D-box motif and is thus unaffected by APC/C^{Cdh1} activity (Lasorella et al. 2006). With Usp1 at a fairly consistent level once outside of $G1^{pRb-}$ phase, it may be the case that cells that spend more time in $G1^{pRb-}$, where both Emi1 and Usp1 are low, levels of Id2 would also be low, leading to a greater bias towards MPEC generation. This could present mechanism through which $CD8^+$ T cells that are geared towards rapid re-entry into cell cycle by APC/C^{Cdh1} inhibition would enhance Id2 levels and thus push cell cycle development towards the T_{eff} phenotype.

Contrary to what had been reported in Immpres, T_{eff} and T_{mem} showed very similar copy numbers of Emi1. The reason for this may be that the data in ImmPRes did not separate pRb+ and pRb- subsets within a population. Our dataset reveals that pRb+ T cells have a far higher expression of Emi1 compared with pRb- cells, in which Emi1 is barely expressed at all. Unsorted T_{mem} are predominately pRb-, so it is likely that a mixed population may appear to have decreased overall levels of Emi1 due to the decreased number of Emi1 expressing pRb+ cells within the population. This finding illustrates the need for caution when undertaking meta-analysis data from which can be skewed by the presence of a population of actively cycling and stalled cycling cells, especially when examining components of the proteome which are cell cycle regulated.

It is important to reflect on the subgroups we might be unable to discriminate against when analysing the proteome of a particular population. For the pRb- group, it is likely that the T_{eff} and T_{mem} contain very different types of cells, some of which are gearing up to re-enter cell cycle immediately, and some which have stalled at the early G1 stage and may have even entered in to a state of quiescence. It is likely that T_{eff} are predominately made up of this first category. This is supported by the enriched GO terms for cyclins present, as well as terms for Cholesterol metabolism, which is known to be associated with improved proliferation (Yang

et al. 2021). While the T_{mem}, which lack these terms and are mostly made up of pRb- cells, could have a larger proportion of the population closer to quiescence. However, there was a clear difference in how pRb- cells of either T_{mem} or T_{eff} compared to naïve T cells with the latter in both cases showing a lack of cell cycle associated proteins entirely, favoring more oxphos metabolic processes seen more in non-proliferating cells generally (Kalucka et al. 2015). Interestingly, when looking at the proportional differences in the proteome between pRb+ T_{eff} and T_{mem}, glycolysis was highlighted as an enriched term within T_{eff}, a metabolic process associated with getting past restriction point. This may indicate that T_{eff} have a greater capacity for S phase re-entry (Kalucka et al. 2015).

When comparing proteins which increase from the pRb- to pRb+ within both phenotypes, they appear to share a number of processes. This includes Cyclins B1, B2, and A2, as well as cell cycle progression supporting E2F2 and its inhibitors E2F7 and E2F8 and APC/C regulator Emi1, all of whom are known APC/C^{cdh1} targets. Other notable proteins common to both phenotypes are a number of Kinesin motor proteins, Kinetochore components, spindle assembly checkpoint proteins, and other proteins associated with M phase. However, of the unique proteins to $T_{eff,}$ three stood out as highly upregulated, these being Sass6, Melk, and Cdca5.

Sass6 has a role in promoting centriole assembly (Ito et al. 2019), and recent studies show Sass6 binds with E2F4 and E2F5 (Hazan et al. 2021), though the downstream effect of this in $CD8^+$ T cells is not yet known. There is early evidence however, which indicates Sass6 may be essential for centriole formation in ES cells (Grzonka and Bazzi 2022). Cdca5 is transcribed by E2F1, and enhances cell proliferation by enhancing the AKT-Erk pathway (H. Chen et al. 2019; Nguyen et al. 2010) and has been shown to enhance the stemness capacity in breast cancer cells and adrenocortical carcinoma (Hao et al. 2022; Shi et al. 2021).

Melk, another target of E2F1 (Sun et al. 2021), phosphorylates Foxm1 leading to an array of different effects including enhancing kinetochore assembly, and enhancing Plk1 mediated degradation of Cdh1 within muscle stem cells (Chen et al. 2020; Costa 2005), and is understood to be essential for glioma stem cell proliferation (Joshi et al. 2013). This may be further evidence that $CD8^+$ T cells share mechanisms with stem cells to maintain their rapid proliferation and could indicate the T_{eff} may be more stem-like in their regulatory systems than T_{mem} at this stage in their development.

Looking further afield, we observed that the components of other processes that involved APC/C regulation, namely the expression of Ube2c and Ube2s and Cdh1 degradation by SCF, did not show any particular bias towards T_{eff} or T_{mem} beyond a general trend of raised copy number in T_{eff} which could simply be a result of increase protein density in general.

While this might seem to contradict our model, which predicts that T_{mem} would have a more active APC/C^{Cdh1} than T_{eff}, there is still a very strong correlation between Emi1 high population, and the pRb+ population. Somewhat surprisingly, when comparing pRb+ populations, T_{mem} had a generally higher proportion of APC/C substrates, as well as high relative count of M phase proteins including Kinetochore components, Spindle formation, and Ube2s and Cdc20, while higher in T_{eff} were Cdk inhibitors p21 and p16. All of which may suggest that, while IL-15 might influence more cells towards a more prolonged G1, the cells that do remain in cycle may be better able to maintain a faster cell cycle than T_{eff}.

Together, these results suggest that both T_{eff} and T_{mem} employ similar strategies of APC/C^{Cdh1} inhibition via Emi1 to attain a rapid proliferative phenotype when cycling, but IL-15 stimulation encourages cell to remain in $G1^{pRb-}$. The decision point for this change in behaviour likely occurs at a time point earlier than that captured in this study. Our proposed model, that Emi1 enables rapid S-phase entry, is unlikely to be the only factor which separates the cell cycle behaviour of T_{eff} and T_{mem}, yet our analysis has indicated a possible mechanism in which Emi1 and Usp1 enable enhanced expression of Id2 and thus a greater capacity for T_{eff} differentiation, though this will need to be investigated in greater depth.

5 Emi1 KO results in re-replication and impaired S phase entry in IL-2 mediated expansion

5.1 Introduction

Emi1 inhibition of APC/C is understood to be an important factor enabling not only rapid S-phase re-entry, but also has a role in enabling differentiation of ES cells (Ballabeni et al. 2011; Bar-On, M. Shapira, et al. 2010). The evidence presented in previous chapters details that $CD8^+$ T cells share a number of regulatory mechanisms with ES cells and that control of APC/C at the G1/S checkpoint is key. We hypothesised that an excess of Emi1 would prevent the formation of APC/C^{Cdh1} within CD8 T cells, enabling the rapidly proliferative phenotype seen in IL-2 treated $CD8^+$ T cells, but that this would not be the case in the slower proliferating IL-15 treated $CD8^+$ T cells.

However, our proteomic analysis was not able to resolve the question of whether Emi1 decrease lead to or was instead a result of cells stalling in G1 following IL-15 stimulation. In order to assess this more directly, it became necessary to design a protocol which is able to prevent Emi1 from functioning and then observe how this impacts cell cycle. Creating a knockout phenotype by conventional ES cell targeting is not possible however, as Emi1 knockout has proved to be embryonic lethal in mice (Lee et al. 2006). Other studies which have tried to define the activity of Emi1 instead focus on knock down (KD) studies utilising siRNA or morpohlino oligonucleotides (Machida and Dutta 2007; Shimizu et al. 2013; Verschuren et al. 2007). However, this approach is not appropriate for $CD8^+$ T cells as there is evidence which shows small RNAs could be detected by Toll-like Receptors, producing off-target effects which may alter T cell functions (Richardt-Pargmann et al. 2011).

Cas9 Crispr allows for a precise gene editing of cells which can be applied *in vitro*. It works by taking advantage of the Cas9 enzyme, which cleaves DNA proximal to the site of the Protospacer Adjacent Motifs (PAM) sequences. To specify its target, a guide sequence (gRNA) which recognizes a specific region near the PAM sequence, is combined with the Trans-Activating CrispR RNA (TracrRNA) which can then bind to the Cas9 enzyme itself. This Cas9 complex then creates double stranded breaks at the gene targeted by the gRNA (Anders et al. 2014; Garneau et al. 2010).

If our hypothesis is correct, then by knocking out Emi1 in cycling T_{eff}, we should expect to see a drop in proliferation as APC/C^{Cdh1} would remain high, obstructing cells from entering into S-phase.

5.1.1 Development of Emi1 KO

$CD8^+$ T cells were transfected with Emi1 targeting Cas9 complex at 48 hours post activation in order to ensure the cells had switched from TCR driven to IL-2 driven proliferation. After this point, cells were left in medium with fresh IL-2 provided daily and samples were collected at the 72 hour and 96 hour time point (Figure 52).

We utilised two guides, G12 and G44, each of which targets the PAM sequence of a separate exon of the Emi1 gene. We also utilised a guide which targeted Thy1, a cell surface expressed marker on T cells which has no known function on cell cycle regulation. Thy1 knockout is easy to verify by flow cytometry and thus serves as an ideal non-target control. Tracking of Indels by Decomposition (TIDE) Analysis, allows use to detect the presence of inserts or deletions (indels) within a sequence (Brinkman et al. 2014). This tool enables us to track which part of a sequence has been disrupted via the presence of indels, and the percentage of genetic material that contains indels, and thus the percentage of our sample which has been successfully knocked out. We determined that both guides were capable of inducing indels which were persistent at both 72hr and 96hr time points(Figure 53 left), and that compared to the no guide control and the non-target control, both guides had a significant impact on cell expansion (Figure 53 right).

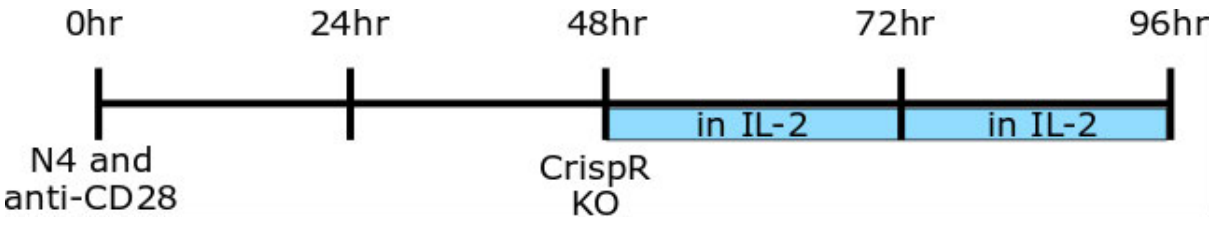

Figure 52 OT-1 T cells were extracted from the lymph nodes and plated with N4 and anti-CD28 at the 0hr time point, and incubated for 48 hours, at which point they were subjected to electroporation with or without the Cas9 CrispR guide complex. The cells were returned to IL-2 which was supplemented daily, with samples taken for analysis at the 72hour and 96 hour time point.

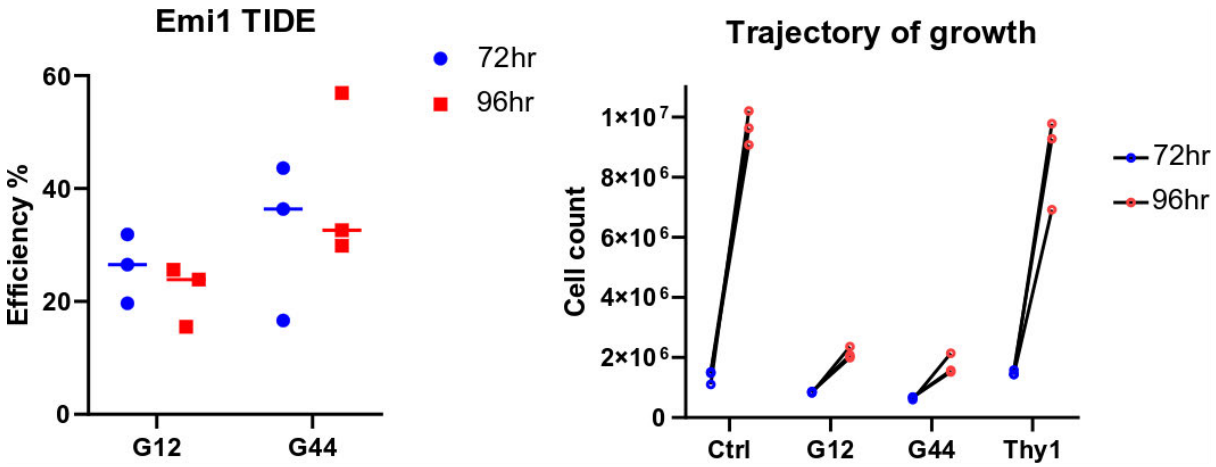

Figure 53 Efficiency of knockout as depicted by the presence of indels using TIDE analysis (as described in Chapter2, left), and the cell count (right) of cells collected at the 72hr and 96hr time point. Cells were subjected to transfection either in the presence the G12 guide or G44 guide, both of which target Emi1 exons, the irrelevant target site Thy1 guide, and without the presence of a guide as a control. n=3 with data from 2 independent expreiments.

When examined by flow cytometry, we confirmed that for cells within the population of $G1^{pRb-}$ we observed a decrease in Emi1 expression for both specific guides, but not for either the Thy1 knockout, or the no-guide negative control (Figure 54). Looking more widely, we observed a very distinct pattern of cells falling out of S-phase or collecting in the 4n, indicating an inability to progress past the G2/M checkpoint, as well as the beginnings of re-replication in which cells had greater than 4n DNA content.

This indicates that the cells dupilicated their genome for a second time before undergoing mitosis and thus cytokinesis. In essence, this would mean that they entered into S phase before entering M phase. These phenotypes were observed as a result of targeting with either Emi1 guide. We observed that the re-replication phenotype became more striking at the 96 hour time point in which a substantial population of events are seen as greater than 4n (Figure 55). This rereplicative phenotype mimics what has been observed in Emi1 knock down studies (Shimizu et al. 2013; Verschuren et al. 2007), providing good evidence that both these guides are capable of selectively knocking out Emi1 up to 48 hours post transfection.

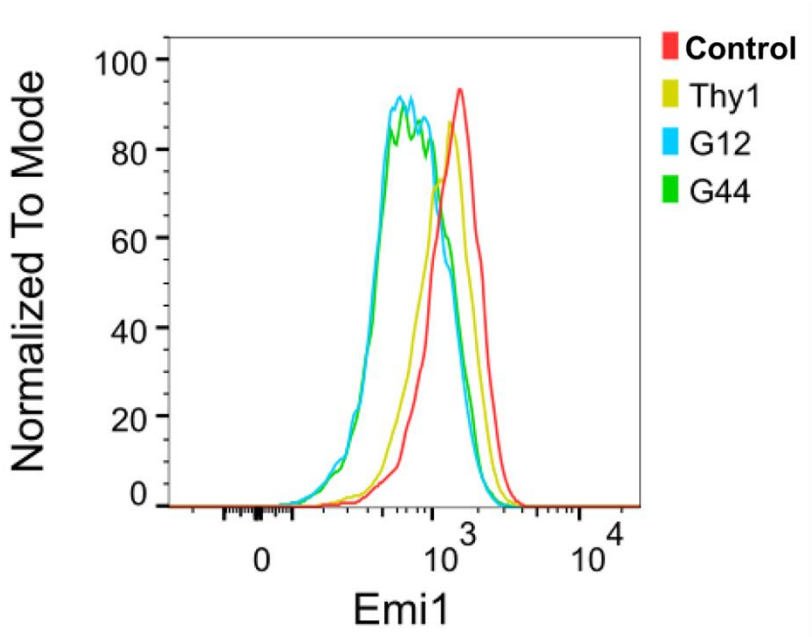

Figure 54 Expression of Emi1 in T-cells within the G1^{pRb-} gate, which was used because the cells were similar in morphology at this stage of the cell cycle. Cells were transfected with either the G12 or G44 guide for Emi1 targeting, the Thy1 targeting guide, or without a guide present at 48 hours.

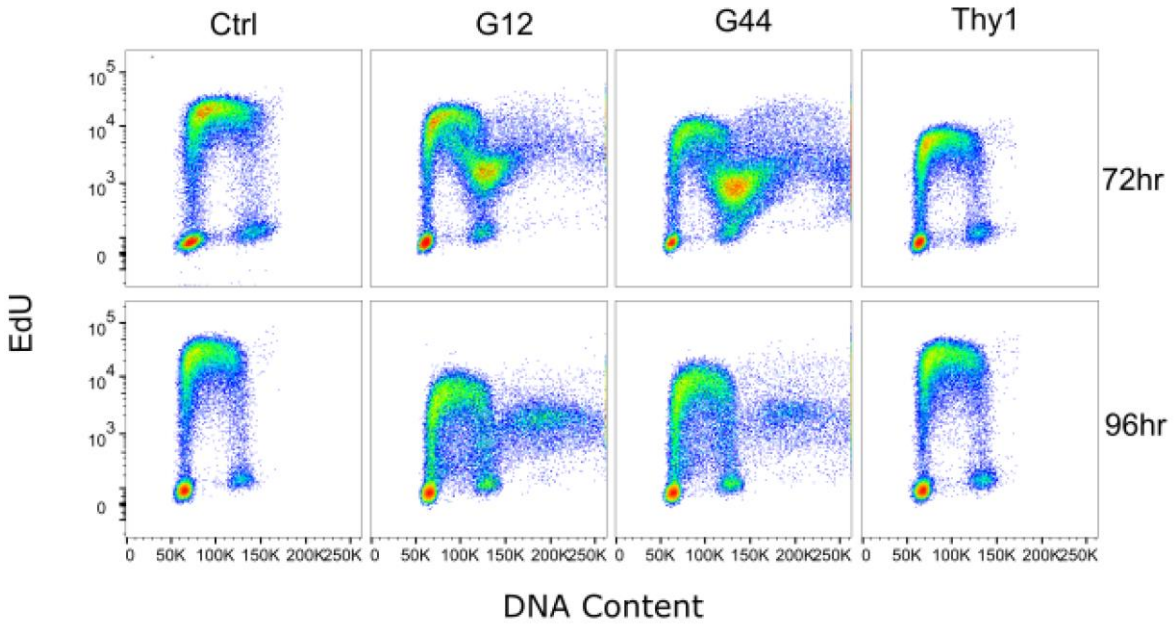

Figure 55 DNA vs EdU profile of N4 and IL-2 stimulated OT-1 T cells taken the 72hr (top) and 96hr (bottom) time points. Cells were transfected with either the G12 or G44 guide for Emi1 targeting, the Thy1 targeting guide, or with no guide and stained at 48 hours.

5.2 Emi1 KO results in change to proliferative behavior of CD8$^+$ T cells

Having demonstrated a working protocol for Emi1 KO of CD8$^+$ T cells, we then set up an experiment to examine the impact that Emi1 KO had on cell cycle phase distribution in both T_{eff} and T_{mem} phenotypes. To achieve this, cells which were transfected with the guides were

split into culture with IL-2 or IL-15, to be supplemented daily and collected at the 72 hour and 96 hour time points (Figure 56).

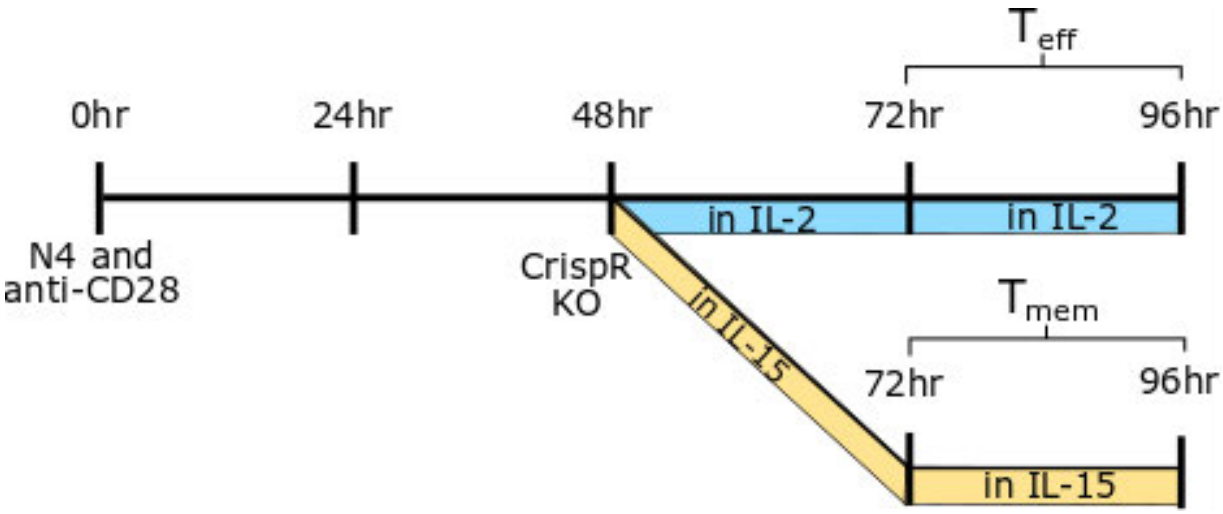

Figure 56 OT-1 T cells were extracted from the lymph nodes and plated with N4 and anti-CD28 at the 0hr time point, and incubated for 48 hours, at which point they were subjected to electroporation with or without the Cas9 CrispR guide construct. The cells were placed into culture with either IL-2 or IL-15 which was supplemented daily, with samples taken for analysis at the 72 hour and 96 hour time point.

In order to maximise the efficiency of obtaining Emi1 knockout cells, we utilised both guides together in the transfection. Standard imaging on a Nikon microscope (Figure 57) showed that each guide separately led to an increase in cells with irregular morphology (the rounded cells with a bright halo), and these irregular cells were increased as a result of combining the guides. A western blot confirmed that this combination knockout significantly reduced Emi1 protein in the T_{eff} phenotype (Figure 58), and preliminary results showed a similar reduction in T_{mem} as well.

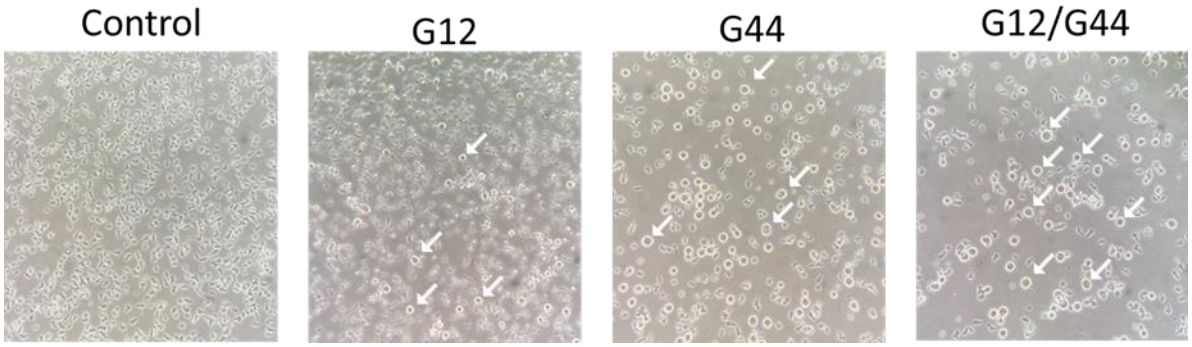

Figure 57 Images taken of cells in culture at the 96 hour time point through the x10/0.25 objective of a Nikon Eclipse TS100. White arrows indicate a few examples of irregular cells.

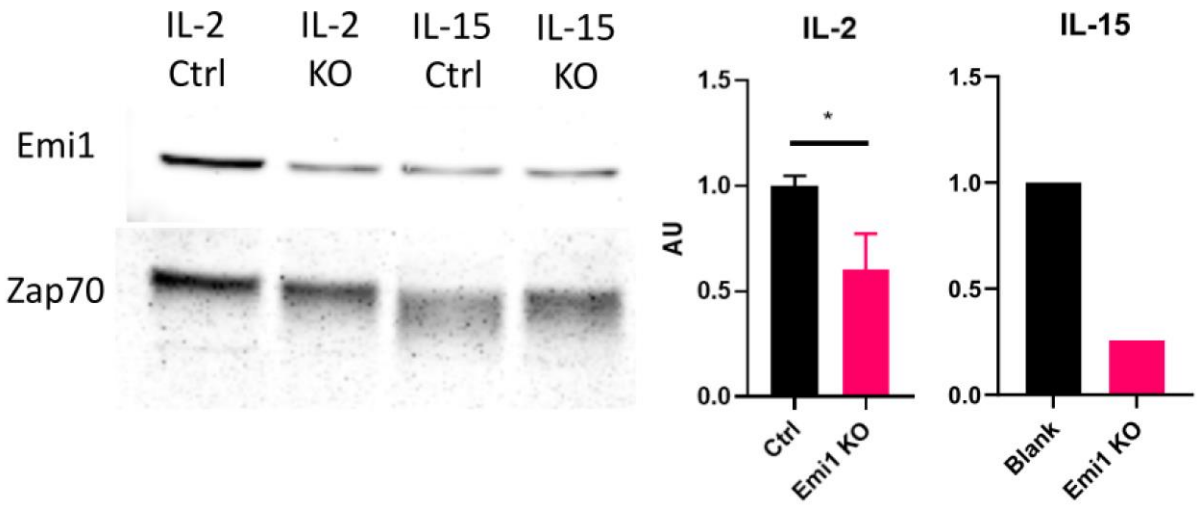

*Figure 58 Western blot (left) of cells taken at the 96hr time point. The levels of Emi1 relative to Zap70 (right) were measured to determine knock out success in IL-2 and IL-15 treated T cells * p<=0.05. IL-2: n=3, IL-15: n=1, conducted in one experiment.*

5.2.1 Cell Cycle phase distribution

In both the T_{eff} and T_{mem} cells, the combined knockout produced a very strong re-replication phenotype seen at both the 72 and 96 hour time points (Figure 59). These cells were gated on forward and side scatter (FSC and SSC) to include the re-replicating subset (see Appendix figure 4). As expected from what was seen under the microscope, the Emi1 KO cells showed a distinctly larger cell size, as demonstrated by an increase is forward scatter (Figure 60). This difference in cell size was most notable at 72 hours, a difference which was still present at 96 hours (Figure 61).

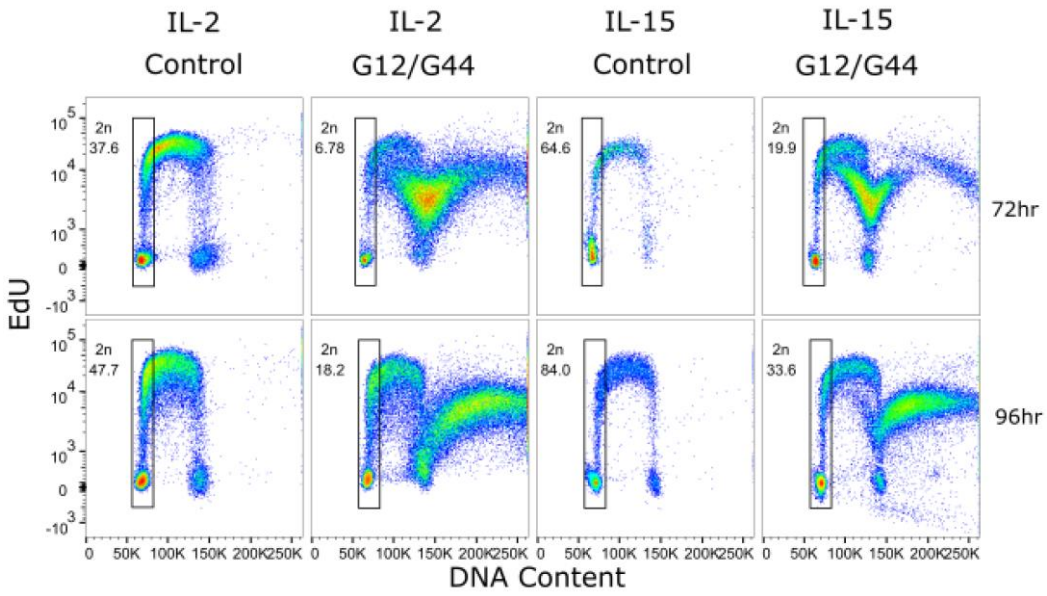

Figure 59 DNA vs EdU profile of IL-2 or IL-15 stimulated OT-1 T cells taken the 72hr (top) and 96hr (bottom) time points following Crispr deletion.

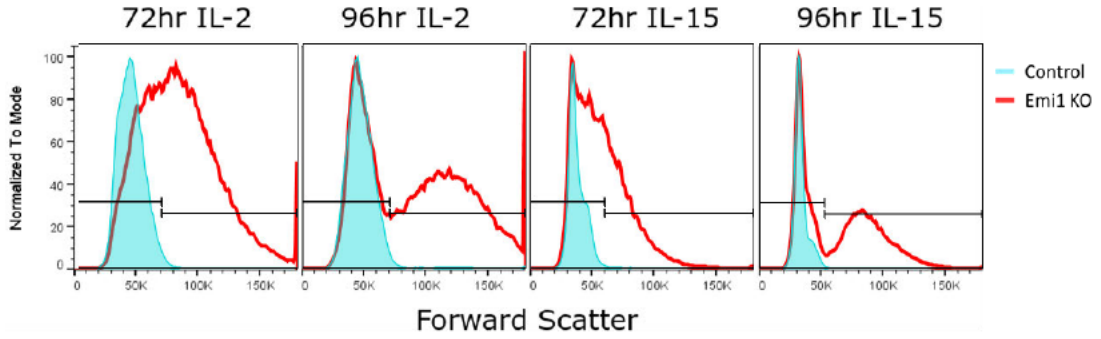

Figure 60 Forwards scatter of total cells treated either with the combination G12/G44 Emi1 guides (red) or without a guide (blue) at 48 hours, then cultured in either IL-2 or IL-15 for a further 24 and 48 hours. Gates indicate cells considered to be FSC^{lo} versus FSC^{hi}

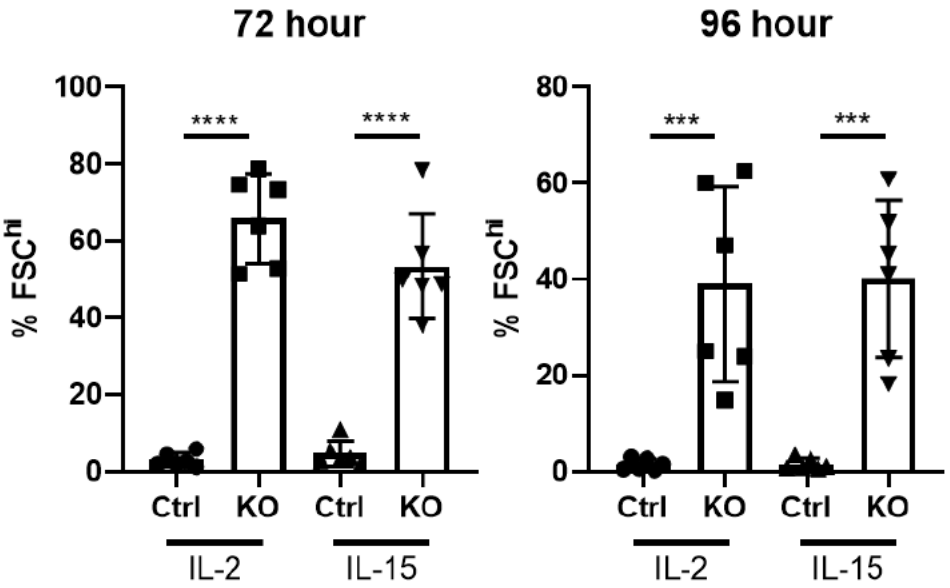

*Figure 61 percentage of cells within the Forward Scatter FSC^{hi} gate for CD8$^+$ T cells which have been transfected with the combination G12/G44 Emi1KO guides or no guide at 48 hours, and cultured in IL-2 for a further 24 hours (left) or 48 hours (right). Significance was attained by ANOVA followed by Tukey's test. ****p<=0.0001, ***p<=0.001, NS= not significant. n=6, data taken from two independent experiments.*

Previous studies have demonstrated that cells undergoing re-replication after having entered S phase do so as a result of poor inhibition of origin licensing processes, leading to a second initialisation of S phase and thus a larger overall cell size (Fu et al. 2021). We were able to confirm this correlation was present in CD8$^+$ T cells by backgating on the increase forward scatter profile, and showing that these events made up the >4n population on the DNA vs EdU profile (Figure 62). To quantify the shift in DNA content, we defined the gates of 2n, 4n, and >4n on the histogram for DNA content (Figure 63) which showed a substantial increase in DNA content within the Emi1 KO groups. Indeed, the number of cells with greater than 4n DNA content was much greater in the knockout groups at both time points, regardless of

cytokine treatment. This demonstrated that Emi1 has an important role in mediating replication in CD8⁺ T cells post S phase entry.

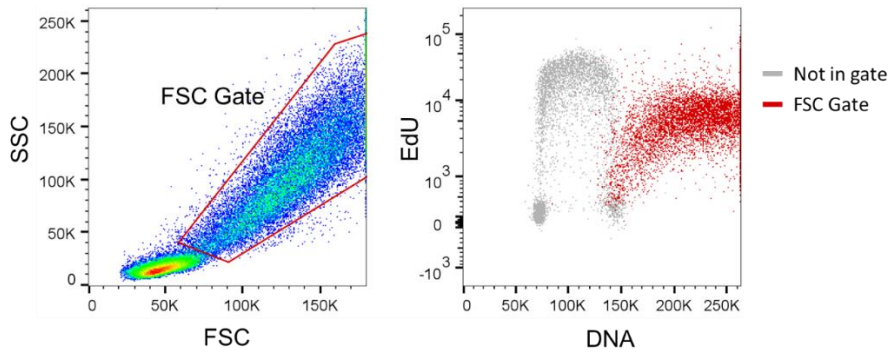

Figure 62 Profiles of Emi1 KO T cells at the 96 hour time point. Forward Scatter vs Side Scatter (left) shows the gating around cells above the average size of lymphocytes. Identification of the large population within the FSC gate in the DNA vs EdU staining (right) shows them as superimposed in red.

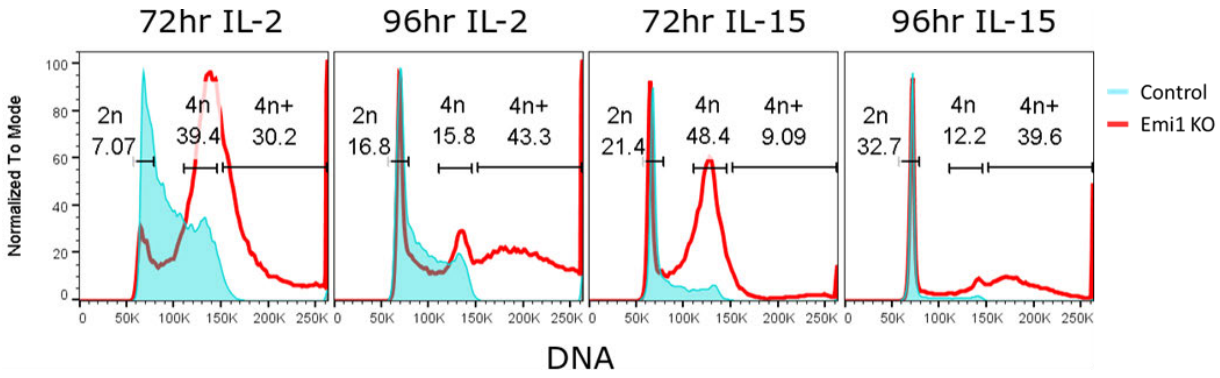

Figure 63 DNA histograms of CD8⁺ T cells transfected with Emi1 targeting guides G12/G44 (red) and without guide (blue) 48 hours post activation, then placed into IL-2 or IL-15 for a further 24 and 48 hours.

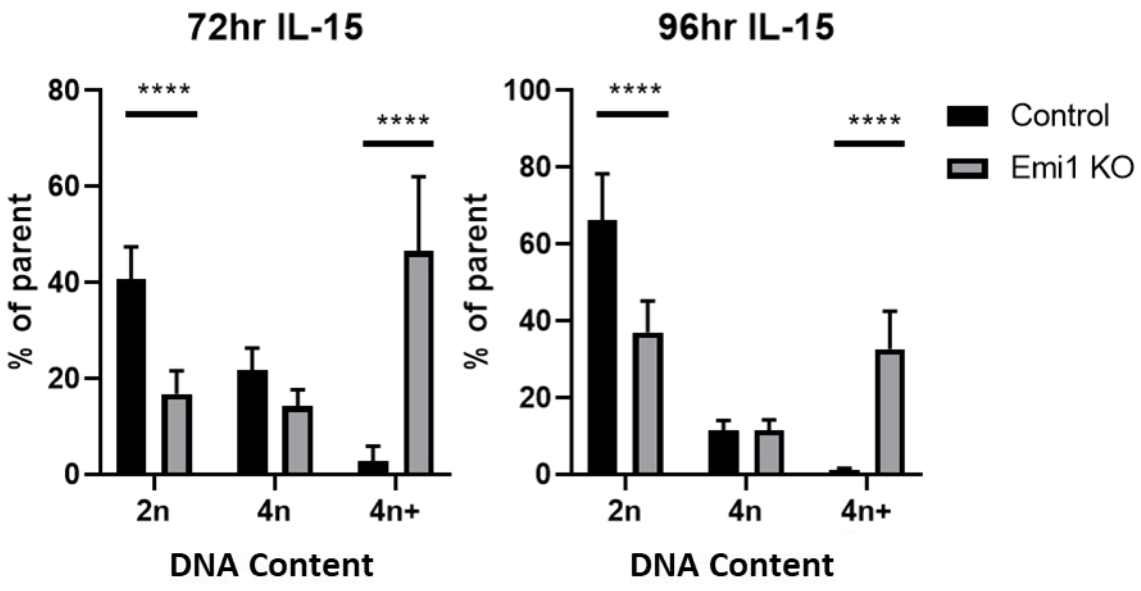

*Figure 64 DNA histograms of CD8⁺ T cells transfected with Emi1 targeting guides G12/G44 and without guide 48 hours post activation, then placed into IL-2 (top) or IL-15 (bottom) for a further 24 hours (left) and 48 hours (right). Significance was determined with paired Student's t-test. ****p=<0.0001, **p=<0.01, *p<0.05. n=6, data taken from two independent experiments.*

To examine the impact that Emi1 KO had to CD8⁺ T cells that had yet to enter S phase, we focused exclusively on the population of cells within the 2n gate and looked at the cell cycle phases measured by pRb and EdU expression (Figure 66). While there was no discernible difference in cell cycle distribution by the 72 hour time point, by 96 hours, the IL-2 treated cells showed a significant reduction in cells entering in to S phase, and an increase in cells which were p-Rb negative. A similar trend was not observed in IL-15 treated cells, indicating that the role of Emi1 on S phase progression is much stronger in T_{eff} than it is in T_{mem}.

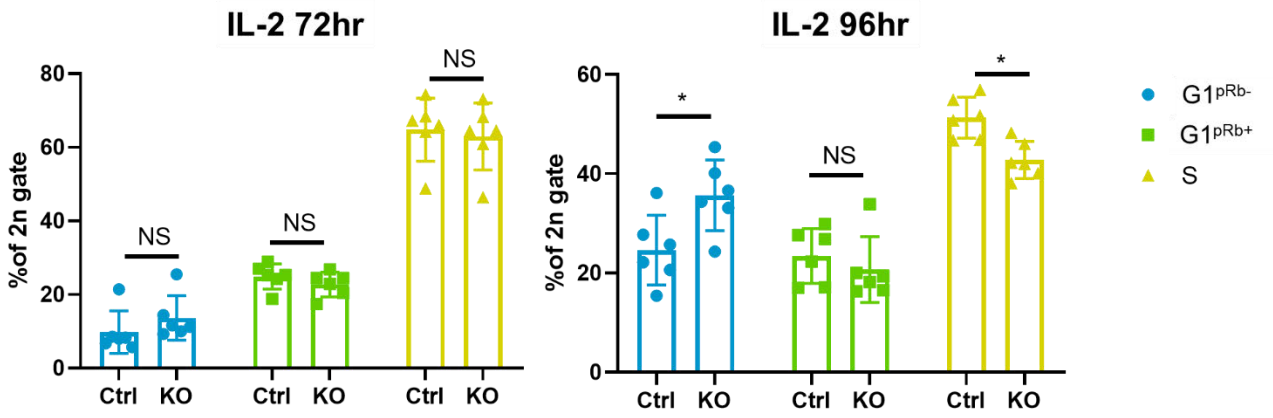

*Figure 65 Cell cycle phase distribution of CD8⁺ T cells treated with IL-2 collected at the 72 hour (left) and 96 hour (right) time point. Cells were transfected with CAS9 complex targeting Emi1 (KO) or nothing (Ctrl). Significance calculated by student's t-test. *p<=0.05, NS= Not Significant. n=6 in two independent experiments*

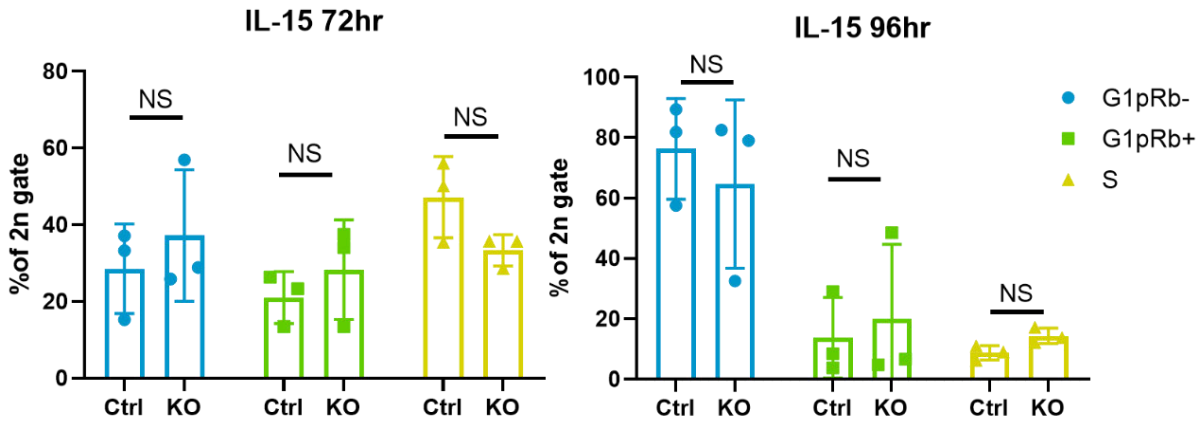

*Figure 66 Cell cycle phase distribution of CD8⁺ T cells treated with IL-2 collected at the 72 hour (left) and 96 hour (right) time point. Cells were transfected with CAS9 complex targeting Emi1 (KO) or nothing (Ctrl). Significance calculated by Student's t-test. *p<=0.05, NS= Not Significant. n=6 in two independent experiments*

Because Emi1 knockout results in re-replication, there is a possibility that the reason more cells are in $G1^{pRb-}$ is because of an increase in genomic instability leading to early cell cycle arrest, rather than an increase in APC/C activity. To rule this out as a cause, we stained the cells for a γH2AX, a known marker of DNA damage. We observed that there was a noticeable shift in γH2AX expression in the Emi1 KO samples, with an increased number in the high expression peak (Figure 67 left). But when isolating the $G1^{pRb-}$ populations, we noted that both control and KO remained in the low expression peak (Figure 67 right), indicating that there was no discernible difference in DNA damage between these two populations.

To confirm that this difference in phase distribution was a result of differences in APC/C activity, we stained the samples for Eg5, a known substrate of APC/C^{Cdh1} (Figure 68). We expect that when APC/C^{Cdh1} is active, Eg5 expression will be low as it would be tagged for degredation, but if APC/C^{Cdh1} is inhibited, Eg5 expression will increase. In T_{eff} cells, while Eg5 levels remain the same in 2n cells at the 72 hour point, there was a significant decrease in Eg5 expression at 96 hours (Figure 69), indicating an increase in APC/C^{Cdh1} activity. This result demonstrates that within T_{eff} cells rely on Emi1 to obstruct APC/C^{Cdh1} for a more rapid entry in to S-phase.

The T_{mem} population was less straightforward. T_{mem} cells did not show a decrease in Eg5 by 96 hours. Instead in two out of three samples we noted an increase in Eg5 at the 72 hour point (Figure 68). This difference reached significance only when two reulst out of the triplicate

were included for analysis (Figure 69), as a result it is difficult to say how representative this data is of the T_{mem} system.

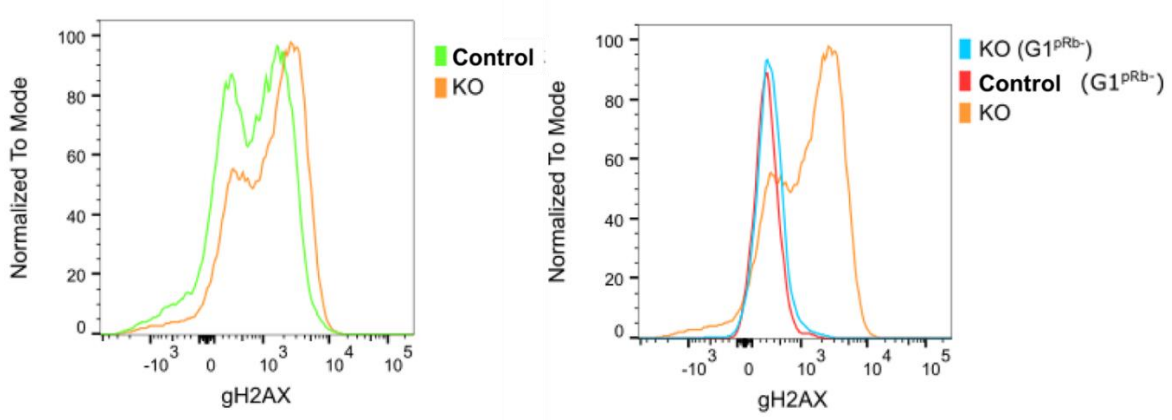

Figure 67 γH2AX expression in N4 stimulated OT-1 T cells at the 96 hour time point, comparing the bimodal peaks of the total population (left) to the 2n p-Rb negative gated population (right)

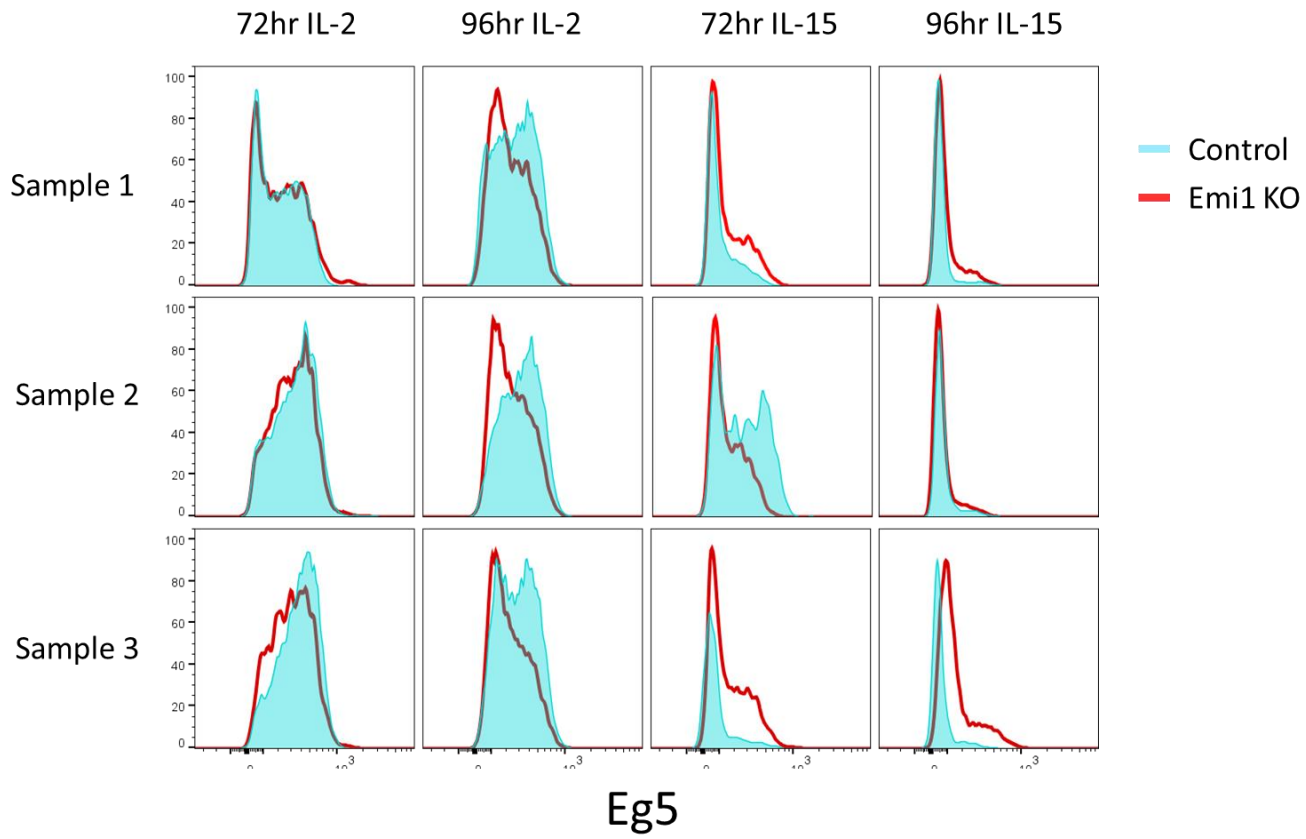

Figure 68 Eg5 intensity for CD8 T cells transfected with the CAS9 complex at the 48hr time point with guides targeting Emi1 (red) or without guides (control). Samples were incubated in IL-2 or IL-15 at 72hr and 96hr. Each row represents a different sample within a set of biological triplicates.

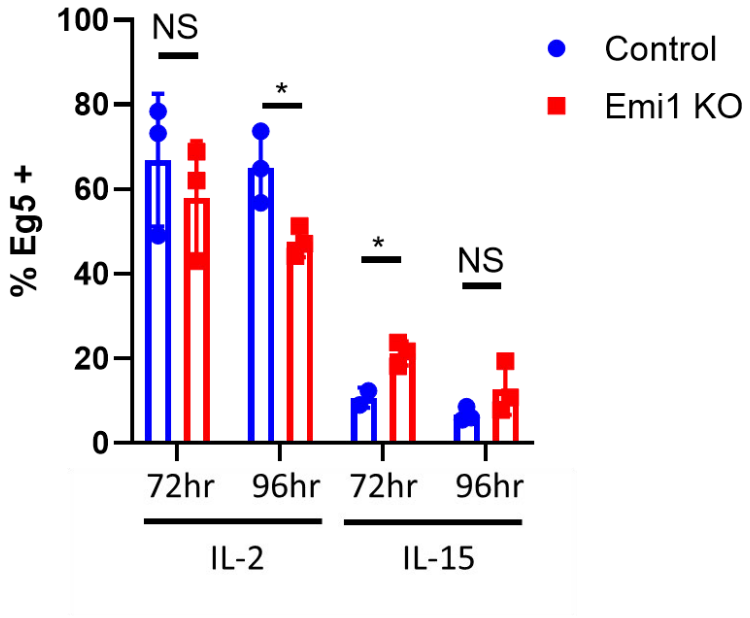

*Figure 69 Eg5 intensity for CD8 T cells transfected with the CAS9 complex at the 48hr time point with guides targeting Emi1 (red) or without guides (control). Samples were incubated in IL-2 or IL-15 at 72hr and 96hr. Significance was determined by students t-test *p<= 0.05, NS= Not Significant. n=3 from one experiment. One data value from the 72hr IL-15 treated control group was removed due to being an outlier at 55.7%.*

5.3 Emi1 KO has different effects on naïve CD8 T cells

Having established the impact Emi1 KO had on already cycling $CD8^+$ T cells, we next attempted to measure the impact of Emi1 as $CD8^+$ T cells entered in to the first cell cycle following initial stimulation. First we established whether the guides had the same efficacy in naïve cells as they did on pre-activated cells (Figure 70). TIDE analysis demonstrated that G44 showed a high presence of indels for the first 48 hours, but this dropped dramatically by the 72 hour time point, while G12 showed a low presence of indels throughout the culture. We therefore decided to utilise only the G44 guide to knock out Emi1 in naïve $CD8^+$ T cells, and continue the culture only to the first 48 hours.

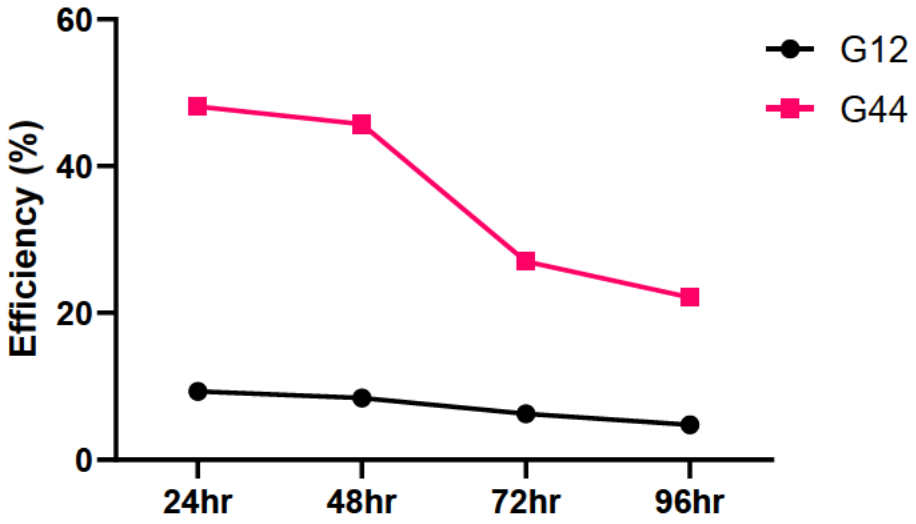

Figure 70 TIDE analysis conducted on CD8⁺ T cells transfected with either the G12 (black) or G44 (red) Emi1 targeting guide while naïve, then cultured with N4 antigen for 48 hours, and then IL-2 for a further 48 hours. Samples were collected at 24 hour intervals. n=1

While there was no discernible difference between the cells at 24 hours, we noted the emergence of re-replication at 48 hours in the KO group (Figure 71), though it was far less pronounced than when transfecting cycling T cells.

Surprisingly, preliminary experiments staining the cells with Eg5 showed an increase in Eg5 in the knockout compared to the control at the 24 hour time point (Figure 73), however this result will need to be repeated to confirm reproducibility.

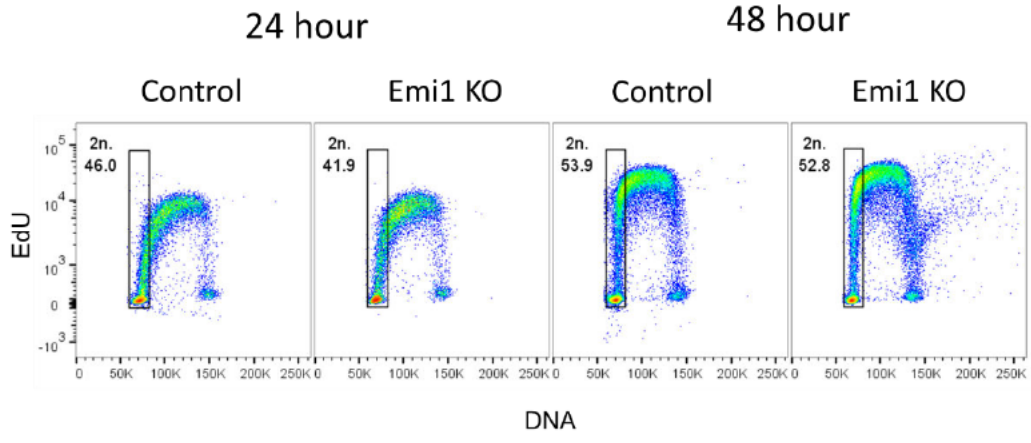

Figure 71 DNA vs EdU profile of naïve CD8⁺ T cells transfected with CAS9 with Emi1 targeting guide or without guide. Cells were then incubated in N4 for 24 hours and 48 hours before staining and analysis by flow cytometry.

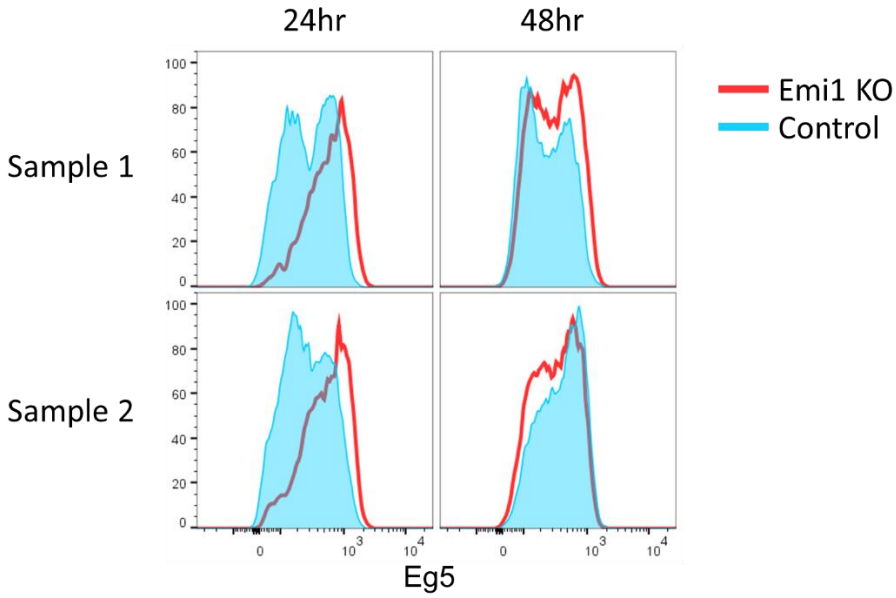

Figure 72 Eg5 intensity of naïve CD8⁺ T cells transfected with CAS9 with Emi1 targeting guide (red) or without guide (blue). Cells were then incubated in N4 for 24 hours and 48 hours before collection.

While our preliminary findings do not contain a robust enough dataset to make firm conclusions on cell cycle phase distribution, we do observe a trend in which by 24 hours, there is an increase in S-phase entry for the knockout group and a decrease in cells at $G1^{pRb+}$ (Figure 73). But by 48 hours, this trend appears to be lost.

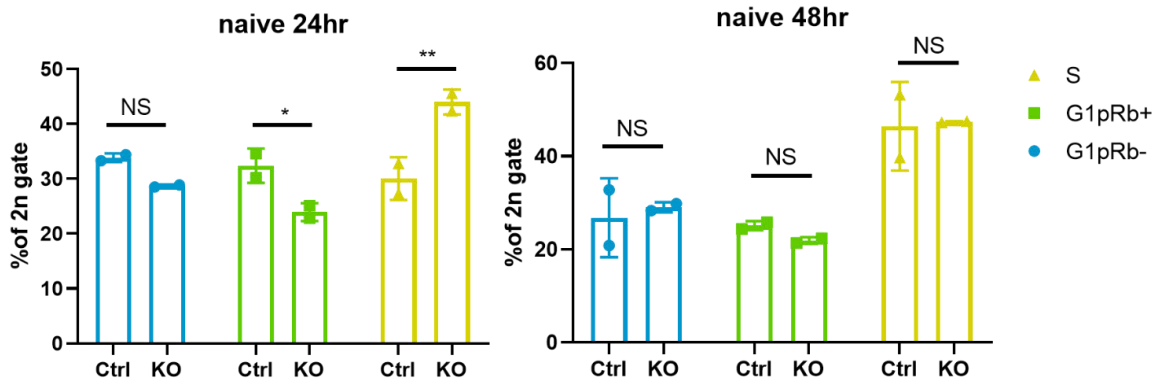

*Figure 73 Cell cycle phase distribution within the 2n gate of CD8⁺ T cells transfected while naïve with CAS9 with Emi1 targeting guide (KO) or without guide (Ctrl). Cells were then incubated in N4 for 24 hours and 48 hours before collection. Significance was determined by Student's t-test. **p<=0.01, *p<=0.05, NS= Not Significant. n=2 from one experiment.*

5.3.1 Impact of Emi1 KO on division index

Having demonstrated that Emi1 knockout has an impact on a CD8⁺ T cell's cell cycle phase distribution, we next set out to see if such an impact could also be seen in the rate of cell division. To achieve this, naïve CD8⁺ T cells were stained with CTV prior to transfection, and then incubated for up to 48 hours. By 24 hours, the cells had begun their entry into cell cycle

as shown by the increase in pRb, and began to rapidly proliferate at 48 hours, with a substantial number of cells reaching the 4th generation (Figure 74). While no discernible difference was detected between control and Emi1 KO by 24 hours, we observed a larger percentage of cells within the earlier generations, and amongst them a marked increase in pRb hi cells in generations 0 and 1.

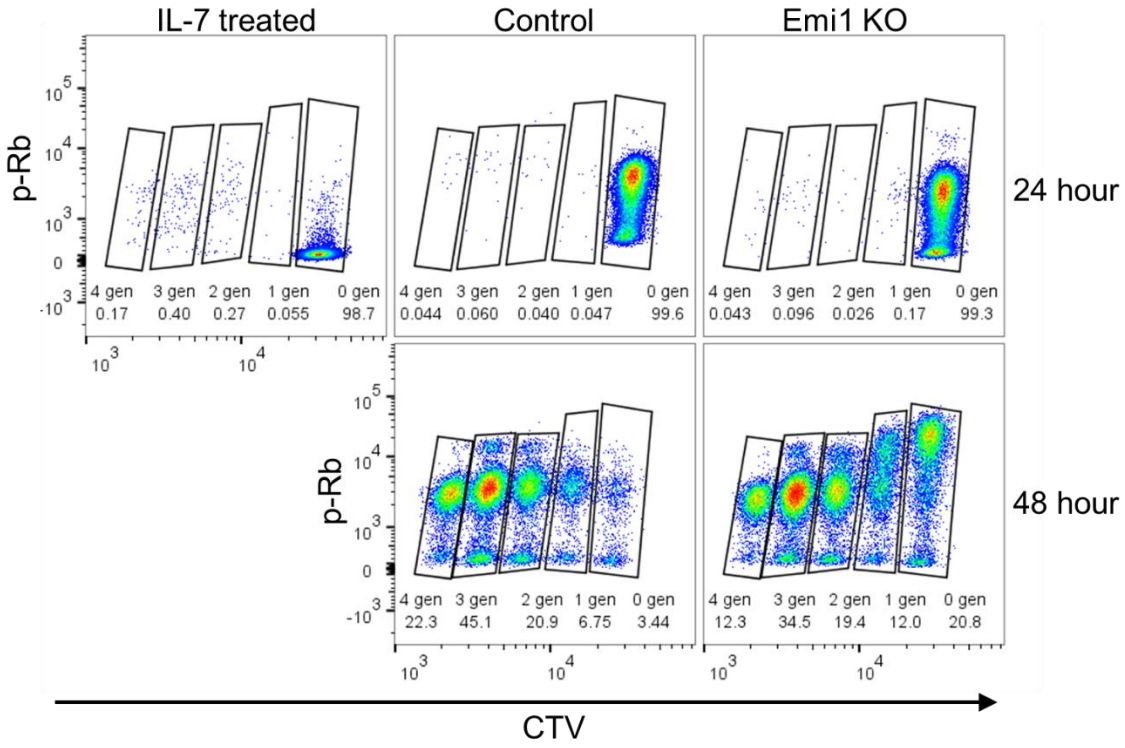

Figure 74 Cell Trace Violet (CTV) vs p-Rb profile of CD8⁺ T cells transfected while naïve with CAS9 with Emi1 targeting guide or without guide. Cells were then incubated in N4 or in IL-7 for 24 hours and 48 hours before collection.

It is possible that this increase of events in the earlier generation is due to the presence of the re-replicating cells rather than cells which are unable to enter S phase as quickly. However, we were unable to measure DNA directly to confirm this due to the incompatibility of the Hoechst and CTV stains. Having already established that rereplicatiing cells correlates with an above average intensity in both forwards and side scatter, we incorporated an FSC-gate to exclude the re-replicating subset (Figure 75). Even with this subsection removed, we could still detect an increased percentage of cells which were still in the earlier generations in the KOs although this was less than without the FSC-gate (Figure 76).

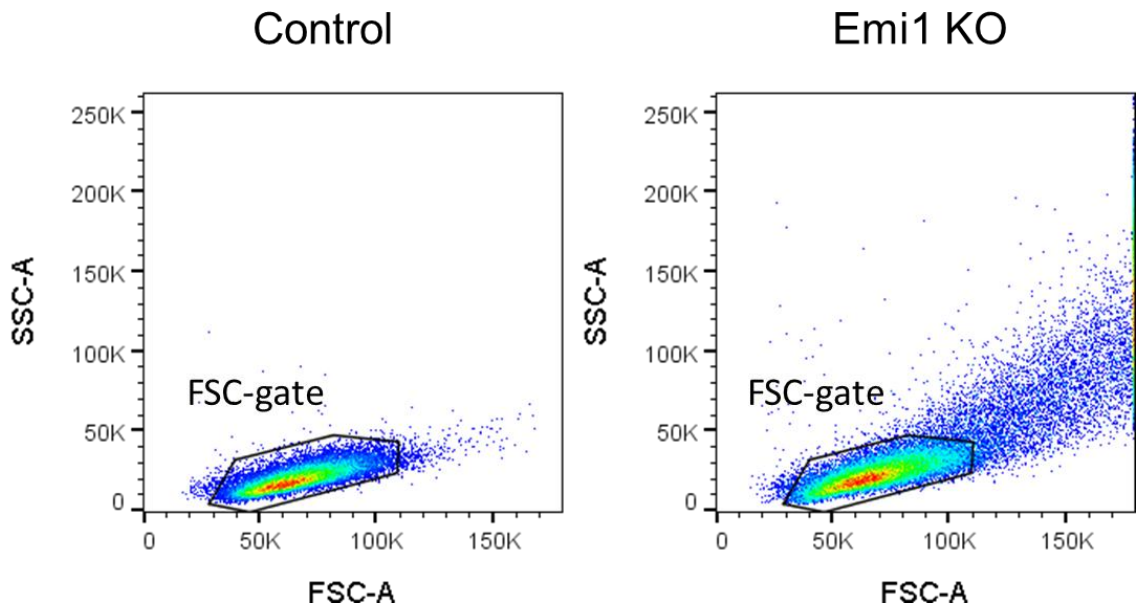

Figure 75 Forward scatter vs Side scatter profiles of CD8⁺ T cells transfected while naïve with CAS9 with Emi1 targeting guide (right) or without guide (left) collected at 48 hours. FSC gate was drawn around the Control cells and used as the basis to identify non-re-replicating cells in the Emi1 KO samples.

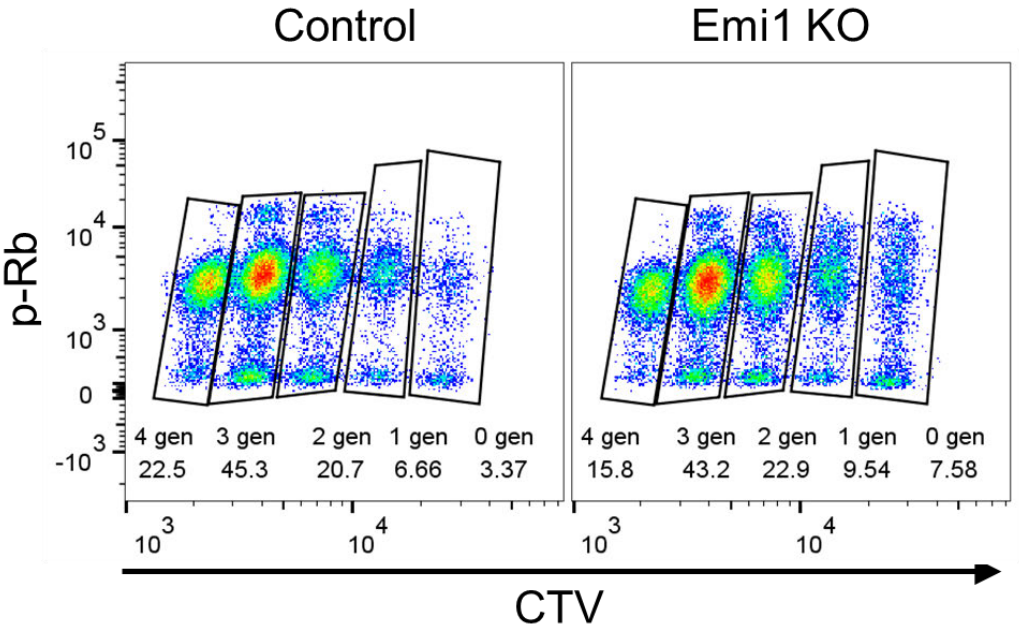

Figure 76 CTV vs p-Rb profile of CD8⁺ T cells transfected while naïve with CAS9 with Emi1 targeting guide or without guide. Cells were then incubated in N4 for 48 hours before collection. Cells greater in size due to re-replication were excluded from these graphs.

When each generation was isolated, we noted that ratio of p-Rb- to p-Rb+ was tilted in favour of the p-Rb+ in the KO population (Figure 77). This was more prominent when the re-replicated cells were included, but removing them did not significantly reduce this phenomenon and while it is most apparent in the earlier generations, this trend of reduced

percentage of pRb- could be observed across all generations. This may indicate that the arrest or slowing down of cell cycle progression occurs post S phase entry, as is the case for re-replicating cells, or just prior to licensing where p-Rb levels are already high.

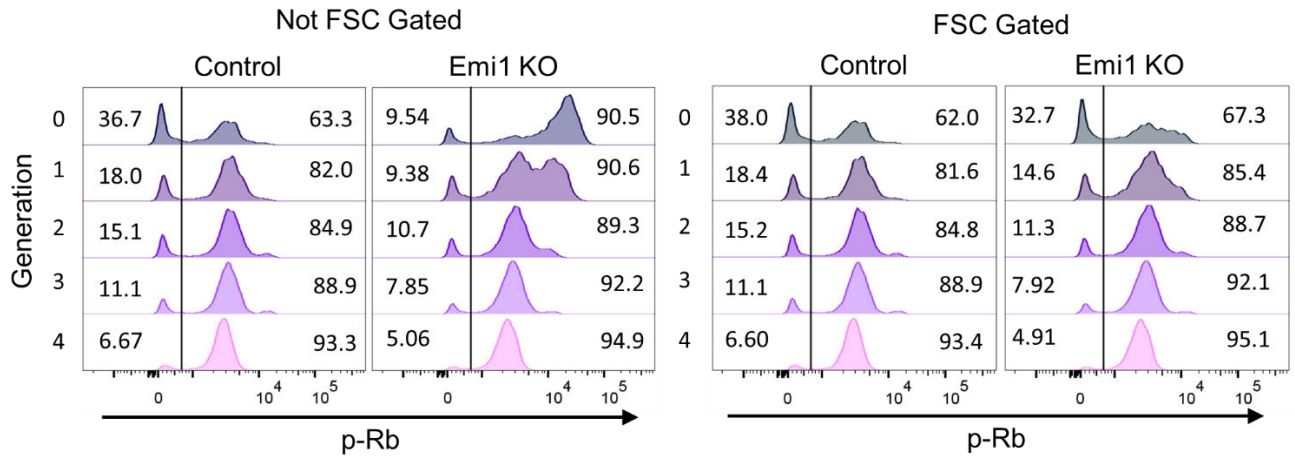

Figure 77 p-Rb Intensities for CD8⁺ T cells transfected while naïve with CAS9 with Emi1 targeting guide or without guide. Cells were then incubated in N4 for 48 hours before collection. Data presented here shows populations including the re-replicating cells (Not FSC Gated) or excluding them (FSC Gated). Each row shows the p-Rb profile of a specific generation as determined by CTV staining. Vertical lines show the cut-off gate for p-Rb positive and p-Rb negative, with numbers showing the percentage in each gate for each generation.

We utilised Flowjo's inbuilt algorithm for measuring division index, which calculates the average number of divisions that a cell from the original population undergoes, in order to quantify whether Emi1 KO had any impact on the rate of cell cycle. Our preliminary data demonstrated that there is an observable decrease in the division index in the Emi1 KO samples, and while this difference is less pronounced when removing the re-replicating cells, there is still a perceivable difference (Figure 79). As we have established that Emi1 is an important protein required for S-phase progression in CD8⁺ T cells, it is therefore likely that this role may have a significant impact on the rate of proliferation. However, this finding would need to be confirmed for reproducibility.

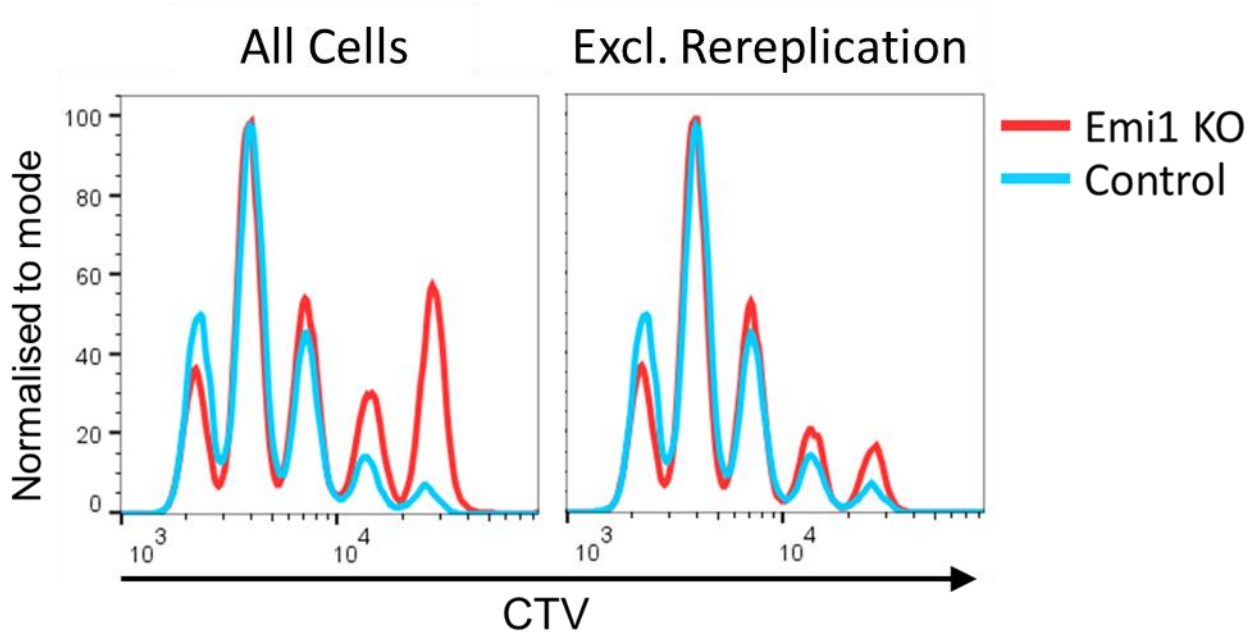

Figure 78 CTV intensities of CD8⁺ T cells transfected while naïve with CAS9 with Emi1 targeting guide (red) or without guide (blue). Cells were then incubated in N4 for 48 hours before collection. Cells greater in size due to re-replication were included (left) or excluded (right) from these graphs.

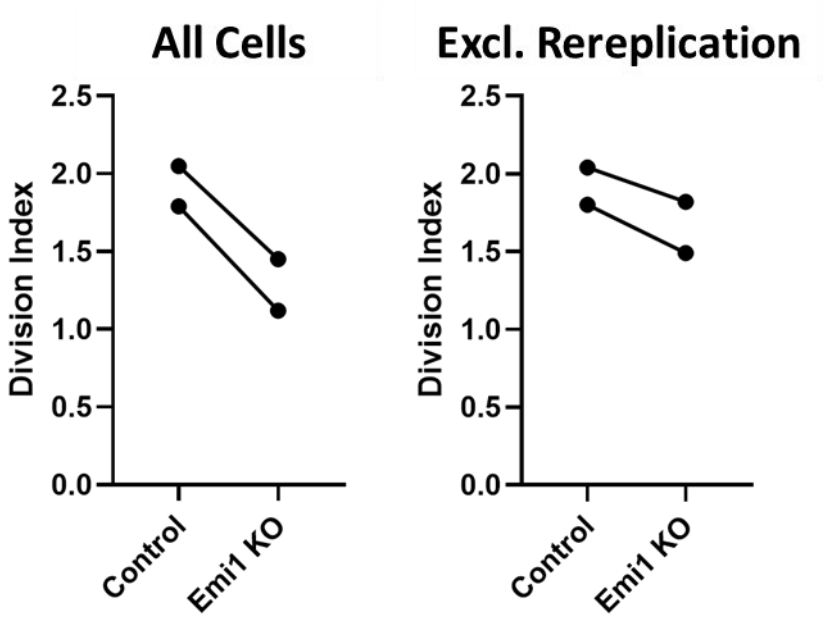

Figure 79 Division index for CD8⁺ T cells transfected while naïve with CAS9 with Emi1 targeting guide (Emi1 KO) or without guide (Control). Cells were then incubated in N4 for 48 hours before collection. Cells greater in size due to re-replication were included (left) or excluded (right) from these graphs. Division index was calculated by FlowJo v10 with CV fixed at 3.0. n=2, from one experiment.

5.4 Discussion

This work is the first to establish a protocol for Cas9 CrispR knock out of Emi1 in both naïve and cycling $CD8^+$ T cells. The efficiency of this method is compromised slightly by the fact that method relies on replication in order to maintain the knockout gene in the population. As such, when CrispR is used to knock out a protein which is essential for cell cycle, any cells which evade transfection will have a competitive advantage and in time will out-proliferate the knocked out cells, reducing both the efficiency and the biological impact of the knock out. The reason behind the low efficiency therefore may in part be due to the $CD8^+$ T cells particularly rapid rate of proliferation once introduced to IL-2.

Because the time it takes for the Cas9 Crispr to find its target is not uniform, the Emi1 KO may be established at different moments of the cell cycle. This could result in a population of cells losing Emi1 expression both before and after R point has been reached. Another factor that impacts the phenotype is the rate of turnover on the target protein. When an interruption to the Emi1 gene is introduced, if there is still a sufficient amount of Emi1 abundance in the cell, then the impact of the KO may not be felt until after origin licensing has taken place, leading to the re-replication phenotype.

These re-replicating cells make up the majority of the cell population within the first 24 hours transfection. As has been observed in Emi1 KD studies, loss of Emi1 post S-phase entry leads to a premature resurgence in APC/C^{Cdh1} activity. This results in the early degradation of Cyclin A and Geminin, and subsequently leads to excess in Cdc6 and Cdt1 before the G2/M checkpoint is reached (Machida and Dutta 2007) (Figure 80). It is likely that this is the reason why EdU uptake decreased in cells 24 hours post Emi1 KO, as cyclin A levels are important for regulating S phase progression (Zhao et al. 2014).

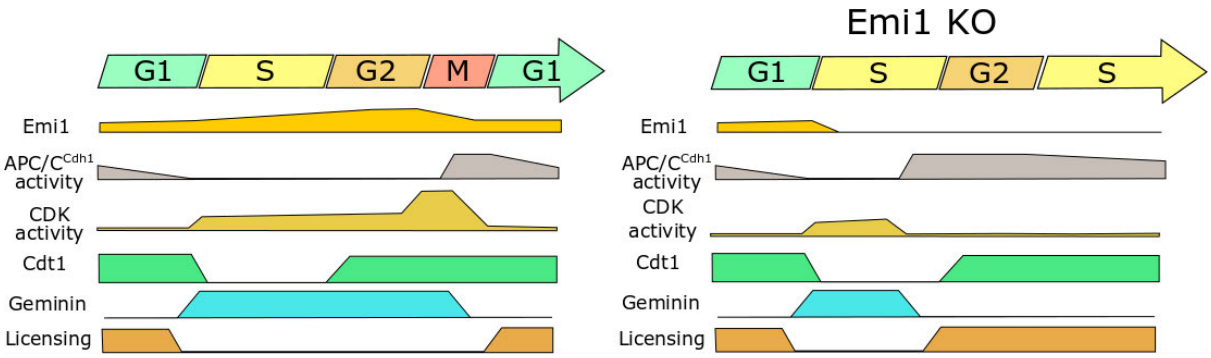

Figure 80 In a wildtype cell, Emi1 ensure APC/C^{Cdh1} levels are reduced, leading to an upregulation of cyclin A and Geminin, reducing Cdt1 as the cells enter S phase, APC/C^{Cdh1} levels remains low until M phase, where they increase, reducing levels of Cyclin A and geminin, allowing uninhibited Cdt1 and Cdc6 to initiate licensing during G1. When Emi1 is disrupted after S phase entry, APC/C^{Cdh1} rise early, reducing cyclin A and Geminin levels while the cells are still in S phase. This allows Cdt1 and Cdc6 to initiate licensing and thereby allows the cells to enter S phase before the cells have undergone mitosis.

It is interesting to note that KD of Emi1 does not result in the same extent of re-replication in all cell types. Re-replication has been observed in a number of cancer cell lines including, breast cancer (MCF-7), colon cancer (RKO), osteosarcoma (SaOS-2), and glioma (T98G) which respond to Emi1 KD with enlarged nuclei and a substantial population of cells >4n. In contrast primary cell lines including fibroblasts (NHDF, HFLIII), and epithelial cells (MCF10A) also showed signs of re-replication, but were not affected to the same extent as transformed cell lines (Shimizu et al. 2013).

A similar study noted that re-replication was far more present in transformed cell lines including HeLA and HCT-116 when compared with primary cell line RPE-1, (Verschuren et al. 2007). Like these transformed cells, there is evidence that stem cells undergo re-replication by loss of Emi1, such as Emi1 KO Zebrafish embryo (Robu, Zhang, and Rhodes 2012) and Emi1 KD in ES cells (Ballabeni et al. 2011). Together this indicates that there is a greater reliance on Emi1 to suppress APC/C^{Cdh1} within transformed cell lines, stem cells, and in $CD8^+$ T cells compared with primary somatic cell lines. This could mean that just as cancer cells are known to reactivate embryonic mechanisms to enhance their own survival and proliferation, $CD8^+$ T cells may as well be returning to embryonic cell cycle regulatory pathways to achieve rapid proliferation.

By focusing on the 2n population we attempted to restrict the analysis to the cells in which the KO is introduced before the cells enter S-phase, and thereby try to assess the importance that Emi1 has in enabling S phase entry. We have demonstrated that IL-2 mediated T_{eff} cells which experience Emi1 KO prior to S-phase entry are less likely to enter S-phase and by 48

hours post transfection, there is a higher proportion of pRb negative cells as predicted by our model. We demonstrated that there is no change in γH2AX concentration within the pRb- population. This likely means that standard forms of DNA damage, including double strand breaks are unlikely to be the main factor in limiting S-phase entry. However, it would be prudent to also assess for single strand breaks, which may not lead to a noticeable increase in γH2AX levels. Instead, levels of p-Chk1, which lies downstream of the single strand break detector ATR, could provide a useful readout (Choi et al. 2010).

Our preliminary data on Emi1 KO in IL-15 induced T_{mem} showed a very different profile. While at 48 hours post transfection, Emi1 KO cells behaved no differently from control cells, there was instead an increase in Eg5 by 24 hours in 2n DNA cells. It is difficult to comment precisely on the mechanism at play in this case, as such a phenomenon has yet to be observed in other models, and indeed it remains to be seen if the preliminary data can be reproduced. However it does highlight the role IL-2 has in creating the Emi1 high environment predicted by our model.

Our preliminary findings on naïve cells show little impact of the Emi1 KO 24 hours post transfection, but a noticeable effect by 48 hours mimicking what was seen in the T_{eff}. This may be because CD25 not expressed in OT-1 up to the first 24 hours post activation, and thus until this point, the cells are unable to receive or respond to IL-2 signal. It is therefore likely that the Emi1 reliant phenotype is dependent on IL-2 signal, and is not achieved by TCR signaling alone. It would be of interest to confirm the importance of IL-2 to upregulating Emi1 by making use of the IL-2 knockout clone as seen in which showed decrease proliferation in respond to CD3/CD28 stimulation, and total cell cycle arrest in response to rapamycin preincubation prior to activation as oppose to only partial inhibition of cell cycle as seen in the wild type (Colombetti et al. 2006). In addition, within 24 hours of activation, Emi1 KO $CD8^+$ T cells with a DNA content of 2n showed a large upregulation of Eg5 expression similar to what is seen with the T_{mem} but far more pronounced. If this proves to be reproducible, it may be an indication of a yet undocumented mechanism of TCR cell cycle initiation.

In summary, we have demonstrated further evidence which suggests $CD8^+$ T cells have stem-like mechanics regulating cell cycle, that an important component of these pathways is Emi1 mediated APC/C^{Cdh1} inhibition, and that this mechanism is potentially activated only by IL-2 stimulation.

6 Discussion

This study is the first attempt to characterize the mechanisms of cell cycle regulation with $CD8^+$ T cells. We have generated a proteomic data set which dissects cell cycle of an asynchronous population and have identified a number of characteristics of cell cycle regulation that show similarities to stem cell processes within $CD8^+$ T cells. In particular, we have gathered evidence which demonstrates that $CD8^+$ T cells hold a shortened G1 phase maintained by constitutively active proteins involved in origin licensing and DNA replication such as Mcm2, Mcm4, and Cdc45. We also identified a likely mechanism for this is suppression of APC/C^{Cdh1} mediated by high expression of Emi1, confirming this by demonstrating that KO of Emi1 leads to a decrease in cells which pass into S phase.

Stem cells are defined by the potential they hold to differentiate into a variety of possible lineages. They are notable for undergoing rapid proliferation in a manner distinct from most other cell types (Li and Kirschner 2014), and there is a growing interest in how these two characteristics may be mechanistically linked. Within neuron cell development, there are three pathways which are pertinent to promoting stem cell maintenance. Notch signaling which repressed expression of differentiation, Wnt pathways which promotes proliferation via β-Catenin induced upregulation of Cyclin D1 and Myc, and Sox family transcription factors, some of which (SoxB1 genes) maintain multipotency and proliferation, while others (*SoxB2*, *SoxD*, and *SoxE* genes) promote lineage specification and repress proliferation, or in the case of *SoxC* genes, induce proliferation and terminal differentiation in certain lineages (Muhr and Hagey 2021).

It has been observed that over the course of a neuron cells development from ES cell, as it differentiates towards a neural stem cell, levels of Cyclin B1 drop, and along with it so does the abundance of B1 family Sox2 and Notch1 as the cell transitions from an amplifying progenitor cell with a high expression of Cyclin D1, to a fully differentiated neuron with low Cyclin abundance as cell reaches quiescence. Some molecular mechanisms which have been elucidated include the activation of Sox2 to maintain stem cell maintenance which drops as Cyclin B1 decreases to prepare for differentiation and high levels of Sox2 obscuring the binding site of β-Catenin preventing the production of Cyclin D1 (Hagey and Muhr 2014) and thus demonstrating an example of molecular crosstalk between cell cycle and differentiation mechanisms. Indeed, Wnt-signalling was observed to have a direct impact on shortening G1

length via upregulation of Cyclins D1 and E2 in pluripotent stem cells (Jang et al. 2019). It was observed that a larger accumulation of the epigenetic mark 5-hydroxymethylcytosine which are recruited by D cyclins in G1 and are enhanced in number during an elongated G1, influence the lineage restriction of a pluripotent stem cell more towards Neuroectoderm, while pluripotent ES cells with a short G1 length were instead biased towards mesoderm (Hagey and Muhr 2014; Pauklin et al. 2016). This pattern was similarly seen in Fucci mice (Pauklin and Vallier 2013) in that Fucci T cells with a longer G1 were biased towards memory phenotype (Kinjyo et al. 2015).

Emi1 is also implicated in lineage restriction within pluripotent ES cells. Geminin, in addition to inhibiting origin licensing, is known to inhibit expression of Sox2, as well as Oct4 and Nanog, encouraging differentiation towards trophectoderm. An effect which can be caused directly by knock down of Emi1 (V. S. Yang et al. 2011). It is therefore reasonable to consider that $CD8^+$ T cell differentiation may similarly be regulated by cell cycle events, and in particular by regulation of Emi1. This would be in fitting with what is known of $CD4^+$ T cells, for which differentiation is an essential step in their differentiation towards the Th1 or Th2 phenotypes (Proserpio et al. 2016).

One possible mechanism of cell cycle mediated control on differentiation in $CD8^+$ T cells would be via Usp1, an APC/C^{Cdh1} substrate downregulated in G1 within HeLa and U2OS cell lines (Cotto-Rios et al. 2011). Usp1 was confirmed to be low in $G1^{pRb-}$ but high consistently elsewhere within the cell cycle within our dataset, as is Emi1. It is likely then that Usp1 would be regulated by Emi1 expression. Id proteins are a family consisting of 4 proteins (Id1-4). They are inhibitors of a number of transcription factors such as the E proteins, or ETS, the inhibition of which promotes cell proliferation and survival. For example, the inhibition of Id1 and Id3 leads to an increase in E-box mediated upregulation of p16, leading to cell cycle arrest in ovarian cancer cells (Mern, Hasskarl, and Burwinkel 2010), and Id2 has been reported to bind hypophosphorylated Rb, and thereby enhancing proliferation (Iavarone et al. 1994). In addition to promoting proliferation, Id proteins are also linked with inhibiting pathways of differentiation and maintaining stemness in a number of lineages. This includes neural stem cells (Niola et al. 2012), thymocytes (Morrow et al. 1999; Rivera et al. 2000) and a large variety of cancer cells (Lasorella, Benezra, and Iavarone 2014). Usp1 stabilises Id1, Id2, and Id3, preventing their degradation, and thus promoting stemness of the population (Williams et al.

2011). This is in direct opposition to APC/C^{Cdh1} which targets Id1 and Id2 for polyubiquitination, as well as Usp1 (Lasorella et al. 2006).

Within $CD8^+$ T cells, there are a few reports that demonstrate the importance of E proteins in mediating differentiation. One shows that loss of E2A and HEB resulted in an overall decrease in Eomes expression, and a subsequent bias in the production of $KLRG1^{hi}$ $CD127^{lo}$ SLECs over $KLRG1^{lo}$ $CD127^{hi}$ MPEC generation (D'Cruz et al. 2012). Complementing this is data demonstrating that SLECs lose enhancer regions pertaining to E2A binding sites, which are still available in MPECs (Schauder et al. 2021). It has also been shown that Id2 inhibition of E2A, and thus decreased expression of Tcf1 results in a decrease in T-bet production, as well as a decrease in the production of Id3 (Masson et al. 2013), whereas the loss of Id3 leads to defective memory production (C. Y. Yang et al. 2011).

This demonstrates a clear axis between Id2 and Id3 where high Id2 pushes cells towards the SLEC phenotype, and high Id3 towards the MPEC phenotype. Considering that Id2 is APC/C^{Cdh1} controlled, but Id3 is not, $CD8^+$ T cells with high APC/C^{Cdh1} activity would conceivably have less Id2, but still maintain Id3 levels, biasing the cells towards the T_{mem} phenotype, but also enhancing the potential for proliferation by downregulating Cdkis such at p16. Cells that are rich in Emi1 and thus have reduced levels of APC/C^{Cdh1} activity would instead have far more Id2 activity, with its stability enhanced by a greater abundance of Usp1, especially given findings that show that Usp1 is higher in cells which terminally differentiate towards the T_{eff} phenotype (Omilusik et al. 2021). These cells would instead be biased towards the T_{eff} phenotype and enhance proliferation by further inhibiting Rb. It may be the respective impact that Id2 and Id3 have on cell cycle processes that leads to our observation that T_{mem} cells had a greater capacity for proliferation even though they are otherwise prevented from cell cycle re-entry, and why we observed T_{eff} had a greater abundance of p16 present in their pRb+ group compared with T_{mem}.

These findings, if verified, would have a number of implications on cancer immunotherapy. One of the major factors for successful anti-tumor responses is the level of stemness within the cohort of tumor recognising T cells, and in particular the expression of Tcf1 (Sade-Feldman et al. 2018). A prominent obstacle in ACT is the fact that during expansion of TILs, usually done in a high dose IL-2 culture, tends to result in a loss of stemness, and even encourage exhaustion (Y. Liu et al. 2021). Recent studies have looked in to potential means to retain

stemness during expansion, such as culturing with AKT and PI3K inhibitors (Feng et al. 2022), and overexpressing c-Jun in CAR T cells, which has the effect of reducing the impact exhaustion has on effector function by promoting Ap-1-Irf complex formation (Lynn et al. 2019). Mechanisms involved with APC/C regulation could offer another avenue of control to the ACT repertoire, either through partial inhibition of Emi1, or upregulation of proteins which regulate Emi1, in order to enhance APC/C activity and thus preserve Id3 mediated Tcf1 expression.

Our analysis showed no difference between copy number of Emi1 between T_{mem} and T_{eff} when separated between pRb^+ and pRb^-. However, we did observe that the majority of IL-15 treated cells presented as pRb^-, while IL-2 were instead predominately pRb^+, indicating that a change in cell cycle behavior had already taken place as a result of the cytokine stimulation. It would be of interest to examine the proteome of these cells at an earlier time point post cytokine induction. In order to better define when cells have entered origin licensing, it would be useful to augment the PRIMMUS panel to incorporate proteins like Geminin, Cdt1, and even Cdc6, providing a more complete picture of the status of S phase progression.

In order to examine the impact of Emi1KO on S phase entry, cells which showed re-replication were excluded from the cell cycle phase analysis by focusing on the 2n population. As a result, a bias against the successfully knocked out cells was introduced, as the 2n population would include far more Emi1 sufficient cells that would continue to divide normally and thus overshadow the Emi1KO population. It is possible that the impact of Emi1 on cell cycle entry in $CD8^+$ T cells is much greater than we have been able to demonstrate. Carrying out a time course assay post activation of naïve T cells would be of interest in order to examine the rate of Rb phosphorylation and Edu uptake in order to catch the exact moment the cells begin to push towards cell cycle and how Emi1 deficiency impacts this.

One way to overcome the challenge of the Emi1KO population being outcompete would be to enhance the efficiency of the CrispR KO protocol. There are a number of steps which could be taken which would improve upon the protocol such as by experimenting with different primers which may target more accessible loci. Another factor is the temperature in which the Cas9 is left to carry out genome editing. Our protocol puts the cells immediately in 37^{o}C following transfection, but certain loci show greater efficiency at lower temperatures (30^{o}C – 33^{o}C) or higher temperatures (39^{o}C) (Xiang et al. 2017). Another method involves the

generation of a mouse line which holds a reporter, such as GFP, which is downstream of the *Emi1* locus but offset by one frame, such that indels introduced by the KO would shift it back into frame. The signal could then be used to identify confirmed Emi1 KO cells during flow cytometry (W. H. Liu et al. 2021). As an alternative to Crispr, an inducible knockout would allow for a more direct means of gene editing. The Cre system works by incorporating a *Locus Of X-over-P1* (*LoxP*) site at the 5' and 3' end of the gene in question, this would enable the DNA recombinase Cre to loop and recombine the DNA at the *LoxP* sites, removing the sequence between them. Cre generation would also be incorporated into the genome such that Cre protein could be generated within the cell along with some means to inhibit it until treated with an agent which would release it at a specific time point (Kim et al. 2018).

Another way to examine the role Emi1 has would be to conduct an overexpression analysis in which Emi1 production was genetically engineered within T cells by means of a viral vector. Our data has shown that IL-15 stimulation causes the majority of activated $CD8^+$ T cells to remain pRb^-. If we hypothesise that Emi1 expression is the key difference between which cells proliferate and which cells remain with inactive E2F, then we would expect introducing Emi1 into IL-15 treated cells would cause their behavior to match that of IL-2 treated cells. Within a number of somatic models of cell cycle, including MCF10A, HeLa, and non-transformed fibroblasts (Bj-5Ta) it has been observed that Emi1 inhibition of APC/C^{Cdh1} activity is essential for these cell lines to pass the S phase checkpoint, and that overexpression of Emi1 in these cells drastically reduces the time between mitosis and decrease in APC activity (Cappell et al. 2016). It would be useful therefore to see if within IL-2 treated cells whether Emi1 overexpression has a similar impact.

While there is still much to determine about the precise impact Emi1 has on $CD8^+$ T cell development, it is clear that it is an essential protein for cell cycle maintenance in a similar manner to that seen with stem cells and many cancer models.

7 References

Alfieri, C., Chang, L., Zhang, Z., Yang, J., Maslen, S., Skehel, M., and Barford, D. 2016. "Molecular Basis of APC/C Regulation by the Spindle Assembly Checkpoint." *Nature* 536(7617):431. doi: 10.1038/NATURE19083.

Alfieri, C., Zhang, S., and Barford, D. 2017. "Visualizing the Complex Functions and Mechanisms of the Anaphase Promoting Complex/Cyclosome (APC/C)." *Open Biol.* 7(11). doi: 10.1098/RSOB.170204.

Allam, A., Conze, D. B., Torchia, M. L. G., Munitic, I., Yagita, H., Sowell, R. T., Marzo, A. L., and Ashwell, J. D. 2009. "The CD8+ Memory T-Cell State of Readiness Is Actively Maintained and Reversible." *Blood* 114(10):2121. doi: 10.1182/BLOOD-2009-05-220087.

Álvarez-Fernández, M., and Malumbres, M. 2020. "Mechanisms of Sensitivity and Resistance to CDK4/6 Inhibition." *Cancer Cell* 37(4):514–29.

del Amo, P. C., Beneytez, J. L., Boelen, L., Ahmed, R., Miners, K. L., Zhang, Y., Roger, L., Jones, R. E., Marraco, S. A. F., Speiser, D. E., Baird, D. M., Price, D. A., Ladell, K., Macallan, D., and Asquith, B. 2018. "Human T SCM Cell Dynamics in Vivo Are Compatible with Long-Lived Immunological Memory and Stemness." *PLoS Biol.* 16(6):e2005523. doi: 10.1371/journal.pbio.2005523.

Anders, C., Niewoehner, O., Duerst, A., and Jinek, M. 2014. "Structural Basis of PAM-Dependent Target DNA Recognition by the Cas9 Endonuclease." *Nat. 2014 5137519* 513(7519):569–73. doi: 10.1038/nature13579.

Appleman, L. J., Berezovskaya, A., Grass, I., and Boussiotis, V. A. 2000. "CD28 Costimulation Mediates T Cell Expansion Via IL-2-Independent and IL-2-Dependent Regulation of Cell Cycle Progression." *J. Immunol.* 164(1):144–51. doi: 10.4049/jimmunol.164.1.144.

Araki, M., Wharton, R. P., Tang, Z., Yu, H., and Asano, M. 2003. "Degradation of Origin Recognition Complex Large Subunit by the Anaphase-Promoting Complex in Drosophila." *EMBO J.* 22(22):6115–26. doi: 10.1093/EMBOJ/CDG573.

Au-Yeung, B. B., Smith, G. A., Mueller, J. L., Heyn, C. S., Jaszczak, R. G., Weiss, A., and Zikherman, J. 2017. "IL-2 Modulates the TCR Signaling Threshold for CD8 but Not CD4 T Cell Proliferation on a Single-Cell Level." *J. Immunol.* 198(6):2445–56. doi: 10.4049/jimmunol.1601453.

Baas, M., Besançon, A., Goncalves, T., Valette, F., Yagita, H., Sawitzki, B., Volk, H. D., Waeckel-Enée, E., Rocha, B., Chatenoud, L., and You, S. 2016. "TGFβ-Dependent Expression of PD-1 and PD-L1 Controls CD8+ T Cell Anergy in Transplant Tolerance." *Elife* 5(JANUARY2016). doi: 10.7554/ELIFE.08133.

Ballabeni, A., Park, I. H., Zhao, R., Wang, W., Lerou, P. H., Daley, G. Q., and Kirschner, M. W. 2011. "Cell Cycle Adaptations of Embryonic Stem Cells." *Proc. Natl. Acad. Sci. U. S. A.* 108(48):19252–57. doi: 10.1073/PNAS.1116794108/SUPPL_FILE/SAPP.PDF.

Ballabeni, A., Zamponi, R., Caprara, G., Melixetian, M., Bossi, S., Masiero, L., and Helin, K. 2009. "Human CDT1 Associates with CDC7 and Recruits CDC45 to Chromatin during S Phase." *J. Biol. Chem.* 284(5):3028–36. doi: 10.1074/JBC.M803609200.

Balomenos, D., Martín-Caballero, J., García, M. I., Prieto, I., Flores, J. M., Serrano, M., and Martínez-A, C. 2000. “The Cell Cycle Inhibitor P21 Controls T-Cell Proliferation and Sex-Linked Lupus Development.” *Nat. Med.* 6(2):171–76. doi: 10.1038/72272.

Bar-On, O., Shapira, anit, Skorecki, K., Hershko, A., and Hershko, D. D. 2010. “Cell Cycle Regulation of APC/C Cdh1 Ubiquitin Ligase in Differentiation of Human Embryonic Stem Cells.” doi: 10.4161/cc.9.10.11727.

Bar-On, O., Shapira, M., Skorecki, K., Hershko, A., and Hershko, D. D. 2010. “Regulation of APC/CCdh1 Ubiquitin Ligase in Differentiation of Human Embryonic Stem Cells.” *Cell Cycle* 9(10):1986–89. doi: 10.4161/CC.9.10.11727.

Barski, A., Cuddapah, S., Kartashov, A. V., Liu, C., Imamichi, H., Yang, W., Peng, W., Lane, H. C., and Zhao, K. 2017. “Rapid Recall Ability of Memory T Cells Is Encoded in Their Epigenome.” *Sci. Rep.* 7(1):1–10. doi: 10.1038/srep39785.

Bashir, T., Dorello, H. V., Amador, V., Guardavaccaro, D., and Pagano, M. 2004. “Control of the SCFSkp2–Cks1 Ubiquitin Ligase by the APC/CCdh1 Ubiquitin Ligase.” *Nat. 2004 4286979* 428(6979):190–93. doi: 10.1038/nature02330.

Bassermann, F., Frescas, D., Guardavaccaro, D., Busino, L., Peschiaroli, A., and Pagano, M. 2008. “The Cdc14B-Cdh1-Plk1 Axis Controls the G2 DNA Damage Response Checkpoint.” *Cell* 134(2):256. doi: 10.1016/J.CELL.2008.05.043.

Bermejo, R., Vilaboa, N., and Calés, C. 2002. “Regulation of CDC6, Geminin, and CDT1 in Human Cells That Undergo Polyploidization.” *Mol. Biol. Cell* 13(11):3989. doi: 10.1091/MBC.E02-04-0217.

Bornstein, G., Bloom, J., Sitry-Shevah, D., Nakayama, K., Pagano, M., and Hershko, A. 2003. “Role of the SCFSkp2 Ubiquitin Ligase in the Degradation of P21Cip1 in S Phase.” *J. Biol. Chem.* 278(28):25752–57. doi: 10.1074/JBC.M301774200.

Boussiotis, V. A., Freeman, G. J., Taylor, P. A., Berezovskaya, A., Grass, I., Blazar, B. R., and Nadler, L. M. 2000. “P27(Kip1) Functions as an Anergy Factor Inhibiting Interleukin 2 Transcription and Clonal Expansion of Alloreactive Human and Mouse Helper T Lymphocytes.” *Nat. Med.* 6(3):290–97. doi: 10.1038/73144.

Brenes, A., Hukelmann, J., Bensaddek, D., and Lamond, A. I. 2019. “Multibatch TMT Reveals False Positives, Batch Effects and Missing Values.” *Mol. Cell. Proteomics* 18(10):1967. doi: 10.1074/MCP.RA119.001472.

Brenes, A. J., Hukelmann, J. L., Spinelli, L., Howden, A. J. M., Marchingo, J. M., Sinclair, L. V., Rollings, C., James, O. J., Phair, I. R., Matthews, S. P., Ross, S. H., Arthur, J. S. C., Swamy, M., Finlay, D. K., Lamond, A. I., and Cantrell, D. A. 2022. “The Immunological Proteome Resource.” *BioRxiv* 2022.08.29.505666. doi: 10.1101/2022.08.29.505666.

Brennan, P., Babbage, J. W., Thomas, G., and Cantrell, D. 1999. “P70s6k Integrates Phosphatidylinositol 3-Kinase and Rapamycin-Regulated Signals for E2F Regulation in T Lymphocytes.” *Mol. Cell. Biol.* 19(7):4729–38. doi: 10.1128/mcb.19.7.4729.

Brinkman, E. K., Chen, T., Amendola, M., and Van Steensel, B. 2014. “Easy Quantitative Assessment of Genome Editing by Sequence Trace Decomposition.” *Nucleic Acids Res.* 42(22):e168–e168. doi: 10.1093/NAR/GKU936.

Brown, N. G., VanderLinden, R., Watson, E. R., Weissmann, F., Ordureau, A., Wu, K. P., Zhang, W., Yu, S., Mercredi, P. Y., Harrison, J. S., Davidson, I. F., Qiao, R., Lu, Y., Dube, P., Brunner, M. R., Grace, C. R. R., Miller, D. J., Haselbach, D., Jarvis, M. A., Yamaguchi, M., Yanishevski, D., Petzold, G., Sidhu, S. S., Kuhlman, B., Kirschner, M. W., Harper, J. W., Peters, J. M., Stark, H., and Schulman, B. A. 2016. "Dual RING E3 Architectures Regulate Multiubiquitination and Ubiquitin Chain Elongation by APC/C." *Cell* 165(6):1440. doi: 10.1016/J.CELL.2016.05.037.

Brownlie, R. J., and Zamoyska, R. 2013. "T Cell Receptor Signalling Networks: Branched, Diversified and Bounded." *Nat. Rev. Immunol.* 13(4):257–69.

Burchill, M. A., Goetz, C. A., Prlic, M., O'Neil, J. J., Harmon, I. R., Bensinger, S. J., Turka, L. A., Brennan, P., Jameson, S. C., and Farrar, M. A. 2003. " Distinct Effects of STAT5 Activation on CD4 + and CD8 + T Cell Homeostasis: Development of CD4 + CD25 + Regulatory T Cells versus CD8 + Memory T Cells ." *J. Immunol.* 171(11):5853–64. doi: 10.4049/jimmunol.171.11.5853.

Cappell, S. D., Chung, M., Jaimovich, A., Spencer, S. L., and Meyer, T. 2016. "Irreversible APCCdh1 Inactivation Underlies the Point of No Return for Cell-Cycle Entry." *Cell* 166(1):167–80. doi: 10.1016/j.cell.2016.05.077.

Cappell, S. D., Mark, K. G., Garbett, D., Pack, L. R., Rape, M., and Meyer, T. 2018. "EMI1 Switches from Being a Substrate to an Inhibitor of APC/CCDH1 to Start the Cell Cycle." *Nature* 558(7709):313–17. doi: 10.1038/s41586-018-0199-7.

Castro, A., Bernis, C., Vigneron, S., Labbé, J. C., and Lorca, T. 2005. "The Anaphase-Promoting Complex: A Key Factor in the Regulation of Cell Cycle." *Oncogene 2005 243* 24(3):314–25. doi: 10.1038/sj.onc.1207973.

Castro, I., Yu, A., Dee, M. J., and Malek, T. R. 2011. " The Basis of Distinctive IL-2– and IL-15–Dependent Signaling: Weak CD122-Dependent Signaling Favors CD8 + T Central-Memory Cell Survival but Not T Effector-Memory Cell Development ." *J. Immunol.* 187(10):5170–82. doi: 10.4049/jimmunol.1003961.

Cellerai, C., Perreau, M., Rozot, V., Bellutti Enders, F., Pantaleo, G., and Harari, A. 2010. "Proliferation Capacity and Cytotoxic Activity Are Mediated by Functionally and Phenotypically Distinct Virus-Specific CD8 T Cells Defined by Interleukin-7R{alpha} (CD127) and Perforin Expression." *J. Virol.* 84(8):3868–78. doi: 10.1128/JVI.02565-09.

Chee, J., Wilson, C., Buzzai, A., Wylie, B., Forbes, C. A., Booth, M., Principe, N., Foley, B., Cruickshank, M. N., and Waithman, J. 2020. "Impaired T Cell Proliferation by Ex Vivo BET-Inhibition Impedes Adoptive Immunotherapy in a Murine Melanoma Model." *Epigenetics* 15(1–2):134. doi: 10.1080/15592294.2019.1656156.

Chen, H., Chen, Jun, Zhao, L., Song, W., Xuan, Z., Chen, Jian, Li, Z., Song, G., Hong, L., Song, P., and Zheng, S. 2019. "CDCA5, Transcribed by E2F1, Promotes Oncogenesis by Enhancing Cell Proliferation and Inhibiting Apoptosis via the AKT Pathway in Hepatocellular Carcinoma." *J. Cancer* 10(8):1846–54. doi: 10.7150/JCA.28809.

Chen, Z., Ji, Z., Ngiow, S. F., Manne, S., Cai, Z., Huang, A. C., Johnson, J., Staupe, R. P., Bengsch, B., Xu, C., Yu, S., Kurachi, M., Herati, R. S., Vella, L. A., Baxter, A. E., Wu, J. E., Khan, O., Beltra, J. C., Giles, J. R., Stelekati, E., McLane, L. M., Lau, C. W., Yang, X.,

Berger, S. L., Vahedi, G., Ji, H., and Wherry, E. J. 2019. “TCF-1-Centered Transcriptional Network Drives an Effector versus Exhausted CD8 T Cell-Fate Decision.” *Immunity* 51(5):840-855.e5. doi: 10.1016/J.IMMUNI.2019.09.013.

Chen, Z., Li, L., Xu, S., Liu, Z., Zhou, C., Li, Z., Liu, Y., Wu, W., Huang, Y., Kuang, M., Fan, S., Li, H., Li, X., Song, G., Wu, W. S., Chen, J., and Hou, Y. 2020. “A Cdh1–FoxM1–Apc Axis Controls Muscle Development and Regeneration.” *Cell Death Dis.* 11(3). doi: 10.1038/S41419-020-2375-6.

Cheng, M., Olivier, P., Diehl, J. A., Fero, M., Roussel, M. F., Roberts, J. M., and Sherr, C. J. 1999. “The P21(Cip1) and P27(Kip1) CDK ‘inhibitors’ Are Essential Activators of Cyclin D-Dependent Kinases in Murine Fibroblasts.” *EMBO J.* 18(6):1571–83. doi: 10.1093/emboj/18.6.1571.

Cheng, Q., Chen, L., Li, Z., Lane, W. S., and Chen, J. 2009. “ATM Activates P53 by Regulating MDM2 Oligomerization and E3 Processivity.” *EMBO J.* 28(24):3857. doi: 10.1038/EMBOJ.2009.294.

Cho, B. K., Wang, C., Sugawa, S., Eisen, H. N., and Chen, J. 1999. “Functional Differences between Memory and Naive CD8 T Cells.” *Proc. Natl. Acad. Sci. U. S. A.* 96(6):2976–81. doi: 10.1073/pnas.96.6.2976.

Cho, J.-H., Kim, H.-O., Kim, K.-S., Yang, D.-H., Surh, C. D., and Sprent, J. 2013. “ Unique Features of Naive CD8 + T Cell Activation by IL-2 .” *J. Immunol.* 191(11):5559–73. doi: 10.4049/jimmunol.1302293.

Choi, J. H., Lindsey-Boltz, L. A., Kemp, M., Mason, A. C., Wold, M. S., and Sancar, A. 2010. “Reconstitution of RPA-Covered Single-Stranded DNA-Activated ATR-Chk1 Signaling.” *Proc. Natl. Acad. Sci. U. S. A.* 107(31):13660–65. doi: 10.1073/PNAS.1007856107/SUPPL_FILE/PNAS.1007856107_SI.PDF.

Choudhury, R., Bonacci, T., Arceci, A., Lahiri, D., Mills, C. A., Kernan, J. L., Branigan, T. B., DeCaprio, J. A., Burke, D. J., and Emanuele, M. J. 2016. “APC/C and SCFcyclin F Constitute a Reciprocal Feedback Circuit Controlling S-Phase Entry.” *Cell Rep.* 16(12):3359–72. doi: 10.1016/J.CELREP.2016.08.058.

Choudhury, R., Bonacci, T., Wang, X., Truong, A., Arceci, A., Zhang, Y., Mills, C. A., Kernan, J. L., Liu, P., and Emanuele, M. J. 2017. “The E3 Ubiquitin Ligase SCF(Cyclin F) Transmits AKT Signaling to the Cell-Cycle Machinery.” *Cell Rep.* 20(13):3212–22. doi: 10.1016/J.CELREP.2017.08.099.

Clute, P., and Pines, J. 1999. “Temporal and Spatial Control of Cyclin B1 Destruction in Metaphase.” *Nat. Cell Biol. 1999 12* 1(2):82–87. doi: 10.1038/10049.

Colombetti, S., Basso, V., Mueller, D. L., and Mondino, A. 2006. “Prolonged TCR/CD28 Engagement Drives IL-2-Independent T Cell Clonal Expansion through Signaling Mediated by the Mammalian Target of Rapamycin.” *J. Immunol.* 176(5):2730–38. doi: 10.4049/jimmunol.176.5.2730.

Coronado, D., Godet, M., Bourillot, P. Y., Tapponnier, Y., Bernat, A., Petit, M., Afanassieff, M., Markossian, S., Malashicheva, A., Iacone, R., Anastassiadis, K., and Savatier, P. 2013. “A Short G1 Phase Is an Intrinsic Determinant of Naïve Embryonic Stem Cell

Pluripotency." *Stem Cell Res.* 10(1):118–31. doi: 10.1016/J.SCR.2012.10.004.

Costa, R. H. 2005. "FoxM1 Dances with Mitosis." *Nat. Cell Biol. 2005 72* 7(2):108–10. doi: 10.1038/ncb0205-108.

Cotto-Rios, X. M., Jones, M. J. K., Busino, L., Pagano, M., and Huang, T. T. 2011. "APC/CCdh1-Dependent Proteolysis of USP1 Regulates the Response to UV-Mediated DNA Damage." *J. Cell Biol.* 194(2):177. doi: 10.1083/JCB.201101062.

Craney, A., Kelly, A., Jia, L., Fedrigo, I., Yu, H., and Rape, M. 2016. "Control of APC/C-Dependent Ubiquitin Chain Elongation by Reversible Phosphorylation." *Proc. Natl. Acad. Sci. U. S. A.* 113(6):1540–45. doi: 10.1073/PNAS.1522423113/-/DCSUPPLEMENTAL.

D'Cruz, L. M., Lind, K. C., Wu, B. B., Fujimoto, J. K., and Goldrath, A. W. 2012. "Loss of E Protein Transcription Factors E2A and HEB Delays Memory-Precursor Formation during the CD8+ T-Cell Immune Response." *Eur. J. Immunol.* 42(8):2031–41. doi: 10.1002/EJI.201242497.

D'Souza, W. N., and Lefrançois, L. 2003. "IL-2 Is Not Required for the Initiation of CD8 T Cell Cycling but Sustains Expansion." *J. Immunol.* 171(11):5727–35. doi: 10.4049/jimmunol.171.11.5727.

Dang, C. V., O'Donnell, K. A., Zeller, K. I., Nguyen, T., Osthus, R. C., and Li, F. 2006. "The C-Myc Target Gene Network." *Semin. Cancer Biol.* 16(4):253–64.

Dankert, J. F., Rona, G., Clijsters, L., Geter, P., Skaar, J. R., Bermudez-Hernandez, K., Sassani, E., Fenyö, D., Ueberheide, B., Schneider, R., and Pagano, M. 2016. "Cyclin F-Mediated Degradation of SLBP Limits H2A.X Accumulation and Apoptosis upon Genotoxic Stress in G2." *Mol. Cell* 64(3):507–19. doi: 10.1016/J.MOLCEL.2016.09.010.

Davison, T. S., Yin, P., Nie, E., Kay, C., and Arrowsmith, C. H. 1998. "Characterization of the Oligomerization Defects of Two P53 Mutants Found in Families with Li–Fraumeni and Li–Fraumeni-like Syndrome." *Oncogene 1998 175* 17(5):651–56. doi: 10.1038/sj.onc.1202062.

Debes, G. F., Arnold, C. N., Young, A. J., Krautwald, S., Lipp, M., Hay, J. B., and Butcher, E. C. 2005. "Chemokine Receptor CCR7 Required for T Lymphocyte Exit from Peripheral Tissues." *Nat. Immunol.* 6(9):889–94. doi: 10.1038/ni1238.

Dempsey, P. W., Vaidya, S. A., and Cheng, G. 2003. "The Art of War: Innate and Adaptive Immune Responses." *C. Cell. Mol. Life Sci* 60. doi: 10.1007/s00018-003-3180-y.

Deng, J., Wang, E. S., Jenkins, R. W., Li, S., Dries, R., Yates, K., Chhabra, S., Huang, W., Liu, H., Aref, A. R., Ivanova, E., Paweletz, C. P., Bowden, M., Zhou, C. W., Herter-Sprie, G. S., Sorrentino, J. A., Bisi, J. E., Lizotte, P. H., Merlino, A. A., Quinn, M. M., Bufe, L. E., Yang, A., Zhang, Y., Zhang, H., Gao, P., Chen, T., Cavanaugh, M. E., Rode, A. J., Haines, E., Roberts, P. J., Strum, J. C., Richards, W. G., Lorch, J. H., Parangi, S., Gunda, V., Boland, G. M., Bueno, R., Palakurthi, S., Freeman, G. J., Ritz, J., Nicholas Haining, W., Sharpless, N. E., Arthanari, H., Shapiro, G. I., Barbie, D. A., Gray, N. S., and Wong, K. K. 2018. "CDK4/6 Inhibition Augments Antitumor Immunity by Enhancing T-Cell Activation." *Cancer Discov.* 8(2):216–33. doi: 10.1158/2159-8290.CD-17-0915.

Dubois, S., Mariner, J., Waldmann, T. A., and Tagaya, Y. 2002. “IL-15Rα Recycles and Presents IL-15 in Trans to Neighboring Cells.” *Immunity* 17(5):537–47. doi: 10.1016/S1074-7613(02)00429-6.

Dunphy, W. G., and Kumagai, A. 1991. “The Cdc25 Protein Contains an Intrinsic Phosphatase Activity.” *Cell* 67(1):189–96. doi: 10.1016/0092-8674(91)90582-J.

Dutta, M., Das, B., Mohapatra, D., Behera, P., Senapati, S., and Roychowdhury, A. 2022. “MicroRNA-217 Modulates Pancreatic Cancer Progression via Targeting ATAD2.” *Life Sci.* 301:120592. doi: 10.1016/J.LFS.2022.120592.

Dyson, N. 1998. “The Regulation of E2F by PRB-Family Proteins.” *Genes Dev.* 12(15):2245–62.

Emanuele, M. J., Enrico, T. P., Mouery, R. D., Wasserman, D., Nachum, S., and Tzur, A. 2020. “Complex Cartography: E2F Transcriptional Control by Cyclin F and Ubiquitin.” *Trends Cell Biol.* 30(8):640. doi: 10.1016/J.TCB.2020.05.002.

Evrin, C., Clarke, P., Zech, J., Lurz, R., Sun, J., Uhle, S., Li, H., Stillman, B., and Speck, C. 2009. “A Double-Hexameric MCM2-7 Complex Is Loaded onto Origin DNA during Licensing of Eukaryotic DNA Replication.” *Proc. Natl. Acad. Sci. U. S. A.* 106(48):20240–45. doi: 10.1073/PNAS.0911500106.

Feng, H., Qiu, L., Shi, Z., Sheng, Y., Zhao, P., Zhou, D., Li, F., Yu, H., You, Y., Wang, H., Li, M., Zhu, S., Du, Y., Cui, J., Sun, J., Liu, Y., Jiang, H., and Wu, X. 2022. “Modulation of Intracellular Kinase Signaling to Improve TIL Stemness and Function for Adoptive Cell Therapy.” *Cancer Med.* doi: 10.1002/CAM4.5095.

Feng, X., Wang, H., Takata, H., Day, T. J., Willen, J., and Hu, H. 2011. “Transcription Factor Foxp1 Exerts Essential Cell-Intrinsic Regulation of the Quiescence of Naive T Cells.” *Nat. Immunol.* 12(6):544. doi: 10.1038/NI.2034.

Fero, M. L., Rivkin, M., Tasch, M., Porter, P., Carow, C. E., Firpo, E., Polyak, K., Tsai, L. H., Broudy, V., Perlmutter, R. M., Kaushansky, K., and Roberts, J. M. 1996. “A Syndrome of Multiorgan Hyperplasia with Features of Gigantism, Tumorigenesis, and Female Sterility in P27Kip1-Deficient Mice.” *Cell* 85(5):733–44. doi: 10.1016/S0092-8674(00)81239-8.

Fixemer, J., Hummel, J. F., Arnold, F., Klose, C. S. N., Hofherr, A., Weissert, K., Kögl, T., Köttgen, M., Arnold, S. J., Aichele, P., and Tanriver, Y. 2020. “Eomes Cannot Replace Its Paralog T-Bet during Expansion and Differentiation of CD8 Effector T Cells” edited by A. Oxenius. *PLOS Pathog.* 16(9):e1008870. doi: 10.1371/journal.ppat.1008870.

Foe, I. T., Foster, S. A., Cheung, S. K., Deluca, S. Z., Morgan, D. O., and Toczyski, D. P. 2011. “Ubiquitination of Cdc20 by the APC Occurs through an Intramolecular Mechanism.” *Curr. Biol.* 21(22):1870–77. doi: 10.1016/j.cub.2011.09.051.

Frye, J. J., Brown, N. G., Petzold, G., Watson, E. R., Grace, C. R. R., Nourse, A., Jarvis, M. A., Kriwacki, R. W., Peters, J. M., Stark, H., and Schulman, B. A. 2013. “EM Structure of Human APC/CCDH1-EMI1 Reveals Multimodal Mechanism of E3 Ligase Shutdown.” *Nat. Struct. Mol. Biol.* 20(7):827. doi: 10.1038/NSMB.2593.

Fu, H., Redon, C. E., Thakur, B. L., Utani, K., Sebastian, R., Jang, S. M., Gross, J. M.,

Mosavarpour, S., Marks, A. B., Zhuang, S. Z., Lazar, S. B., Rao, M., Mencer, S. T., Baris, A. M., Pongor, L. S., and Aladjem, M. I. 2021. “Dynamics of Replication Origin Over-Activation.” *Nat. Commun. 2021 121* 12(1):1–15. doi: 10.1038/s41467-021-23835-0.

Fujii-Yamamoto, H., Min Kim, J., Arai, K., and Masai, H. 2005. “Cell Cycle and Developmental Regulations of Replication Factors in Mouse Embryonic Stem Cells.” *J. Biol. Chem.* 280(13):12976–87. doi: 10.1074/jbc.M412224200.

Fujimitsu, K., Grimaldi, M., and Yamano, H. 2016. “Cyclin-Dependent Kinase 1-Dependent Activation of APC/C Ubiquitin Ligase.” *Science* 352(6289):1121–24. doi: 10.1126/SCIENCE.AAD3925.

Fukushima, H., Ogura, K., Wan, L., Lu, Y., Li, V., Gao, D., Liu, P., Lau, A. W., Wu, T., Kirschner, M. W., Inuzuka, H., and Wei, W. 2013. “SCF-Mediated Cdh1 Degradation Defines a Negative Feedback System That Coordinates Cell-Cycle Progression.” *Cell Rep.* 4(4):803–16. doi: 10.1016/J.CELREP.2013.07.031.

Galkina, E., Florey, O., Zarbock, A., Smith, B. R. E., Preece, G., Lawrence, M. B., Haskard, D. O., and Ager, A. 2007. “T Lymphocyte Rolling and Recruitment into Peripheral Lymph Nodes Is Regulated by a Saturable Density of L-Selectin (CD62L).” *Eur. J. Immunol.* 37(5):1243–53. doi: 10.1002/eji.200636481.

Garneau, J. E., Dupuis, M. È., Villion, M., Romero, D. A., Barrangou, R., Boyaval, P., Fremaux, C., Horvath, P., Magadán, A. H., and Moineau, S. 2010. “The CRISPR/Cas Bacterial Immune System Cleaves Bacteriophage and Plasmid DNA.” *Nat. 2010 4687320* 468(7320):67–71. doi: 10.1038/nature09523.

Gattinoni, L., Lugli, E., Ji, Y., Pos, Z., Paulos, C. M., Quigley, M. F., Almeida, J. R., Gostick, E., Yu, Z., Carpenito, C., Wang, E., Douek, D. C., Price, D. A., June, C. H., Marincola, F. M., Roederer, M., and Restifo, N. P. 2011. “A Human Memory T Cell Subset with Stem Cell-like Properties.” *Nat. Med.* 17(10):1290–97. doi: 10.1038/nm.2446.

Gattinoni, L., Zhong, X.-S., Palmer, D. C., Ji, Y., Hinrichs, C. S., Yu, Z., Wrzesinski, C., Boni, A., Cassard, L., Garvin, L. M., Paulos, C. M., Muranski, P., and Restifo, N. P. 2009. “Wnt Signaling Arrests Effector T Cell Differentiation and Generates CD8 + Memory Stem Cells.” 15. doi: 10.1038/nm.1982.

Goel, S., DeCristo, M. J., Watt, A. C., BrinJones, H., Sceneay, J., Li, B. B., Khan, N., Ubellacker, J. M., Xie, S., Metzger-Filho, O., Hoog, J., Ellis, M. J., Ma, C., Ramm, S., Krop, I. E., Winer, E. P., Roberts, T. M., Kim, H.-J., McAllister, S. S., and Zhao, J. J. 2017. “CDK4/6 Inhibition Triggers Anti-Tumor Immunity.” *Nature* 548(7668):471. doi: 10.1038/NATURE23465.

Gonzalez, N. M., Zou, D., Gu, A., and Chen, W. 2021. “Schrödinger’s T Cells: Molecular Insights Into Stemness and Exhaustion.” *Front. Immunol.* 12:3480. doi: 10.3389/FIMMU.2021.725618/BIBTEX.

Gookin, S., Min, M., Phadke, H., Chung, M., Moser, J., Miller, I., Carter, D., and Spencer, S. L. 2017. “A Map of Protein Dynamics during Cell-Cycle Progression and Cell-Cycle Exit” edited by J. Pines. *PLOS Biol.* 15(9):e2003268. doi: 10.1371/journal.pbio.2003268.

Graef, P., Buchholz, V. R., Stemberger, C., Flossdorf, M., Henkel, L., Schiemann, M., Drexler, I., Höfer, T., Riddell, S. R., and Busch, D. H. 2014. “Serial Transfer of Single-Cell-Derived

Immunocompetence Reveals Stemness of CD8+ Central Memory T Cells." *Immunity* 41(1):116–26. doi: 10.1016/j.immuni.2014.05.018.

Grange, M., Giordano, M., Mas, A., Roncagalli, R., Firaguay, G., Nunes, J. A., Ghysdael, J., Schmitt-Verhulst, A. M., and Auphan-Anezin, N. 2015. "Control of CD8 T Cell Proliferation and Terminal Differentiation by Active STAT5 and CDKN2A/CDKN2B." *Immunology* 145(4):543–57. doi: 10.1111/imm.12471.

Greil, C., Engelhardt, M., and Wäsch, R. 2022. "The Role of the APC/C and Its Coactivators Cdh1 and Cdc20 in Cancer Development and Therapy." *Front. Genet.* 13:27. doi: 10.3389/FGENE.2022.941565.

Grimmler, M., Wang, Y., Mund, T., Cilenšek, Z., Keidel, E. M., Waddell, M. B., Jäkel, H., Kullmann, M., Kriwacki, R. W., and Hengst, L. 2007. "Cdk-Inhibitory Activity and Stability of P27Kip1 Are Directly Regulated by Oncogenic Tyrosine Kinases." *Cell* 128(2):269–80. doi: 10.1016/j.cell.2006.11.047.

Gruber, T., Hermann-Kleiter, N., Hinterleitner, R., Fresser, F., Schneider, R., Gastl, G., Penninger, J. M., and Baier, G. 2009. "PKC-θ Modulates the Strength of T Cell Responses by Targeting Cbl-b for Ubiquitination and Degradation." *Sci. Signal.* 2(76):ra30–ra30. doi: 10.1126/scisignal.2000046.

Grzonka, M., and Bazzi, H. 2022. "Mouse SAS-6 Is Required for Centriole Formation in Embryos and Integrity in Embryonic Stem Cells." *BioRxiv* 2022.08.11.503634. doi: 10.1101/2022.08.11.503634.

Guiley, K. Z., Stevenson, J. W., Lou, K., Barkovich, K. J., Kumarasamy, V., Wijeratne, T. U., Bunch, K. L., Tripathi, S., Knudsen, E. S., Witkiewicz, A. K., Shokat, K. M., and Rubin, S. M. 2019. "P27 Allosterically Activates Cyclin-Dependent Kinase 4 and Antagonizes Palbociclib Inhibition." *Science (80-.).* 366(6471). doi: 10.1126/science.aaw2106.

Hagey, D. W., and Muhr, J. 2014. "Sox2 Acts in a Dose-Dependent Fashion to Regulate Proliferation of Cortical Progenitors." *Cell Rep.* 9(5):1908–20. doi: 10.1016/j.celrep.2014.11.013.

Hames, R. S., Wattam, S. L., Yamano, H., Bacchieri, R., and Fry, A. M. 2001. "APC/C-Mediated Destruction of the Centrosomal Kinase Nek2A Occurs in Early Mitosis and Depends upon a Cyclin A-Type D-Box." *EMBO J.* 20(24):7117. doi: 10.1093/EMBOJ/20.24.7117.

Hand, T. W., Cui, W., Woo Jung, Y., Sefik, E., Joshi, N. S., Chandele, A., Liu, Y., and Kaech, S. M. 2010. "Differential Effects of STAT5 and PI3K/AKT Signaling on Effector and Memory CD8 T-Cell Survival." 107(38):16601–6. doi: 10.1073/pnas.

Hao, B., Zheng, N., Schulman, B. A., Wu, G., Miller, J. J., Pagano, M., and Pavletich, N. P. 2005. "Structural Basis of the Cks1-Dependent Recognition of P27Kip1 by the SCFSkp2 Ubiquitin Ligase." *Mol. Cell* 20(1):9–19. doi: 10.1016/J.MOLCEL.2005.09.003.

Hao, H., Yuan, X., Xiao-Yu, Z., Yang, D., Fu-Jian, W., You, H., Xing-Hua, L., and Tong-Cun, Z. 2022. "CDCA5 Promotes the Progression of Breast Cancer and Serves as a Potential Prognostic Biomarker." *Oncol. Rep.* 48(4). doi: 10.3892/OR.2022.8387.

Hao, Z., Sheng, Y., Duncan, G. S., Li, W. Y., Dominguez, C., Sylvester, J., Su, Y. W., Lin, G. H. Y., Snow, B. E., Brenner, D., You-Ten, A., Haight, J., Inoue, S., Wakeham, A., Elford, A.,

Hamilton, S., Liang, Y., Zúñiga-Pflücker, J. C., He, H. H., Ohashi, P. S., and Mak, T. W. 2017. “K48-Linked KLF4 Ubiquitination by E3 Ligase Mule Controls T-Cell Proliferation and Cell Cycle Progression.” *Nat. Commun. 2017 81* 8(1):1–14. doi: 10.1038/ncomms14003.

Hazan, R., Mori, M., Danielian, P. S., Guen, V. J., Rubin, S. M., Cardoso, W. V., and Lees, J. A. 2021. “E2F4’s Cytoplasmic Role in Multiciliogenesis Is Mediated via an N-Terminal Domain That Binds Two Components of the Centriole Replication Machinery, Deup1 and SAS6.” *Mol. Biol. Cell* 32(20). doi: 10.1091/MBC.E21-01-0039.

Heckler, M., Ali, L. R., Clancy-Thompson, E., Qiang, L., Ventre, K. S., Lenehan, P., Roehle, K., Luoma, A., Boelaars, K., Peters, V., Boschert, T., Wang, E. S., Suo, S., Marangoni, F., Mempel, T. R., Long, H. W., Wucherpfennig, K. W., Dougan, M., Gray, S., Yuan, G.-C., Goel, S., Tolaney, S. M., and Dougan, S. K. 2021. “Inhibition of CDK4/6 Promotes CD8 T Cell Memory Formation 1 2.” *Author Manuscr. Publ. OnlineFirst*. doi: 10.1158/2159-8290.CD-20-1540.

Heuser, C., and Gattinoni, L. 2022. “C-Myb Redefines the Hierarchy of Stem-like T Cells.” 23. doi: 10.1038/s41590-022-01319-7.

Honda, K., Mihara, H., Kato, Y., Yamaguchi, A., Tanaka, H., Yasuda, H., Furukawa, K., and Urano, T. 2000. “Degradation of Human Aurora2 Protein Kinase by the Anaphase-Promoting Complex-Ubiquitin-Proteasome Pathway.” *Oncogene* 19(24):2812–19. doi: 10.1038/SJ.ONC.1203609.

Howden, A. J. M., Hukelmann, J. L., Brenes, A., Spinelli, L., Sinclair, L. V., Lamond, A. I., and Cantrell, D. A. 2019. “Quantitative Analysis of T Cell Proteomes and Environmental Sensors during T Cell Differentiation.” *Nat. Immunol.* 20(11):1542–54. doi: 10.1038/s41590-019-0495-x.

Huang, H., Regan, K. M., Lou, Z., Chen, J., and Tindall, D. J. 2006. “CDK2-Dependent Phosphorylation of FOXO1 as an Apoptotic Response to DNA Damage.” *Science (80-.).* 314(5797):294–97. doi: 10.1126/science.1130512.

Huang, X. D., Summers, M. K., Pham, V., Lill, J. R., Liu, J., Lee, G., Kirkpatrick, D. S., Jackson, P. K., Fang, G., and Dixit, V. M. 2011. “Deubiquitinase USP37 Is Activated by CDK2 to Antagonize APCCDH1 and Promote S Phase Entry.” *Mol. Cell* 42(4):511–23. doi: 10.1016/j.molcel.2011.03.027.

Hwang, J. R., Byeon, Y., Kim, D., and Park, S. G. 2020. “Recent Insights of T Cell Receptor-Mediated Signaling Pathways for T Cell Activation and Development.” *Exp. Mol. Med.* 52(5):750–61.

Hwang, S. M., Im, S. H., and Rudra, D. 2022. “Signaling Networks Controlling ID and E Protein Activity in T Cell Differentiation and Function.” *Front. Immunol.* 13:4321. doi: 10.3389/FIMMU.2022.964581/BIBTEX.

Iavarone, A., Garg, P., Lasorella, A., Hsu, J., and Israel, M. A. 1994. “The Helix-Loop-Helix Protein Id-2 Enhances Cell Proliferation and Binds to the Retinoblastoma Protein.” *Genes Dev.* 8(11):1270–84. doi: 10.1101/GAD.8.11.1270.

Immpress.co.uk. n.d. “ImmPRes.Co.Uk.” *Univ. Dundee*. Retrieved June 17, 2021

(http://immpres.co.uk/).

Ito, D., Zitouni, S., Jana, S. C., Duarte, P., Surkont, J., Carvalho-Santos, Z., Pereira-Leal, J. B., Ferreira, M. G., and Bettencourt-Dias, M. 2019. "Pericentrin-Mediated SAS-6 Recruitment Promotes Centriole Assembly." *Elife* 8. doi: 10.7554/ELIFE.41418.

Jacobberger, J. W., Frisa, P. S., Sramkoski, R. M., Stefan, T., Shults, K. E., and Soni, D. V. 2008. "A New Biomarker for Mitotic Cells." *Cytom. Part A* 73A(1):5–15. doi: 10.1002/cyto.a.20501.

Jang, J., Han, D., Golkaram, M., Audouard, M., Liu, G., Bridges, D., Hellander, S., Chialastri, A., Dey, S. S., Petzold, L. R., and Kosik, K. S. 2019. "Control over Single-Cell Distribution of G1 Lengths by WNT Governs Pluripotency." *PLoS Biol.* 17(9). doi: 10.1371/JOURNAL.PBIO.3000453.

Ji, Y., Pos, Z., Rao, M., Klebanoff, C. A., Yu, Z., Sukumar, M., Reger, R. N., Palmer, D. C., Borman, Z. A., Muranski, P., Wang, E., Schrump, D. S., Marincola, F. M., Restifo, N. P., and Gattinoni, L. 2011. "Repression of the DNA-Binding Inhibitor Id3 by Blimp-1 Limits the Formation of Memory CD8+ T Cells." *Nat. Immunol. 2011 1212* 12(12):1230–37. doi: 10.1038/ni.2153.

Jiang, X., Tang, L., Yuan, Y., Wang, J., Zhang, D., Qian, K., Cho, W. C., and Duan, L. 2022. "NcRNA-Mediated High Expression of HMMR as a Prognostic Biomarker Correlated With Cell Proliferation and Cell Migration in Lung Adenocarcinoma." *Front. Oncol.* 12:1. doi: 10.3389/FONC.2022.846536/FULL.

Joshi, K., Banasavadi-Siddegowda, Y., Mo, X., Kim, S. H., Mao, P., Kig, C., Nardini, D., Sobol, R. W., Chow, L. M. L., Kornblum, H. I., Waclaw, R., Beullens, M., and Nakano, I. 2013. "MELK-Dependent FOXM1 Phosphorylation Is Essential for Proliferation of Glioma Stem Cells." *Stem Cells* 31(6):1051. doi: 10.1002/STEM.1358.

Joshi, N. S., Cui, W., Chandele, A., Lee, H. K., Urso, D. R., Hagman, J., Gapin, L., and Kaech, S. M. 2007. "Inflammation Directs Memory Precursor and Short-Lived Effector CD8+ T Cell Fates via the Graded Expression of T-Bet Transcription Factor." *Immunity* 27(2):281–95. doi: 10.1016/j.immuni.2007.07.010.

Jung Park, E., Hee Kim, J., Hyun Seong, R., Geun Kim, C., Dai Park, S., and Hwan Hong, S. 1999. "Characterization of a Novel Mouse CDNA, ES18, Involved in Apoptotic Cell Death of T-Cells." *Nucleic Acids Res.* 27(6).

Jutz, S., Leitner, J., Schmetterer, K., Doel-Perez, I., Majdic, O., Grabmeier-Pfistershammer, K., Paster, W., Huppa, J. B., and Steinberger, P. 2016. "Assessment of Costimulation and Coinhibition in a Triple Parameter T Cell Reporter Line: Simultaneous Measurement of NF-KB, NFAT and AP-1." *J. Immunol. Methods* 430:10–20. doi: 10.1016/j.jim.2016.01.007.

Kaech, S. M., and Cui, W. 2012. "Transcriptional Control of Effector and Memory CD8+ T Cell Differentiation." *Nat. Rev. Immunol. 2012 1211* 12(11):749–61. doi: 10.1038/nri3307.

Kaech, S. M., Tan, J. T., Wherry, E. J., Konieczny, B. T., Surh, C. D., and Ahmed, R. 2003. "Selective Expression of the Interleukin 7 Receptor Identifies Effector CD8 T Cells That Give Rise to Long-Lived Memory Cells." *Nat. Immunol.* 4(12):1191–98. doi:

10.1038/ni1009.

Kalucka, J., Missiaen, R., Georgiadou, M., Schoors, S., Lange, C., De Bock, K., Dewerchin, M., and Carmeliet, P. 2015. “Metabolic Control of the Cell Cycle.” *Cell Cycle* 14(21):3379. doi: 10.1080/15384101.2015.1090068.

Kamura, T., Hara, T., Kotoshiba, S., Yada, M., Ishida, N., Imaki, H., Hatakeyama, S., Nakayama, K., and Nakayama, K. I. 2003. “Degradation of P57Kip2 Mediated by SCFSkp2-Dependent Ubiquitylation.” *Proc. Natl. Acad. Sci. U. S. A.* 100(18):10231–36. doi: 10.1073/PNAS.1831009100.

Karpievitch, Y. V, Polpitiya, A. D., Anderson, G. A., Smith, R. D., and Dabney, A. R. 2010. “Liquid Chromatography Mass Spectrometry-Based Proteomics: Biological and Technological Aspects.” *Ann. Appl. Stat.* 4(4):1797–1823. doi: 10.1214/10-AOAS341.

Kavazović, I. I., Han, H., Balzaretti, G., Slinger, E., W LemmermannID, N. A., ten Brinke, A., Merkler, D., KosterID, J., Bryceson, Y. T., de Vries, N., Jonjić, S., Klarenbeek, P. L., PolićID, B., Eldering, E., and WensveenID, F. M. 2020. “Eomes Broadens the Scope of CD8 T-Cell Memory by Inhibiting Apoptosis in Cells of Low Affinity.” doi: 10.1371/journal.pbio.3000648.

Kelly, J. M., Sterry, S. J., Cose, S., Turner, S. J., Fecondo, J., Rodda, S., Fink, P. J., and Carbone, F. R. 1993. “Identification of Conserved T Cell Receptor CDR3 Residues Contacting Known Exposed Peptide Side Chains from a Major Histocompatibility Complex Class I-Bound Determinant.” *Eur. J. Immunol.* 23(12):3318–26. doi: 10.1002/eji.1830231239.

Kelly, V., al-Rawi, A., Lewis, D., Kustatscher, G., and Ly, T. 2022. “Low Cell Number Proteomic Analysis Using In-Cell Protease Digests Reveals a Robust Signature for Cell Cycle State Classification.” *Mol. Cell. Proteomics* 21(1):100169. doi: 10.1016/J.MCPRO.2021.100169.

Kim, H., Kim, M., Im, S.-K., and Fang, S. 2018. “Mouse Cre-LoxP System: General Principles to Determine Tissue-Specific Roles of Target Genes.” *Lab. Anim. Res.* 34(4):147. doi: 10.5625/LAR.2018.34.4.147.

Kim, P. S., and Ahmed, R. 2010. “Features of Responding T Cells in Cancer and Chronic Infection.” *Curr. Opin. Immunol.* 22(2):223–30. doi: 10.1016/j.coi.2010.02.005.

Kinjyo, I., Qin, J., Tan, S.-Y., Wellard, C. J., Mrass, P., Ritchie, W., Doi, A., Cavanagh, L. L., Tomura, M., Sakaue-Sawano, A., Kanagawa, O., Miyawaki, A., Hodgkin, P. D., and Weninger, W. 2015. “Real-Time Tracking of Cell Cycle Progression during CD8+ Effector and Memory T-Cell Differentiation.” *Nat. Commun.* 6:6301. doi: 10.1038/ncomms7301.

Kiyokawa, H., Kineman, R. D., Manova-Todorova, K. O., Soares, V. C., Huffman, E. S., Ono, M., Khanam, D., Hayday, A. C., Frohman, L. A., and Koff, A. 1996. “Enhanced Growth of Mice Lacking the Cyclin-Dependent Kinase Inhibitor Function of P27Kip1.” *Cell* 85(5):721–32. doi: 10.1016/S0092-8674(00)81238-6.

Klotz-Noack, K., McIntosh, D., Schurch, N., Pratt, N., and Blow, J. J. 2012. “Re-Replication Induced by Geminin Depletion Occurs from G2 and Is Enhanced by Checkpoint Activation.” *J. Cell Sci.* 125(10):2436–45. doi: 10.1242/JCS.100883/263217/AM/RE-REPLICATION-INDUCED-BY-GEMININ-DEPLETION-OCCURS.

Knox, J. J., Cosma, G. L., Betts, M. R., and McLane, L. M. 2014. “Characterization of T-Bet and Eomes in Peripheral Human Immune Cells.” *Front. Immunol.* 5(MAY). doi: 10.3389/fimmu.2014.00217.

Koenen, P., Heinzel, S., Carrington, E. M., Happo, L., Alexander, W. S., Zhang, J. G., Herold, M. J., Scott, C. L., Lew, A. M., Strasser, A., and Hodgkin, P. D. 2013. “Mutually Exclusive Regulation of T Cell Survival by IL-7R and Antigen Receptor-Induced Signals.” *Nat. Commun. 2013 41* 4(1):1–10. doi: 10.1038/ncomms2719.

Koo, S. J., Fernández-Montalván, A. E., Badock, V., Ott, C. J., Holton, S. J., von Ahsen, O., Toedling, J., Vittori, S., Bradner, J. E., and Gorjánácz, M. 2016. “ATAD2 Is an Epigenetic Reader of Newly Synthesized Histone Marks during DNA Replication.” *Oncotarget* 7(43):70323. doi: 10.18632/ONCOTARGET.11855.

Kowalczyk, M. S., Tirosh, I., Heckl, D., Rao, T. N., Dixit, A., Haas, B. J., Schneider, R. K., Wagers, A. J., Ebert, B. L., and Regev, A. 2015. “Single-Cell RNA-Seq Reveals Changes in Cell Cycle and Differentiation Programs upon Aging of Hematopoietic Stem Cells.” *Genome Res.* 25(12):1860. doi: 10.1101/GR.192237.115.

Kramer, E. R., Scheuringer, N., Podtelejnikov, A. V., Mann, M., and Peters, J. M. 2000. “Mitotic Regulation of the APC Activator Proteins CDC20 and CDH1.” *Mol. Biol. Cell* 11(5):1555–69. doi: 10.1091/mbc.11.5.1555.

Krasny, L., and Huang, P. H. 2021. “Data-Independent Acquisition Mass Spectrometry (DIA-MS) for Proteomic Applications in Oncology.” *Mol. Omi.* 17(1):29–42. doi: 10.1039/D0MO00072H.

Kretschmer, L., Flossdorf, M., Mir, J., Cho, Y. L., Plambeck, M., Treise, I., Toska, A., Heinzel, S., Schiemann, M., Busch, D. H., and Buchholz, V. R. 2020. “Differential Expansion of T Central Memory Precursor and Effector Subsets Is Regulated by Division Speed.” *Nat. Commun.* 11(1):1–12. doi: 10.1038/s41467-019-13788-w.

Kurts, C., Kosaka, H., Carbone, F. R., Miller, J. F. A. P., and Heath, W. R. 1997. “Class I-Restricted Cross-Presentation of Exogenous Self-Antigens Leads to Deletion of Autoreactive CD8+ T Cells.” *J. Exp. Med.* 186(2):239–45. doi: 10.1084/jem.186.2.239.

Kye, Y. C., Lee, G. W., Lee, S. W., Ju, Y. J., Kim, H. O., Yun, C. H., and Cho, J. H. 2021. “STAT1 Maintains Naïve CD8+ T Cell Quiescence by Suppressing the Type I IFN-STAT4-MTORC1 Signaling Axis.” *Sci. Adv.* 7(36). doi: 10.1126/SCIADV.ABG8764/SUPPL_FILE/SCIADV.ABG8764_SM.PDF.

Labaer, J., Garrett, M. D., Stevenson, L. F., Slingerland, J. M., Sandhu, C., Chou, H. S., Fattaey, A., and Harlow, E. 1997. “New Functional Activities for the P21 Family of CDK Inhibitors.” *Genes Dev.* 11(7):847–62. doi: 10.1101/gad.11.7.847.

Lasorella, A., Benezra, R., and Iavarone, A. 2014. “The ID Proteins: Master Regulators of Cancer Stem Cells and Tumour Aggressiveness.” *Nat. Rev. Cancer 2014 142* 14(2):77–91. doi: 10.1038/nrc3638.

Lasorella, A., Stegmüller, J., Guardavaccaro, D., Liu, G., Carro, M. S., Rothschild, G., De La Torre-Ubieta, L., Pagano, M., Bonni, A., and Iavarone, A. 2006. “Degradation of Id2 by the Anaphase-Promoting Complex Couples Cell Cycle Exit and Axonal Growth.” *Nat.*

2006 4427101 442(7101):471–74. doi: 10.1038/nature04895.

Lau, A. W., Inuzuka, H., Fukushima, H., Wan, L., Liu, P., Gao, D., Sun, Y., and Wei, W. 2013. "Regulation of APCCdh1 E3 Ligase Activity by the Fbw7/Cyclin E Signaling Axis Contributes to the Tumor Suppressor Function of Fbw7." *Cell Res. 2013 237* 23(7):947–61. doi: 10.1038/cr.2013.67.

Lee, H., Lee, D. J., Oh, S. P., Park, H. D., Nam, H. H., Kim, J. M., and Lim, D.-S. 2006. " Mouse Emi1 Has an Essential Function in Mitotic Progression during Early Embryogenesis ." *Mol. Cell. Biol.* 26(14):5373–81. doi: 10.1128/MCB.00043-06/SUPPL_FILE/FIGLEGENDSFORSUPPDATA_43_06.DOC.

Lewis, D. A., and Ly, T. 2021. "Cell Cycle Entry Control in Naïve and Memory CD8+ T Cells." *Front. Cell Dev. Biol.* 9:727441. doi: 10.3389/FCELL.2021.727441.

Li, A., and Blow, J. J. 2005. "Cdt1 Downregulation by Proteolysis and Geminin Inhibition Prevents DNA Re-Replication in Xenopus." *EMBO J.* 24(2):395. doi: 10.1038/SJ.EMBOJ.7600520.

Li, D., Gál, I., Vermes, C., Alegre, M.-L., Chong, A. S. F., Chen, L., Shao, Q., Adarichev, V., Xu, X., Koreny, T., Mikecz, K., Finnegan, A., Glant, T. T., and Zhang, J. 2004. "Cutting Edge: Cbl-b: One of the Key Molecules Tuning CD28- and CTLA-4-Mediated T Cell Costimulation." *J. Immunol.* 173(12):7135–39. doi: 10.4049/jimmunol.173.12.7135.

Li, G., Yang, Q., Zhu, Y., Wang, H. R., Chen, X., Zhang, X., and Lu, B. 2013. "T-Bet and Eomes Regulate the Balance between the Effector/Central Memory T Cells versus Memory Stem Like T Cells." *PLoS One* 8(6). doi: 10.1371/JOURNAL.PONE.0067401.

Li, V. C., and Kirschner, M. W. 2014. "Molecular Ties between the Cell Cycle and Differentiation in Embryonic Stem Cells." *Proc. Natl. Acad. Sci. U. S. A.* 111(26):9503–8. doi: 10.1073/PNAS.1408638111/-/DCSUPPLEMENTAL.

Liao, W., Lin, J. X., and Leonard, W. J. 2013. "Interleukin-2 at the Crossroads of Effector Responses, Tolerance, and Immunotherapy." *Immunity* 38(1):13–25.

Liu, Q., Langdon, W. Y., and Zhang, J. 2014. "E3 Ubiquitin Ligase Cbl-b in Innate and Adaptive Immunity." *Cell Cycle* 13(12):1875–84.

Liu, W. H., Völse, K., Senft, D., and Jeremias, I. 2021. "A Reporter System for Enriching CRISPR/Cas9 Knockout Cells in Technically Challenging Settings like Patient Models." *Sci. Rep.* 11(1):12649. doi: 10.1038/S41598-021-91760-9.

Liu, Y., Zhou, N., Zhou, L., Wang, J., Zhou, Y., Zhang, T., Fang, Yi, Deng, J., Gao, Y., Liang, X., Lv, J., Wang, Z., Xie, J., Xue, Y., Zhang, Huafeng, Ma, J., Tang, K., Fang, Yiliang, Cheng, F., Zhang, C., Dong, B., Zhao, Y., Yuan, P., Gao, Q., Zhang, Haizeng, Xiao-Feng Qin, F., and Huang, B. 2021. "IL-2 Regulates Tumor-Reactive CD8+ T Cell Exhaustion by Activating the Aryl Hydrocarbon Receptor." *Nat. Immunol. 2021 223* 22(3):358–69. doi: 10.1038/s41590-020-00850-9.

Lockyer, H. M., Tran, E., and Nelson, B. H. 2007. "STAT5 Is Essential for Akt/P70S6 Kinase Activity during IL-2-Induced Lymphocyte Proliferation." *J. Immunol.* 179(8):5301–8. doi: 10.4049/jimmunol.179.8.5301.

Lord, J. D., McIntosh, B. C., Greenberg, P. D., and Nelson, B. H. 2000. " The IL-2 Receptor Promotes Lymphocyte Proliferation and Induction of the c- Myc, Bcl-2, and Bcl-x Genes Through the Trans- Activation Domain of Stat5 ." *J. Immunol.* 164(5):2533–41. doi: 10.4049/jimmunol.164.5.2533.

Lukas, C., Sørensen, C. S., Kramer, E., Santoni-Ruglu, E., Lindeneg, C., Peters, J. M., Bartek, J., and Lukas, J. 1999. "Accumulation of Cyclin B1 Requires E2F and Cyclin-A-Dependent Rearrangement of the Anaphase-Promoting Complex." *Nature* 401(6755):815–18. doi: 10.1038/44611.

Ly, T., Ahmad, Y., Shlien, A., Soroka, D., Mills, A., Emanuele, M. J., Stratton, M. R., and Lamond, A. I. 2014. "A Proteomic Chronology of Gene Expression through the Cell Cycle in Human Myeloid Leukemia Cells." *Elife* 3:e01630. doi: 10.7554/eLife.01630.

Ly, T., Endo, A., and Lamond, A. I. 2015. "Proteomic Analysis of the Response to Cell Cycle Arrests in Human Myeloid Leukemia Cells." *Elife* 2015(4). doi: 10.7554/ELIFE.04534.

Ly, T., Whigham, A., Clarke, R., Brenes-Murillo, A. J., Estes, B., Madhessian, D., Lundberg, E., Wadsworth, P., and Lamond, A. I. 2017. "Proteomic Analysis of Cell Cycle Progression in Asynchronous Cultures, Including Mitotic Subphases, Using PRIMMUS." *Elife* 6. doi: 10.7554/eLife.27574.

Lynn, R. C., Weber, E. W., Sotillo, E., Gennert, D., Xu, P., Good, Z., Anbunathan, H., Lattin, J., Jones, R., Tieu, V., Nagaraja, S., Granja, J., de Bourcy, C. F. A., Majzner, R., Satpathy, A. T., Quake, S. R., Monje, M., Chang, H. Y., and Mackall, C. L. 2019. "C-Jun Overexpression in CAR T Cells Induces Exhaustion Resistance." *Nat. 2019 5767786* 576(7786):293–300. doi: 10.1038/s41586-019-1805-z.

Macallan, D. C., Busch, R., and Asquith, B. 2019. "Current Estimates of T Cell Kinetics in Humans." *Curr. Opin. Syst. Biol.* 18:77–86.

Macallan, D. C., Wallace, D., Zhang, Y., De Lara, C., Worth, A. T., Ghattas, H., Griffin, G. E., Beverley, P. C. L., and Tough, D. F. 2004. "Rapid Turnover of Effector-Memory CD4+ T Cells in Healthy Humans." *J. Exp. Med.* 200(2):255–60. doi: 10.1084/jem.20040341.

Machida, Y. J., and Dutta, A. 2007. "The APC/C Inhibitor, Emi1, Is Essential for Prevention of Rereplication." *Genes Dev.* 21(2):184. doi: 10.1101/GAD.1495007.

Macintyre, A. N., Finlay, D., Preston, G., Sinclair, L. V., Waugh, C. M., Tamas, P., Feijoo, C., Okkenhaug, K., and Cantrell, D. A. 2011. "Protein Kinase B Controls Transcriptional Programs That Direct Cytotoxic T Cell Fate but Is Dispensable for T Cell Metabolism." *Immunity* 34(2):224–36. doi: 10.1016/j.immuni.2011.01.012.

Mailand, N., and Diffley, J. F. X. 2005. "CDKs Promote DNA Replication Origin Licensing in Human Cells by Protecting Cdc6 from APC/C-Dependent Proteolysis." *Cell* 122(6):915–26. doi: 10.1016/j.cell.2005.08.013.

Margottin-Goguet, F., Hsu, J. Y., Loktev, A., Hsieh, H. M., Reimann, J. D. R., and Jackson, P. K. 2003. "Prophase Destruction of Emi1 by the SCFβTrCP/Slimb Ubiquitin Ligase Activates the Anaphase Promoting Complex to Allow Progression beyond Prometaphase." *Dev. Cell* 4(6):813–26. doi: 10.1016/S1534-5807(03)00153-9.

Martín-Otal, C., Navarro, F., Casares, N., Lasarte-Cía, A., Sánchez-Moreno, I., Hervás-Stubbs,

S., Lozano, T., and Lasarte, J. J. 2022. “Impact of Tumor Microenvironment on Adoptive T Cell Transfer Activity.” *Int. Rev. Cell Mol. Biol.* 370:1–31. doi: 10.1016/BS.IRCMB.2022.03.002.

Masson, F., Minnich, M., Olshansky, M., Bilic, I., Mount, A. M., Kallies, A., Speed, T. P., Busslinger, M., Nutt, S. L., and Belz, G. T. 2013. “Id2-Mediated Inhibition of E2A Represses Memory CD8+ T Cell Differentiation.” *J. Immunol.* 190(9):4585–94. doi: 10.4049/JIMMUNOL.1300099.

Mavrommati, I., Faedda, R., Galasso, G., Li, J., Burdova, K., Fischer, R., Kessler, B. M., Carrero, Z. I., Guardavaccaro, D., Pagano, M., and D’Angiolella, V. 2018. “β-TrCP- and Casein Kinase II-Mediated Degradation of Cyclin F Controls Timely Mitotic Progression.” *Cell Rep.* 24(13):3404–12. doi: 10.1016/J.CELREP.2018.08.076.

McGarry, T. J., and Kirschner, M. W. 1998. “Geminin, an Inhibitor of DNA Replication, Is Degraded during Mitosis.” *Cell* 93(6):1043–53. doi: 10.1016/S0092-8674(00)81209-X.

McLane, L. M., Banerjee, P. P., Cosma, G. L., Makedonas, G., Wherry, E. J., Orange, J. S., and Betts, M. R. 2013. “Differential Localization of T-Bet and Eomes in CD8 T Cell Memory Populations.” *J. Immunol.* 190(7):3207–15. doi: 10.4049/jimmunol.1201556.

Meghnem, D., Morisseau, S., Frutoso, M., Trillet, K., Maillasson, M., Barbieux, I., Khaddage, S., Leray, I., Hildinger, M., Quéméner, A., Jacques, Y., and Mortier, E. 2017. “Cutting Edge: Differential Fine-Tuning of IL-2- and IL-15-Dependent Functions by Targeting Their Common IL-2/15Rβ/Γc Receptor.” *J. Immunol.* 198(12):4563–68. doi: 10.4049/JIMMUNOL.1700046.

Mehlhop-Williams, E. R., and Bevan, M. J. 2014. “Memory CD8+ T Cells Exhibit Increased Antigen Threshold Requirements for Recall Proliferation.” *J. Exp. Med.* 211(2):345–56. doi: 10.1084/jem.20131271.

Mern, D. S., Hasskarl, J., and Burwinkel, B. 2010. “Inhibition of Id Proteins by a Peptide Aptamer Induces Cell-Cycle Arrest and Apoptosis in Ovarian Cancer Cells.” *Br. J. Cancer 2010 1038* 103(8):1237–44. doi: 10.1038/sj.bjc.6605897.

Michelini, R. H., Doedens, A. L., Goldrath, A. W., and Hedrick, S. M. 2013. “Differentiation of CD8 Memory T Cells Depends on Foxo1.” *J. Exp. Med.* 210(6):1189–1200. doi: 10.1084/jem.20130392.

Miotto, B., Chibi, M., Xie, P., Koundrioukoff, S., Moolman-Smook, H., Pugh, D., Debatisse, M., He, F., Zhang, L., and Defossez, P. A. 2014. “The RBBP6/ZBTB38/MCM10 Axis Regulates DNA Replication and Common Fragile Site Stability.” *Cell Rep.* 7(2):575–87. doi: 10.1016/J.CELREP.2014.03.030.

Mishima, T., Fukaya, S., Toda, S., Ando, Y., Matsunaga, T., and Inobe, M. 2017. “Rapid G0/1 Transition and Cell Cycle Progression in CD8+ T Cells Compared to CD4+ T Cells Following in Vitro Stimulation.” *Microbiol. Immunol.* 61(5):168–75. doi: 10.1111/1348-0421.12479.

Mombaerts, P., Iacomini, J., Johnson, R. S., Herrup, K., Tonegawa, S., and Papaioannou, V. E. 1992. “RAG-1-Deficient Mice Have No Mature B and T Lymphocytes.” *Cell* 68(5):869–77. doi: 10.1016/0092-8674(92)90030-G.

Mondino, A., Colombetti, S., Basso, V., and Mueller, D. L. 2006. “Mammalian Target of Rapamycin through Signaling Mediated by the IL-2-Independent T Cell Clonal Expansion Prolonged TCR/CD28 Engagement Drives.” doi: 10.4049/jimmunol.176.5.2730.

Moriggl, R., Sexl, V., Piekorz, R., Topham, D., and Ihle, J. N. 1999. “Stat5 Activation Is Uniquely Associated with Cytokine Signaling in Peripheral T Cells.” *Immunity* 11(2):225–30. doi: 10.1016/S1074-7613(00)80097-7.

Moriggl, R., Topham, D. J., Teglund, S., Sexl, V., McKay, C., Wang, D., Hoffmeyer, A., Van Deursen, J., Sangster, M. Y., Bunting, K. D., Grosveld, G. C., and Ihle, J. N. 1999. “Stat5 Is Required for IL-2-Induced Cell Cycle Progression of Peripheral T Cells.” *Immunity* 10(2):249–59. doi: 10.1016/S1074-7613(00)80025-4.

Morotti, M., Albukhari, A., Alsaadi, A., Artibani, M., Brenton, J. D., Curbishley, S. M., Dong, T., Dustin, M. L., Hu, Z., McGranahan, N., Miller, M. L., Santana-Gonzalez, L., Seymour, L. W., Shi, T., Van Loo, P., Yau, C., White, H., Wietek, N., Church, D. N., Wedge, D. C., and Ahmed, A. A. 2021. “Promises and Challenges of Adoptive T-Cell Therapies for Solid Tumours.” *Br. J. Cancer 2021 12411* 124(11):1759–76. doi: 10.1038/s41416-021-01353-6.

Morrow, M. A., Mayer, E. W., Perez, C. A., Adlam, M., and Siu, G. 1999. “Overexpression of the Helix–Loop–Helix Protein Id2 Blocks T Cell Development at Multiple Stages.” *Mol. Immunol.* 36(8):491–503. doi: 10.1016/S0161-5890(99)00071-1.

Muhr, J., and Hagey, D. W. 2021. “The Cell Cycle and Differentiation as Integrated Processes: Cyclins and CDKs Reciprocally Regulate Sox and Notch to Balance Stem Cell Maintenance.” *BioEssays* 43(7):2000285. doi: 10.1002/BIES.202000285.

Nakayama, K., Ishida, N., Shirane, M., Inomata, A., Inoue, T., Shishido, N., Horii, I., Loh, D. Y., and Nakayama, K. I. 1996. “Mice Lacking P27Kip1 Display Increased Body Size, Multiple Organ Hyperplasia, Retinal Dysplasia, and Pituitary Tumors.” *Cell* 85(5):707–20. doi: 10.1016/S0092-8674(00)81237-4.

Nakayama, K., Nagahama, H., Minamishima, Y. A., Matsumoto, M., Nakamichi, I., Kitagawa, K., Shirane, M., Tsunematsu, R., Tsukiyama, T., Ishida, N., Kitagawa, M., Nakayama, K. I., and Hatakeyama, S. 2000. “Targeted Disruption of Skp2 Results in Accumulation of Cyclin E and P27Kip1, Polyploidy and Centrosome Overduplication.” *EMBO J.* 19(9):2069. doi: 10.1093/EMBOJ/19.9.2069.

Nelson, B. H. 2004. “IL-2, Regulatory T Cells, and Tolerance.” *J. Immunol.* 172(7):3983–88. doi: 10.4049/jimmunol.172.7.3983.

Nguyen, M. H., Koinuma, J., Ueda, K., Ito, T., Tsuchiya, E., Nakamura, Y., and Daigo, Y. 2010. “Phosphorylation and Activation of Cell Division Cycle Associated 5 by Mitogen-Activated Protein Kinase Play a Crucial Role in Human Lung Carcinogenesis.” *Cancer Res.* 70(13):5337–47. doi: 10.1158/0008-5472.CAN-09-4372.

Niola, F., Zhao, X., Singh, D., Castano, A., Sullivan, R., Lauria, M., Nam, H. S., Zhuang, Y., Benezra, R., Di Bernardo, D., Iavarone, A., and Lasorella, A. 2012. “Id Proteins Synchronize Stemness and Anchorage to the Niche of Neural Stem Cells.” *Nat. Cell Biol.* 14(5):477. doi: 10.1038/NCB2490.

Nolz, J. C., and Richer, M. J. 2020. “Control of Memory CD8+ T Cell Longevity and Effector Functions by IL-15.” *Mol. Immunol.* 117:180–88.

Oh, S. P., Seki, T., Goss, K. A., Imamura, T., Yi, Y., Donahoe, P. K., Li, L., Miyazono, K., Ten Dijke, P., Kim, S., and Li, E. 2000. “Activin Receptor-like Kinase 1 Modulates Transforming Growth Factor-Beta 1 Signaling in the Regulation of Angiogenesis.” *Proc. Natl. Acad. Sci. U. S. A.* 97(6):2626–31. doi: 10.1073/PNAS.97.6.2626.

Omilusik, K. D., Nadjsombati, M. S., Yoshida, T. M., Shaw, L. A., Goulding, J., and Goldrath, A. W. 2021. “Ubiquitin Specific Protease 1 Expression and Function in T Cell Immunity.” *J. Immunol.* 207(5):1377. doi: 10.4049/JIMMUNOL.2100303.

Paolino, M., Thien, C. B. F., Gruber, T., Hinterleitner, R., Baier, G., Langdon, W. Y., and Penninger, J. M. 2011. “ Essential Role of E3 Ubiquitin Ligase Activity in Cbl-b–Regulated T Cell Functions .” *J. Immunol.* 186(4):2138–47. doi: 10.4049/jimmunol.1003390.

Parry, D. H., and O’Farrell, P. H. 2001. “The Schedule of Destruction of Three Mitotic Cyclins Can Dictate the Timing of Events during Exit from Mitosis.” *Curr. Biol.* 11(9):671–83. doi: 10.1016/S0960-9822(01)00204-4.

Parvin, J. D. 2009. “The BRCA1-Dependent Ubiquitin Ligase, Gamma-Tubulin, and Centrosomes.” *Environ. Mol. Mutagen.* 50(8):649–53. doi: 10.1002/EM.20475.

Pauklin, S., Madrigal, P., Bertero, A., and Vallier, L. 2016. “Initiation of Stem Cell Differentiation Involves Cell Cycle-Dependent Regulation of Developmental Genes by Cyclin D.” *Genes Dev.* 30(4):421. doi: 10.1101/GAD.271452.115.

Pauklin, S., and Vallier, L. 2013. “The Cell-Cycle State of Stem Cells Determines Cell Fate Propensity.” *Cell* 155(1):135. doi: 10.1016/J.CELL.2013.08.031.

Paul, D., Kales, S. C., Cornwell, J. A., Afifi, M. M., Rai, G., Zakharov, A., Simeonov, A., and Cappell, S. D. 2022. “Revealing β-TrCP Activity Dynamics in Live Cells with a Genetically Encoded Biosensor.” *Nat. Commun. 2022 131* 13(1):1–14. doi: 10.1038/s41467-022-33762-3.

Pollizzi, K. N., Patel, C. H., Sun, I. H., Oh, M. H., Waickman, A. T., Wen, J., Delgoffe, G. M., and Powell, J. D. 2015. “MTORC1 and MTORC2 Selectively Regulate CD8+ T Cell Differentiation.” *J. Clin. Invest.* 125(5):2090–2108. doi: 10.1172/JCI77746.

Proserpio, V., Piccolo, A., Haim-Vilmovsky, L., Kar, G., Lönnberg, T., Svensson, V., Pramanik, J., Natarajan, K. N., Zhai, W., Zhang, X., Donati, G., Kayikci, M., Kotar, J., McKenzie, A. N. J., Montandon, R., Billker, O., Woodhouse, S., Cicuta, P., Nicodemi, M., and Teichmann, S. A. 2016. “Single-Cell Analysis of CD4+ T-Cell Differentiation Reveals Three Major Cell States and Progressive Acceleration of Proliferation.” *Genome Biol.* 17(1). doi: 10.1186/S13059-016-0957-5.

Quan, Y., Xia, Y., Liu, L., Cui, J., Li, Z., Cao, Q., Chen, X. S., Campbell, J. L., and Lou, H. 2015. “Cell-Cycle-Regulated Interaction between Mcm10 and Double Hexameric Mcm2-7 Is Required for Helicase Splitting and Activation during S Phase.” *Cell Rep.* 13(11):2576–86. doi: 10.1016/J.CELREP.2015.11.018.

Rao, R. R., Li, Q., Odunsi, K., and Shrikant, P. A. 2010. “The MTOR Kinase Determines Effector

versus Memory CD8+ T Cell Fate by Regulating the Expression of Transcription Factors T-Bet and Eomesodermin." *Immunity* 32(1):67–78. doi: 10.1016/j.immuni.2009.10.010.

Reber, A., Lehner, C. F., and Jacobs, H. W. 2006. "Terminal Mitoses Require Negative Regulation of Fzr/Cdh1 by Cyclin A,Preventing Premature Degradation of Mitotic Cyclins and String/Cdc25." *Development* 133(16):3201–11. doi: 10.1242/DEV.02488.

Richardt-Pargmann, D., Wechsler, M., Krieg, A. M., Vollmer, J., and Jurk, M. 2011. "Positive T Cell Co-Stimulation by TLR7/8 Ligands Is Dependent on the Cellular Environment." *Immunobiology* 216(1–2):12. doi: 10.1016/J.IMBIO.2010.03.011.

Richer, M. J., Pewe, L. L., Hancox, L. S., Hartwig, S. M., Varga, S. M., and Harty, J. T. 2015. "Inflammatory IL-15 Is Required for Optimal Memory T Cell Responses." *J. Clin. Invest.* 125(9):3477–90. doi: 10.1172/JCI81261.

Rivera, R. R., Johns, C. P., Quan, J., Johnson, R. S., and Murre, C. 2000. "Thymocyte Selection Is Regulated by the Helix-Loop-Helix Inhibitor Protein, Id3." *Immunity* 12(1):17–26. doi: 10.1016/S1074-7613(00)80155-7.

Robu, M. E., Zhang, Y., and Rhodes, J. 2012. "Rereplication in Emi1-Deficient Zebrafish Embryos Occurs through a Cdh1-Mediated Pathway." *PLoS One* 7(10):e47658. doi: 10.1371/JOURNAL.PONE.0047658.

Rollings, C. M., Sinclair, L. V, Brady, H. J. M., Cantrell, D. A., and Ross, S. H. 2018. "Interleukin-2 Shapes the Cytotoxic T Cell Proteome and Immune Environment-Sensing Programs." *Sci. Signal.* 11(526):eaap8112. doi: 10.1126/scisignal.aap8112.

Rowley, J., Monie, A., Hung, C. F., and Wu, T. C. 2009. "Expression of IL-15RA or an IL-15/IL-15RA Fusion on CD8+ T Cells Modifies Adoptively Transferred T-Cell Function in Cis." *Eur. J. Immunol.* 39(2):491–506. doi: 10.1002/eji.200838594.

Rowshanravan, B., Halliday, N., and Sansom, D. M. 2018. "CTLA-4: A Moving Target in Immunotherapy." *Blood* 131(1):58–67. doi: 10.1182/BLOOD-2017-06-741033.

Russell, P., and Nurse, P. 1987. "Negative Regulation of Mitosis by Wee1+, a Gene Encoding a Protein Kinase Homolog." *Cell* 49(4):559–67. doi: 10.1016/0092-8674(87)90458-2.

Sade-Feldman, M., Yizhak, K., Bjorgaard, S. L., Ray, J. P., de Boer, C. G., Jenkins, R. W., Lieb, D. J., Chen, J. H., Frederick, D. T., Barzily-Rokni, M., Freeman, S. S., Reuben, A., Hoover, P. J., Villani, A. C., Ivanova, E., Portell, A., Lizotte, P. H., Aref, A. R., Eliane, J. P., Hammond, M. R., Vitzthum, H., Blackmon, S. M., Li, B., Gopalakrishnan, V., Reddy, S. M., Cooper, Z. A., Paweletz, C. P., Barbie, D. A., Stemmer-Rachamimov, A., Flaherty, K. T., Wargo, J. A., Boland, G. M., Sullivan, R. J., Getz, G., and Hacohen, N. 2018. "Defining T Cell States Associated with Response to Checkpoint Immunotherapy in Melanoma." *Cell* 175(4):998-1013.e20. doi: 10.1016/j.cell.2018.10.038.

Sansam, C. L., Shepard, J. L., Lai, K., Ianari, A., Danielian, P. S., Amsterdam, A., Hopkins, N., and Lees, J. A. 2006. "DTL/CDT2 Is Essential for Both CDT1 Regulation and the Early G2/M Checkpoint." *Genes Dev.* 20(22):3117–29. doi: 10.1101/GAD.1482106.

Schauder, D. M., Shen, J., Chen, Y., Kasmani, M. Y., Kudek, M. R., Burns, R., and Cui, W. 2021. "E2A-Regulated Epigenetic Landscape Promotes Memory CD8 T Cell Differentiation." *Proc. Natl. Acad. Sci. U. S. A.* 118(16):e2013452118. doi:

10.1073/PNAS.2013452118/SUPPL_FILE/PNAS.2013452118.SAPP.PDF.

Schülein, C., Eilers, M., and Popov, N. 2011. “PI3K-Dependent Phosphorylation of Fbw7 Modulates Substrate Degradation and Activity.” *FEBS Lett.* 585(14):2151–57. doi: 10.1016/J.FEBSLET.2011.05.036.

Seddon, B., Legname, G., Tomlinson, P., and Zamoyska, R. 2000. “Long-Term Survival but Impaired Homeostatic Proliferation of Naïve T Cells in the Absence of P56lck.” *Science* 290(5489):127–31. doi: 10.1126/SCIENCE.290.5489.127.

Seddon, B., and Zamoyska, R. 2002. “TCR Signals Mediated by Src Family Kinases Are Essential for the Survival of Naive T Cells.” *J. Immunol.* 169(6):2997–3005. doi: 10.4049/JIMMUNOL.169.6.2997.

Sherr, C. J., and Roberts, J. M. 1999. “CDK Inhibitors: Positive and Negative Regulators of G1-Phase Progression.” *Genes Dev.* 13(12):1501–12. doi: 10.1101/gad.13.12.1501.

Shi, X., Liu, Y., Cheng, S., Hu, H., Zhang, J., Wei, M., Zhao, L., and Xin, S. 2021. “Cancer Stemness Associated With Prognosis and the Efficacy of Immunotherapy in Adrenocortical Carcinoma.” *Front. Oncol.* 11:1995. doi: 10.3389/FONC.2021.651622/BIBTEX.

Shifrut, E., Carnevale, J., Tobin, V., Roth, T. L., Woo, J. M., Bui, C. T., Li, P. J., Diolaiti, M. E., Ashworth, A., and Marson, A. 2018. “Genome-Wide CRISPR Screens in Primary Human T Cells Reveal Key Regulators of Immune Function.” *Cell* 175(7):1958-1971.e15. doi: 10.1016/j.cell.2018.10.024.

Shimizu, N., Nakajima, N. I., Tsunematsu, T., Ogawa, I., Kawai, H., Hirayama, R., Fujimori, A., Yamada, A., Okayasu, R., Ishimaru, N., Takata, T., and Kudo, Y. 2013. “Selective Enhancing Effect of Early Mitotic Inhibitor 1 (Emi1) Depletion on the Sensitivity of Doxorubicin or x-Ray Treatment in Human Cancer Cells.” *J. Biol. Chem.* 288(24):17238–52. doi: 10.1074/jbc.M112.446351.

Siddiqui, I., Schaeuble, K., Chennupati, V., Fuertes Marraco, S. A., Calderon-Copete, S., Pais Ferreira, D., Carmona, S. J., Scarpellino, L., Gfeller, D., Pradervand, S., Luther, S. A., Speiser, D. E., and Held, W. 2019. “Intratumoral Tcf1 + PD-1 + CD8 + T Cells with Stem-like Properties Promote Tumor Control in Response to Vaccination and Checkpoint Blockade Immunotherapy.” *Immunity* 50(1):195-211.e10. doi: 10.1016/j.immuni.2018.12.021.

Singh, A., Jatzek, A., Plisch, E. H., Srinivasan, R., Svaren, J., and Suresh, M. 2010. “Regulation of Memory CD8 T-Cell Differentiation by Cyclin-Dependent Kinase Inhibitor P27Kip1.” *Mol. Cell. Biol.* 30(21):5145–59. doi: 10.1128/mcb.01045-09.

Sivaprasad, U., Machida, Y. J., and Dutta, A. 2007. “APC/C – the Master Controller of Origin Licensing?” *Cell Div.* 2:8. doi: 10.1186/1747-1028-2-8.

Smith, K. A., and Ruscetti, F. W. 1981. “T-Cell Growth Factor and the Culture of Cloned Functional T Cells.” *Adv. Immunol.* 31(C):137–75. doi: 10.1016/S0065-2776(08)60920-7.

Song, L., and Rape, M. 2010. “Regulated Degradation of Spindle Assembly Factors by the Anaphase-Promoting Complex.” *Mol. Cell* 38(3):369. doi: 10.1016/J.MOLCEL.2010.02.038.

Spolski, R., Li, P., and Leonard, W. J. 2018. “Biology and Regulation of IL-2: From Molecular Mechanisms to Human Therapy.” *Nat. Rev. Immunol.* 18(10):648–59.

Stauber, D. J., Debler, E. W., Horton, P. A., Smith, K. A., and Wilson, I. A. 2006. “Crystal Structure of the IL-2 Signaling Complex: Paradigm for a Heterotrimeric Cytokine Receptor.” *Proc. Natl. Acad. Sci. U. S. A.* 103(8):2788–93. doi: 10.1073/pnas.0511161103.

Stead, E., White, J., Faast, R., Conn, S., Goldstone, S., Rathjen, J., Dhingra, U., Rathjen, P., Walker, D., and Dalton, S. 2002. “Pluripotent Cell Division Cycles Are Driven by Ectopic Cdk2, Cyclin A/E and E2F Activities.” *Oncogene 2002 2154* 21(54):8320–33. doi: 10.1038/sj.onc.1206015.

Stengel, K. R., Thangavel, C., Solomon, D. A., Angus, S. P., Zheng, Y., and Knudsen, E. S. 2009. “Retinoblastoma/P107/P130 Pocket Proteins. Proteins Dynamics and Interactions with Target Gene Promoters.” *J. Biol. Chem.* 284(29):19265–71. doi: 10.1074/jbc.M808740200.

Sterner, R. C., and Sterner, R. M. 2021. “CAR-T Cell Therapy: Current Limitations and Potential Strategies.” *Blood Cancer J.* 11(4):69. doi: 10.1038/S41408-021-00459-7.

Sudakin, V., Chan, G. K. T., and Yen, T. J. 2001. “Checkpoint Inhibition of the APC/C in HeLa Cells Is Mediated by a Complex of BUBR1, BUB3, CDC20, and MAD2.” *J. Cell Biol.* 154(5):925. doi: 10.1083/JCB.200102093.

Sullivan, B. M., Juedes, A., Szabo, S. J., Von Herrath, M., and Glimcher, L. H. 2003. *Antigen-Driven Effector CD8 T Cell Function Regulated by T-Bet*.

Sullivan, M., Lehane, C., and Uhlmann, F. 2001. “Orchestrating Anaphase and Mitotic Exit: Separase Cleavage and Localisation of Slk19.” *Nat. Cell Biol.* 3(9):771. doi: 10.1038/NCB0901-771.

Sun, H., Ma, H., Zhang, H., and Ji, M. 2021. “Up-Regulation of MELK by E2F1 Promotes the Proliferation in Cervical Cancer Cells.” *Int. J. Biol. Sci.* 17(14):3875. doi: 10.7150/IJBS.62517.

Tan, H., Yang, K., Li, Y., Shaw, T. I., Wang, Y., Blanco, D. B., Wang, X., Cho, J.-H., Wang, H., Rankin, S., Guy, C., Peng, J., and Chi, H. 2017. “Integrative Proteomics and Phosphoproteomics Profiling Reveals Dynamic Signaling Networks and Bioenergetics Pathways Underlying T Cell Activation.” *Immunity* 46(3):488–503. doi: 10.1016/J.IMMUNI.2017.02.010.

Tewari, K., Walent, J., Svaren, J., Zamoyska, R., and Suresh, M. 2006. “Differential Requirement for Lck during Primary and Memory CD8+ T Cell Responses.” *Proc. Natl. Acad. Sci. U. S. A.* 103(44):16388–93. doi: 10.1073/pnas.0602565103.

Thornton, B. R., and Toczyski, D. P. 2003. “Securin and B-Cyclin/CDK Are the Only Essential Targets of the APC.” *Nat. Cell Biol. 2003 512* 5(12):1090–94. doi: 10.1038/ncb1066.

Tinoco, R., Alcalde, V., Yang, Y., Sauer, K., and Zuniga, E. I. 2009. “TGF-β Signaling in T Cells Is Essential for CD8 T Cell Suppression and Viral Persistence In Vivo.” *Immunity* 31(1):145. doi: 10.1016/J.IMMUNI.2009.06.015.

Tomasik, J., Jasiński, M., and Basak, G. W. 2022. “Next Generations of CAR-T Cells - New Therapeutic Opportunities in Hematology?” *Front. Immunol.* 13:6578. doi: 10.3389/FIMMU.2022.1034707/BIBTEX.

Tomoda, K., Kubota, Y., and Kato, J. Y. 1999. “Degradation of the Cyclin-Dependent-Kinase Inhibitor P27(Kip1) Is Instigated by Jab1.” *Nature* 398(6723):160–65. doi: 10.1038/18230.

Tough, D. F., and Sprent, J. 1994. “Turnover of Naive- and Memory-Phenotype T Cells.” *J. Exp. Med.* 179(4):1127. doi: 10.1084/JEM.179.4.1127.

Tyanova, S., Temu, T., and Cox, J. 2016. “The MaxQuant Computational Platform for Mass Spectrometry-Based Shotgun Proteomics.” *Nat. Protoc.* 11(12):2301–19. doi: 10.1038/nprot.2016.136.

Uhlmann, F., Lottspelch, F., and Nasmyth, K. 1999. “Sister-Chromatid Separation at Anaphase Onset Is Promoted by Cleavage of the Cohesin Subunit Scc1.” *Nat. 1999 4006739* 400(6739):37–42. doi: 10.1038/21831.

Utzschneider, D. T., Gabriel, S. S., Chisanga, D., Gloury, R., Gubser, P. M., Vasanthakumar, A., Shi, W., and Kallies, A. 2020. “Early Precursor T Cells Establish and Propagate T Cell Exhaustion in Chronic Infection.” *Nat. Immunol. 2020 2110* 21(10):1256–66. doi: 10.1038/s41590-020-0760-z.

Uzunova, K., Dye, B. T., Schutz, H., Ladurner, R., Petzold, G., Toyoda, Y., Jarvis, M. A., Brown, N. G., Poser, I., Novatchkova, M., Mechtler, K., Hyman, A. A., Stark, H., Schulman, B. A., and Peters, J. M. 2012. “APC15 Mediates CDC20 Auto-Ubiquitylation by APC/CMCC and MCC Disassembly.” *Nat. Struct. Mol. Biol.* 19(11):1116. doi: 10.1038/NSMB.2412.

Vartanian, R., Masri, J., Martin, J., Cloninger, C., Holmes, B., Artinian, N., Funk, A., Ruegg, T., and Gera, J. 2011. “AP-1 Regulates Cyclin D1 and c-MYC Transcription in an AKT-Dependent Manner in Response to MTOR Inhibition: Role of AIP4/Itch-Mediated JUNB Degradation.” *Mol. Cancer Res.* 9(1):115–30. doi: 10.1158/1541-7786.MCR-10-0105.

Verschuren, E. W., Ban, K. H., Masek, M. A., Lehman, N. L., and Jackson, P. K. 2007. “Loss of Emi1-Dependent Anaphase-Promoting Complex/Cyclosome Inhibition Deregulates E2F Target Expression and Elicits DNA Damage-Induced Senescence.” *Mol. Cell. Biol.* 27(22):7955. doi: 10.1128/MCB.00908-07.

Wade Harper, J., Adami, G. R., Wei, N., Keyomarsi, K., and Elledge, S. J. 1993. “The P21 Cdk-Interacting Protein Cip1 Is a Potent Inhibitor of G1 Cyclin-Dependent Kinases.” *Cell* 75(4):805–16. doi: 10.1016/0092-8674(93)90499-G.

Waickman, A. T., and Powell, J. D. 2012. “MTOR, Metabolism, and the Regulation of T-Cell Differentiation and Function.” *Immunol. Rev.* 249(1):43–58. doi: 10.1111/j.1600-065X.2012.01152.x.

Wang, H., Nicolay, B. N., Chick, J. M., Gao, X., Geng, Y., Ren, H., Gao, H., Yang, G., Williams, J. A., Suski, J. M., Keibler, M. A., Sicinska, E., Gerdemann, U., Haining, W. N., Roberts, T. M., Polyak, K., Gygi, S. P., Dyson, N. J., and Sicinski, P. 2017. “The Metabolic Function of Cyclin D3-CDK6 Kinase in Cancer Cell Survival.” *Nature* 546(7658):426–30. doi: 10.1038/nature22797.

Wang, R., Dillon, C. P., Shi, L. Z., Milasta, S., Carter, R., Finkelstein, D., McCormick, L. L., Fitzgerald, P., Chi, H., Munger, J., and Green, D. R. 2011. "The Transcription Factor Myc Controls Metabolic Reprogramming upon T Lymphocyte Activation." *Immunity* 35(6):871–82. doi: 10.1016/j.immuni.2011.09.021.

Wang, Y., Zhou, T., Chen, H., Wen, S., Dao, P., and Chen, M. 2022. "Rad54L Promotes Bladder Cancer Progression by Regulating Cell Cycle and Cell Senescence." *Med. Oncol.* 39(12):1–11. doi: 10.1007/S12032-022-01751-7/TABLES/1.

Watanabe, Nobumoto, Arai, H., Nishihara, Y., Taniguchi, M., Watanabe, Naoko, Hunter, T., and Osada, H. 2004. "M-Phase Kinases Induce Phospho-Dependent Ubiquitination of Somatic Wee1 by SCFbeta-TrCP." *Proc. Natl. Acad. Sci. U. S. A.* 101(13):4419–24. doi: 10.1073/PNAS.0307700101.

Wei, H., Geng, J., Shi, B., Liu, Z., Wang, Y.-H., Stevens, A. C., Sprout, S. L., Yao, M., Wang, H., and Hu, H. 2016. "Foxp1 Controls Naive CD8+ T Cell Quiescence by Simultaneously Repressing Key Pathways in Cellular Metabolism and Cell Cycle Progression." *J. Immunol.* 196(9):3537. doi: 10.4049/JIMMUNOL.1501896.

Weinberg, R. A. 1995. "The Retinoblastoma Protein and Cell Cycle Control." *Cell* 81(3):323–30. doi: 10.1016/0092-8674(95)90385-2.

Wherry, E. J. 2011. "T Cell Exhaustion." *Nat. Immunol. 2011 126* 12(6):492–99. doi: 10.1038/ni.2035.

White, J., Stead, E., Faast, R., Conn, S., Cartwright, P., and Dalton, S. 2005. "Developmental Activation of the Rb–E2F Pathway and Establishment of Cell Cycle-Regulated Cyclin-Dependent Kinase Activity during Embryonic Stem Cell Differentiation." *Mol. Biol. Cell* 16(4):2018. doi: 10.1091/MBC.E04-12-1056.

Wichert, S., Fonkianos, K., and Strimmer, K. 2004. "Identifying Periodically Expressed Transcripts in Microarray Time Series Data." *Bioinformatics* 20(1):5–20. doi: 10.1093/BIOINFORMATICS/BTG364.

Williams, S. A., Maecker, H. L., French, D. M., Liu, J., Gregg, A., Silverstein, L. B., Cao, T. C., Carano, R. A. D., and Dixit, V. M. 2011. "USP1 Deubiquitinates ID Proteins to Preserve a Mesenchymal Stem Cell Program in Osteosarcoma." *Cell* 146(6):918–30. doi: 10.1016/j.cell.2011.07.040.

Wiśniewski, J. R., Hein, M. Y., Cox, J., and Mann, M. 2014. "A 'Proteomic Ruler' for Protein Copy Number and Concentration Estimation without Spike-in Standards." *Mol. Cell. Proteomics* 13(12):3497–3506. doi: 10.1074/MCP.M113.037309.

Wolfraim, L. A., Walz, T. M., James, Z., Fernandez, T., and Letterio, J. J. 2004. " P21 Cip1 and P27 Kip1 Act in Synergy to Alter the Sensitivity of Naive T Cells to TGF-β-Mediated G 1 Arrest through Modulation of IL-2 Responsiveness ." *J. Immunol.* 173(5):3093–3102. doi: 10.4049/jimmunol.173.5.3093.

Wu, G., Xu, G., Schulman, B. A., Jeffrey, P. D., Harper, J. W., and Pavletich, N. P. 2003. "Structure of a β-TrCP1-Skp1-β-Catenin Complex: Destruction Motif Binding and Lysine Specificity of the SCFβ-TrCP1 Ubiquitin Ligase." *Mol. Cell* 11(6):1445–56. doi: 10.1016/S1097-2765(03)00234-X.

Wu, T.-S., Lee, J.-M., Lai, Y.-G., Hsu, J.-C., Tsai, C.-Y., Lee, Y.-H., and Liao, N.-S. 2002. " Reduced Expression of Bcl-2 in CD8 + T Cells Deficient in the IL-15 Receptor α-Chain ." *J. Immunol.* 168(2):705–12. doi: 10.4049/jimmunol.168.2.705.

Xiang, G., Zhang, X., An, C., Cheng, C., and Wang, H. 2017. "Temperature Effect on CRISPR-Cas9 Mediated Genome Editing." *J. Genet. Genomics* 44(4):199–205. doi: 10.1016/J.JGG.2017.03.004.

Xue, H. H., Kovanen, P. E., Pise-Masison, C. A., Berg, M., Radovich, M. F., Brady, J. N., and Leonard, W. J. 2002. "Il-2 Negatively Regulates IL-7 Receptor α Chain Expression in Activated T Lymphocytes." *Proc. Natl. Acad. Sci. U. S. A.* 99(21):13759–64. doi: 10.1073/pnas.212214999.

Yamada, T., Park, C. S., Mamonkin, M., and Lacorazza, H. D. 2009. "The Transcription Factor ELF4 Controls Proliferation and Homing of CD8+ T Cells via the Krüppel-like Factors KLF4 and KLF2." *Nat. Immunol.* 10(6):618. doi: 10.1038/NI.1730.

Yang, C. Y., Best, J. A., Knell, J., Yang, E., Sheridan, A. D., Jesionek, A. K., Li, H. S., Rivera, R. R., Lind, K. C., D'Cruz, L. M., Watowich, S. S., Murre, C., and Goldrath, A. W. 2011. "The Transcriptional Regulators Id2 and Id3 Control the Formation of Distinct Memory CD8+ T Cell Subsets." *Nat. Immunol.* 12(12):1221–29. doi: 10.1038/NI.2158.

Yang, F., Kou, J., Liu, Z., Li, W., and Du, W. 2021. "MYC Enhances Cholesterol Biosynthesis and Supports Cell Proliferation Through SQLE." *Front. Cell Dev. Biol.* 9:655889. doi: 10.3389/FCELL.2021.655889/FULL.

Yang, V. S., Carter, S. A., Hyland, S. J., Tachibana-Konwalski, K., Laskey, R. A., and Gonzalez, M. A. 2011. "Geminin Escapes Degradation in G1 of Mouse Pluripotent Cells and Mediates the Expression of Oct4, Sox2, and Nanog." *Curr. Biol.* 21(8):692. doi: 10.1016/J.CUB.2011.03.026.

Yao, C., Lou, G., Sun, H. W., Zhu, Z., Sun, Y., Chen, Z., Chauss, D., Moseman, E. A., Cheng, J., D'Antonio, M. A., Shi, W., Shi, J., Kometani, K., Kurosaki, T., Wherry, E. J., Afzali, B., Gattinoni, L., Zhu, Y., McGavern, D. B., O'Shea, J. J., Schwartzberg, P. L., and Wu, T. 2021. "BACH2 Enforces the Transcriptional and Epigenetic Programs of Stem-like CD8+ T Cells." *Nat. Immunol. 2021 223* 22(3):370–80. doi: 10.1038/s41590-021-00868-7.

Yeo, C. J. J., and Fearon, D. T. 2011. "T-Bet-Mediated Differentiation of the Activated CD8+ T Cell." *Eur. J. Immunol.* 41(1):60–66. Retrieved April 18, 2021 (/pmc/articles/PMC3130140/).

Yoon, H., Kim, T. S., and Braciale, T. J. 2010. "The Cell Cycle Time of CD8+ T Cells Responding in Vivo Is Controlled by the Type of Antigenic Stimulus." *PLoS One* 5(11). doi: 10.1371/journal.pone.0015423.

Youngblood, B., Hale, J. S., Kissick, H. T., Ahn, E., Xu, X., Wieland, A., Araki, K., West, E. E., Ghoneim, H. E., Fan, Y., Dogra, P., Davis, C. W., Konieczny, B. T., Antia, R., Cheng, X., and Ahmed, R. 2017. "Effector CD8 T Cells Dedifferentiate into Long-Lived Memory Cells." *Nature* 552(7685):404–9. doi: 10.1038/nature25144.

Zetterberg, A., and Larsson, O. 1985. "Kinetic Analysis of Regulatory Events in G1 Leading to Proliferation or Quiescence of Swiss 3T3 Cells." *Proc. Natl. Acad. Sci. U. S. A.*

82(16):5365–69. doi: 10.1073/pnas.82.16.5365.

Zetterberg, A., and Larsson, O. 1991. “Coordination between Cell Growth and Cell Cycle Transit in Animal Cells.” *Cold Spring Harb. Symp. Quant. Biol.* 56:137–47. doi: 10.1101/SQB.1991.056.01.018.

Zetterberg, A., Larsson, O., and Wiman, K. G. 1995. “What Is the Restriction Point?” *Curr. Opin. Cell Biol.* 7(6):835–42. doi: 10.1016/0955-0674(95)80067-0.

Zhang, J., Gao, Q., Li, P., Liu, X., Jia, Y., Wu, W., Li, J., Dong, S., Koseki, H., and Wong, J. 2011. “S Phase-Dependent Interaction with DNMT1 Dictates the Role of UHRF1 but Not UHRF2 in DNA Methylation Maintenance.” *Cell Res.* 21(12):1723. doi: 10.1038/CR.2011.176.

Zhao, H., Zhang, S., Xu, D., Lee, M. Y., Zhang, Z., Lee, E. Y. C., and Darzynkiewicz, Z. 2014. “Expression of the P12 Subunit of Human DNA Polymerase δ (Pol δ), CDK Inhibitor P21(WAF1), Cdt1, Cyclin A, PCNA and Ki-67 in Relation to DNA Replication in Individual Cells.” *Cell Cycle* 13(22):3529–40. doi: 10.4161/15384101.2014.958910.

Zheng, L., Dominski, Z., Yang, X.-C., Elms, P., Raska, C. S., Borchers, C. H., and Marzluff, W. F. 2003. “Phosphorylation of Stem-Loop Binding Protein (SLBP) on Two Threonines Triggers Degradation of SLBP, the Sole Cell Cycle-Regulated Factor Required for Regulation of Histone MRNA Processing, at the End of S Phase.” *Mol. Cell. Biol.* 23(5):1590. doi: 10.1128/MCB.23.5.1590-1601.2003.

Zhou, X., Ji, H., Ye, D., Li, Hong, Liu, F., Li, Haiyan, Xu, J., Li, Y., and Xiang, F. 2020. “Knockdown of ATAD2 Inhibits Proliferation and Tumorigenicity Through the Rb-E2F1 Pathway and Serves as a Novel Prognostic Indicator in Gastric Cancer.” *Cancer Manag. Res.* 12:337–51. doi: 10.2147/CMAR.S228629.

Zielke, N., and Edgar, B. A. 2015. “FUCCI Sensors: Powerful New Tools for Analysis of Cell Proliferation.” *Wiley Interdiscip. Rev. Dev. Biol.* 4(5):469–87. doi: 10.1002/WDEV.189.

Zielke, N., Querings, S., Rottig, C., Lehner, C., and Sprenger, F. 2008. “The Anaphase-Promoting Complex/Cyclosome (APC/C) Is Required for Rereplication Control in Endoreplication Cycles.” *Genes Dev.* 22(12):1690–1703. doi: 10.1101/GAD.469108.

8 Appendix

8.1 Dynamics of CD8 T cell proliferation

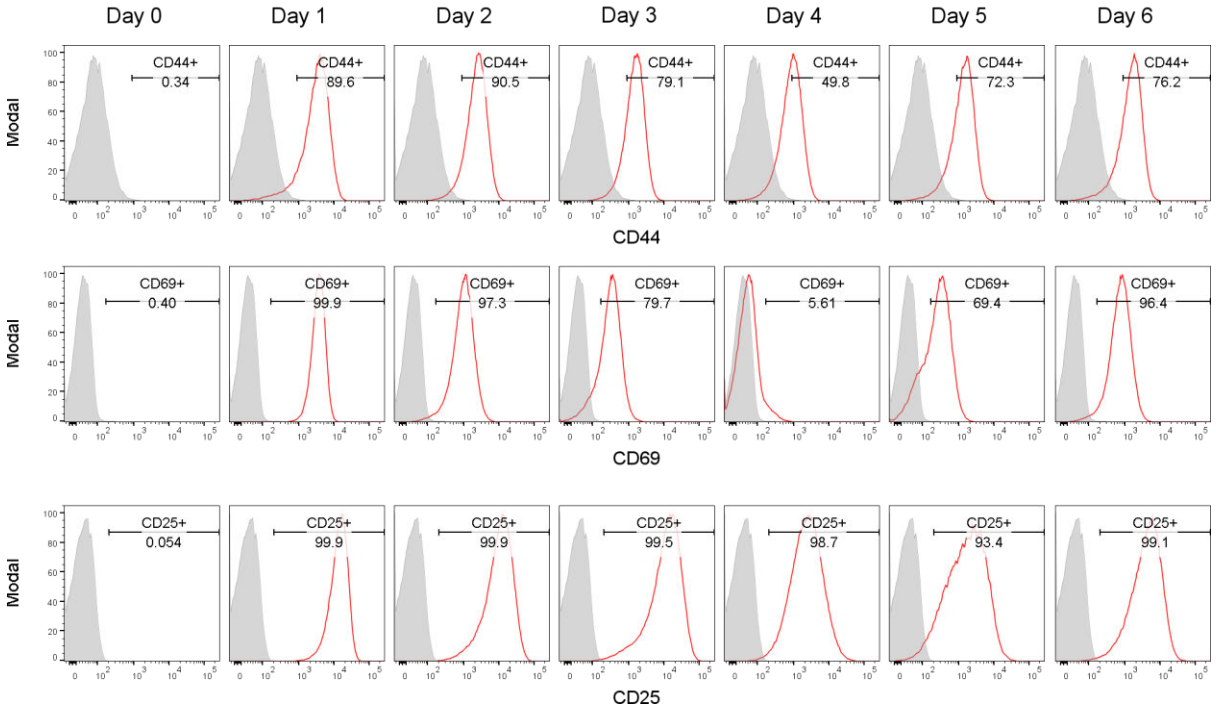

OT-1 CD8⁺ T cells were extracted from lymph nodes and incubated with N4 antigen at Day 0 to day 2, at which point the cells were washed and returned to culture with IL-2, and supplemented with IL-2 at day 4. Cells were taken each day and stained for activation markers CD44, CD69 and CD25 to track activation. Grey are the naïve cells at day 0.

8.2 Phenotype of CD8 T cells following IL-2 or IL-15 treatment from day 3 of culture

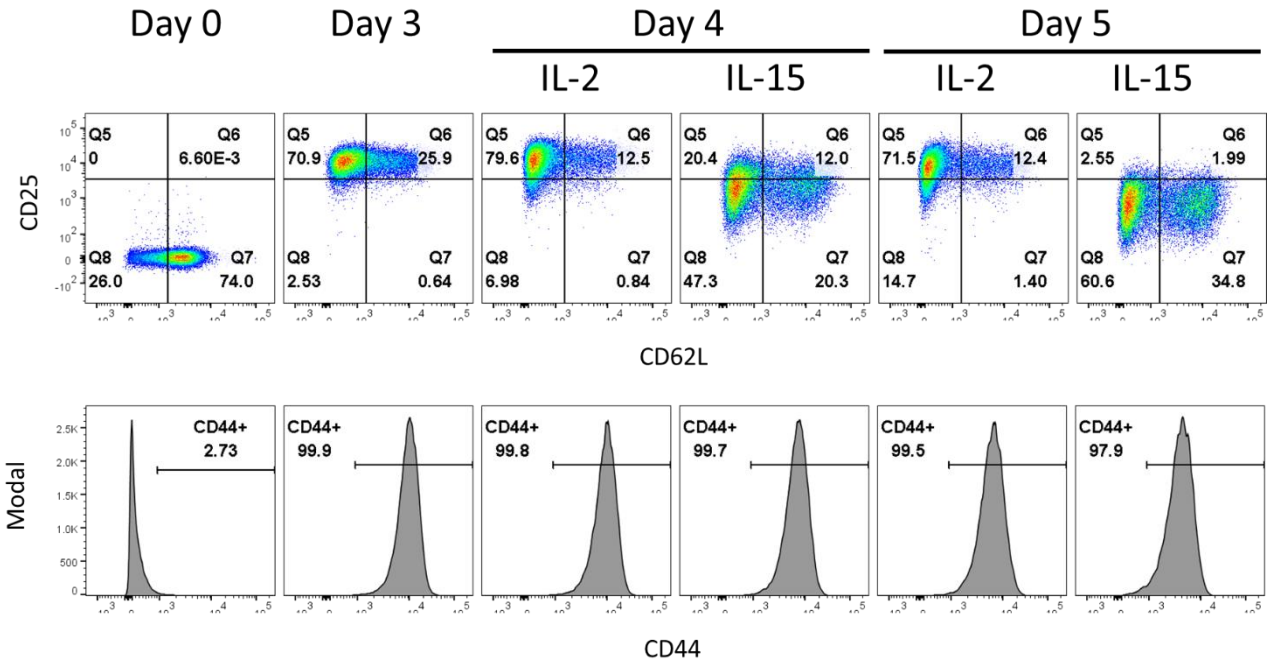

OT-1 CD8⁺ T cells were activated in N4 antigen for 2 days and then kept in IL-2 for 1 day. Cells were then separated in to IL-2 or IL-15 and collected daily. T for naïve cells (day 0) and from day 3, at which point the culture was split between IL-2 and IL-15 stimulation.

8.3 Cell Cycle phase distribution of cultures with different frequencies of IL-2 supplementation

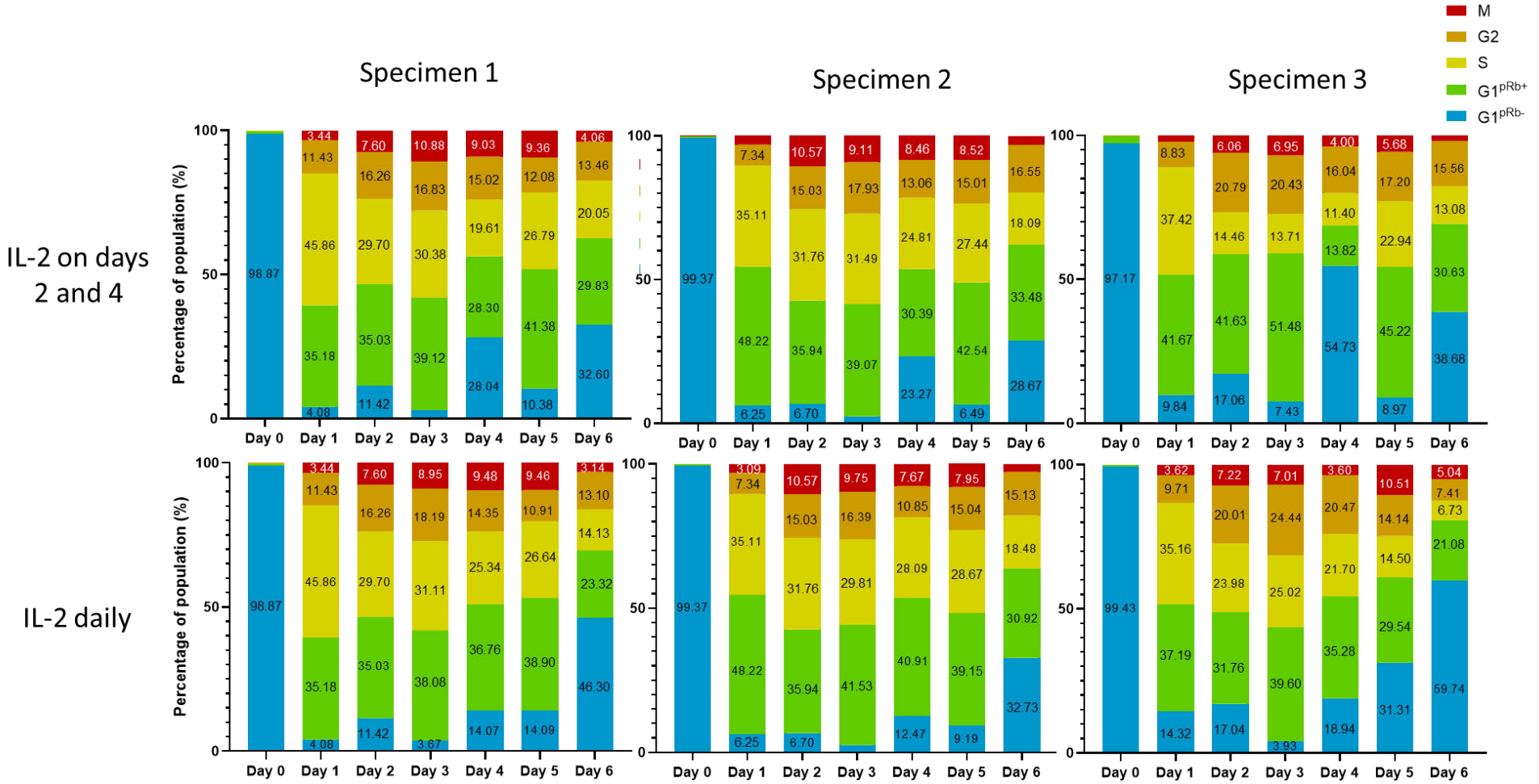

Cell cycle analysis of OT-1 cells activated with N4 antigen for 2 days, then provided IL-2 either on days 2 and 4 (top row) or daily from Day 2 (bottom row). Cells were separated into cell cycle phases by cell cycle markers p-Rb and pH3 Ser10. Data provided on a set of triplicate conducted over two experiments. We observed fluctuations in the number of cells which were pRb-, increasing following 48 hours without IL-2 supplementation, which was not observed as consistently in daily IL-2 supplementation.

8.4 Gating strategy used on CD8 T cells post transfection

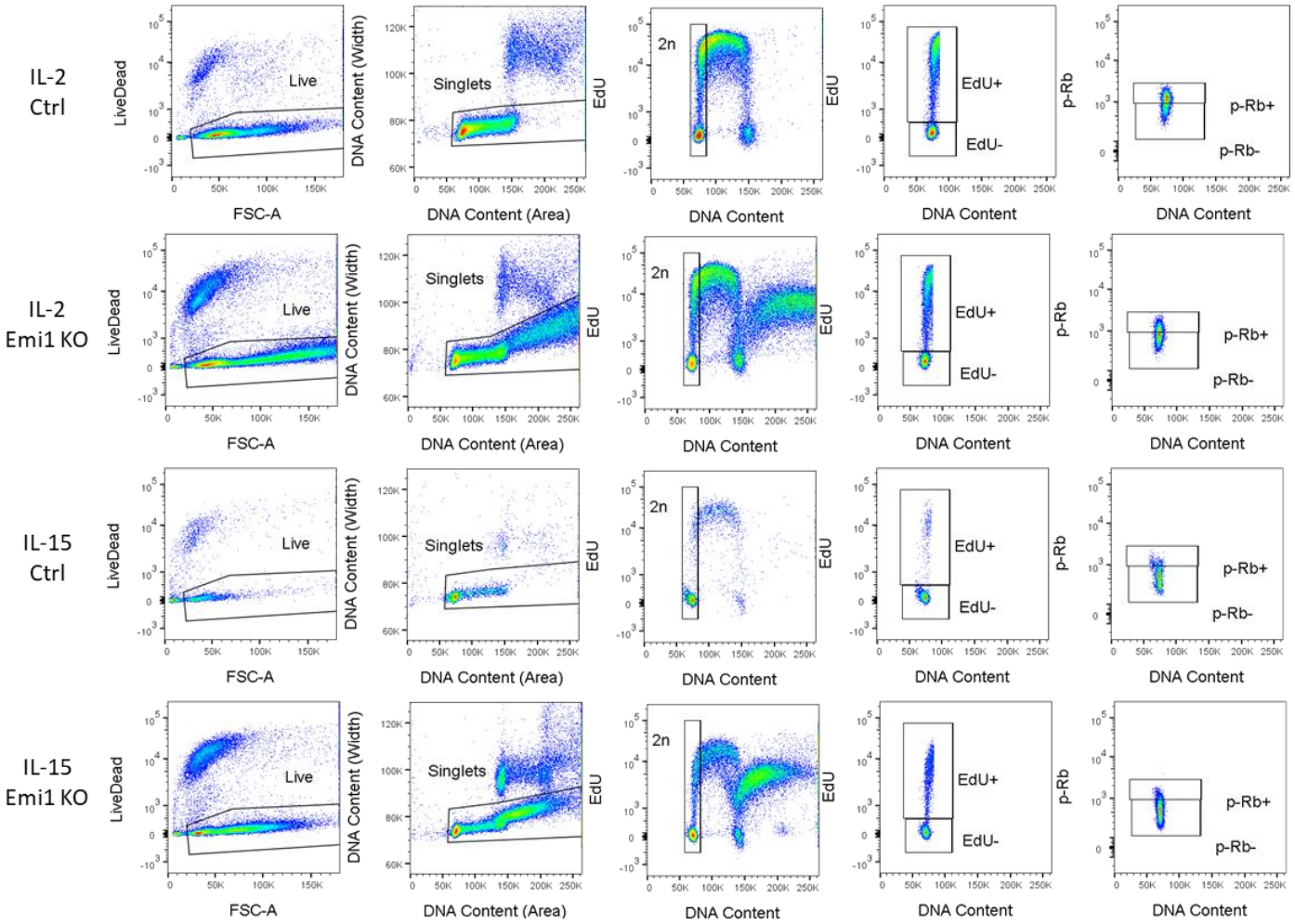

Gating strategy for T cells following transfection with Emi1 targeting Cas9 Crispr complex or complex free control. Cells were first separated for dead cells and then screened for doublets. Due to the expanded size of re-replicating cells, doublet screening was augmented to include these populations using DNA content on Area and Width to discriminate against true doublets. From this population the 2n gate was based on the DNA and EdU profile, and from this group Edu- and Edu+ were quantified, and within the Edu- gate, pRb+ and pRb- were quantified.